Progress in Retinal and Eye Research 101 (2024) 101273

Contents lists available at ScienceDirect

Progress in Retinal and Eye Research

journal homepage: www.elsevier.com/locate/preteyeres

Alzheimer's disease pathophysiology in the Retina

Bhakta Prasad Gaire [a], Yosef Koronyo [a], Dieu-Trang Fuchs [a], Haoshen Shi [a], Altan Rentsendorj [a], Ron Danziger [b], Jean-Philippe Vit [a], Nazanin Mirzaei [a], Jonah Doustar [a], Julia Sheyn [a], Harald Hampel [c], Andrea Vergallo [c], Miyah R. Davis [a], Ousman Jallow [a], Filippo Baldacci [c,d], Steven R. Verdooner [e], Ernesto Barron [f,g], Mehdi Mirzaei [h], Vivek K. Gupta [h], Stuart L. Graham [h,i], Mourad Tayebi [j], Roxana O. Carare [k], Alfredo A. Sadun [f,g], Carol A. Miller [l], Oana M. Dumitrascu [m], Shouri Lahiri [b], Liang Gao [n], Keith L. Black [a], Maya Koronyo-Hamaoui [a,b,o,*]

[a] Department of Neurosurgery, Maxine Dunitz Neurosurgical Research Institute, Cedars-Sinai Medical Center, Los Angeles, CA, USA
[b] Department of Neurology, Cedars-Sinai Medical Center, Los Angeles, CA, USA
[c] Sorbonne University, Alzheimer Precision Medicine (APM), AP-HP, Pitié-Salpêtrière Hospital, Paris, France
[d] Department of Clinical and Experimental Medicine, Neurology Unit, University of Pisa, Pisa, Italy
[e] NeuroVision Imaging Inc., Sacramento, CA, USA
[f] Department of Ophthalmology, David Geffen School of Medicine at University of California Los Angeles, Los Angeles, CA, USA
[g] Doheny Eye Institute, Los Angeles, CA, USA
[h] Department of Clinical Medicine, Health and Human Sciences, Macquarie Medical School, Macquarie University, Sydney, NSW, Australia
[i] Department of Clinical Medicine, Macquarie University, Sydney, NSW, Australia
[j] School of Medicine, Western Sydney University, Campbelltown, NSW, Australia
[k] Department of Clinical Neuroanatomy, University of Southampton, Southampton, UK
[l] Department of Pathology Program in Neuroscience, Keck School of Medicine, University of Southern California, Los Angeles, CA, USA
[m] Department of Neurology, Mayo Clinic, Scottsdale, AZ, USA
[n] Department of Bioengineering, University of California Los Angeles, Los Angeles, CA, USA
[o] Department of Biomedical Sciences, Division of Applied Cell Biology and Physiology, Cedars-Sinai Medical Center, Los Angeles, CA, USA

ARTICLE INFO

Keywords:
Neurodegenerative diseases
Retinal imaging
Inflammation
Retinal vascular pathology
Visual impairments
Alzheimer's disease

ABSTRACT

The retina is an emerging CNS target for potential noninvasive diagnosis and tracking of Alzheimer's disease (AD). Studies have identified the pathological hallmarks of AD, including amyloid β-protein (Aβ) deposits and abnormal tau protein isoforms, in the retinas of AD patients and animal models. Moreover, structural and functional vascular abnormalities such as reduced blood flow, vascular Aβ deposition, and blood-retinal barrier damage, along with inflammation and neurodegeneration, have been described in retinas of patients with mild cognitive impairment and AD dementia. Histological, biochemical, and clinical studies have demonstrated that the nature and severity of AD pathologies in the retina and brain correspond. Proteomics analysis revealed a similar pattern of dysregulated proteins and biological pathways in the retina and brain of AD patients, with enhanced inflammatory and neurodegenerative processes, impaired oxidative-phosphorylation, and mitochondrial dysfunction. Notably, investigational imaging technologies can now detect AD-specific amyloid deposits, as well as vasculopathy and neurodegeneration in the retina of living AD patients, suggesting alterations at different disease stages and links to brain pathology. Current and exploratory ophthalmic imaging modalities, such as optical coherence tomography (OCT), OCT-angiography, confocal scanning laser ophthalmoscopy, and hyperspectral imaging, may offer promise in the clinical assessment of AD. However, further research is needed to deepen our understanding of AD's impact on the retina and its progression. To advance this field, future studies require replication in larger and diverse cohorts with confirmed AD biomarkers and standardized retinal imaging techniques. This will validate potential retinal biomarkers for AD, aiding in early screening and monitoring.

* Corresponding author. Cedars-Sinai Medical Center, 127 S. San Vicente Blvd., Los Angeles, CA, 90048, USA.
E-mail address: maya.koronyo@csmc.edu (M. Koronyo-Hamaoui).

https://doi.org/10.1016/j.preteyeres.2024.101273
Received 11 February 2023; Received in revised form 23 April 2024; Accepted 10 May 2024
Available online 15 May 2024

Abbreviations

3R tau	3-repeats tau
4R tau	4-repeats tau
α -SMA	α-smooth muscle actin
ABC	Amyloid/Braak/CERAD score
Aβ	amyloid β-protein
abd	Aβ deposits
ACE	angiotensin-converting enzyme
AD	Alzheimer's disease
AF	autofluorescence
aMCI	amnestic MCI
AMD	age-related macular degeneration
ANX776	Annexin A5
ANOVA	analysis of variance
APOE	apolipoprotein E
APP	amyloid precursor protein
AQP4	aquaporin 4
ARIA	amyloid-related imaging abnormalities
AUC	area under the curve
BBB	blood-brain barrier
BM/bm	bone marrow/basement membrane
B	black
BRB	blood-retinal barrier
BV/bv	blood vessel
C	central/Caucasian
CAA	cerebral amyloid angiopathy
Caps	capillaries
CCasp3	cleaved-caspase-3
CD	cluster of differentiation
CDR	clinical dementia rating
CERAD	consortium to establish a registry for Alzheimer's disease
CFZ	capillary-free zone
CLEC7A	C-type lectin domain family 7 member A
CLN	clusterin
CNS	central nervous system
ColIV	collagen IV
COVID-19	coronavirus disease 2019
COU	context of use
CSF	cerebrospinal fluid
c/SLO	confocal/scanning laser ophthalmoscope
DAB	3,3′ Diaminobenzidine
Degen	*degenerating*
DEPs	differentially expressed proteins
dH2O	distilled water
DIC	differential interference contrast
DL	deep-learning
DMP	distal mid-periphery
DVA	dynamic vessel analyzer
E	equal
EC	entorhinal cortex
EEG	electroencephalogram
ELISA	enzyme-linked immunosorbent assay
ERG	electroretinogram
F	far-peripheral/female
FA	fluorescein angiography
FAD	familial AD
FAZ	foveal avascular zone
FC	fold change
FDG-PET	fluorodeoxyglucose-positron emission tomography
fib	fibrils
FITC	fluorescein isothiocyanate
FLIO	fluorescence lifetime imaging ophthalmoscopy
FOV	field of view
FWHM	full width at half maximum
GA	glatiramer acetate
GCL	ganglion cell layer
GFAP	glial fibrillary acidic protein
GFP	green fluorescent protein
GS	glutamine synthetase
HA11	h-2 class I histocompatibility antigen
H	Hipnotic
Hipp	hippocampus
HR	high resolution
HSI	hyperspectral imaging
I	inferior
IBA1	ionized calcium-binding adapter molecule 1
ICAM1	intercellular adhesion molecule 1
ICG	Indocyanine Green
IHC	immunohistochemistry
IL-1β	interleukin-1β
ILM	inner limiting membrane
IN	inferior-nasal
INL	inner nuclear layer
IPAD	intramural peri-arterial drainage
IPL	inner plexiform layer
IR	inner retina/immunoreactivity
ISF	interstitial fluid
IT	inferior-temporal
iAβo	intracellular Aβ oligomers
i.v.	intravenous
λ	wavelength
L vessel	longitudinal vessel
LAMP1/2	lysosomal-associated membrane protein 1 and 2
LBD	Lewy body dementia
LMICs	low- and middle-income countries
LRP1	low-density lipoprotein receptor-related protein 1
M	mid-peripheral/male/month
mAb	monoclonal antibody
MC	Müller cell
MCI	mild cognitive impairment
mg	milligram
MGnD/DAM	neurodegenerative or disease-associated microglial state
mid	mid-peripheral retina
miR	micro-RNA
mm	millimeter
MMSE	Mini-Mental State Examination
Mo	monocyte
MOCA	Montreal cognitive assessment
mRGC	melanopsin-containing RGC
MRI	magnetic resonance imaging
MS	mass spectrometry
N	nasal
NC	normal cognition
NF-κB	nuclear factor-κB
RNFL	retinal nerve fiber layer
NIA-AA	national institute of ageing and Alzheimer's Association
NFTs	neurofibrillary tangles
NIR	near infrared
nm	nanometer
NORM	normalized
NS	superior-nasal
OCT	optical coherence tomography
OCTA	OCT angiography
OD	optic disc/oculus dexter
ODD	optic disc diameter
OLM	outer limiting membrane
ONL	outer nuclear layer

OPL	outer plexiform layer
OR	outer retina
OS	outer segment/oculus sinister
PP/P. pole	posterior pole
PBS	phosphate-buffered saline
PCA	posterior cortical atrophy
PD	Parkinson's disease
PDGFRβ	platelet-derived growth factor receptor-beta
PET	positron emission tomography
PERG	pattern ERG
pfib	protofibrils
pg	picogram
PHF	paired helical filament
PICALM	phosphatidylinositol binding clathrin assembly protein
pl	plaque
PMP	proximal mid-periphery
PR	photoreceptor
PRL	PR layer
PSEN1	presenilin-1
pTau	hyperphosphorylated Tau
PReT	primary retinal tauopathy
PV	primary visual cortex
r	Pearson's correlation coefficient
RAGE	receptor for advanced glycation end products
RAI	retinal amyloid index
RGC	retinal ganglionic cell
RH	red high
RNA	ribonucleic acid
RGCL	retinal GCL
RNFL	retinal NFL
RPE	retinal pigment epithelium
S	superior
s.c.	subcutaneous
scFv	single-chain Fv fragment
scRNAseq	single-cell RNA sequencing
SD-OCT	spectral domain-OCT
ST	superior-temporal
SSB	Sudan Black B
T/Temp	temporal
tAD	typical AD
TEM	transmission electron microscopy
tg	transgenic
TJ	tight junction
TMEM119	transmembrane protein 119
TREM2	triggering receptor expressed on myeloid cells 2
TUBB	β-III Tubulin
TUNEL	terminal deoxynucleotidyl transferase dUTP nick end labeling
UWF	ultra-widefield
μg	microgram
μm	micrometer
v	vascular
v vessel	vertical vessel
VA	visual association cortex
VEP	visual evoked potential
ViS4M	Visual-Stimuli 4-arm Maze
VTI	vessel tortuosity index
w/o	with or without
WT	wild type
ZO-1	zonula occludens-1

1. Introduction

Charlotte Bronte's words in *Jane Eyre* that "the soul, fortunately, has an interpreter – often an unconscious but still a faithful interpreter – in the eye" still ring true in the modern battle against Alzheimer's disease (AD), given the growing body of evidence highlighting ocular manifestations of the disease. AD is a devastating neurodegenerative disorder characterized by an irreversible decline in cognitive and functional abilities, with few disease-modifying treatment options currently available (Boxer and Sperling, 2023; Dhillon, 2021; Haddad et al., 2022; Lista et al., 2022; McDade et al., 2022; Scheltens et al., 2016; Sims et al., 2023; van Dyck et al., 2023). However, what if there was a way to gain insight into the brains of AD patients before the onset of this debilitating decline? What if the eye, more specifically the retina, could provide a "faithful interpretation" of the complex structural and molecular processes occurring in the brains of these patients? Advances in ocular imaging technologies have made this possibility a reality that may offer a unique window into the pathology of AD and serve as a much-needed tool in the battle against this increasingly prevalent condition.

According to the National Institute on Aging (NIA), an estimated 6.7 million elderly Americans have been afflicted by AD – the most frequent form of senile dementia and one of the leading causes of death in the United States (Alzheimer's, 2023). Worldwide, more than 55 million people live with AD and related dementias, with the cost of care projected to increase to nearly $1 trillion by 2050 (Alzheimer's, 2023; WHO, 2023; Wiese et al., 2023). As the elderly population continues to grow, the number of individuals affected by AD is expected to reach an alarming 139 million by 2050, posing a substantial burden of emotional, physical, and financial strain (Ferri et al., 2005; Sloane et al., 2002). In addition, recent data from the Household Pulse Survey show that nearly half of adults (48%) in the United States reported having had COVID-19, with nearly one-third of those (29%) still experiencing symptoms of Long COVID. Neurologic functional and structural studies in patients with COVID-19 have shown greater cognitive decline and reduction in gray matter thickness compared to age-matched controls who never had COVID-19 (Douaud et al., 2022). While clinical studies correlating COVID-19 and AD-related cognitive decline are limited (Shajahan et al., 2023), there is speculation that neuroinflammatory changes induced by COVID-19 infection may contribute to a higher incidence of neurodegenerative complications and disorders such as AD (Chen et al., 2022a; Wang et al., 2022a).

AD is typified by the cerebral accumulation of amyloid β-protein (Aβ) plaques, which eventually develop into neuritic plaques, along with hyperphosphorylated tau (pTau)-containing neurofibrillary tangles (NFTs) (De-Paula et al., 2012; Grundke-Iqbal et al., 1986; Hampel et al., 2021b; Kosik et al., 1986; Masters et al., 1985; Yarns et al., 2022). In addition, low-grade chronic neuroinflammation, including brain-resident glial activation and peripheral immune cell infiltration, along with small vessel and blood-brain barrier (BBB) dysfunctions, characterize the early pathophysiological landscape of AD (Montagne et al., 2017; Ni Chasaide and Lynch, 2020; Pascoal et al., 2021; Welikovitch et al., 2020; Zhong et al., 2018). These pathological changes lead to progressive synaptic dysfunction and degeneration of neurons, culminating in cognitive decline and, in the later stages of the disease, severe dementia, disability, and ultimately death. AD follows a clinical-biological continuum, with long-lasting asymptomatic stages driven by underlying pathological processes, particularly Aβ aggregation, which precedes the clinical symptoms by over 20 years (Bateman et al., 2012; Buchhave et al., 2012; Dubois et al., 2016; Fagan et al., 2014; Hampel et al., 2021a; Holtzman et al., 2011; Sperling et al., 2011; Sperling et al., 2013). However, early detection of Alzheimer's pathology can still be challenging in the clinical setting (Hu et al., 2023a; Porsteinsson et al., 2021). Recent findings from clinical trials involving anti-Aβ monoclonal antibody therapies have yielded promising outcomes. These treatments were effective in clearing brain Aβ plaques and had benefits in slowing the rate of cognitive decline, especially among

patients in the early clinical stages of AD (Boxer and Sperling, 2023; Cummings et al., 2024; Landhuis, 2024). However, intervention later in the disease progression has proven less effective (Haass and Selkoe, 2022; Landhuis, 2024; Osborne et al., 2023). At this later stage of the disease, Aβ clearance may have done little to ameliorate cognitive decline as irreversible vascular damage, gliosis, and neurotoxicity have already impacted the brain (Frozza et al., 2018; Gallardo and Holtzman, 2017; Holmes et al., 2008; Tolar et al., 2020). Nonetheless, the large time frame between the preclinical disease stage and the prevalence of clinical symptoms provides an opportunity for early detection and effective intervention before extensive damage to the brain's structural and functional networks occurs (Hampel et al., 2019).

Current AD diagnostic biomarkers, including brain imaging of amyloid and tau burden using positron emission tomography (PET) and assessment of cerebrospinal fluid (CSF) bioproducts, have been validated for different context of use (COU) in AD clinical trials and healthcare management (Bao et al., 2017; Hameed et al., 2020). However, widespread adoption of these biomarkers in AD clinical practice is hindered by several limitations, such as invasiveness, health risks associated with exposure to radioactive isotopes, high costs, limited accessibility, and resource demands. Blood-based biomarkers are currently under validation for potential implementation in clinical practice to facilitate decision-making in clinical studies and large-scale AD screening and monitoring (Gonzalez-Ortiz et al., 2022; Hampel et al., 2018; Teunissen et al., 2022). However, the likely interference of systemic metabolism and clearance on brain-derived molecules may introduce variability in blood-based results. Moreover, biomarkers present in bodily fluids do not allow direct visualization of central nervous system (CNS) pathology at the site of injury, including their spatial distribution. Hence, despite major advances in AD biomarkers, there remains a necessity for more widely applicable techniques to improve diagnosis and monitoring of the disease.

Unlike the brain, which is shielded by the opaque skull, the retina is an optically accessible space that can be directly visualized non-invasively at the vascular, cellular, and molecular levels with high resolution. This offers an affordable means to monitor CNS abnormalities in the clinical setting. The retina shares a common embryonic origin with the brain and is its direct anatomical extension (Byerly and Blackshaw, 2009; Purves and Fitzpatrick, 2001; Sadda et al., 2022; Trost et al., 2016). Given that both the brain and retina are encompassed by comparable neuronal and glial cells and blood barriers (Jindal, 2015; Jorge et al., 2019), their shared vulnerability to neuropathological processes is not surprising. Indeed, emerging evidence from human histopathological, biochemical, and in vivo imaging studies has revealed that AD-specific pathology not only affects the brain but also manifests in the retina of AD patients (Alexandrov et al., 2011; Ashraf et al., 2023; Cao et al., 2021; den Haan et al., 2022; den Haan et al., 2018; Du et al., 2022; Dumitrascu et al., 2020; Dumitrascu et al., 2021; Grimaldi et al., 2019; Gupta et al., 2021; Hadoux et al., 2019; Hart de Ruyter et al., 2023; Hart et al., 2016; Koronyo et al., 2017; Koronyo et al., 2023; Koronyo-Hamaoui et al., 2011; La Morgia et al., 2016; Lee et al., 2020b; Lemmens et al., 2020; Mirzaei et al., 2020; More et al., 2019; Ngolab et al., 2021; Qiu et al., 2020; Schon et al., 2012; Schultz et al., 2020; Shi et al., 2023; Shi et al., 2021; Shi et al., 2020b; Snyder et al., 2021; Tadokoro et al., 2021b; Tsai et al., 2014; Walkiewicz et al., 2024; Xu et al., 2022). The pathological hallmarks identified in the retina of AD patients were accompanied by vascular abnormalities, gliosis, and neuronal degeneration (Asanad et al., 2019; Ascaso et al., 2014; Berisha et al., 2007; Blanks et al., 1989, 1996a, 1996b; Frost et al., 2013; Gao et al., 2015b; Grimaldi et al., 2019; Hinton et al., 1986; Kesler et al., 2011; Kim et al., 2022; Kirbas et al., 2013; Koronyo et al., 2023; La Morgia et al., 2016; Marziani et al., 2013; Sadun and Bassi, 1990; Shi et al., 2020b, 2023; Xu et al., 2022). Retinal Aβ deposition and other AD-related pathology seemed to follow a similar trajectory to that of the brain at different disease stages (Doustar et al., 2020; Gupta et al., 2016; Habiba et al., 2021; Koronyo et al., 2017, 2023; Schultz et al., 2020; Shi et al., 2020b, 2023). Fig. 1 presents a timeline highlighting key retinal pathological and imaging findings in AD patients.

Early retinal changes have been reported in both AD patients and animal models, suggesting that the pathological hallmarks, along with associated inflammation, vasculopathy, and neurodegeneration, occur in the retina during the early stages of the disease (Berisha et al., 2007; Chiasseu et al., 2017; Dumitrascu et al., 2020, 2021; Frost et al., 2013; Gaynor et al., 2019; Grimaldi et al., 2018; Habiba et al., 2021; Koronyo et al., 2023; Koronyo-Hamaoui et al., 2011; Lu et al., 2010; More et al., 2019; More and Vince, 2015; Ngolab et al., 2021; Shi et al., 2020a, 2020b, 2023; Zhang et al., 2019, 2021b, 2021c). Furthermore, individuals with mild cognitive impairment (MCI) and AD dementia frequently present with visual impairments, aberrant electroretinogram (ERG) patterns, and disruptions in circadian rhythms (Hart et al., 2016; La Morgia et al., 2016; Perrin et al., 2009; Petersen et al., 1999; Risacher et al., 2020; Wang and Holtzman, 2020). Such deficits, often among the earliest symptoms noted, can be partially attributed to retinal pathology observed in these patients. Overall, these findings advocate for further exploration of visual-related abnormalities and encourage the use of the retina as a potential site for early diagnosis and screening of AD in at-risk populations (Alber et al., 2020, 2023; London et al., 2013).

Given the availability of various ophthalmic imaging modalities to visualize vascular and structural abnormalities in the clinical setting, as well as the feasibility of detecting retinal amyloid deposits, there is an urgent need to expand research on distinct neuropathological features of AD in the retina. In this review, we summarize up-to-date histopathological and biochemical evidence of AD biomarkers in the retina, highlight the parallels between brain and retinal abnormalities seen in AD, and discuss current strategies for using retinal imaging to detect AD-related pathology.

2. Histopathological evidence of AD hallmarks in the retina

2.1. Retinal Aβ pathology in AD

Although plaques were initially described in the brain of an AD patient in the early 1900s (Alzheimer, 1906; Alzheimer et al., 1995), it was not until a century later, in 2010, that Aβ plaques were identified in the retina of AD patients (Koronyo-Hamaoui et al., 2011). Histological analyses of retinal flatmounts revealed the presence and increased deposition of Aβ in the retina of autopsy-confirmed AD patients, including cases at the early functional impairment stages (MCI), compared to minimal to no Aβ deposits in non-AD individuals (Koronyo-Hamaoui et al., 2011). Subsequent studies using fluorescence and non-fluorescence histological and biochemical techniques in retinal flatmounts and cross-sections confirmed the existence and/or elevated levels of retinal Aβ in these patients as compared to individuals with normal cognition (NC) (Alexandrov et al., 2011; Cao et al., 2021; den Haan et al., 2018; Du et al., 2022; Grimaldi et al., 2019; Koronyo et al., 2017; Koronyo et al., 2023; Koronyo-Hamaoui et al., 2011; La Morgia et al., 2016; Lee et al., 2020b; Qiu et al., 2020; Schultz et al., 2020; Shi et al., 2023; Shi et al., 2020b; Tsai et al., 2014; Xu et al., 2022). Further characterization of retinal Aβ deposits was performed in various human cohorts, describing their size, morphology, ultrastructure, Aβ-alloform content (*e.g.*, $Aβ_{40}$, $Aβ_{42}$), localization (*e.g.*, extracellular, intracellular, vascular, perivascular), as well as their spatiotemporal distribution across anatomical regions and retinal layers (Figs. 2–4).

The histological studies that used Aβ-labeling compounds or Aβ immunostaining, demonstrated the presence of diffused and classical Aβ plaques, fibrillar Aβ aggregates, and neuritic-like plaques in the retina of AD patients (Fig. 2E, 2F–H and Fig. 3F) (Koronyo et al., 2017; Koronyo-Hamaoui et al., 2011; Qiu et al., 2020). Multiple monoclonal antibodies specifically recognizing diverse Aβ epitopes (*e.g.*, 6E10, 4G8, 6F3D, 12F4, 11A50-B10, JRF/cAβ40/28, JRF/cAβ 42/26, JRF/Aβtot/17, scFvA13) and Aβ-labeling compounds, such as curcumin, thioflavin-S, Gallyas silver, Congo red, and amyloid-binding fluorescent

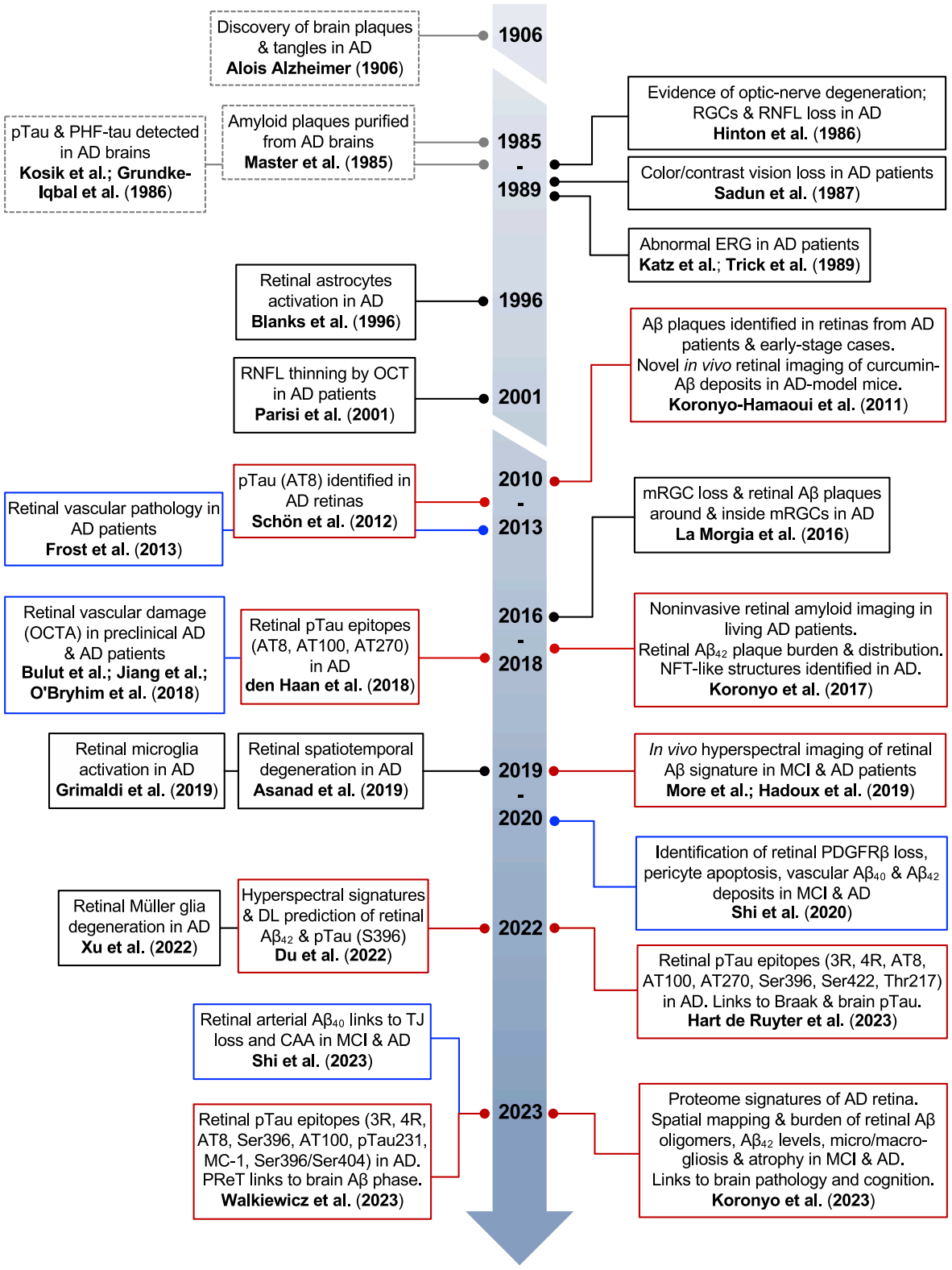

Fig. 1. Landmark findings of retinal pathology in AD patients. Timeline highlighting the key discoveries of retinal pathological, biochemical, and imaging biomarkers in Alzheimer's disease (AD) patients since the first report of neuropathological plaques and tangles in the brain of an AD patient in 1906. Gray dotted rectangles highlight the key brain hallmarks, blue rectangles mark retinal vascular-related abnormalities, red rectangles highlight the identification of AD-hallmark pathologies in the retina of patients, and black rectangles define other AD-relevant pathologic biomarkers in the AD retina.

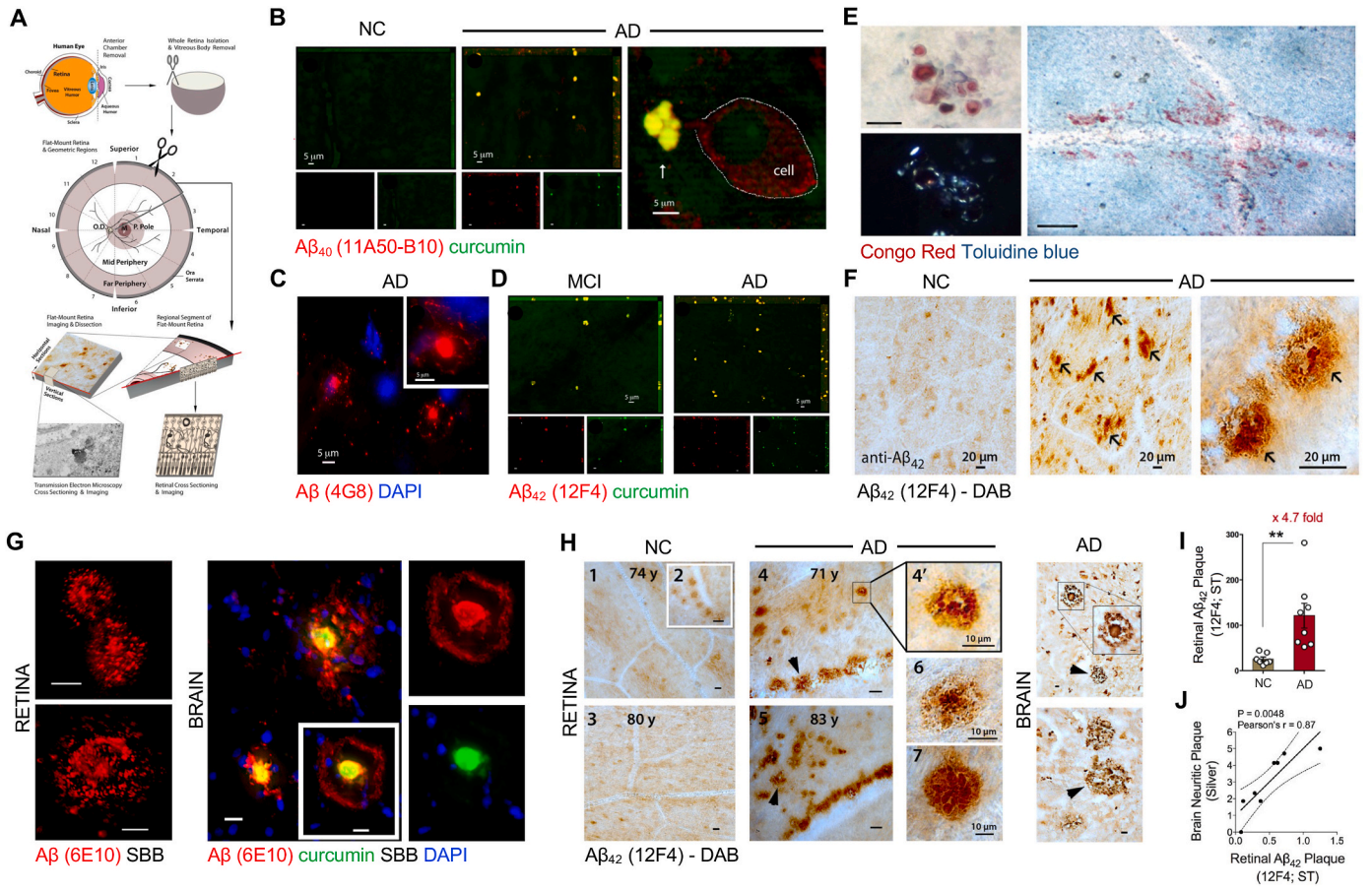

Fig. 2. Aβ plaques identified in retinal flatmounts of AD patients. (**A**) Schematic illustration of eye dissection, retinal isolation, and preparation of retinal flatmount and cross-section for histological and biochemical analyses. P. Pole (posterior pole), O.D. (optic disc), M (macula), and F (fovea). (**B**) Representative images of a retinal flatmount stained with curcumin and anti-human $A\beta_{40}$ mAb (11A5-B10) in individuals with normal cognition (NC) and AD. No Aβ plaques were observed in NC retinas (left), while AD retinas exhibited evident Aβ plaques (middle). Higher magnification images (right) show extracellular $A\beta_{40}$ plaques (white arrow) and intracellular $A\beta_{40}$ (dotted line). (**C**) Representative images of Aβ plaques (4G8 mAb) in the inner retina, depicting classical plaque morphology with a central dense core and radiating fibrillar arms. (**D**) Representative maximum intensity projection images of retinal flatmounts stained with curcumin and anti-$A\beta_{42}$ (12F4 mAb) in mild cognitively impaired (MCI) and AD patients. Abundant Aβ plaques were widespread in AD retinas. (**E**) Representative retinal flatmount images of AD patients depicting amyloid deposits stained with Congo red and toluidine blue (top-left), as well as amyloid fibrils' birefringence (apple-green, bottom left) under polarized light. Scale bar: 25 μm. Congo red–positive amyloid plaques in AD patient retinas (right). Scale bar: 100 μm. Two intersecting blood vessels surrounded (along blood vessels and perivascular) by extensive Congo red–positive staining. **(F)** Representative images of NC and AD retinal flatmount depicting Aβ plaques stained with anti-$A\beta_{42}$ mAb (12F4) and visualized with peroxidase-based labeling (DAB), highlighting the presence of Aβ plaques along a retinal blood vessel. (**G**) Representative images of retinal flatmounts and brain cortical tissues from AD patients stained with anti-Aβ antibody (6E10) and Longvida curcumin, depicting the colocalization of curcumin and 6E10 in cortical Aβ plaques. Scale bars: 10 μm. (**H**) Representative images of retinal flatmounts of AD patients and NC subjects and brain cortical tissues from AD patients stained with 12F4 and DAB labeling, displaying diverse morphology of Aβ aggregates. Scale bars: 20 μm, unless otherwise indicated. (**I**) IR area of $12F4^{+}$-$A\beta_{42}$-containing plaques in the superior-temporal (ST) quadrant of retinal flatmounts in a subset of definite AD patients (N = 8) and matched NC subjects (N = 7). (**J**) Pearson's (*r*) correlation analysis between retinal $12F4^{+}$-plaque burden and cerebral neuritic plaques (Gallyas silver stain) (N = 8). Statistics: Data from individual subjects (circles) as well as group means ± SEMs are shown. Fold change is shown in red. $^{**}P < 0.01$ by unpaired two-tailed Student's *t*-test. Panels A, E, G-J were modified from (Koronyo et al., 2017), Panels B–D were modified from (Koronyo-Hamaoui et al., 2011), and Panel F was modified from (La Morgia et al., 2016) with permission.

probe ARCAM-1, were used to identify Aβ deposits in the AD retina (Cao et al., 2021; den Haan et al., 2018; Du et al., 2022; Dumitrascu et al., 2024; Grimaldi et al., 2019; Koronyo et al., 2017; Koronyo-Hamaoui et al., 2011; La Morgia et al., 2016; Lee et al., 2020b; Qiu et al., 2020; Shi et al., 2023; Shi et al., 2020b; Tsai et al., 2014; Xu et al., 2022). Of note, amyloid deposits were detected using Congo red staining in retinal flatmounts from AD patients, and the birefringence (apple-green) of Congo red–stained retinas under polarized light validated the formation of amyloid fibrils, often surrounding and along blood vessels (Fig. 2E) (Koronyo et al., 2017). Similarly, Qiu et al., reported an increased number of polarimetric positive deposits, containing amyloid fibrils confirmed by thioflavin-S fluorescence under polarization sensitive microscopy, in the postmortem retina of AD patients compared to controls (Qiu et al., 2020). The detected retinal Aβ deposits were, on average, smaller in size (~5–20 μm in diameter) than those observed in the AD brain (Fig. 2H) (Cao et al., 2021; den Haan et al., 2018; Koronyo et al., 2017; Koronyo-Hamaoui et al., 2011; La Morgia et al., 2016; Qiu et al., 2020).

The ultrastructure of Aβ aggregates in the human retina was further investigated using transmission electron microscopy (TEM). In these experiments, vertical and en face retinal sections from AD patients were analyzed following $12F4^{+}$-$A\beta_{42}$ and peroxidase-based DAB pre-labeling or immunogold anti-$A\beta_{42}$ labeling, revealing retinal Aβ plaques containing central dense amyloid cores with radiating fibrillar arms, $A\beta_{42}$ protofibrils and fibrils of 10–15 nm wide parallel β-sheets, and other types of $A\beta_{42}$ assemblies (Fig. 3G and H) (Koronyo et al., 2017, 2023). Retinal Aβ fibrils with parallel β-sheets were found to be identical to those in the AD brains (Iadanza et al., 2016), and such fibrils were also

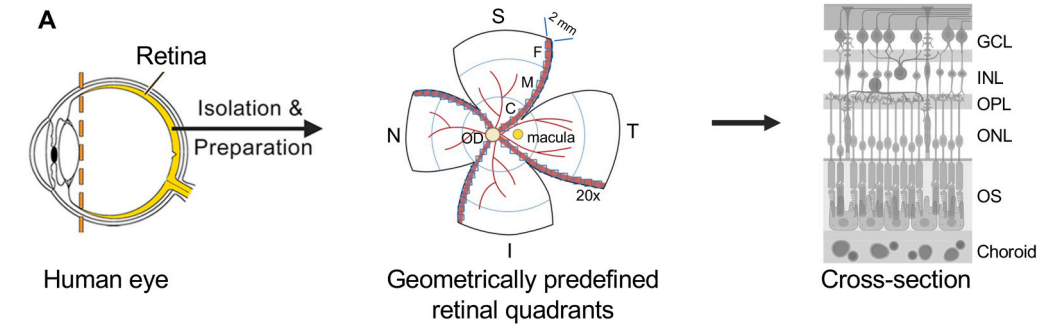

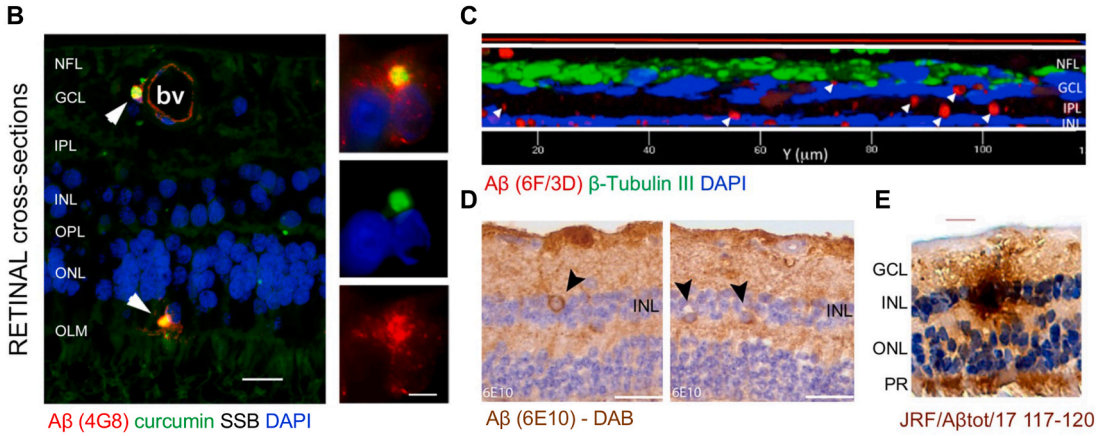

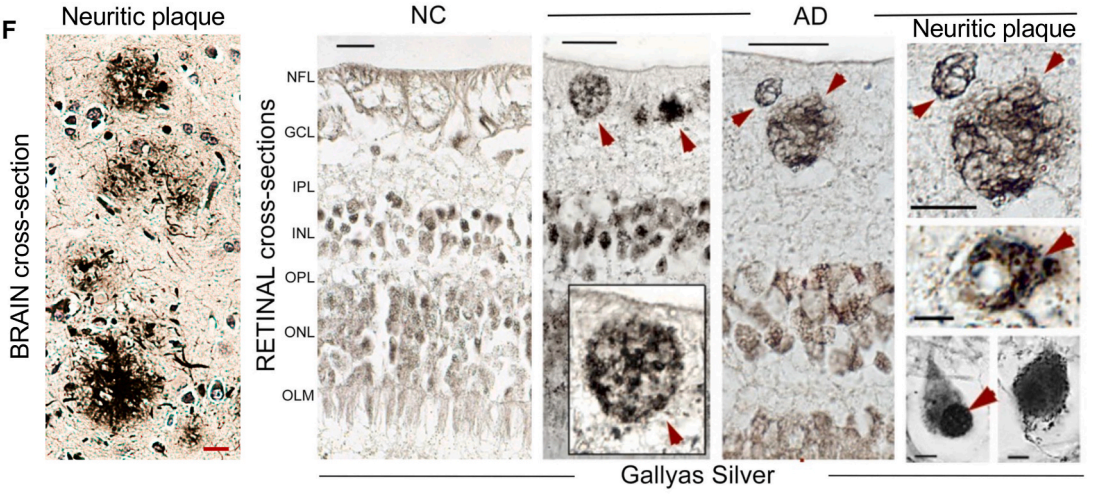

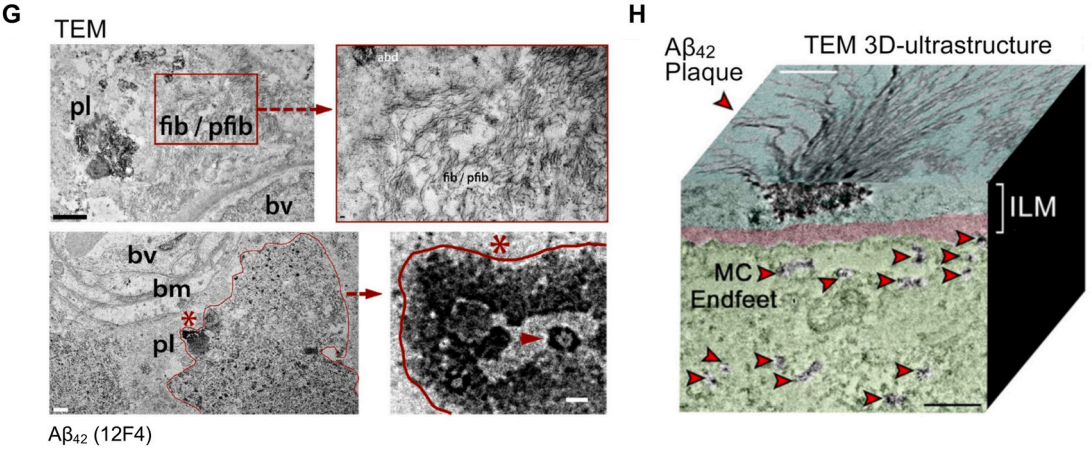

(caption on next page)

Fig. 3. Aβ deposition and distribution in retinal cross-sections from MCI and AD patients. (**A**) Schematic depiction of retinal cross-section preparation in predefined geometrical regions within the superior-temporal (ST), inferior-temporal (IT), inferior-nasal (IN), and superior-nasal (SN) quadrants. Retinal strips (red line, ~2 mm width) from each quadrant, extending from the optic disc (OD) to the ora serrata, were dissected for cross-section preparation and further defined into subregions for histological analysis: proximal to OD – central (C) and distal from OD – mid-periphery (M) and far-periphery (F). Ten images (3C, 4M, 3F at 20× magnification), on average, are captured from each retinal section for quantitative analysis. (**B-E**) Representative fluorescent and non-fluorescent microscopic images demonstrating Aβ plaques in retinal cross-sections from confirmed AD patients. (**B**) Double-positive 4G8 mAbs (red) and curcumin (green) Aβ deposits were detected in the ONL and in the GCL, near and inside blood vessel (bv) walls. Left scale bar: 20 μm. Enlarged image, right scale bar: 5 μm. SSB: Sudan Black B. (**C**) A magnified, orthogonal view of a set of Z-stack images, from an AD retinal flatmount, demonstrated 6F/3D^{+} Aβ deposits (red; indicated by white arrowheads) in the RNFL, GCL, IPL, and INL. The green fluorescence is beta-3 tubulin immunoreactivity, demonstrating neuronal processes associated with retinal ganglion cell axons in the RNFL. (**D**) Representative retinal cross-section images showing 6E10^{+} Aβ plaques (non-fluorescent DAB) around amacrine cells (left) and horizontal cells (right) in the INL. Scale bars: 50 μm. (**E**) A retinal cross-section image from a representative MCI patient stained for total Aβ using JRF/Aβtot/17 (117–120) mAb and visualized with peroxidase-based DAB. In this MCI patient, a retinal Aβ plaque is observed in the INL. Scale bar: 20 μm. (**F**) Gallyas silver staining of a brain cross-section from an AD patient showing neuritic plaques in the frontal cortex (left image, scale bar: 20 μm). Retinas from NC individuals generally exhibited intact tissue (left image in retinal cross-section). Retinas from AD patients exhibited a classic Aβ plaque and compact deposits (red arrowheads): higher-magnification image in the inset (left). Retinal neuritic plaques (red arrowheads) were identified in the GCL of AD patients (middle). Neuritic components of senile plaques in GCL at higher magnification (right, top). Scale bar: 10 μm. Soma-positive silver stain aggregates and nuclear-dominant silver stain (red arrowheads) are observed in the GCL and INL (right, middle and bottom). Scale bar: 5 μm. (**G-H**) TEM analyses of retinal sections from AD patients. Retinas were pre-stained for $A\beta_{42}$ with 12F4 mAbs and visualized with DAB. (**G**) Top left: TEM image showing ultrastructure of an $A\beta_{42}$ plaque (pl), fibrils (fib), and protofibrils (pfib) near a blood vessel (bv) in vertical sections. Scale bar: 1 μm. Higher-magnification image (top right), indicating presence of 10- to 150-nm-wide $A\beta_{42}$ fibrils as well as protofibrils and Aβ deposits (abd). Scale bar: 50 nm. Bottom left: Aβ plaque-like structure, marked by an asterisk and bordering red line, near basement membrane (bm) of a blood vessel (scale bar: 0.5 μm). Higher-magnification image (bottom right) showing Aβ plaque-like area, with structures resembling paranuclei containing annular oligomers (arrowhead; scale bar: 40 nm). (**H**) 3D-reconstruction of vertical and en face TEM images show a retinal $A\beta_{42}$ plaque ultrastructure with fibril arms emanating from its dense core and Aβ-containing deposits in Müller cell (MC) end-feet close to the inner limiting membrane (ILM; red arrowheads). Scale bar: 1 μm. Panels A, E, and H were modified from (Koronyo et al., 2023), Panels B, F, and G were modified from (Koronyo et al., 2017), Panel C was modified from (Lee et al., 2020b), and Panel D was modified from (den Haan et al., 2018) with permission.

located adjacent to the basement membrane of blood vessels. Notably, analysis of retinal flatmounts allowed for the detection of classical Aβ plaques or plaque-like structures (Fig. 2) (Cao et al., 2021; Dumitrascu et al., 2024; Koronyo et al., 2017; Koronyo-Hamaoui et al., 2011; La Morgia et al., 2016; Lee et al., 2020b; Qiu et al., 2020; Tsai et al., 2014; Xu et al., 2022), whereas analysis of cross-sections often showed distinct patterns of Aβ immunolabeling (Fig. 3) (Cao et al., 2021; den Haan et al., 2018; Du et al., 2022; Grimaldi et al., 2019; Koronyo et al., 2017; Koronyo et al., 2023; Lee et al., 2020b; Shi et al., 2023; Shi et al., 2020b; Xu et al., 2022). Moreover, growing evidence suggests an uneven distribution of Aβ pathology with regional vulnerability in the retina, across cell layers and geometrical regions (see Fig. 3A). For instance, our team found that Aβ deposits appear earlier (in MCI) and more densely in the inner retina, particularly within the superior-temporal and inferior-temporal peripheral subregions (Fig. 4D–F) (Koronyo et al., 2017, 2023).

Of all Aβ alloforms, $A\beta_{42}$ is considered the most neurotoxic and pathognomonic to AD. Evidence indicates that it rapidly aggregates into oligomers and fibrils, while $A\beta_{42}$ oligomers were shown to directly disrupt synaptic plasticity and integrity, long-term potentiation, neurite outgrowth, axonal transport, and cognition (Barucker et al., 2015; Cohen et al., 2013; Lee et al., 2022; Li et al., 2020b; Pauwels et al., 2012; Shankar et al., 2008; Varga et al., 2015). Additionally, $A\beta_{42}$ interacts with tau protein and related downstream neurotoxic pathways (Hampel et al., 2021b). $A\beta_{42}$-containing plaques, exhibiting various morphologies including diffuse, immature, and mature-classical plaques, have been found to manifest and increase in burden by 4.7-fold in flatmount retinas of AD patients compared to age- and sex-matched healthy controls (Koronyo et al., 2017; La Morgia et al., 2016). The burden of these plaques in the retina tightly correlates with brain Aβ-plaque burden (Fig. 2I and J). Examination of 12F4^{+}-$A\beta_{42}$ immunoreactive area in superior- and inferior-temporal retinal cross-sections from MCI and AD patients compared to NC controls, indicated 5-9-fold increases in $A\beta_{42}$ load in these patients, respectively, with a highly significant correlation to cortical Aβ-plaque load (Fig. 4) (Koronyo et al., 2023). Substantial perivascular and vascular deposits of $A\beta_{40}$ and $A\beta_{42}$ were also evident in retinas from MCI and AD patients (Koronyo et al., 2017; La Morgia et al., 2016; Shi et al., 2020b, 2023). Furthermore, Aβ oligomers, which have been found to be synaptotoxic in the AD brain (Selkoe, 2008; Zempel et al., 2013), were identified mostly inside retinal ganglion cells (RGCs), with significant overall increases in postmortem retinas of MCI and AD patients compared to NC controls (Fig. 5) (Koronyo et al., 2023).

In support of these histological findings, the biochemical studies also indicate elevated Aβ levels in the retinas of AD patients (Alexandrov et al., 2011; Koronyo et al., 2023; Schultz et al., 2020; Shi et al., 2020b). For instance, retinal $A\beta_{1\text{-}42}$ and $A\beta_{1\text{-}40}$, detected by sensitive sandwich ELISA kits, showed significant increases in AD patients compared to matched NC controls (Koronyo et al., 2023; Shi et al., 2020b). Specifically, the average concentrations of $A\beta_{1\text{-}42}$ in AD patients were found to be 0.26 ng/mg in the retina and approximately 2.40 ng/mg in the brain, contrasting with 0.04 ng/mg and around 0.90 ng/mg in the retina and brain, respectively, of NC individuals (Koronyo et al., 2023; Roberts et al., 2017). Another study detected increased levels of high-molecular-weight retinal $A\beta_{42}$ and $A\beta_{40}$ peptides in AD patients (Schultz et al., 2020). Patients with elevated cerebral Aβ-plaque scores and carriers of the apolipoprotein E ε4 (APOEε4) allele had elevated levels of retinal $A\beta_{42}$ and $A\beta_{40}$. Notably, retinal $A\beta_{42}$ and $A\beta_{40}$ levels significantly correlated with their respective levels in the hippocampus and with the severity of cerebral NFTs burden (Schultz et al., 2020).

Furthermore, clinical investigations using hyperspectral imaging (HSI) modality, pioneered by More and colleagues (More et al., 2016; More and Vince, 2015), have successfully delineated the unique optical signature of Aβ deposits in both retinal and brain tissues. Subsequent studies involving living AD patients have demonstrated significant spectral deviations attributable to the Aβ optical signature in the retina of these patients compared to NC controls (Hadoux et al., 2019; Lemmens et al., 2020; More et al., 2019). Another recent study further detected the specific spectral signature of $A\beta_{42}$ deposits in retinal cross-sections from AD patients and demonstrated the feasibility of a novel HSI combined with a deep learning-based framework method to predict retinal $A\beta_{42}$ deposits in label-free retinal tissues (Du et al., 2022).

Despite the majority of peer-reviewed studies utilizing biochemical, histological, and in vivo retinal imaging techniques that validated Aβ deposition in the retina of AD patients (Alexandrov et al., 2011; Cao et al., 2021; Du et al., 2022; Dumitrascu et al., 2020, 2021; Grimaldi et al., 2019; Hadoux et al., 2019; Kile et al., 2020; Koronyo et al., 2017, 2023; Koronyo-Hamaoui et al., 2011; La Morgia et al., 2016; Lee et al., 2020b; Lemmens et al., 2020; More et al., 2019; Ngolab et al., 2021; Qiu et al., 2020; Schultz et al., 2020; Shi et al., 2020b, 2023; Tadokoro et al., 2021b; Tsai et al., 2014; Xu et al., 2022), a few studies were unable to replicate these findings. Four studies failed to detect retinal Aβ when analyzing conventional eye cross-sections of AD patients (Hinton et al.,

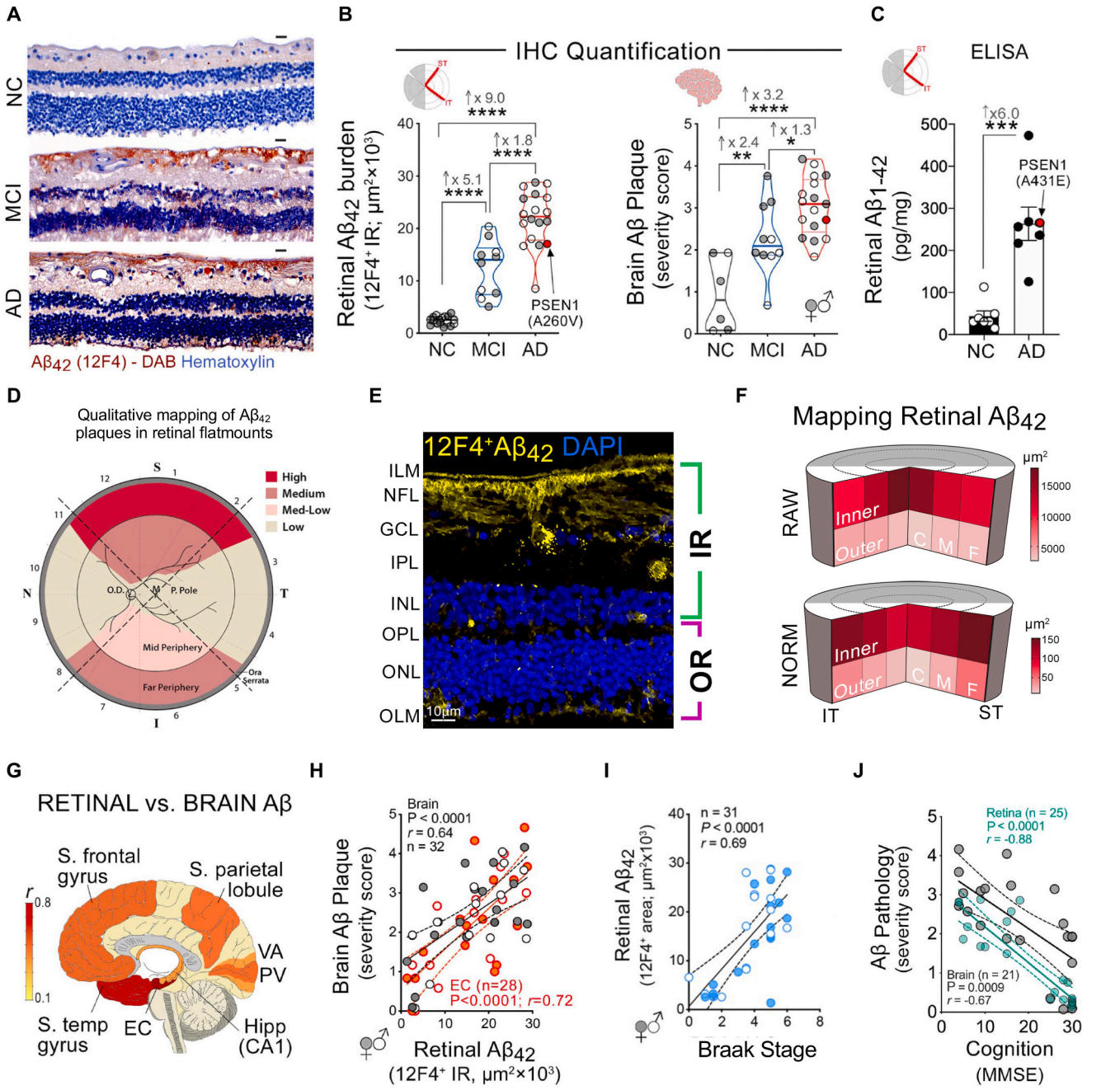

Fig. 4. Parallels between retinal and brain Aβ pathology in MCI and AD patients. (A) Representative retinal cross-section images from MCI and AD patients compared to NC controls immunolabeled with 12F4^{+}-Aβ_{42} using peroxidase-based DAB and hematoxylin counterstaining. Scale bar: 20 µm. (**B**, left) Violin plots display IR area of retinal 12F4^{+}-Aβ_{42} in age- and sex-matched patients with premortem clinical diagnoses of NC (N = 17), MCI (N = 10), or AD (N = 18). (**B**, right) Aβ-plaque severity scores in a subset of corresponding brains from NC (N = 6), MCI (N = 10), and AD (N = 17) subjects (by silver and Thioflavin-S or 4G8 mAbs). Red circles represent the autosomal-dominant AD patient with an A260V mutation in *PSEN1*. (**C**) Retinal A$\beta_{1–42}$ levels determined by ELISA are shown in a cohort of NC controls (N = 7) and AD patients (N = 7). The red circle represents an autosomal-dominant AD patient with an A431E mutation in *PSEN1*. (**D**) Qualitative geometric hot spot regions for Aβ deposits found in retinal flatmounts of AD patients (S, superior; T, temporal; I, inferior; N, nasal; cumulative data from multiple experiments). (**E**) A typical Aβ_{42} immunoreactivity pattern (yellow) is observed in the inner retina (IR) and the outer retina (OR) in cross-sections from an AD patient. (**F**) Pie charts display Aβ_{42} distribution across the IR and OR, as well as the C, M, and F subregions of the ST and IT retina: raw data and normalized (NORM) per retinal thickness (density); higher burden in darker red. (**G**) Mid-sagittal brain illustration shows color-grading magnitude of Pearson's (*r*) correlation values between retinal Aβ_{42} burden and brain pathology in the hippocampus (Hipp), superior (S.) frontal gyrus and temporal (temp) gyrus, S. parietal lobule, entorhinal cortex (EC), primary visual (PV), and visual association (VA) cortices. Pearson's (*r*) correlations between (**H**) retinal Aβ_{42} area and Aβ plaques in the brain (gray; average of 7 brain regions) or in EC (orange), (**I**) retinal Aβ_{42} area and Braak stage, and (**J**) retinal Aβ_{42} area (green) or brain Aβ burden (gray) and the Mini-Mental State Examination (MMSE)-cognitive scores. Statistics: Data from individual subjects (circles) as well as group means ± SEMs are shown. Median, lower, and upper quartiles are indicated on each violin plot. Fold changes are shown in gray. *$P < 0.05$, **$P < 0.01$, ***$P < 0.001$, ****$P < 0.0001$, by one-way ANOVA and Tukey's post hoc multiple comparison test, or by two-tailed unpaired Student's *t*-test. Panels A–C, E-J were modified from (Koronyo et al., 2023), and Panel D was modified from (Koronyo et al., 2017) with permission.

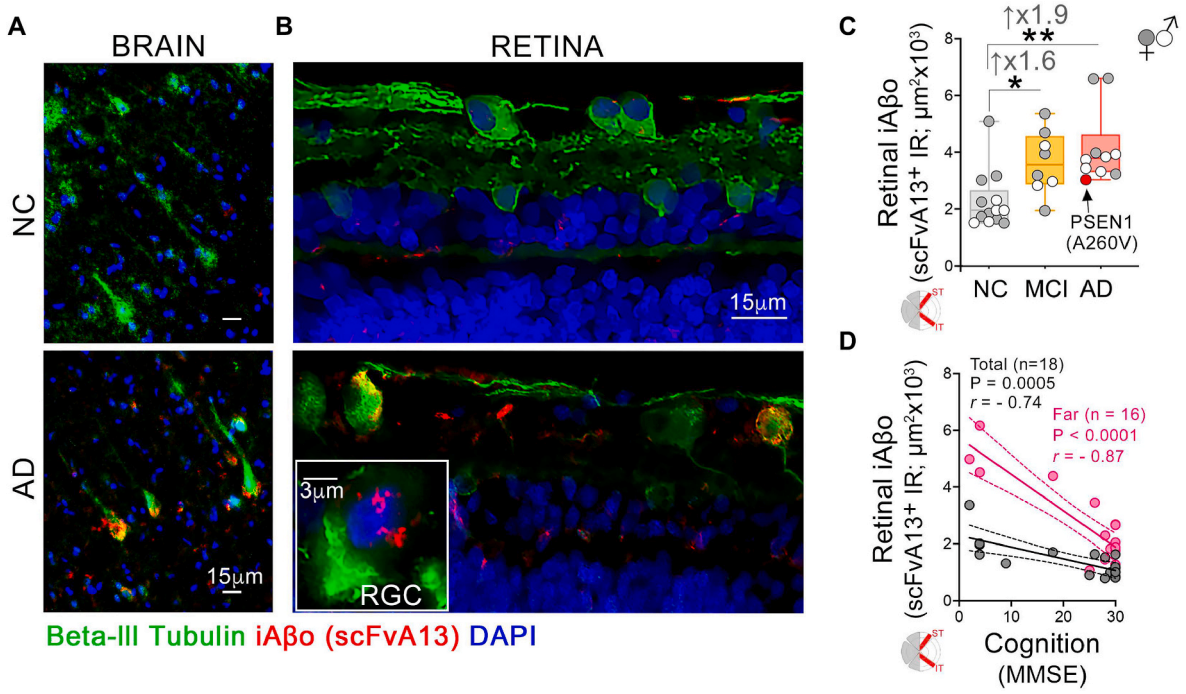

Fig. 5. Identification of intracellular Aβ oligomers in postmortem brain and retina of MCI and AD patients. Representative images of postmortem (**A**) brain and (**B**) retinal cross-sections show the existence of intracellular Aβ oligomers (iAβo) detected by the single-chain Fv fragment (scFv)A13 (red) conformation-sensitive and sequence-specific antibody. The scFvA13 selectively recognized AD-relevant Aβ oligomers inside cortical pyramidal and retinal neurons (Beta-III Tubulin, green) in AD patients, with a minimal signal in NC controls. Insert image: iAβo^{+}-RGC. (**C**) IR area of scFvA13^{+}iAβo in the ST/IT retina in MCI (N = 8) and AD patients (N = 10) versus NC controls (N = 13). The red circle depicts the autosomal-dominant AD patient with the *PSEN1*-A260V mutation. (**D**) Pearson's (*r*) correlations between retinal iAβo in the ST/IT regions (gray circles for total area, and pink circles for far-peripheral subregions) and MMSE cognitive scores. Statistics: Data points are presented with group means ± SEMs are shown. Fold changes are shown in gray. $^{*}P < 0.05$, $^{**}P < 0.01$, by one-way ANOVA with Tukey's post hoc multiple comparison test. All panels are adopted from (Koronyo et al., 2023) with permission.

1986; Ho et al., 2014; Schon et al., 2012; Williams et al., 2017), and a study by den Haan and colleagues identified the presence of Aβ deposits when analyzing retinal cross-sections from the superior peripheral region but without observing an apparent increase in AD patients compared to healthy controls (den Haan et al., 2018). In fact, this group described retinal Aβ deposits with comparable sizes as reported by Koronyo and colleagues (Koronyo et al., 2017), but reported a distinct morphology from that of brain plaques (den Haan et al., 2018). Overall, these groups that were unable to detect 6F/3D- or 4G8-positive Aβ deposits in retinas from AD patients (Ho et al., 2014; Schon et al., 2012; Williams et al., 2017) applied traditional ocular histological techniques in thin cross-sections, which are not optimal for detecting highly amyloidogenic protein aggregates in anisotropic retinal tissue.

Based on the reported methods, the failed studies may have encountered multiple methodological challenges, such as suboptimal tissue isolation, fixation, processing, and labeling procedures, as well as limited scanning of retinal areas within thin cross-sections, especially in temporal-to-nasal sections that are less frequently impacted by AD (Ho et al., 2014; Schon et al., 2012; Williams et al., 2017). Nevertheless, studies that applied more optimal procedures were all able to replicate the original findings. For instance, Xu et al. observed Aβ deposits in retinal flatmounts and cross-sections from AD patients using the same 6F/3D and 4G8 monoclonal antibodies (Xu et al., 2022), indicating that negative results in prior studies (Ho et al., 2014; Schon et al., 2012; Williams et al., 2017) were likely due to applying inadequate protocols and incomplete tissue screening. In addition, the same team (Hinton et al., 1986), who identified RGC degeneration but could not detect retinal amyloidosis in AD patients in 1986, later detected fibrillar Aβ deposits by Congo-red staining in retinal flatmounts from AD patients using more suitable histological methods, especially by examining larger retinal flatmount regions (Fig. 3A) (Koronyo et al., 2017). These findings underscore the critical importance of using proper experimental procedures for detecting amyloidogenic protein aggregates in the human retina, particularly in studying retinal Aβ pathology in AD. Taken together, to mitigate potential methodological inconsistencies, groups and workshops that harmonize these methods for studying AD core pathologies in the retina are warranted (Alber et al., 2023; Snyder et al., 2021).

Findings in animal models of AD have mirrored the retinal outcomes described in human studies (Alexandrov et al., 2011; Chang et al., 2020, 2021; Chen et al., 2013; Chibhabha et al., 2020; Cutler et al., 2015; Doustar et al., 2020; Du et al., 2015; Dutescu et al., 2009; Edwards et al., 2014; Grimaldi et al., 2018; Guo et al., 2021; Gupta et al., 2016; Habiba et al., 2020, 2021; Hadoux et al., 2019; Hart et al., 2016; Kimbrough et al., 2015; Koronyo et al., 2012; Koronyo-Hamaoui et al., 2011; Lee et al., 2010; Liu et al., 2009; Mei et al., 2020; More and Vince, 2015; Nazari et al., 2022; Ning et al., 2008; Park et al., 2014; Parnell et al., 2012; Parthasarathy et al., 2015; Peng et al., 2015; Perez et al., 2009; Pogue et al., 2015; Sarkar et al., 2018; Shi et al., 2020a, 2022; Sidiqi et al., 2020; Tsai et al., 2014; Vandenabeele et al., 2021; Wang et al., 2023b; Williams et al., 2013; Zhang et al., 2021c). In transgenic rodent models of AD, retinal Aβ deposits were often detected at early stages of the disease (Habiba et al., 2021; Koronyo-Hamaoui et al., 2011; Zhang et al., 2021b), associated with enhanced gliosis, and colocalized within sites of neuronal apoptosis and degeneration (Bevan et al., 2020; Burgaletto et al., 2021; Doustar et al., 2017; Grimaldi et al., 2018; Gupta et al., 2016; Koronyo et al., 2012, 2017; Koronyo-Hamaoui et al., 2011; La Morgia et al., 2016; Liu et al., 2009; Ning et al., 2008; Oliveira-Souza et al., 2017; Perez et al., 2009; Salobrar-Garcia et al., 2020b; Tsai et al., 2014). In addition, Aβ oligomers have been observed in the retina of various transgenic animal models of AD, with an increased burden in AD-model mice compared to non-transgenic wild type (WT) littermate

controls (Bartley et al., 2022; Bitel et al., 2012; Du et al., 2015; Habiba et al., 2020, 2021). Our group also reported age-dependent increases in total retinal and vascular $A\beta_{40}$ and $A\beta_{42}$ deposits in the $APP_{SWE}/PS1_{\Delta E9}$ transgenic mice (Doustar et al., 2020; Shi et al., 2020b, 2022).

Overall, the accumulating evidence from both AD patients and animal models confirms the presence of AD-specific Aβ species in the retina, suggesting a shared vulnerability of the retina and brain to AD pathological processes.

2.2. Retinal tauopathy in AD

The accumulation of aberrant microtubule-associated protein tau isoforms (*e.g.*, pTau, NFTs) represents another hallmark of AD in the brain, crucial for disease diagnosis and staging, and closely linked with neuronal injury and cognitive decline (Ballatore et al., 2007; Hanseeuw et al., 2019; Jadhav et al., 2015; Zhang et al., 2021a). In postmortem retinas of confirmed AD patients, pTau inclusions were identified in 2012 using anti-AT8 monoclonal antibodies (Schon et al., 2012). Results from this study were corroborated by subsequent studies showing elevated levels of pathological tau isoforms, including increased microglial uptake of retinal pTau, in the retina of AD patients (den Haan et al., 2018; Du et al., 2022; Grimaldi et al., 2019; Hart de Ruyter et al., 2023; Nunez-Diaz et al., 2024; Shi et al., 2024; Walkiewicz et al., 2024). Total tau (HT7, 43D), 3-repeat and 4-repeat tau isoforms (RD3, RD4), and diverse pTau epitopes, analyzed by phosphorylation site-specific antibodies such as AT8 (Ser202/Thr205), AT270 (Thr181), AT100 (Thr212/Ser214), pS396 (Ser396), pT217 (Thr217), and pT231 (Thr231), were detected in retinal cross-sections from AD patients (Fig. 6). These pTau isoforms were predominantly localized within the synapse-dense inner plexiform layer (IPL) and outer plexiform layer (OPL) of AD patients but were also notably observed in the inner retinal layers, including the retinal nerve fiber layer (RNFL), inner nuclear layer (INL), and ganglion cell layer (GCL).

A histopathological analysis of the postmortem brain and retinal tissue from AD patients revealed that retinal pTau isoforms (Ser202/Thr205 and Thr217) were concentrated in retinal amacrine and horizontal cells in the INL of AD patients, and both pTau epitopes were significantly elevated in AD cases compared to non-tauopathy neurodegenerative cases or controls (Braak 0) (Hart de Ruyter et al., 2023). However, there were no significant differences in other pTau epitopes (Thr212/Ser214, Thr181, and Ser396) between the groups. Importantly, the presence of retinal pTau Ser202/Thr205 and Thr217 correlated with the Braak stage for NFTs and with the presence of pTau Ser202/Thr205 in the hippocampus and cortex of these patients (Hart de Ruyter et al., 2023). Another recent study that characterized the distribution of different pTau isoforms (AT8, Ser396, AT100, pTau231, Ser396/Ser404, Ser396, and 3R, 4R) and tau tangles (anti-NFT MC-1 antibody), in the AD retina demonstrated that retinal primary tauopathy is associated with the brain Aβ phase (Walkiewicz et al., 2024). Furthermore, the optical signature of pS396 (Ser396)-tau was identified in the AD retina using HSI methodology, and pS396-tau was predicted in unstained tissues aided by deep learning image analysis (Fig. 6F–J) (Du et al., 2022). A few studies were unable to confirm the presence of pTau in the human AD retina (Ho et al., 2014; Williams et al., 2017), possibly due to examining small anatomical locations and the application of non-optimal methodologies, as specified above. In addition, inconsistencies were noted in the identification, or lack of, specific pTau isoforms in the retina among the groups that found pTau in the AD retina, which again emphasizes the need to harmonize retinal pathological methodologies.

To date, one study has reported the existence of NFT-like structures in postmortem retinas of AD patients using Gallyas silver stain (Fig. 6B) (Koronyo et al., 2017). Nevertheless, the colocalization of pTau at sites of neuronal loss in the human AD retina (Asanad et al., 2019; Grimaldi et al., 2019; Koronyo et al., 2017) may indicate a similar pathophysiological vulnerability to pTau accumulation in both the retina and brain. Despite this, we still have a limited understanding of tauopathy in the human retina, its distribution, immature and mature formation, propagation, and subsequent impact on retinal inflammation and degeneration. Furthermore, the relationships between aberrant retinal tau forms and other retinal AD processes with brain AD pathology and cognitive function, are understudied.

In murine models of AD, associations between retinal tauopathy and cognition have been observed. In these models, researchers detected disease-associated pTau species from the GCL to the outer nuclear layer (ONL) (Buccarello et al., 2017; Burgaletto et al., 2021; Buscho et al., 2022; Chang et al., 2020; Chiasseu et al., 2017; de Ruyter, 2020; den Haan et al., 2018; Du et al., 2015; Grimaldi et al., 2018; Guo et al., 2019; Kim et al., 2021a; Latina et al., 2021; Lee et al., 2012; Schon et al., 2012; Wang et al., 2023b; Yang et al., 2013; Zhao et al., 2013), including intracellular pTau aggregates (Zhao et al., 2013) and tau tangles in the GCL (Grimaldi et al., 2018). An accumulation of total tau and epitope-specific pTau in the retina reportedly precedes the onset of neurobehavioral deficits and brain tauopathy in AD-model mice (Chiasseu et al., 2017).

2.3. Retinal inflammation in AD

Chronic, low-grade inflammation is a typical sign of AD neuropathology in the brain (Akiyama et al., 2000; Tao et al., 2018). Genome-wide association studies, along with histological, proteomic, and single-cell RNA sequencing (scRNAseq) analyses, indicate that dysregulated immune processes, particularly heightened innate immune responses, playing a central role (Calsolaro and Edison, 2016; Heneka et al., 2015; Jansen et al., 2019; Karch and Goate, 2015; Lambert et al., 2013). Neuroinflammation in AD predominantly involves a phenotypic shift in glial cells, notably reactive astrocytes and activated microglia surrounding cerebral Aβ plaque sites, which exacerbates disease progression (Chaudhury et al., 2003; Heneka et al., 2015; McGeer and McGeer, 2004; Olabarria et al., 2010; Pelkmans et al., 2024; Wyss-Coray et al., 2003). These glial cells undergo transcriptional and functional changes leading to overactivity, directly involved in the seeding, aggregation, and propagation of abnormal Aβ and tau forms (Castellani and Schwartz, 2020; Hampel et al., 2020; Pascoal et al., 2021). Detrimental microglial polarization leads to increased secretion of pro-inflammatory chemokines and cytokines such as tumor necrosis factor-α, enhancing neurotoxicity (McAlpine and Tansey, 2008). Additionally, impaired Aβ-phagocytic activity by brain-resident microglia appears to hinder cerebral Aβ clearance (Butovsky et al., 2006; Hickman et al., 2008; Krabbe et al., 2013; Zuroff et al., 2017). Microglia also play a role in synaptic remodeling, with pathological conditions resulting in excessive synapse pruning that was shown to lead to synaptic loss in animal models of AD (Hansen et al., 2018; Hong et al., 2016; Rajendran and Paolicelli, 2018; Salter and Stevens, 2017). In addition, scRNAseq experiments have identified a distinct neurodegenerative or disease-associated microglia (MGnD/DAM) activation state near Aβ plaques in the brains of transgenic AD murine models (Keren-Shaul et al., 2017; Krasemann et al., 2017), regulated by the triggering receptor expressed on myeloid cells 2-APOE (TREM2-APOE) pathway (Krasemann et al., 2017).

Analyses of retinal cross-sections and flatmounts from patients with MCI or AD dementia revealed marked inflammatory processes (Blanks et al., 1996a; Grimaldi et al., 2019; Koronyo et al., 2023; Xu et al., 2022). Blanks and colleagues observed elevated levels of glial fibrillary acidic protein (GFAP) expression in retinal astrocytes and Müller glia within the GCL of patients with AD (Blanks et al., 1996a). Grimaldi et al. detected significant increases in reactive $GFAP^+$ astrocytes and activated microglia, alongside elevated Aβ and pTau pathology in retinas from AD patients compared to age-matched controls (Grimaldi et al., 2019). They also identified upregulation of innate immune response mediators such as interleukin-1β (IL-1β), complement component 3, osteopontin, and TREM2 in these retinal tissues. Recent research by Xu et al., corroborated

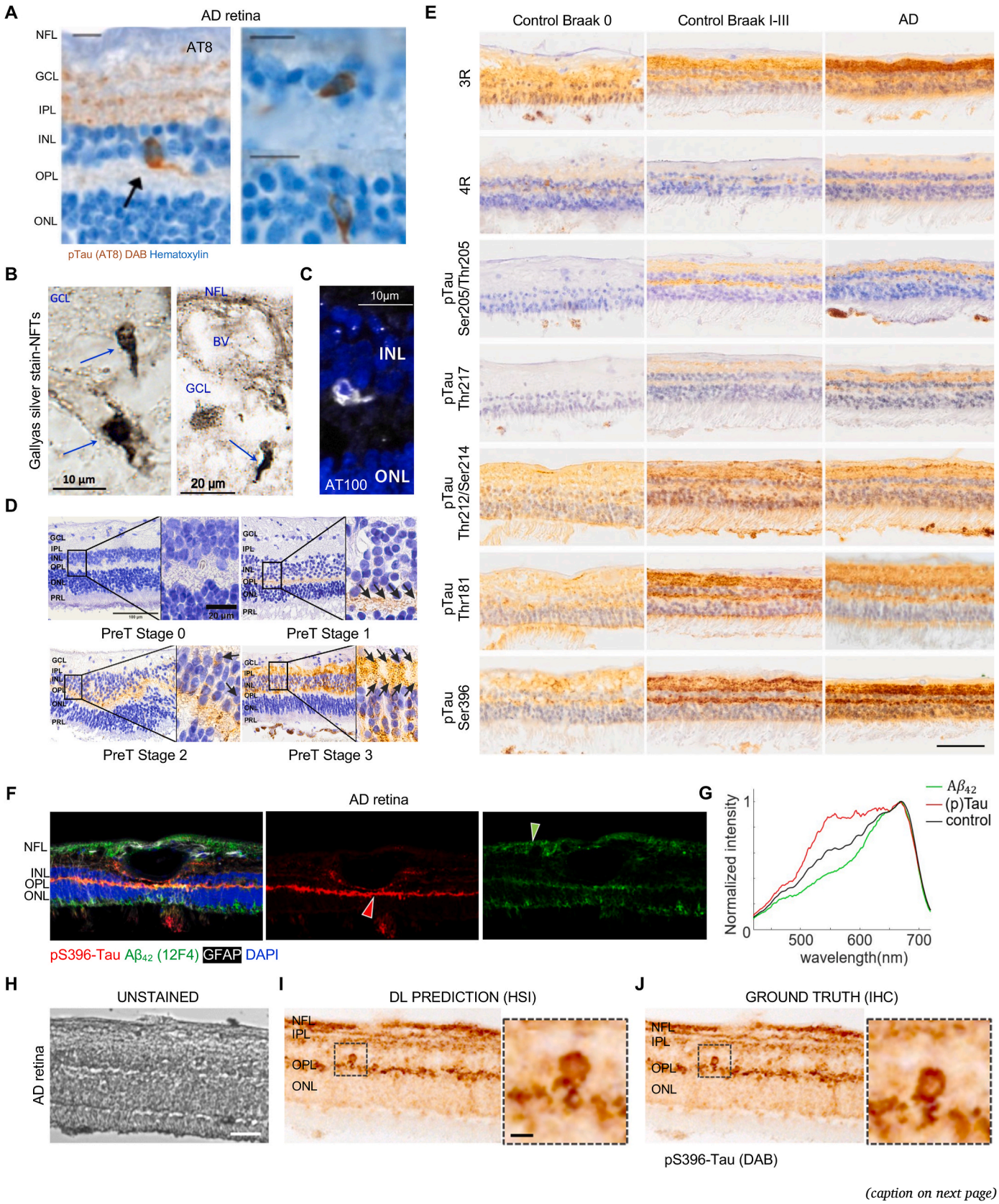

(caption on next page)

these findings, showing increased activated microgliosis, as assessed by the ionized calcium-binding adapter molecule 1 (IBA1) marker, in the INL and OPL of retinal mid-peripheral regions of AD patients (Xu et al., 2022).

Interestingly, this study also reported lower levels of retinal astrocytes and Müller glial cells in patients with AD as assessed by GFAP and glutamine synthetase expression (Xu et al., 2022).

Fig. 6. Tau isoforms and hyperspectral signatures of pTau and Aβ$_{42}$ identified in retinal cross-sections from AD patients. Representative images of retinal cross-sections from AD patients following (**A**) immunostaining with AT8 mAb against hyperphosphorylated-(p)Tau (Ser202, Thr205) and peroxidase DAB labeling, followed by hematoxylin counterstaining, reveal intracellular pTau accumulation in the INL (arrow) and neuronal processes of the IPL. Scale bar: 10 μm; (**B**) Gallyas silver staining, indicating the presence of neurofibrillary tangles (NFTs)-like structures, especially in the GCL (blue arrows); and (**C**) immunofluorescence staining with AT100 mAb against pTau (Thr212, Ser214), showing intracellular signals (white) in the INL. (**D**) Representative retinal cross-section images stained with pTau (Ser202, Thr205) and visualized with peroxidase DAB labeling, followed by hematoxylin counterstaining, depict the sequential pattern of primary retinal tauopathy (PReT) among the non-AD and AD retina: PReT stage 0, no p-tau pathology in the retina; PReT stage 1, initial pTau accumulation in the OPL; PReT stage 2, additional pTau presence in neurons of the INL; PReT stage 3, further accumulation of pTau in the OPL and INL, as well as in the IPL. (**E**) Representative images of superior peripheral retinal cross-sections from individuals with the following brain pathology: Braak stage 0, Braak stage I–III, and AD, stained for various tau isoforms, including the 3 and 4-repeats (3R, 4R) tau and five pTau epitopes, followed by DAB labelling (brown), and hematoxylin counterstaining for nuclei (violet). Scale bar: 50 μm. (**F**) Immunofluorescence staining showing positive signals for pS396-Tau (red), 12F4-Aβ$_{42}$ (green), GFAP^{+} astrocytes (white), and DAPI nuclei (blue) in a retinal cross-section of an AD patient. (**G**) Distinct optical signatures of Aβ$_{42}$ (green line) and pS396-Tau (red line) identified by hyperspectral imaging in the human AD retina. Representative images of AD retinal cross-sections showing (**H**) an unstained section (gray), (**I**) deep-learning (DL) predicted image (brown) based on the identified pTau optical signature, and (**J**) 'ground truth' immunostaining for pS396-Tau and peroxidase DAB labeling (brown). DL prediction (**I**) accurately indicated on unstained tissues the true pTau patterns, and demonstrated pS396-Tau signals that appear as intracellular and synaptic aggregates in the RNFL, IPL, and OPL. High magnification images (in I and J) show retinal NFT-like structures. Scale bar: 50 μm for large images, and 10 μm for bordered inserts. Panel A was modified from (Schon et al., 2012), Panel B was modified from (Koronyo et al., 2017), Panel D was modified from (Walkiewicz et al., 2024), Panel E was modified from (Hart de Ruyter et al., 2023), and Panels F–H were modified from (Du et al., 2022) with permission.

In a recent study, Koronyo et al., found significant increases in IBA1^{+} microgliosis and GFAP^{+} or S100 calcium-binding protein B (S100β)$^{+}$ macrogliosis (astrocyte and Müller glia markers), often surrounding Aβ deposits, in the neurosensory retina of patients with MCI and AD compared to NC controls (Koronyo et al., 2023). Elevated IBA1^{+} microgliosis was particularly notable at the retinal synapse-rich plexiform layers (IPL and OPL) in these patients, suggesting a potential role of retinal microglia in excessive synaptic pruning and cognitive decline. Additionally, there was a notable sex dysmorphism, with significantly higher levels of retinal microgliosis observed in female AD patients compared to male patients. This study also highlighted the direct involvement of retinal microglia in Aβ uptake (Koronyo et al., 2023), mirroring findings in the AD brain (Lee and Landreth, 2010; Paresce et al., 1996). The extent of retinal microgliosis and macrogliosis closely correlated with increased retinal Aβ$_{42}$ burden (Koronyo et al., 2023), indicating that Aβ in the retina triggers glial activation akin to processes observed in the AD brain (Heneka et al., 2015). Consistent with previous findings (Xu et al., 2022), Koronyo and colleagues revealed that over 80% fewer retinal microglia engaged in Aβ$_{42}$ internalization in MCI and AD patients compared to NC controls (Koronyo et al., 2023), suggesting impaired Aβ phagocytosis despite increased microgliosis in these patients. Further investigation is needed to determine whether this defective microglial Aβ phagocytosis in the MCI and AD retina is a consequence or a driver of the disease. In response to retinal tau pathology, a recent study by Nuñez-Diaz et al. demonstrated an increased uptake of pTau (using the PHF-1 and AT8 antibodies) by microglial cells in retinal flatmounts from AD patients compared to control subjects (Nunez-Diaz et al., 2024). Overall, the histological evidence depicting augmented inflammatory processes in the retina of MCI and AD patients compared to NC controls is summarized in Fig. 7.

Various studies in animal models of AD have also provided evidence of enhanced retinal inflammation (Antes et al., 2015; Edwards et al., 2014; Gao et al., 2015a; Grimaldi et al., 2018; Liu et al., 2009; Ning et al., 2008; Perez et al., 2009; Pogue et al., 2015; Shi et al., 2020a, 2022; Tsai et al., 2014; Yang et al., 2013). Salobrar-Garcia et al., described morphological changes in retinal microglia consistent with neuroinflammatory phenotypes in 3xTg AD mice (Salobrar-Garcia et al., 2020b). In a study by our team, we demonstrated that nuclear factor-kappa B (NF-κB) expression is significantly increased in the retina of 12-month-old double-transgenic APP$_{SWE}$/PS1$_{ΔE9}$ (ADtg) mice, indicating an increased pro-inflammatory response in the retina of these mice (Shi et al., 2020a). Recently, we identified the existence of MGnD/DAM microglia that were increased in the retina of APP$_{SWE}$/PS1$_{L166P}$ transgenic mouse models of AD (Shi et al., 2022). The transcriptional regulation of retinal MGnD microglial phenotype through micro-RNA (miR)-155 inhibition not only limited retinal inflammation but also reduced vascular amyloidosis and protected inner BRB integrity in these AD mouse models (Shi et al., 2022). In aged, late-stage APP$_{SWE}$/PS1$_{ΔE9}$ (ADtg) mouse models compared to WT littermate controls, dysregulation of multiple inflammatory markers, as determined by mass spectrometry analysis, was similarly evident in both the brain and retina (Doustar et al., 2020). Notably, immunomodulation therapy with glatiramer acetate (GA) in ADtg mice led to the recruitment of blood-borne neuroprotective monocytes to Aβ-plaque sites in the brain and retina, effective in Aβ phagocytosis and clearance. GA immunization further mitigated various aspects of AD-related pathology, preserved synapses and cognition (Butovsky et al., 2006, 2007; Koronyo et al., 2012, 2015; Koronyo-Hamaoui et al., 2020; Li et al., 2020b), and elicited parallel regulatory effects on inflammatory markers, such as ICAM1, LAMP1/2, and HA11, in both the brain and retina of ADtg mice (Doustar et al., 2020). Another study analyzed the effects of monocyte blood enrichment and transient overexpression of the Aβ-degrading angiotensin-converting enzyme (ACE) in monocytes (ACE*10* model) on AD-like progression in APP$_{SWE}$/PS1$_{ΔE9}$ ADtg mice (Koronyo-Hamaoui et al., 2020). This study demonstrated that increased retinal and cerebral infiltration of ACE-overexpressing monocytes was associated with reduced Aβ burden and gliosis, preserved synapses, and improved cognitive functions (Fig. 8). Furthermore, in *App*$^{NL-F/NL-F}$ knock-in mouse models of AD, retinal microglia were found to be involved in the uptake of pTau, which increased with disease progression (Nunez-Diaz et al., 2024). Overall, advances in understanding the intricate inflammatory dynamics across peripheral (*e.g.*, blood, bone marrow) and CNS (*e.g.*, brain, retina) tissues offer promising avenues to uncover novel insights into AD pathogenesis, which may lead to the discovery of novel diagnostic and therapeutic strategies.

2.4. Retinal neurodegeneration in AD

Brain neurodegeneration in AD is characterized by progressive damage to synapses and neuronal circuits, which are linked to various neurobehavioral functions including cognition, sensation, mood, vision, and orientation. Evidence suggests that this neuronal and synaptic loss is responsible for the various characteristic symptoms of AD (Crews and Masliah, 2010; Lan et al., 2022; Moya-Alvarado et al., 2016; Wilson et al., 2010). Consistent with the observed distribution of retinal Aβ deposits and pTau in AD patients, mounting histological and in vivo imaging findings indicate structural damage to key components of the visual pathway. Hinton and colleagues provided the first evidence for RGC loss, retinal NFL thinning, and optic nerve atrophy in postmortem tissues from AD patients (Hinton et al., 1986). Subsequent studies have further showed significant retinal neurodegeneration, including retinal atrophy and thinning, in AD patients (Asanad et al., 2019; Berisha et al., 2007; Blanks et al., 1989; Blanks et al., 1996a; Blanks et al., 1996b; Cheung et al., 2021; Cunha et al., 2017a; Janez-Escalada et al., 2019;

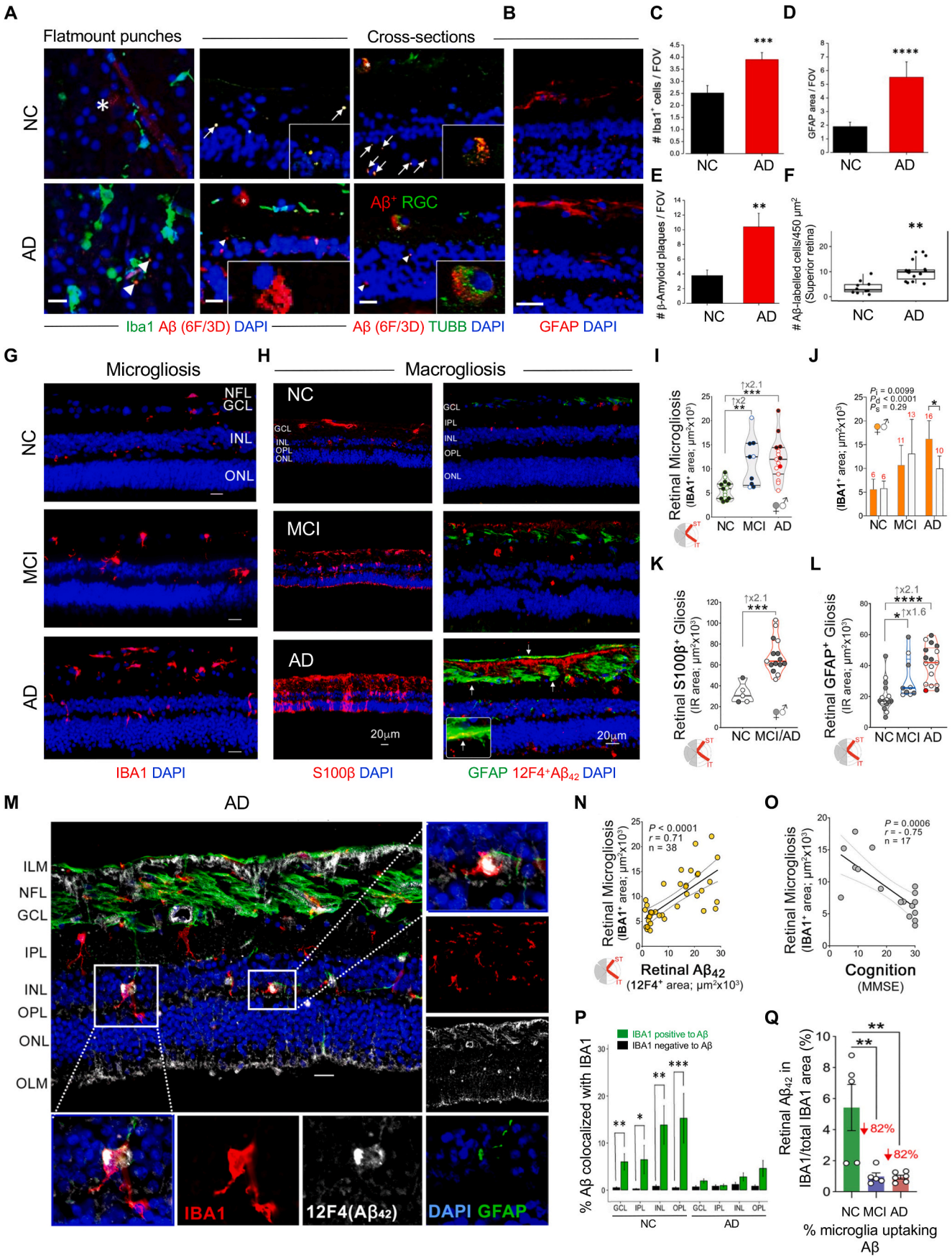

(caption on next page)

Fig. 7. Retinal gliosis and Aβ phagocytosis by microglia in MCI and AD patients. (**A**) Representative immunofluorescence images of retinal flatmount punches from AD patients and NC controls stained for Aβ (6F/3D; red) and IBA1$^+$ microglia (green). Also displayed are representative images of retinal cross-sections immunostained for Aβ (6F/3D; red), β-III Tubulin (TUBB, green), and nuclei (DAPI, blue). Aβ immunofluorescence was evident within TUBB-positive RGCs and in extracellular spaces. Aβ immunoreactivity in RGC (asterisk); in neuropil and extracellular spaces (arrowheads); and colocalization with IBA1 microglia or TUBB neurons are shown. Scale bars: 20 μm. (**B**) Representative images of retinal cross-sections depicting increased astrogliosis (GFAP, red) in AD retina. Scale bar: 20 μm. Quantification of retinal: (**C**) IBA1$^+$ IR area (N = 73/10 fields/patients), (**D**) GFAP$^+$ IR area (N = 44/6 fields/patients), (**E**) number of Aβ plaques per field of view (FOV) (N = 45/5 fields/patients), and (**F**) number of Aβ-positive RGCs, in AD patients (N = 15) versus NC controls (N = 10). (**G, H**) Representative fluorescence images showing (**G**) IBA1$^+$ microgliosis (red), (**H**) retinal S100β$^+$ (red)- or GFAP$^+$ (green), macrogliosis for reactive astrocytes and Müller glia in retinal cross-sections from NC, MCI, and AD patients. Retinal GFAP$^+$ macrogliosis is detected surrounding sites of 12F4$^+$-Aβ_{42} deposits (red), especially in the ganglion cell layer (GCL), in patients with MCI or AD versus NC. White arrows indicate Aβ colocalized within GFAP$^+$ macroglia. Scale bar: 20 μm. (**I**) Retinal IBA1- IR areas in NC (N = 15), MCI (N = 9), and AD (N = 15). (**J**) Bar graph displays means and standard deviations of retinal IBA1$^+$ microgliosis by sex in NC (N = 9F/6M), MCI (N = 6F/3M), and AD (N = 5F/10M). (**K, L**) Quantitative IHC analyses of (**K**) retinal S100β in NC (N = 5) and MCI/AD (N = 15), as well as (**L**) retinal GFAP IR areas in NC (N = 16), MCI (N = 8), and AD (N = 17). (**M**) Fluorescence image shows retinal IBA1$^+$ microgliosis (red) colocalized at sites of 12F4$^+$-Aβ_{42} deposits (white) with GFAP$^+$ macrogliosis (green) and DAPI nuclei (blue). Scale bar: 20 μm. Retinal IBA1$^+$ microglia often internalize Aβ_{42} (enlarged images). (**N, O**) Pearson's (*r*) correlation analyses between retinal IBA1$^+$ immunoreactive area and (**N**) retinal Aβ_{42} load, and (**O**) the MMSE cognitive scores. (**P**) Percent of 6F/3D-Aβ$^+$ colocalized within IBA1$^+$ microglia, showing a comparison between IBA1$^+$ cells positive for Aβ (green) versus IBA1$^+$ cells negative for Aβ (black), across different retinal layers in AD patients (N = 5) and NC controls (N = 7). (**Q**) Percent of 12F4-Aβ_{42}^+ colocalized within IBA1$^+$ microglia out of the total IBA1$^+$ microglia in retinal tissues from patients with MCI (N = 5) and AD (N = 6), as well as NC controls (N = 5). The red circle in panels I and L indicate an ADAD patient with the *PSEN1*-A260V mutation. Fold increases and percent reductions between the groups are indicated on the graphs. Statistics: Data from individual subjects (circles) as well as group means ± SEMs are shown. Median and lower and upper quartiles are indicated on each violin plot. Fold changes are shown in gray. $^*P < 0.05$, $^{**}P < 0.01$, $^{***}P < 0.001$, $^{****}P < 0.0001$, by one-way or two-way ANOVA and Tukey's post hoc multiple comparison test, or by two-tailed unpaired Student's *t*-test. F = female, M = male. Panels A and P were modified from (Xu et al., 2022), Panels B–E were modified from (Grimaldi et al., 2019), Panel F was modified from (Lee et al., 2020b), and Panels G–O and Q were modified from (Koronyo et al., 2023) with permission.

Kesler et al., 2011; Kirbas et al., 2013; Koronyo et al., 2017; Koronyo et al., 2023; La Morgia et al., 2016; Lopez-de-Eguileta et al., 2019; Mathew et al., 2023; Mutlu et al., 2018; Oktem et al., 2015; Polo et al., 2017; Sadun and Bassi, 1990; Salobrar-Garcia et al., 2019; Shao et al., 2018; Shi et al., 2014; Zhao et al., 2023). More in-depth histomorphometric analyses have revealed significant reductions in retinal thickness in different cell layers (GCL, INL, IPL and ONL) and geometrical subregions (central, mid-periphery, and far-periphery) in retinal cross-sections of MCI and AD patients (Fig. 9A–E) (Asanad et al., 2019; Koronyo et al., 2023). Koronyo and colleagues reported significant neuronal degeneration in the GCL, INL, and ONL of AD patients compared to age- and sex-matched NC controls (Koronyo et al., 2017). Similarly, Asanad and colleagues conducted a detailed topographical quantification and found thinning of both inner retinal layers (RNFL, GCL, IPL, INL) and the outer retinal layer (ONL) in AD patients (Asanad et al., 2019), corroborating previous descriptions of retinal thinning. RNFL thinning was most pronounced in the superior-temporal region (Asanad et al., 2019). In a histopathological study with a larger human cohort, the degree of atrophy quantified in the neurosensory retina of MCI and AD patients was comparable to the brain atrophy observed in these patients (Fig. 9D–G) (Koronyo et al., 2023). Notably, the pattern of retinal atrophy was very similar to the distribution of retinal amyloid deposits, frequently observed in the inner cell layers and superior-temporal retinal subregions in AD patients (Dumitrascu et al., 2020, 2021; Koronyo et al., 2017; Koronyo-Hamaoui et al., 2011; La Morgia et al., 2016; Lee et al., 2020b). Furthermore, retinal neurodegeneration was predominantly observed at sites of Aβ deposition and closely correlated with increased retinal Aβ_{42} burden and oligomeric-Aβ load (Fig. 9H) (Koronyo et al., 2017, 2023). In addition, increased retinal thinning in MCI and AD patients strongly correlated with brain Aβ burden (Fig. 9I) and cognitive deficits as assessed by MMSE scores (Fig. 9J) (Koronyo et al., 2023). Given the well-documented impact of misfolded Aβ_{42}, particularly its oligomeric forms, on the neuronal and synaptic degeneration characteristic of AD (Barucker et al., 2015; Cohen et al., 2013; Lee et al., 2022; Li et al., 2020b; Pauwels et al., 2012; Shankar et al., 2008; Varga et al., 2015), the robust association between retinal Aβ_{42} or Aβ oligomers and retinal atrophy suggests a mechanistic link involving Aβ-induced neurodegeneration in the retina of AD patients.

The degeneration of specific retinal cell types, such as RGCs, photoreceptors, and pericytes, has been identified in a series of studies in postmortem retinas of AD patients compared to NC controls (Koronyo et al., 2017, 2023; La Morgia et al., 2016; Shi et al., 2020b). A significant Nissl-positive neuronal loss (22–29%) was documented in retinal cross-sections, particularly in the GCL, in AD patients compared to NC controls (Fig. 10A–C) (Koronyo et al., 2017). Analysis of the apoptotic cell marker, cleaved caspase-3 (CCasp3), revealed a substantial 4.2-fold increase in expression in distinct retinal cell layers in AD retina (Fig. 10D and E), with a notable CCasp3 increase in RGCs. There was a significantly higher percentage of CCasp3$^+$ apoptotic RGCs in AD patients (42.6%) compared to age- and sex-matched NC controls (13.7%) (Koronyo et al., 2023). These histological findings corroborate the clinical evidence that the first component affected in AD in the visual system involves the RGCs, and especially the larger caliber RGCs (M-cells) that synapse in the magnocellular layers 1 and 2 of the lateral geniculate nucleus (LGN) (Erskine et al., 2016; Javitt et al., 2023; Sadun and Bassi, 1990; Sartucci et al., 2010). These RGCs and their axonal projections feed the M pathway that is responsible for low spatial frequency contrast sensitivity and motion detection (Amthor et al., 2005; Gilmore et al., 1994; Gilmore and Whitehouse, 1995; Liu and Sanes, 2017; Zhao et al., 2014), type of visual impairments often observed in MCI and AD patients (Javaid et al., 2016; Lim et al., 2013; Liu et al., 2019; Risacher et al., 2013; Ye et al., 2018). Early RGC dysfunction was further identified by electroretinography in preclinical AD patients, preceding cognitive decline (Asanad et al., 2021). In addition, La Morgia and colleagues found an increased degeneration of melanopsin-containing RGCs (mRGCs), which was closely linked to Aβ accumulation within and around these cells (Fig. 10F–K) (La Morgia et al., 2016). This small subpopulation of ganglion cells is known to drive circadian photoentrainment that regulates the sleep-awake cycles. The selective loss of mRGCs in AD patients may indicate that Aβ is particularly detrimental to certain retinal cell subtypes and provides the first potential retina-based mechanistic explanation for well-documented circadian rhythm disturbances in these patients (La Morgia et al., 2017; Oh et al., 2019). As it relates to other retinal cell types, our team further detected a marked pericyte degeneration in retinal microvasculature from MCI and AD patients (Fig. 10L-P) (Shi et al., 2020b). This substantial pericyte loss likely exacerbates retinal vascular dysfunction and subsequent neurodegeneration of cells vital for the visual pathway, such as RGCs and photoreceptors (Koronyo et al., 2023). Collectively, retinal neurodegeneration in AD coincides with areas of AD-related pathology, demonstrating correlations with disease severity and cerebral atrophy. This phenomenon may contribute to visual and circadian rhythm dysfunctions.

Retinal neurodegeneration has also been reported in animal models of AD (Chiu et al., 2012; Grimaldi et al., 2018; Gupta et al., 2016; Ning

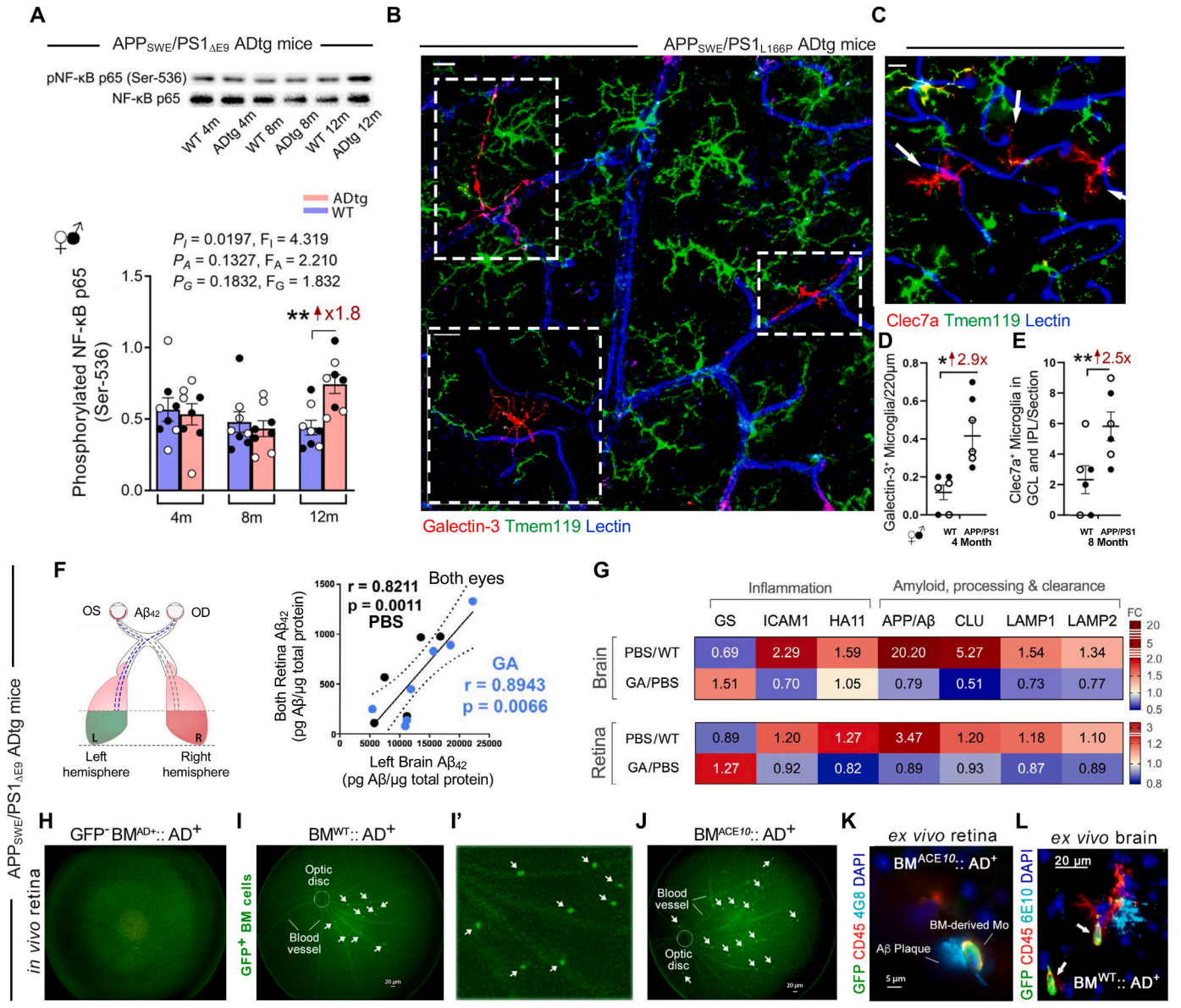

(caption on next page)

et al., 2008; Salobrar-Garcia et al., 2020a; Sanchez-Puebla et al., 2024). For instance, several studies in transgenic murine models of AD reported significant RNFL thinning (Buccarello et al., 2017; Kim et al., 2021b; Lim et al., 2020; Matei et al., 2022; Song et al., 2020). In addition, apoptotic cells were detected in the GCL of double-transgenic $APP_{SWE}/PS1_{M146L}$ and $APP_{SWE}/PS1_{\Delta E9}$ mouse models (Ning et al., 2008). Significant reductions in retinal thickness were detected in several cell layers, spanning from the GCL to the ONL, in ADtg mice compared to their WT littermate controls (Koronyo-Hamaoui et al., 2011; Liu et al., 2009). Another study found that decreased retinal thickness is a result of the thinning of different retinal layers, such as the GCL, IPL, INL, OPL, and photoreceptors (Chiquita et al., 2019). While RNFL thinning commonly causes reduced retinal thickness, the impact of other retinal cell layer degeneration cannot be overlooked. Loss of photoreceptor cells (rods and cones) in the ONL, as well as neuronal cells in the inner retinal layers (such as RGCs, bipolar cells, horizontal cells, or amacrine cells), also contributes to overall retinal thinning (Chiquita et al., 2019; Kim et al., 2021b; Zhang et al., 2021b). A recent study in 5xFAD mice at different age groups revealed that retinal neurodegeneration was closely associated with Aβ pathology, following a progressive pattern in the retina similar to that of the brain (Lim et al., 2020). Aβ deposition in the retina also led to axonal neurodegeneration in the GCL of these mice. As the disease progresses, widespread retinal dysfunctions are observed, as evidenced by reduced ganglion, bipolar, and amacrine cell responses to light and alterations in ERG patterns (Lim et al., 2020). These AD-related processes manifest in the degeneration of photoreceptors, interneurons, and other inner retinal structures (Lim et al., 2020). In summation, numerous studies conducted in both humans and mouse models have demonstrated a complex pattern of AD-induced neurodegeneration spanning all retinal layers, which may negatively impact a wide spectrum of retinal functions.

2.5. *Retinal vascular pathology in AD*

AD pathology is typically associated with abnormalities in cerebral vasculature (Abbasi, 2017; Fisher et al., 2022; Greenberg et al., 2020; Li et al., 2014). The major vascular complication associated with AD in humans is cerebral amyloid angiopathy (CAA), which is mainly

Fig. 8. Retinal inflammation in transgenic murine models of AD. Data from transgenic mouse models of AD, including the $APP_{SWE}/PS1_{\Delta E9}$ mice (referred to as ADtg, AD^{+}, or $APP_{SWE}/PS1_{\Delta E9}$) and the $APP_{SWE}/PS1_{L166P}$ (APP/PS1) mice are shown. (**A**) A representative Western blot gel showing the levels of phosphorylated (p) NF-κB p65 and NF-κB p65 subunit (NF-κB p65) in retinal lysates from $APP_{SWE}/PS1_{\Delta E9}$ mice compared to age- and sex-matched wild type (WT) littermates at 4-, 8-, and 12- months of age (upper panel). The densitometric analyses of Western blot protein bands of pNF-κB p65, normalized to β-actin, is shown (lower panel) (N = 8 for each age and genotype). (**B**) A representative image from a retinal flatmount of an $APP_{SWE}/PS1_{L166P}$ mouse, immunofluorescently stained for Galectin-3^{+} microglia (red), $Tmem119^{+}$ microglia (green), and lectin for blood vessels (blue). Scale bars: 10 μm. (**C**) A representative image from a retinal flatmount of an $APP_{SWE}/PS1_{L166P}$ mouse, immunofluorescently stained for $Clec7a^{+}$ microglia (red), $Tmem119^{+}$ microglia (green), and lectin for blood vessels (blue). Scale bars: 10 μm. (**D-E**) IR area of (**D**) Galectin-3^{+} microglia in 4-month-old APP/PS1 mice and (**E**) $Clec7a^{+}$microglia in 8-month-old APP/PS1 mice (N = 6 each group). (**F-G**) Aged, 20-22-month-old, $APP_{SWE}/PS1_{\Delta E9}$ (ADtg) mice underwent weekly subcutaneous (s.c.) immunization with glatiramer acetate (GA) or were injected with PBS as controls, for a duration of 8 weeks. (**F**, left) Protein homogenates from retinas isolated from the OS (left) and OD (right) eyes, and the respective left (L) and right (R) brain hemispheres, were quantified for levels of $A\beta_{1\text{-}40}$ and $A\beta_{1\text{-}42}$ by ELISA, and global proteome changes were assessed by mass spectrometry (MS). (**F**, right) Pearson's (*r*) correlation analysis demonstrates a tight correlation between levels of $A\beta_{1\text{-}42}$ in the brain and the retina (average of both eyes and left-brain hemispheres). Stronger correlation was found among the GA-treated ADtg mice (N = 14). (**G**) Heat map displaying relative fold changes of differentially expressed proteins identified by the MS analysis, indicating molecular parallels between the retina and the brain in AD-related models following GA immunization. Highlighted are inflammatory markers (glutamine synthetase—GS, intercellular adhesion molecule 1—ICAM1, h-2 class I histocompatibility antigen—HA11) and AD-related amyloid-associated markers (amyloid-β A4 protein—APP/Aβ, clusterin—CLU, lysosomal-associated membrane protein 1 and 2—LAMP1/2) that were significantly up- or down-regulated in brain and retinal tissues of ADtg versus WT mice or of GA-immunized versus PBS-control ADtg mice (N = 4–6 mice per group). (**H-L**) The effects of monocyte blood enrichment and transient angiotensin-converting enzyme (ACE) overexpression in monocytes (ACE*10* model) on AD-like progression was studied. At 2 months of age, the $APP_{SWE}/PS1_{\Delta E9}$ (AD^{+}) mice underwent a partial bone marrow (BM) transplantation following irradiation with head shielding. Recipient AD^{+} mice received an intravenous (i.v.) injection of 5 million GFP-labelled BM cells from donor mice with either monocytes that are WT for ACE expression (GFP^{+} BM^{WT}), monocytes with ACE overexpression (GFP^{+} BM^{ACE10}), or monocytes from AD^{+} mice ($GFP^{-}BM^{AD+}$). (**H-J**) A Micron III® rodent retinal microscope was used to visualize in vivo monocyte infiltration into the retinas of AD^{+} chimeric mice. Representative in vivo retinal fluorescence imaging of infiltrating GFP^{+} BM cells in living AD^{+} chimeric mice: (**H**) control AD^{+} mouse that received $GFP^{-}BM^{AD+}$ transplantation, (**I**) AD^{+} mouse that received $GFP^{+}BM^{WT}$ transplantation (**I′**, enlarged image showing GFP^{+} BM cells in the retina), (**J**) AD^{+} mouse that received $GFP^{+}BM^{ACE10}$ transplantation. Arrows indicate GFP^{+} BM cells. (**K**) A representative microscope image of a retinal flatmount extracted from a GFP^{+} BM^{ACE10}-AD^{+} chimeric mouse whose retina had been previously imaged in vivo. The flatmount retina was *ex vivo* immunostained for GFP (BM-derived cells, green), myelomonocytes (CD45, red), Aβ (4G8, cyan), and nuclei (DAPI, blue). BM-derived GFP^{+} ACE^{10} monocytes migrate to the retina and surround retinal $4G8^{+}$-Aβ plaques. (**L**) Representative fluorescence image of coronal brain section from a GFP^{+} BM^{WT}-AD^{+} chimeric mouse showing infiltrating $GFP^{+}/CD45^{hi}$ monocytes (arrows) migrating to the $6E10^{+}$-Aβ plaque site. Statistics: Data from individual subjects (circles) as well as group means ± SEMs are shown. Fold changes are shown in red. $^{*}P < 0.05$, $^{**}P < 0.01$, by two-way ANOVA with Sidak's post-hoc multiple comparison test or unpaired two-tailed Student's *t*-test. Panel A was modified from (Shi et al., 2020a), Panels B–E were modified from (Shi et al., 2022), Panels F–G were modified from (Doustar et al., 2020), and Panels H–L were modified from (Koronyo-Hamaoui et al., 2020) with permission.

characterized by parenchymal and meningeal vascular amyloid accumulation, primarily consisting $A\beta_{40}$ deposits around smooth muscle cells of arteries (Arvanitakis et al., 2011; Biffi and Greenberg, 2011; Ellis et al., 1996; Viswanathan and Greenberg, 2011). CAA is often accompanied by distortions in small blood vessels (Charidimou et al., 2017; Fischer et al., 1990; Hassler, 1965; Kalaria, 2016), uncoupling and degeneration of the neurovascular unit, and breakdown of the BBB (Bell and Zlokovic, 2009; Claudio, 1996; Ryu and McLarnon, 2009; Sengillo et al., 2013; van de Haar et al., 2016a, 2016b; Zipser et al., 2007; Zlokovic, 2011). While CAA is a distinct clinical entity, a high percentage (more than 85%) of AD patients exhibit varying degrees of CAA severity (Arvanitakis et al., 2011; Jellinger, 2010; Viswanathan and Greenberg, 2011). Other vascular changes associated with AD include, but are not limited to, aberrant angiogenesis (Biron et al., 2011; Desai et al., 2009), vascular nonperfusion and reduce blood flow (Binnewijzend et al., 2016; Bonte et al., 1986; Hirsch et al., 1997), vascular inflammation (Grammas and Ovase, 2001; Tripathy et al., 2007), and accumulation of vascular tau (Castillo-Carranza et al., 2017; Williams et al., 2005). Notably, vascular amyloidosis was shown to increase the rigidity of blood vessels and decrease blood flow in the brains of APP-overexpressing mice (Kimbrough et al., 2015). A range of epidemiological and clinical studies have also suggested that common vascular risk factors, such as systemic hypertension and atherosclerosis, are associated with AD progression, potentially contributing to the deposition of atherosclerotic plaques within cerebral vessels, elevated neuritic plaque burden, and subsequent cognitive decline (Dolan et al., 2010a, 2010b; Gabin et al., 2017; Honig et al., 2005; Launer, 2002; Launer et al., 2000; Reitz et al., 2007; Yao et al., 2023).

As described in the AD brain, emerging evidence indicates a wide spectrum of abnormalities in both structural and functional vascular parameters in the retinas of AD patients. Notably, these retinal changes include reduced blood flow (Berisha et al., 2007; Feke et al., 2015), enlarged foveal avascular zone (FAZ) (O'Bryhim et al., 2018), capillary-free zone (Arthur et al., 2023), compromised microvascular network (Abbasi, 2017; Berisha et al., 2007; Cabrera DeBuc et al., 2018; Cheung et al., 2014; Einarsdottir et al., 2016; Feke et al., 2015; Frost et al., 2013; Frost et al., 2010; O'Bryhim et al., 2018; Williams et al., 2015), vein narrowing (Berisha et al., 2007; Cabrera DeBuc et al., 2018; Cheung et al., 2014; Feke et al., 2015; Frost et al., 2013), distorted vascular branching complexity (Cheung et al., 2014; Frost et al., 2013), increased vascular tortuosity (Cheung et al., 2014), and notably, increased vascular amyloidosis and especially arterial $A\beta_{40}$ deposition (Koronyo et al., 2017; Shi et al., 2020b, 2023).

Several clinical and histopathological studies have reported a close association between retinal vascular abnormalities and increased risk for AD [(Baker et al., 2007; Berisha et al., 2007; Cabrera DeBuc et al., 2018; Cheung et al., 2014; Chiara et al., 2022; Di Pippo et al., 2023; Feke et al., 2015; Frost et al., 2013; Liew et al., 2008; Mei et al., 2021; Pead et al., 2023; Querques et al., 2019; Sharafi et al., 2019; Shi et al., 2020b, 2023; Shin et al., 2021; Sun et al., 2024; Williams et al., 2015; Wu et al., 2020; Yoon et al., 2019; Zabel et al., 2019b), reviewed in (Shi et al., 2021)]. For example, Cheung et al., found that patients with AD have altered microvascular networks in the retina, including narrower retinal venules and a sparser and more tortuous retinal vessels, compared with matched non-AD controls (Cheung et al., 2014). These findings suggest that changes in retinal microvascular structures, such as increased venular and arteriolar tortuosity, are associated with AD risk. Williams et al., using retinal fundus imaging, demonstrated that patients with AD have a sparser retinal microvascular network, reduced fractal dimension, and increased arteriole tortuosity compared to NC subjects (Williams et al., 2015). Berisha et al., further reported that patients with AD exhibit a significant narrowing of the venous blood column diameter and reduced venous blood flow rate (Berisha et al., 2007). Another study uncovered a reduced retinal blood flow in MCI and AD patients compared to NC controls. Interestingly, retinal venous blood flow was significantly reduced in MCI patients, which was further decreased in AD, suggesting a gradual effect on retinal venous blood flow during AD progression (Feke et al., 2015). Notably, vascular amyloidosis alongside other microvascular changes were identified and characterized in the postmortem retinas of MCI and AD patients, and the retinal vascular changes were strongly correlated with CAA severity (Koronyo et al., 2017; Shi et al., 2020b, 2023). These discoveries support the abundant

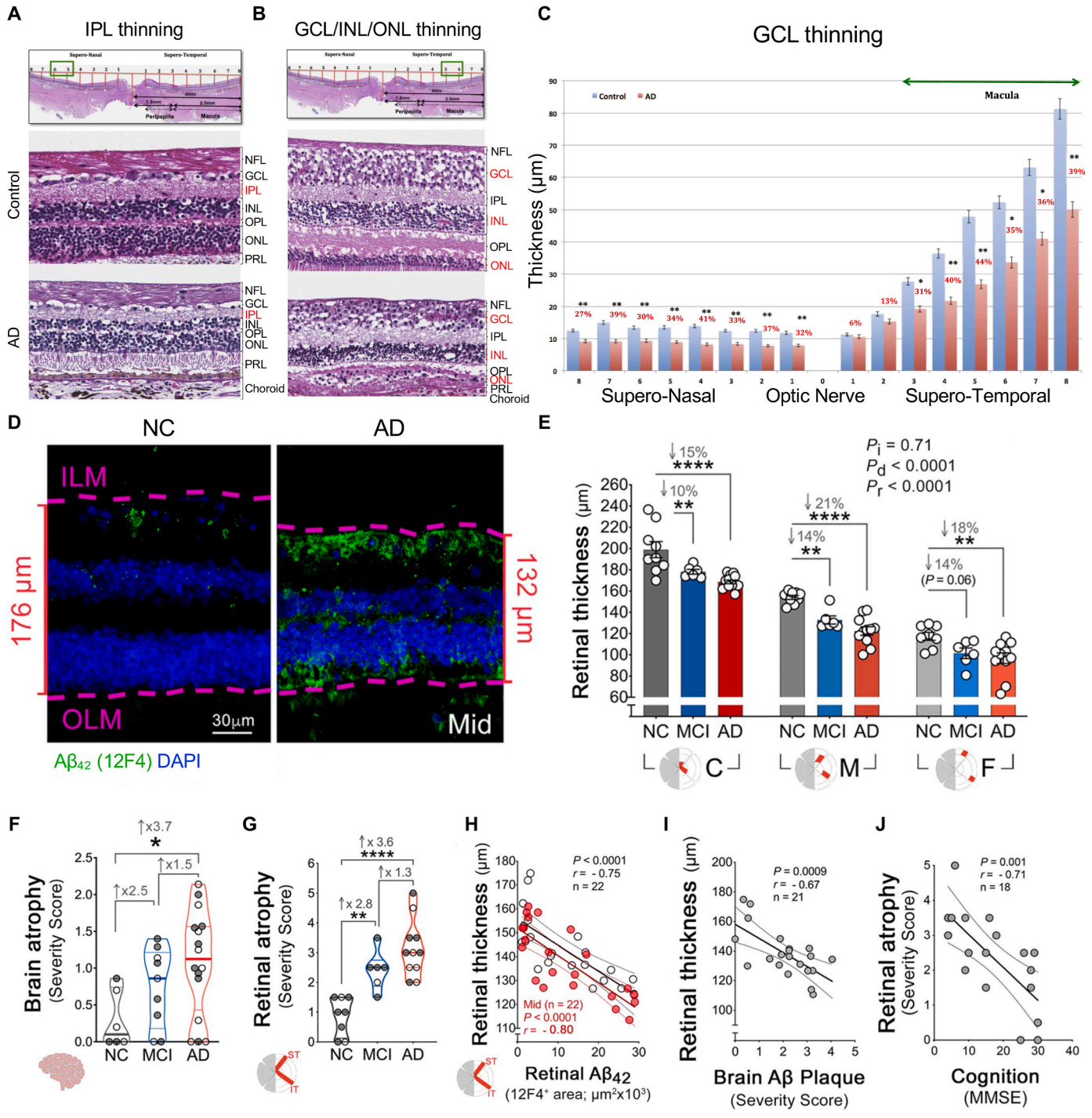

Fig. 9. Histopathological findings of retinal atrophy in MCI and AD patients. (**A-B**) Representative images of retinal cross-sections from human donors with normal cognition (control) and AD dementia stained with hematoxylin (blue, nuclei) and eosin (pink, tissue), illustrating reduced thickness of the (**A**) IPL, and (**B**) GCL, INL, and ONL (red) in AD patients. Retinal analysis was conducted in pre-defined geometric regions, including the superior-nasal and superior-temporal within sectors of ascending distances from the optic nerve. A low magnification view of the retina is shown in the top images with the corresponding magnified retinal region marked in the *green box*. (**C**) Mean GCL thickness across geometrical sectors in AD (red, N = 8) versus control (blue, N = 11) retinas. Error bars denote standard deviation. (**D**) Representative retinal cross-section images immunostained for 12F4^{+}-Aβ_{42} (green) and nuclei (DAPI, blue), demonstrated that along with retinal Aβ_{42} accumulation there is a reduction in tissue thickness in an AD retina (132 μm) versus a NC retina (176 μm). Thickness was measured from the ILM to OLM (purple dashed lines). (**E**) Retinal thickness in the superior- and inferior-temporal retina in predefined subregions, central (C), mid-periphery (M), and far-periphery (F), from patients with AD (N = 11), MCI (N = 6), or NC (N = 8–9). (**F-G**) Severity scores analysis of (**F**) brain AD (N = 16), MCI (N = 9), or NC (N = 6) and (**G**) retinal atrophy in the same cohorts of human donors with AD (N = 11), MCI (N = 6), or NC (N = 8–9). (**H-J**) Pearson's (r) correlation analysis of (**H**) retinal thickness against retinal Aβ_{42}, (**I**) retinal thickness against brain Aβ plaques, and (**J**) retinal atrophy against MMSE cognitive score. Statistics: Data from individual subjects (circles) as well as group means ± SEMs, unless otherwise indicated, are shown. Median, lower, and upper quartiles are indicated on each violin plot. Fold changes are shown in gray. *$P < 0.05$, **$P < 0.01$, ****$P < 0.0001$, by one-way or two-way ANOVA and Tukey's post hoc multiple comparison test. Panels A–C were modified from (Asanad et al., 2019), and Panels D–J were modified from (Koronyo et al., 2023).

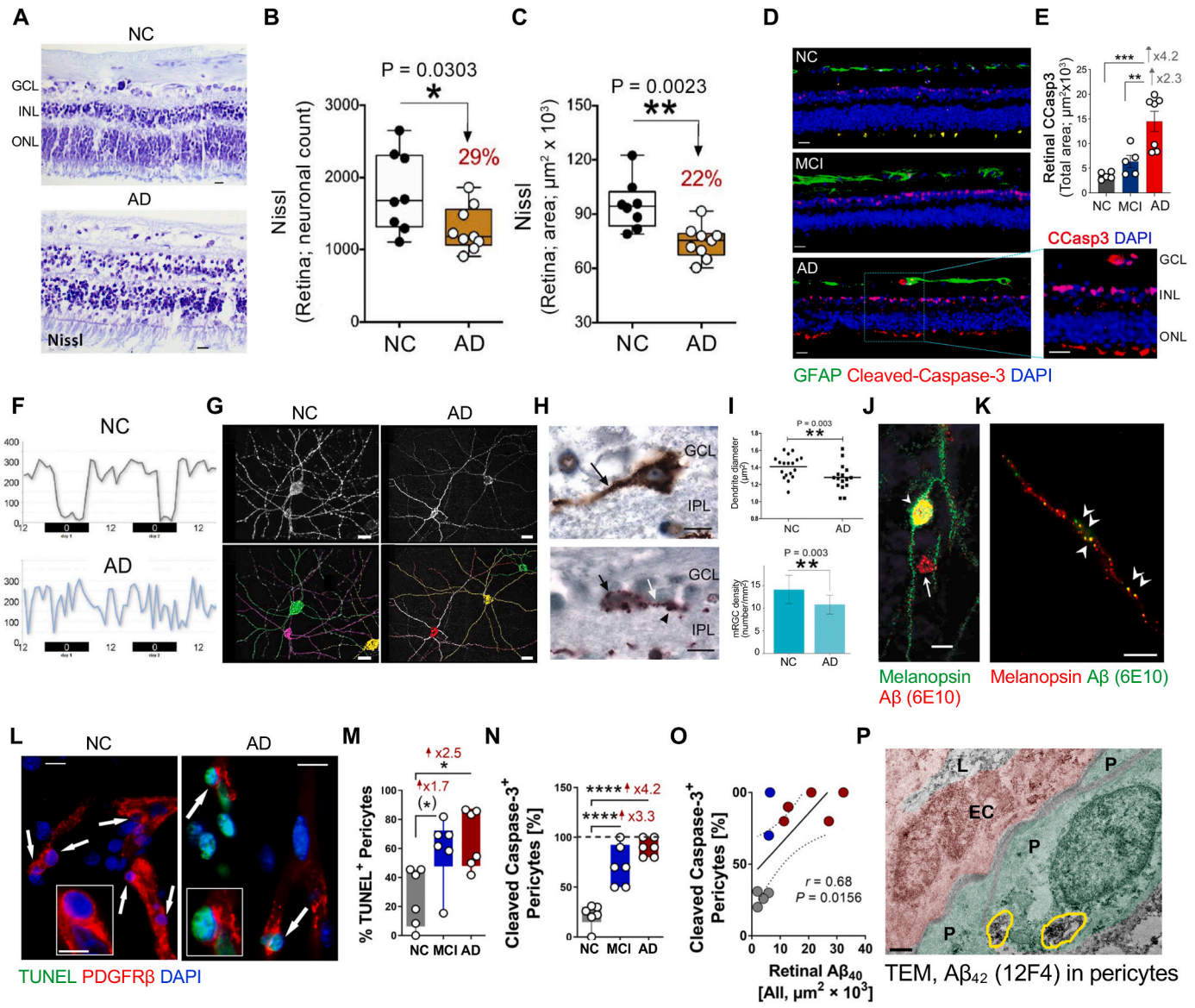

(caption on next page)

potential for retinal vascular targets for AD monitoring and diagnosis. Nevertheless, there remains a substantial lack of understanding on the precise cellular and molecular mechanisms involved in retinal vascular AD pathology, largely due to prior studies focusing on live imaging of retinal vascular structure and blood flow dynamics in AD patients.

To address this gap, our group identified, characterized, quantified, and topographically mapped a set of AD-relevant vascular parameters. We detected significant early increases in vascular $A\beta_{40}$ and $A\beta_{42}$ deposits, alongside the degeneration of pericytes and endothelial tight junctions (TJ) in retinal tissues of patients with MCI and AD compared to age- and sex-matched NC controls (Koronyo et al., 2017; Koronyo-Hamaoui et al., 2011; La Morgia et al., 2016; Shi et al., 2020b, 2023). Retinal vascular Aβ was colocalized both in perivascular spaces and within vessel walls, involving different layers such as the tunica media, tunica adventitia, and tunica intima, within pericytes, the lumen, and outside the basement membrane (Fig. 11) (Koronyo et al., 2017; Shi et al., 2020b). In particular, vascular $A\beta_{40}$ immunoreactivity was increased by 7.2- and 12-fold in the vertical and longitudinal vessels of the AD retina, respectively, compared to the retina of NC controls. Similarly, vascular $A\beta_{42}$ immunoreactivity was 4.4- and 5.6-fold higher in AD retinal vertical and longitudinal vessels. These findings were consistent with the known cerebrovascular Aβ pathology observed in AD patients (Bakker et al., 2016; Bennett, 2001; Vinters, 1987; Vinters and Gilbert, 1983). TEM analysis confirmed the ultrastructure of retinal $A\beta_{42}$ fibrils and protofibrils near the blood vessel basal membrane, on the outer vascular surface adjacent to pericytes, within pericytes, and attached to an endothelial cell surface inside a blood vessel lumen (Koronyo et al., 2017; Shi et al., 2020b).

The BBB is established by endothelial cells firmly joined by TJ proteins forming the vessel walls, together with astrocyte end-feet and supporting pericytes in the basement membrane. Similarly, in the retina, the blood-retinal barrier (BRB) is comprised of an inner barrier with vascular endothelial cells and an outer barrier formed by the retinal pigment epithelium (RPE). Both the BBB and the inner BRB maintain their integrity through the presence of TJ and gap junction proteins, alongside support from pericytes (Cai et al., 2018; Campbell and Humphries, 2012; Zenaro et al., 2017). These components play crucial roles in regulating the selective passage of substances between the blood and the brain or retina, respectively, while preventing the entry of potentially harmful agents. Compromised BBB in AD is considered to be a significant driver of cerebral amyloid deposition, attributed to impaired efflux of Aβ and inadequate clearance through the circulating

Fig. 10. Degeneration of retinal cell types in MCI and AD patients. (**A**) Representative images of Nissl neuronal staining in retinal cross-sections from a definite AD patient and an age- and sex-matched NC subject. Altered retinal neuronal staining is observed in AD patients, including changes in cytoplasmic staining patterns (chromatolysis) in the GCL, INL, and ONL, likely associated with neuronal loss. Scale bar: 20 μm. (**B–C**) Nissl neuronal count and total area in a subset of AD patients (N = 9) and age- and sex-matched NC controls (N = 8). Percent reduction in AD versus NC is indicated in red. (**D**) Representative retinal cross-sections labelled against the early apoptotic marker – cleaved caspase-3 (CCasp3; red), macroglia (GFAP, green), and nuclei (DAPI, blue), from NC (N = 5), MCI (N = 5), or AD subjects (N = 7). The zoomed-in image illustrates the presence of CCasp3$^+$ cells within the GCL and INL. Scale bar: 20 μm. (**E**) Quantitative CCasp3-immunoreactive area in the ST/IT retina. (**F**) Representative actigraphic profiles are shown for an individual with NC and an AD patient; the latter showing a severe disruption in their rest–activity circadian rhythm. (**G**) Morphological analysis of melanopsin retinal ganglion cells (mRGCs) in retinal flatmounts from a NC control and AD patient (upper panel). A 3-dimensional reconstruction of mRGCs created by z-stack images and analysis of cell processes using the filament trace module in Imaris (Bitplane); 3 mRGCs (green, purple, and yellow) and their dendritic processes are visualized (lower panel). Scale bars: 25 μm (NC) and 24 μm (AD). (**H**) Immunostaining for mRGCs in retinal cross-sections from a NC control (upper image) and AD patient (lower image). Note the homogeneous staining of the cell body and dendrite (black arrow) in the NC and the patchy staining of melanopsin in the cell body (black arrow) in the AD retina. A single dendrite can be seen with a focal attenuation (white arrow) and varicosity (black arrowhead). Scale bar: 10 μm (**I**) Dendrite diameter analysis of 18 cells from 3 NC to 16 cells from 4 AD patients (top). The mRGC density (cell number per area) in NC (N = 13) and AD patients (N = 14) (bottom). (**J-K**) Representative images of retinal flatmounts from AD patients demonstrating: (**J**) intracellular Aβ deposition (6E10, red) within mRGC (green; white arrowhead) and an extracellular retinal Aβ deposit (red, white arrow) in the vicinity of mRGCs' neurites. Scale bar: 20 μm; and (**K**) mRGC neurite (melanopsin, red) from an AD retina showing colocalization with Aβ (6E10, green; white arrowheads). Scale bar: 20 μm. (**L-P**) Retinal pericyte apoptosis in MCI and AD patients compared with NC controls. (**L**) Representative images of retinal cross-sections immunolabeled for TUNEL$^+$ apoptotic cells (green), vascular PDGFRβ$^+$ pericytes (red), and nuclei (DAPI, blue). Zoomed-in insets show multiple TUNEL$^+$ pericytes in the AD retina. Scale bar: 10 μm. (**M**) Percent of TUNEL$^+$ pericytes within 10–15 pericytes counted from each retinal cross-section of MCI (N = 6) and AD patients (N = 6) versus NC controls (N = 6). (**N**) Percent cleaved caspase-3$^+$ pericyte within 10–15 pericytes counted from each human donor: AD (N = 6), MCI (N = 6), and NC (N = 6). The dashed line represents the 100% reference point. (**O**) Pearson's (r) correlation between percent cleaved caspase-3$^+$ pericytes and retinal 11A50-B10$^+$Aβ$_{40}$ IR area in a subset of human donors (NC-gray, MCI-blue, AD-red circles) (N = 11). (**P**) Representative TEM image of retinal vertical section from an AD human donor. Retina was pre-stained with anti-Aβ$_{42}$ mAb (12F4) and peroxidase-based DAB. TEM analysis reveals the location and ultrastructure of retinal vascular-associated Aβ deposits (demarcated by yellow shapes). Retinal Aβ$_{42}$ deposits within pericytes (P, green), detected in the cytoplasm and adjacent to mitochondria. Scale bar: 0.5 μm. Endothelial cell (EC, pink) and blood vessel lumen (L, gray) are shown. Statistics: Data from individual subjects (circles) as well as group means ± SD (B, C, I) and means ± SEMs (E, M, N) are shown. Fold changes or percent reductions are also indicated. $^*P < 0.05$, $^{**}P < 0.01$, $^{***}P < 0.001$, $^{****}P < 0.0001$, by one-way or two-way ANOVA and Tukey's post hoc multiple comparison test, or by two-tailed unpaired Student's *t*-test. Panels A–C were modified from (Koronyo et al., 2017), Panels D–E were modified from (Koronyo et al., 2023), Panels F–K were modified from (La Morgia et al., 2016), and Panels L–P were modified from (Shi et al., 2020b) with permission.

blood (Banks et al., 2003; DeMattos et al., 2002; Do et al., 2016; Sweeney et al., 2018; Zhao et al., 2015; Zlokovic et al., 1993). Particularly, BBB impairment in AD can result in faulty transport of Aβ due to alterations in the expression of Aβ transporters. For instance, microvessels in the AD brain exhibit reduced expression of low-density lipoprotein receptor-related protein-1 (LRP-1), a crucial Aβ clearance receptor at the BBB responsible for transporting Aβ out of the brain into the bloodstream (Jaeger et al., 2009; Kim et al., 2016; Sweeney et al., 2018). On the other hand, patients with AD develop increased levels of the receptor for advanced glycation end products (RAGE) in brain microvessels. RAGE transports Aβ in the opposite direction to LRP-1, mediating the re-entry of circulating Aβ into the brain (Sweeney et al., 2018). Animal models of AD exhibit similar expression patterns of increased influx receptor (RAGE) and decreased efflux receptor (LRP-1) for Aβ transport were reported (Do et al., 2016). Furthermore, the expression of the vascular endothelial Aβ transporter phosphatidylinositol binding clathrin assembly protein (PICALM) is diminished in the brains of AD-model mouse, leading to the cessation of Aβ deposit removal to the bloodstream (Zhao et al., 2015). Another important component in regulating vascular function is the capillary pericytes that express platelet-derived growth factor receptor-beta (PDGFRβ). Pericytes are critically involved in blood flow perfusion, vascular remodeling, regression, and stabilization, as well as in the generation and maintenance of blood barriers (Armulik et al., 2011; Bergers and Song, 2005; Hamilton et al., 2010). A significant degeneration of pericytes has been reported in the context of AD, in the mouse brain (Sagare et al., 2023; Zlokovic, 2011), as well as in the retina of AD patients and murine models (Shi et al., 2020a, 2020b), potentially affecting transportation across the endothelial barriers.

Mirroring the AD brain, our investigation of the BRB revealed a significant 32% reduction in the expression of vascular LRP-1 in retinal tissues of AD patients, along with 38% and 72% attenuated vascular (v) PDGFRβ expression and 3.3- and 4.2-fold increased pericyte apoptosis (by CCasp3 marker) in the neurosensory retina of MCI and AD patients, respectively (Shi et al., 2020b). Reduced expression of retinal vPDGFRβ was closely associated with the accumulation of retinal vascular Aβ$_{40}$ and Aβ$_{42}$ deposits. Intriguingly, retinal vPDGFRβ expression levels were inversely correlated with cerebral Aβ-plaque burden and CAA scores, whereas they were directly correlated with cognitive deficits assessed by the Mini-Mental State Examination (MMSE) (Shi et al., 2020b). A more recent study investigating the BRB revealed significant decreases in the expression of endothelial zonula occludens-1 (ZO-1) by 74% and 67% and claudin-5 by 28% and 40% in retinal tissues from MCI and AD patients, respectively, compared to NC controls (Shi et al., 2023). These retinal TJ protein deficiencies significantly correlated with increases in retinal vascular Aβ$_{40}$ deposits, especially in the arteries. Notably, the levels of retinal arterial Aβ$_{40}$ and endothelial claudin-5 were closely associated with CAA severity scores (Fig. 12). Furthermore, retinal ZO-1 deficiency exhibited moderate correlations with various parameters of cerebral AD pathology, including NFTs, neuropil threads, CAA, Braak staging, and ABC scores, as well as with cognitive function (Shi et al., 2023). These findings suggest that certain retinal vascular changes manifest early in the AD continuum and may serve as predictors of CAA severity and AD progression.

Several studies in murine models of AD have demonstrated retinal vascular pathologies, including increased neovascularization (Antes et al., 2015; Biron et al., 2011; El-Darzi et al., 2022). For instance, in the 5xFAD mouse model, El-Darzi et al., observed significant retinal neovascularization that led to disruption of the RPE structure (El-Darzi et al., 2022). In transgenic APP$_{SWE}$/PS1$_{\Delta E9}$ (ADtg) mouse models, we discovered retinal capillary degeneration and attenuated expression of PDGFRβ, accompanied by vascular Aβ deposits, occurring at both young and adult, later-stage ages. These retinal vascular changes correlated with inner BRB damage, including reduced TJ proteins (i.e., claudin-1 and ZO-1), enhanced inflammation (NF-κB p65 phosphorylation), and BRB leakage (Fig. 13) (Shi et al., 2020a). Another preclinical study found that retinal MGnD microglia in the APP$_{SWE}$/PS1$_{L166P}$ murine AD model were associated with increased retinal inflammation, vascular amyloidosis, and BRB impairment (Shi et al., 2022). Increased BRB permeability, measured using fluorescein, Texas-Red-dextran, and FITC-dextran molecules in ADtg mice, was detected as early as 7 months of age (Shi et al., 2020a), earlier than the respective cerebral leakage (Lahiri et al., 2019).

Overall, the findings from studies on both AD patients and murine

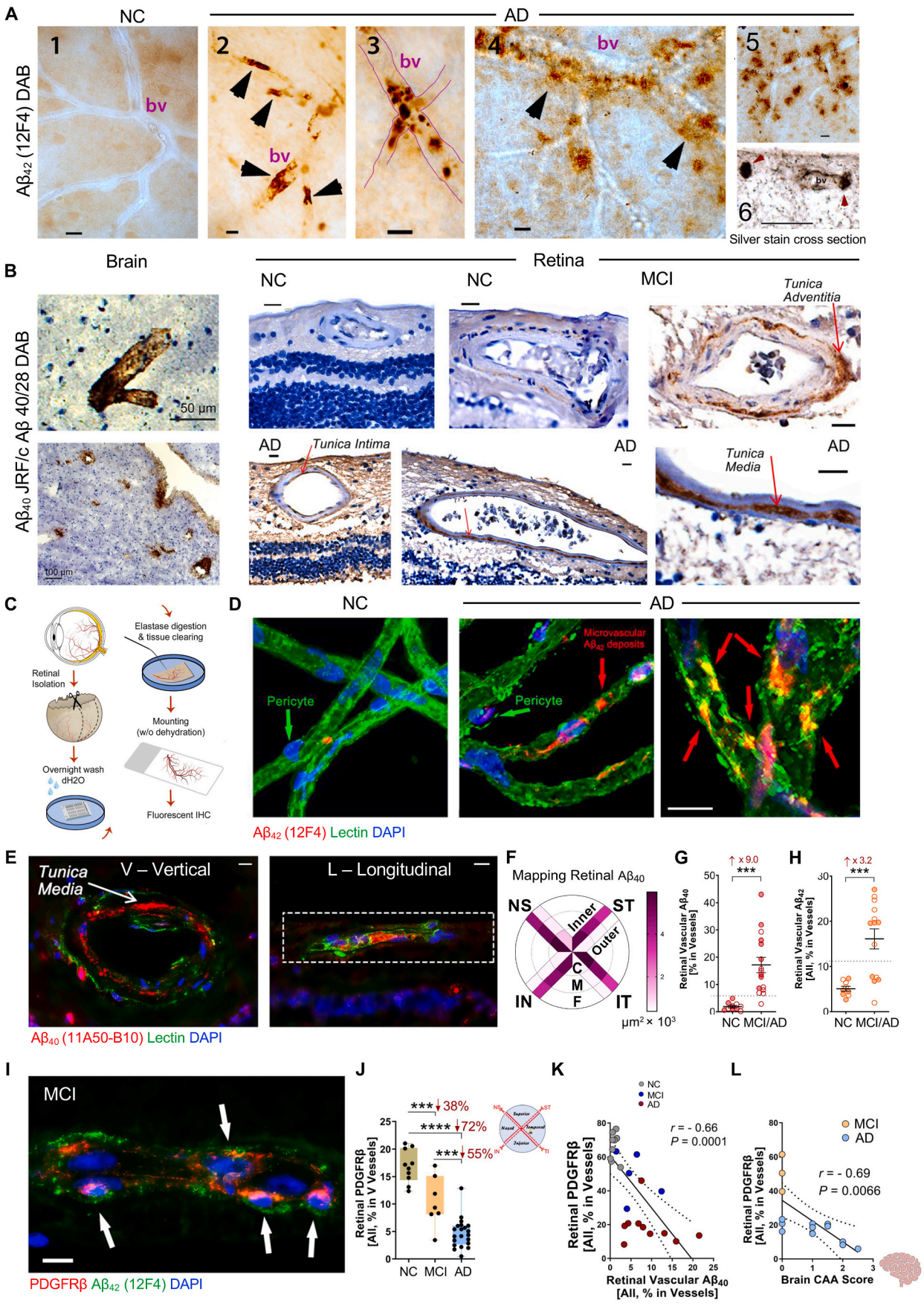

(caption on next page)

Fig. 11. Vascular $A\beta_{40}$ and $A\beta_{42}$ deposits and PDGFRβ deficiency in retinas from MCI and AD patients. (**A**1-5) Representative images of retinal flatmounts from NC and AD subjects stained with $12F4^{+}$-$A\beta_{42}$ and peroxidase-based labeling. The NC retina appears clear of Aβ deposits in blood vessels compared to AD (black arrowheads). Retinal Aβ deposits are apparent inside blood vessels (bv, 2 and 3), as well as peri- and para-vascularly (4 and 5) in AD patients. (**A**6) Gallyas silver staining in a retinal cross-section from an AD patient reveals Aβ deposits near and surrounding a blood vessel (bv). Scale bars: 20 μm. (**B**) Representative images of AD brains and retinal cross-sections immunostained against $A\beta_{40}$ (JRF/cAβ40/28) with DAB labeling and hematoxylin counterstaining in cohorts of AD, MCI, and NC human subjects. Red arrows indicate vascular $A\beta_{40}$ staining in the tunica media, adventitia, or intima; right bottom image is an enlargement of the area indicated by the arrow from the lower middle image. Scale bars: 20 μm, unless otherwise indicated. (**C**) Schematic illustration of modified retinal microvascular network isolation and immunofluorescence staining. After isolation from donor eyes, 7-mm-wide strips were prepared from the temporal hemiretina spanning from the ora serrata to the optic disk. Following fixation, washing, and elastase digestion, the microvascular network is mounted onto slides without dehydration. Immunofluorescence staining was applied on isolated retinal vascular network. (**D**) Representative immunofluorescence images of isolated retinal microvasculature stained for $A\beta_{42}$ (12F4, red), blood vessels (lectin, green), and nuclei (DAPI, blue) in age- and sex-matched human donors with NC and AD. Arrows indicate $A\beta_{42}$ deposits (red arrows) in capillaries of an AD retina, a zoomed-in image (right) shows co-localization of $A\beta_{42}$ within the retinal vascular walls (yellow spots), and retinal pericytes (green arrow). Scale bar: 10 μm. (**E**) Representative immunofluorescence images of retinal cross-sections from AD patients stained for $A\beta_{40}$ (11A50–B10, red) within vertical (V; left) and longitudinal (L; right) blood vessels (lectin, green). Dashed geometric white shapes indicate pre-defined areas for quantitative analysis. Scale bars: 10 μm. (**F**) Mapping of vascular $A\beta_{40}$ in four retinal quadrants, pre-defined C/M/F, and inner/outer retinal subregions. The intensity of the magenta color represents the density of retinal $A\beta_{40}$ burden in each pre-defined geographic region. (**G-H**) Quantitative analyses of percent retinal **(G)** vascular $A\beta_{40}$ IR area in NC control (N = 10) and MCI/AD groups (N = 16) and **(H)** vascular $A\beta_{42}$ IR area in NC control (N = 9) and MCI/AD groups (N = 14). Dotted lines display the suggested threshold separating between the NC control and MCI/AD groups. Males in filled circles and females in clear circles. (**I**) Microscopic image of longitudinal vessel from MCI retina showing vascular $A\beta_{42}$ deposition (green), often colocalized with $PDGFR\beta^{+}$ pericytes (red, white arrows). Scale bars: 10 μm. (**J**) Quantitative analysis of percent retinal PDGFRβ IR area in V vessels from the four quadrants of the retina (ST, IT, IN, NS) in NC (N = 10), MCI (N = 7) and AD (N = 21) retinas. (**K-L**) Pearson's (r) correlation between percent retinal PDGFRβ IR area in sum of V and L blood vessels against **(K)** retinal vascular $A\beta_{40}$ in NC (N = 9), MCI (N = 5), and AD (N = 10) retinas and **(L)** brain cerebral amyloid angiopathy (CAA) scores in the MCI (N = 3) and AD (N = 11) retinas. Statistics: Data from individual subjects (circles) as well as group means ± SEMs are shown. Fold changes and percent reductions are shown in red. $^{***}P < 0.001$, $^{****}P < 0.0001$, by one-way ANOVA with Sidak's post-hoc multiple comparison test or unpaired 2-tailed Student's *t*-test. Panel A was modified from (Koronyo et al., 2017), and Panels B–L were modified from (Shi et al., 2020b) with permission.

models indicate significant impacts on various components of the retinal neurovascular network due to AD-related pathological processes. These studies suggest a complex interplay between AD-associated vascular abnormalities—such as vascular amyloidosis, capillary degeneration, and diminished expression of TJs and PDGFRβ—and subsequent inflammatory responses, glial cell activation, tauopathy, and neurodegeneration. Further investigation is needed to fully understand these connections. Fig. 14 illustrates the key aspects of AD-related vascular and BRB abnormalities observed in postmortem retinas of MCI and AD patients.

2.6. Ocular and brain glymphatic clearance of AD-related pathological hallmarks

The clearance of solute wastes from the brain and retina is of immense importance for normal CNS physiology. Multiple pathways have been identified for the removal of Aβ, including the BBB transport, degradation, interstitial fluid (ISF) bulk flow, and CSF absorption. In contrast, tau is mainly cleared through intracellular degradation (Tarasoff-Conway et al., 2015). In AD pathogenesis, the clearance mechanisms of Aβ and pTau are impaired, leading to abnormal deposition of Aβ and NFTs (Harrison et al., 2020; Mawuenyega et al., 2010; Zuroff et al., 2017). The recently described glymphatic system is responsible for waste removal from para-arterial to para-venous spaces via aquaporin-4 (AQP4) water channels in the astrocytic endfeet. This system consists of three components: CSF influx, CSF–ISF exchange, and CSF–ISF movement into the perivenous space of deep cerebral veins. Waste can then recirculate with the CSF or be absorbed into the lymphatic system (Nedergaard, 2013). The glymphatic system facilitates efficient clearance of interstitial solutes, including Aβ and pTau, from the brain (Harrison et al., 2020; Nedergaard, 2013; Wostyn et al., 2015). This accounts for 55–65% of extracellular Aβ clearance and may also play a role in non-endocytosed tau clearance (Tarasoff-Conway et al., 2015).

A mouse model of tauopathy suggests that dysfunctional glymphatic system clearance can exacerbate or even induce pathological accumulation of tau (Harrison et al., 2020). Additionally, AQP4 channels were found to be a major driver of the glymphatic clearance system, allowing for the elimination of extracellular tau from the brain to the CSF and subsequently to deep cervical lymph nodes, resulting in tau clearance and neuroprotection (Ishida et al., 2022). Of note, increased CAA in a mouse model of AD was found to contribute to the deterioration of arterial structure and function, ultimately impeding perivascular Aβ removal (Kim et al., 2020), possibly due to a compromised glymphatic system. Reduced glymphatic flow in the ADtg mouse brain was associated with wide-spread astrogliosis and amyloid-related obstruction, potentially hindering the normal routes of glymphatic transport (Ben--Nejma et al., 2023). The link between an impaired glymphatic clearance system, brain Aβ accumulation, and memory deficits was reinforced by other studies, underscoring the critical role of glymphatic clearance in AD pathogenesis (Smith et al., 2019; Xu et al., 2015).

As the role of the glymphatic clearance system in the AD brain is increasingly explored, the ocular glymphatic system remains a relatively new topic, and its mechanisms are not well understood. Nonetheless, a few studies have shown its involvement in different retinal diseases, such as glaucoma, age-related macular degeneration, uveitis, and macular edema (Petzold, 2016; Uddin and Rutar, 2022; Wostyn et al., 2016). It is believed that the ocular and brain glymphatic fluid transport systems share similar characteristics pertaining to waste clearance. Indeed, a recent study has elucidated a novel finding regarding the ocular glymphatic system: the posterior segment of the eye (retina) exhibits its own distinct lymphatic drainage pathway, anatomically integrated with the CNS's meningeal lymphatic network and converging at the deep cervical lymph nodes. In particular, the lymphatics of the optic nerve facilitate this connection, establishing a direct conduit between the retina and the brain. Such interconnectivity facilitates synchronized immune responses, with a mechanism for coordinated immune surveillance, potentially priming the brain to respond to impending threats (Yin et al., 2024).

The glymphatic fluid transport system comprises a CSF influx along the periarterial space, an efflux path along the perivenous space, and a final collection site by the dural and cervical lymphatic vessels (Wang et al., 2020a; Wostyn et al., 2017). Recent findings by Wang et al., suggest that the glymphatic pathway, facilitated by astrocytic AQP4 water channels in the retina, enables the removal of metabolites and fluid from the intraocular space, as well as the efflux of Aβ tracers through the optic nerve and meningeal lymph vessels (Wang et al., 2020a). Radial Müller cells spanning the retina, as well as fibrous astrocytes along the optic nerve, express abundant AQP4, and the expression of AQP4 in astrocyte endfeet is diminished in AD pathogenesis (Silva et al., 2021). Furthermore, extensive Müller cell degeneration has been reported in the AD retina (Xu et al., 2022). These studies suggest that retinal astrocytes and Müller glia may play an

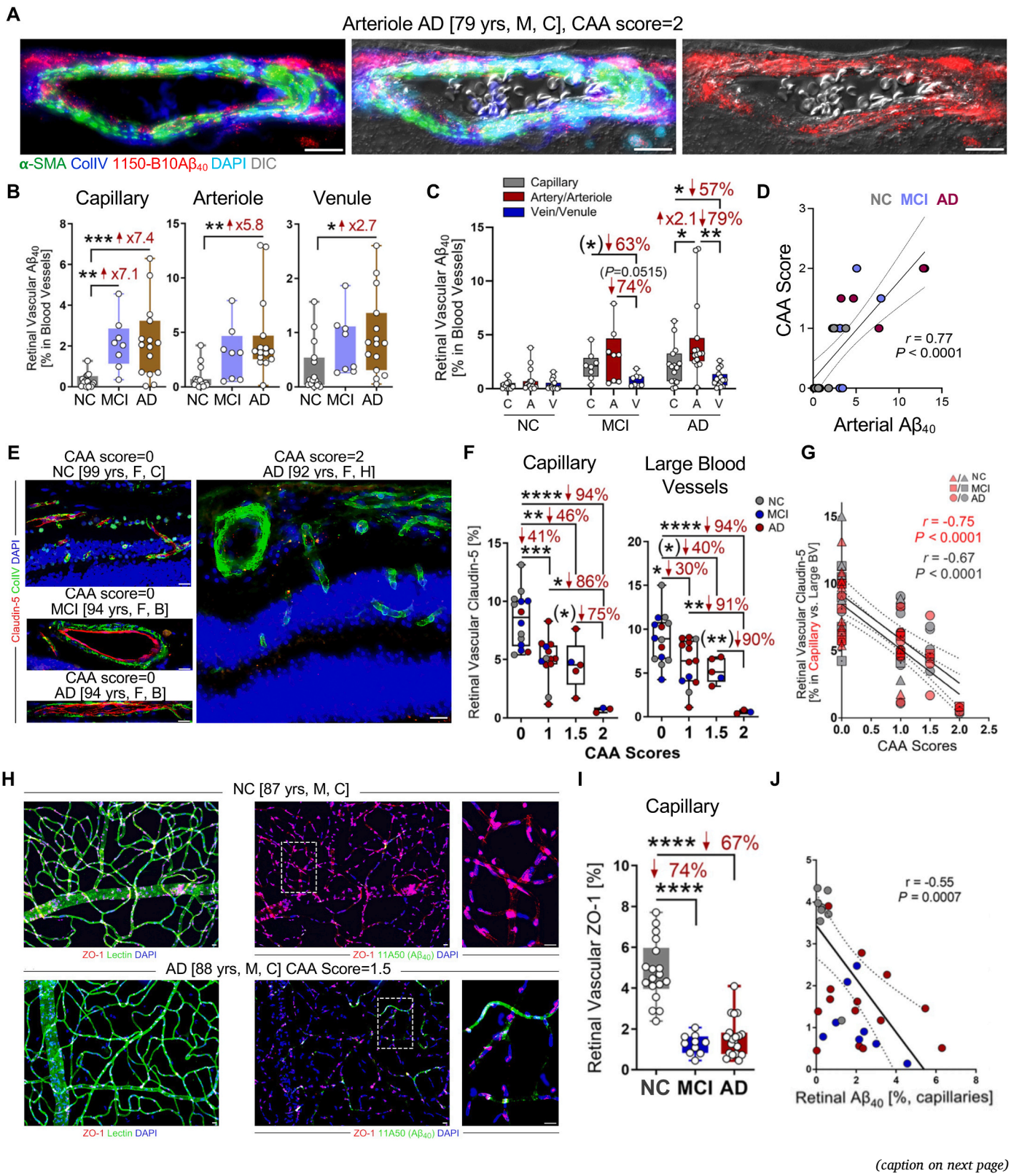

(caption on next page)

important role in clearing retinal waste products and maintaining normal eye physiology.

It has been speculated that Aβ could be cleared from the retina via perivascular transport, and pathological changes in AD may interfere with glymphatic flow, leading to neurotoxicity due to Aβ accumulation (Wostyn et al., 2015). During AD pathogenesis, amyloid build-up along the blood vessels may reduce the large, low-resistance perivascular spaces necessary for glymphatic flux (Hughes et al., 2013), thus creating a vicious cycle of Aβ accumulation, neuronal death, and impaired glymphatic drainage. Our group recently demonstrated increased

Fig. 12. Arterial Aβ$_{40}$ deposition and tight junction deficits in retinas from MCI and AD patients associate with CAA severity. (**A**) Representative immunofluorescent images of retinal cross-sections from an AD patient stained for α-smooth muscle actin (α-SMA, green), collagen IV (ColIV, blue), vascular 11A50-B10^{+}-Aβ$_{40}$ (red), and nuclei (DAPI, cyan), alongside imaging of the differential interference contrast (DIC) channel. Retinal Aβ$_{40}$ deposition is often observed within arteriole walls. Scale bars: 20 μm. (**B**) Quantitative analysis of retinal vascular Aβ$_{40}$ immunoreactive area in retinal blood vessel types—capillaries, arterioles, and venules—stratified by diagnostic groups: NC (N = 15), MCI (N = 8), and AD (N = 15). (**C**) Quantitative analysis of retinal vascular Aβ$_{40}$ immunoreactive area stratified by blood vessel type within the diagnostic group in the same cohort. (**D**) Pearson's (r) correlations between retinal arterial Aβ$_{40}$ versus brain CAA scores (N = 25). (**E**) Representative images of retinal cross-sections immunostained for endothelial tight junction protein, claudin-5 (red), ColIV (green), and DAPI (blue) in NC, MCI, and AD subjects with different degrees of CAA severity scores. Scale bars: 20 μm. (**F**) Percent retinal endothelial claudin-5 IR area separately in capillaries and large blood vessels from all experimental groups stratified by CAA severity scores (N = 35). (**G**) Pearson's (r) correlation between claudin-5 in retinal capillaries (red) and large blood vessels (gray) and CAA severity scores (N = 35). (**H**) Representative images of isolated retinal microvascular networks immunostained for endothelial tight junction zonula occludens protein-1 (ZO-1, red) and lectin for blood vessels (green) or ZO-1 (red) and 11A50-B10^{+} Aβ$_{40}$ (green) and DAPI (blue), in an AD patient and in age- and sex-matched NC control. Scale bars: 20 μm. Right panels are zoomed-in images from regions surrounded by dashed lines showing increased capillary Aβ$_{40}$ deposits with reduced ZO-1 expression in the AD retina. (**I**) Percent retinal endothelial ZO-1 IR area in capillaries of NC (N = 22), MCI (N = 10), and AD (N = 21) retinas. (**J**) Pearson's (r) correlation between retinal Aβ$_{40}$ and ZO-1 in capillaries (N = 30). Statistics: Data from individual subjects (circles) as well as group means ± SEMs are shown. Fold changes and percent reductions are shown in red. $^{*}P < 0.05$, $^{**}P < 0.01$, $^{***}P < 0.001$, $^{****}P < 0.0001$, by one-way ANOVA, or two-way analysis of variance with Tukey's post hoc multiple comparison. All panels were modified from (Shi et al., 2023) with permission.

deposition of retinal vascular and perivascular Aβ in ADtg mice as well as in the retina of MCI and AD patients compared to cognitively normal subjects (Shi et al., 2020a, 2020b, 2023). Retinal Aβ deposits were found in perivascular regions near pericytes, in the lumen adjacent to endothelial cells, inside pericytes, and within the vascular wall (tunica media, tunica adventitia, and tunica intima). These findings suggest that retinal amyloid deposition around and inside blood vessels may impede ocular glymphatic drainage, resulting in aberrant amyloid accumulation. In particular, the failure of Aβ clearance via the intramural peri-arterial drainage (IPAD) pathway in the brain is believed to be central to the development of CAA, resulting in neuronal and homeostatic dysfunctions often associated with cognitive impairment (Kelly et al., 2024). Regarding the retina, Shi et al., demonstrated increased Aβ$_{40}$ deposition in the tunica media of retinal arteries compared to venules and capillaries in patients with MCI and AD, suggesting compromised Aβ clearance via the IPAD system extending to the retina (Shi et al., 2023). Further research is warranted to explore the role of the ocular glymphatic system in retinal amyloid accumulation and vascular pathology, as well as its potential connections to the glymphatic system in the brain.

3. Clinical ophthalmic modalities to detect and monitor AD

The growing recognition of AD pathology in the retina has motivated investigators to develop various retinal imaging modalities for AD diagnosis and monitoring. Experimental retinal imaging of AD-specific amyloid deposits along with microvasculature and neuronal structure imaging hold promise for large-scale screening of at-risk populations and for monitoring responses to AD therapies. Diverse ophthalmic imaging techniques, such as ocular fundus imaging, scanning laser ophthalmoscopy, OCT, OCTA, as well as hyperspectral and multimodal imaging have been utilized to evaluate the hallmarks and other pathological processes of AD in the retina (summarized in Table 1).

3.1. Imaging of retinal degeneration in AD patients

A growing number of studies using cross-sectional imaging with OCT or OCTA have revealed structural abnormalities and neurodegenerative changes in the AD retina, including at stages preceding clinical disease manifestation [(Bulut et al., 2018; Cunha et al., 2016a; Ferrari et al., 2017; Janez-Escalada et al., 2019; Kromer et al., 2014; Parisi et al., 2001; Polans et al., 2017; Polo et al., 2017; Rotenstreich et al., 2022; Salobrar-Garcia et al., 2019); reviewed in (Doustar et al., 2017)]. These studies have shown significant thinning of the RNFL (Asanad et al., 2020; Ashraf et al., 2023; Chan et al., 2019; Chen et al., 2023; Coppola et al., 2015; den Haan et al., 2017; Ferrari et al., 2017; Hedges et al., 1996; Janez-Escalada et al., 2019; Kim et al., 2022; Kromer et al., 2014; Mejia-Vergara et al., 2020; Parisi et al., 2001; Polo et al., 2017; Salobrar-Garcia et al., 2019), the GCL and OPL (Salobrar-Garcia et al., 2019), the GCL and IPL (Ferrari et al., 2017; Janez-Escalada et al., 2019), the total retina and retinal layers including the RNFL, GCL, IPL, INL, and the outer segment layers (Janez-Escalada et al., 2019), as well as macular degeneration (Polo et al., 2017) in AD patients [reviewed in (Cunha et al., 2016a; Doustar et al., 2017; Parisi, 2003)]. Aside from OCT, analysis of blue-light high-resolution fundus photography in AD patients also indicates thinner RNFL, higher cup-to-disc ratio, and either diffuse optic nerve atrophy or temporal pallor, with a correlation between AD Assessment Scale scores and changes in the optic nerve head (Hedges et al., 1996; Tsai et al., 1991). However, these changes are not specific to AD, as they can also manifest in other ocular and neurodegenerative diseases. Additionally, they may stem from age-related axonal loss in the optic nerve (Harwerth et al., 2008; Kim et al., 2005; Lu et al., 2010).

Of note, a few studies have failed to demonstrate significant changes in retinal thickness among MCI or AD patients compared to healthy controls (Jentsch et al., 2015; Shin et al., 2021). This discrepancy may stem from various factors, including the lack of standardization and harmonization of ophthalmic devices, differences in image processing and analytical methods, small sample sizes, variations in disease stage, diverse study populations concerning ethnicity, sex and age, absence of AD biomarker confirmation, and disparities in inclusion/exclusion criteria. Moreover, the absence of consideration for other comorbidities could significantly influence results, given that neurodegeneration occurs in multiple neurological and ocular conditions, underscoring the necessity to address these factors in future studies.

Nevertheless, most meta-analysis studies utilizing OCT have indicated significant structural changes in the MCI and AD retina. A meta-analysis of OCT studies, involving 380 AD and 68 MCI patients and 293 healthy controls, showed a marked decline in the mean RNFL thickness in all four quadrants in MCI, and to a larger extent, in AD patients compared to controls (Coppola et al., 2015). Thomson et al., systematically reviewed five OCT imaging studies including 214 MCI eyes and 421 healthy control eyes and showed a statistically significant thinning of the mean RNFL in MCI compared to controls (Thomson et al., 2015). In another meta-analysis study by den Haan and colleagues, which included 25 studies and involved 887 AD patients, 216 MCI patients, and 864 healthy controls, significant reductions in peripapillary RNFL thickness were observed among MCI and AD patients, while total macular thickness was notably decreased in AD patients compared to healthy controls (den Haan et al., 2017). A subsequent meta-analysis study involving a human cohort comprising 1257 AD patients, 305 MCI patients, and 1460 controls observed significant differences in various retinal atrophy parameters, such as GC-IPL thickness, ganglion cell complex thickness, macular volume and thickness, peripapillary RNFL thickness, and choroidal thickness, between AD patients and control subjects (Chan et al., 2019). However, mixed results were obtained when comparing these parameters between MCI and control subjects. For example, while total RNFL, macular GC-IPL, and peripapillary RNFL were generally thinner in MCI patients as compared to

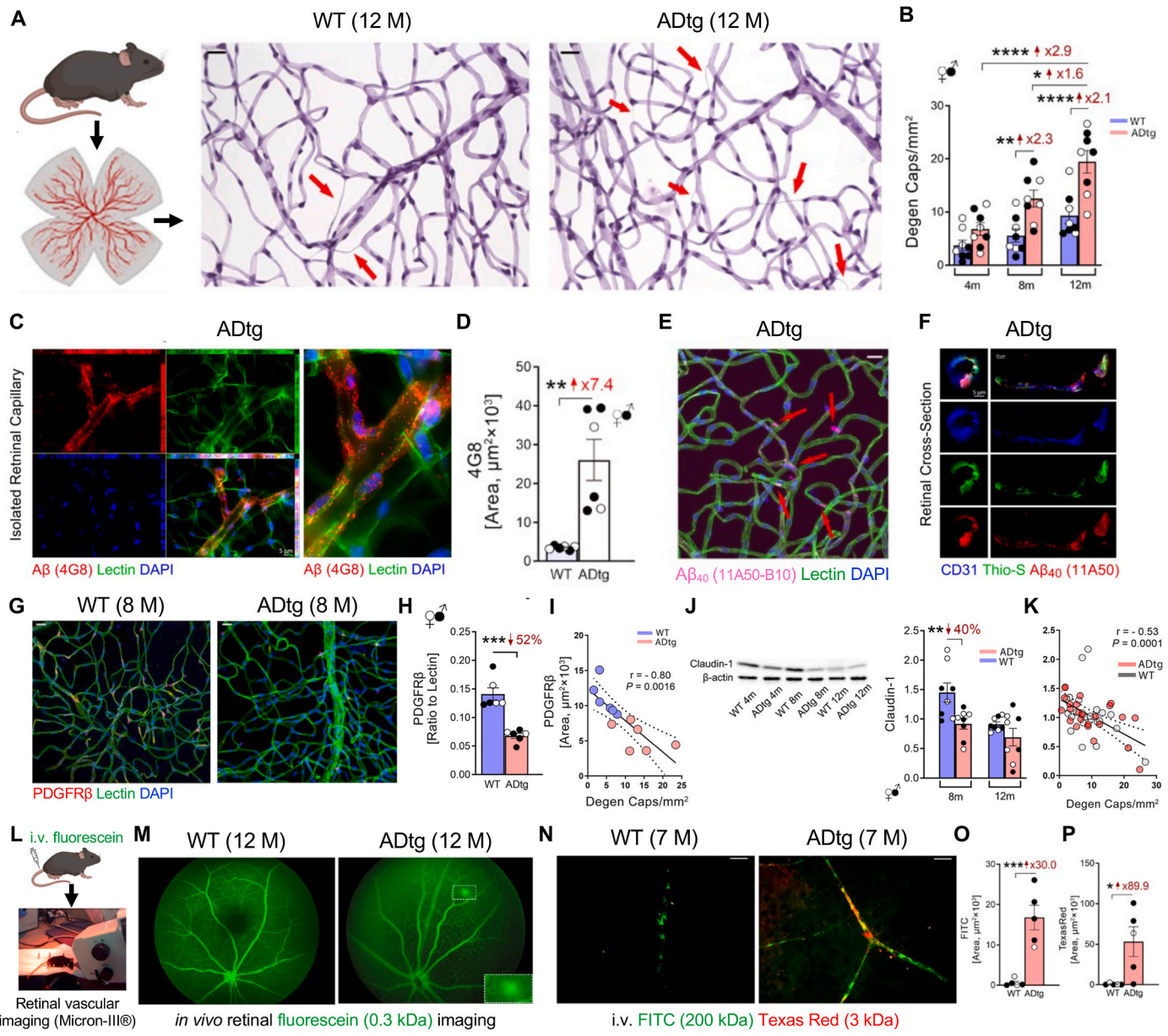

Fig. 13. Retinal vascular abnormalities in transgenic murine models of AD. (**A**, left) Illustration of mouse retinal flatmount isolation. (**A**, middle-right) Representative images of periodic acid-Schiff (PAS)-stained, hematoxylin-counterstained isolated retinal microvasculature from 12-months (M)-old transgenic $APP_{SWE}/PS1_{\Delta E9}$ (ADtg) mice and matched non-tg WT littermates. Acellular degenerated retinal capillaries are indicated by red arrows. Scale bars: 20 µm. (**B**) Number of degenerated retinal capillaries (Degen Caps) in WT (N = 8) and ADtg (N = 8) mice by age groups of 4-, 8-, and 12- months. (**C**) Representative fluorescence image of the isolated retinal microvasculature immunostained for Aβ (4G8, red), blood vessels (lectin, green), and nuclei (DAPI, blue) in an 8-month-old ADtg mouse. Aβ signals were observed in retinal vessel walls and vascular cells. (**D**) Vascular $4G8^{+}$ Aβ IR area in WT (N = 6) versus ADtg (N = 6) mice. (**E**) A representative image of isolated retinal microvasculature network from an 8-month-old ADtg mouse immunostained for $A\beta_{40}$ (11A50-B10, magenta), blood vessels (lectin, green), and nuclei (DAPI, blue). Scale bar: 20 µm. (**F**) Representative fluorescent images of a retinal cross-section immunolabelled for blood vessels (CD31, blue), fibrillar Aβ with thioflavin-S (Thio-S, green), and $A\beta_{40}$ (11A50-B10, red) in an 8-month-old ADtg mouse. Images show both vertical (left) and longitudinal (right) blood vessels. (**G**) Representative fluorescence images of isolated retinal microvasculature immunostained for pericytes (PDGFRβ, red), blood vessels (lectin, green), and nuclei (DAPI, blue) in ADtg and WT littermate mice. Scale bars: 20 µm. (**H**) Quantitative analysis of the ratio between PDGFRβ IR area and lectin IR area in each microscopic field of isolated retinal microvasculature from ADtg (N = 6) versus WT (N = 6) littermate controls. (**I**) Pearson's (r) correlation between degenerated retinal capillary count and PDGFRβ IR area (N = 12). (**J**, left) Representative Western blot (WB) gel of claudin-1 levels and β-actin control in retinal protein lysates from ADtg mice and WT littermate controls. (**J**, right) Densitometric analyses of WB protein bands of retinal claudin-1 normalized to β-actin control in 8- and 12-month-old ADtg (N = 8) versus WT (N = 8) mice. (**K**) Pearson's (r) correlation between degenerated retinal capillary count and the densitometric analysis of retinal claudin-1 levels as assessed by WB. (**L-M**) Illustration of the procedure and live noninvasive retinal vascular imaging following i.v. injection of fluorescein dye in 12-month-old ADtg and WT mice. (**L**) A Micron-III® rodent retinal microscope was used to visualize retinal blood vessels. (**M**) In vivo fluorescein imaging in a WT mouse shows intact retinal microvasculature, whereas retinal imaging in an ADtg mouse shows retinal microvasculature leakage. Inset image shows the magnified view of fluorescein leakage. (**N**) Representative images of retinal flatmounts obtained from a 7-month-old WT and ADtg mice that received i.v. tail injections of FITC-dextran (green) and Texas Red-dextran (red). Quantitative analysis of (**O**) FITC- or (**P**) Texas Red-fluorescence area in each microscopic field of retinal flatmounts from WT (N = 5) versus ADtg (N = 5) mice. Statistics: Data from individual mouse (circles) as well as group means ± SEMs are shown. Fold changes and percent reductions are shown in red. $^{*}P < 0.05$, $^{**}P < 0.01$, $^{***}P < 0.001$, $^{****}P < 0.0001$, by two-way ANOVA with Sidak's post-hoc multiple comparison test or unpaired two-tailed Student's *t*-test. All panels were modified from (Shi et al., 2020a) with permission.

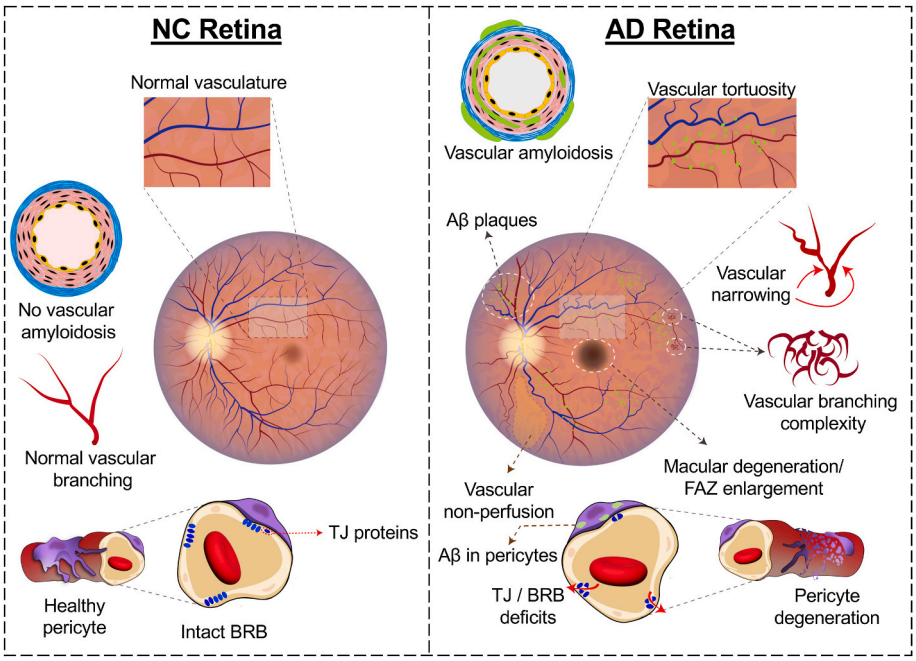

Fig. 14. Schematic summary of retinal vascular abnormalities in MCI and AD patients. Illustration depicting a myriad of vascular abnormalities in the retina of MCI and AD patients, as described by a growing number of histological and in-vivo imaging studies. Retinal vascular changes observed in the AD retina include vascular amyloidosis, predominantly accumulation of $A\beta_{40}$ in retinal peri-vascular space and within arterial walls, tortuosity, dimeter reduction (thinning), abnormal vascular branching complexity, enlarged foveal avascular zone (FAZ), vascular non-perfusion or decreased blood flow, pericyte degeneration, and BRB disruption with loss of tight junction (TJ) proteins. Such changes in retinal vasculature may ultimately lead to functional impairments observed in AD patients. Green signals and dots indicate Aβ deposits in the AD retina.

controls, the differences did not reach statistical significance. Nevertheless, nasal RNFL thickness was significantly reduced in MCI patients compared to the control group (Chan et al., 2019). A later OCT meta-analysis study that pooled data from 17 studies comprised of 622 MCI and 1154 control subjects, reported significant RNFL thinning in MCI patients compared to controls (Noah et al., 2020). Similarly, another meta-analysis study including 15 reports on MCI patients and healthy controls, found that among the patients about 60% showed significant RNFL thinning or reduced macular volume, and 50% showed a significant thinning of macular GCL-IPL complexes (Mejia-Vergara et al., 2020). This study demonstrated substantial heterogeneity in macular volume and RNFL thinning in these patients compared to the control subjects.

A recent meta-analysis study involving 4802 participants with clinically diagnosed patients with AD and MCI, or NC controls, revealed a significant correlation between retinal thickness, in particularly the RNFL thickness, and hippocampal atrophy (Chen et al., 2023). Whole retinal thickness was significantly correlated with hippocampal volume not only in AD dementia, but especially in MCI, despite a substantial heterogeneity in the structural parameters and the imaging methods among the different studies (Chen et al., 2023). Consistent with prior findings, Ashraf et al., conducted a meta-analysis of 38 studies involving 2404 patients and reported a decrease in retinal thickness among AD patients with confirmed brain Aβ (Ashraf et al., 2023). The thinning of the peripapillary and macular RNFL in AD patients was notably more pronounced in the superior quadrant of the retina compared to the inferior quadrant (Ashraf et al., 2023), notwithstanding the considerable heterogeneity across multiple studies in this analysis. The variability in retinal thickness among these patients, particularly in the MCI stage, may derived from two contrasting processes: heightened gliosis and inflammation, which can increase retinal thickness, alongside neurodegeneration, resulting in retinal atrophy and thinning. These intricate pathological mechanisms call for the adoption of precise molecular imaging markers to track AD pathology in the retina. Nevertheless, despite the use of various commercially available OCT devices, retinal thickness changes in AD patients were nearly universal. Further standardization is crucial for OCT measurements as biomarkers for monitoring the AD continuum.

It is important to recognize that retinal degeneration, including RNFL thinning, does not appear to be specific to AD. RNFL thinning has been observed in normal aging (Celebi and Mirza, 2013), and in other diseases such as glaucoma (Lee et al., 2019; Miki et al., 2014), multiple sclerosis (Al-Mujaini et al., 2021), stroke (Wang et al., 2014; Zhang et al., 2020), brain atrophy (Shi et al., 2019), epilepsy (Balestrini et al., 2016), progressive supranuclear palsy (Woo et al., 2022), as well as fibromyalgia (Garcia-Martin et al., 2016b) and thalassemia (Datta et al., 2020). Hence, for enhanced diagnostic accuracy in AD, relying solely on a neurodegenerative structural marker like RNFL thinning seems insufficient, further warranting confirmation with an AD-specific biomarker, such as Aβ.

3.2. *Retinal amyloid imaging in AD patients*

Demonstration of Aβ deposits in retinal tissues from patients with AD has transformed the field of AD retinal biomarkers. The optical accessibility inherent to the eye has inspired the exploration of non-invasive retinal imaging modalities. With their cost-effectiveness and high spatial resolution, these techniques enable the detection of amyloid deposits in a clinically feasible manner, thus potentially facilitating future early diagnosis and monitoring of AD. The in vivo imaging of retinal curcumin-labelled amyloid deposits was initially developed and demonstrated by our group in murine models of AD (Koronyo-Hamaoui et al., 2011). Subsequently, retinal amyloid imaging was feasible in living AD patients by utilizing a modified confocal scanning laser ophthalmoscope (cSLO) with a wide-angle view and oral administration of highly bioavailable Longvida® curcumin (Koronyo et al., 2017). Curcumin is a phytopolylphenol fluorophore that binds to Aβ fibrils and oligomers with high affinity and specificity (Kumaraswamy et al., 2013; Masuda et al., 2011; Mutsuga et al., 2012; Ryu et al., 2006; Yanagisawa et al., 2010, 2011). Importantly, we revealed a significant increase in the

Table 1
Ophthalmic imaging modalities utilized in AD patients.

Imaging modalities	Applications	Findings	Advantages	Limitations	References
OCT/SD-OCT	• Distinct cell layer thickness •Optic nerve (ON) fiber & corneal features •Two & three-dimensional cross-sections	•RNFL Thickness: - Reduced in various quadrants & macula in aMCI & AD dementia -Differentiated healthy subjects from AD -Correlated with cognitive performance -Thinner RNFL linked to increased dementia risk, including AD -Reduced in LBD & PD patients •Peripapillary RNFL Analysis: -Most studies support its use as a marker for cognitive impairment or discriminating between cognitively normal & impaired groups •Macular Volume: -Reduced macular volume in AD -Increased macular volume in aMCI -Correlated with MMSE •Inner & Outer Layer Thickness: -Thinner layers (GCL, INL, IPL, ONL) in MCI & AD -Morphological changes in cognitively unimpaired carriers of FAD mutations •Choroidal Thickness: - Reduced in MCI & AD	•Noninvasive imaging •Eye-safe near-infrared or visible-light •No contact required •Sub-surface images •Micrometer-level depth resolution •Rapid & accurate imaging •Direct visualization of tissue morphology •Full-depth scan in a single exposure	•Susceptible to ocular opacity (*e.g.,* cataracts), vitreous hemorrhages, & dense cataracts •No visualization of single cells •Limited to imaging 2 mm below the surface •Limited field of view	(Almeida et al., 2019; Armstrong et al., 2021; Asanad et al., 2020; Asanad et al., 2019; Ascaso et al., 2014; Bayhan et al., 2015; Berisha et al., 2007; Chaitanuwong et al., 2023; Cheung et al., 2015; Choi et al., 2016; Chua et al., 2022; Cipollini et al., 2020; Coppola et al., 2015; Cunha et al., 2017a; Cunha et al., 2017b; Cunha et al., 2016a; Cunha et al., 2016b; den Haan et al., 2019; Farzinvash et al., 2022; Ferrari et al., 2017; Galvin et al., 2021; Gao et al., 2015b; Garcia-Martin et al., 2016a; Garcia-Martin et al., 2014; Gharbiya et al., 2014; Girbardt et al., 2021; Iseri et al., 2006; Janez-Escalada et al., 2019; Jindahra et al., 2020; Kesler et al., 2011; Kim et al., 2021a; Kim et al., 2022; Kim and Kang, 2019; Kirbas et al., 2013; Kromer et al., 2014; Kwon et al., 2017; La Morgia et al., 2023; Larrosa et al., 2014; Lian et al., 2020; Liu et al., 2015; Lopez-de-Eguileta et al., 2020; Lopez-de-Eguileta et al., 2019; Lu et al., 2010; Marquie et al., 2020; Marziani et al., 2013; Mathew et al., 2023; Mei et al., 2021; Moreno-Ramos et al., 2013; Moschos et al., 2012; Mutlu et al., 2018; Paquet et al., 2007; Parisi et al., 2001; Rotenstreich et al., 2022; Salobrar-Garcia et al., 2019; Salobrar-Garcia et al., 2015; Sanchez et al., 2020; Sanchez et al., 2018; Santangelo et al., 2020; Santos et al., 2018; Sen et al., 2020; Shao et al., 2018; Shi et al., 2014; Sun et al., 2024; Tao et al., 2019; Trebbastoni et al., 2016; van de Kreeke et al., 2019; van der Heide et al., 2023a; van der Heide et al., 2023b; Wang et al., 2022b; Yoon et al., 2019; Zabel et al., 2019a)
OCTA	•Two & three-dimensional visualization of retinal & choroidal microvasculature •Blood flow rate	•Vascular/Capillary Densities: - Reduced retinal vascular network, superficial & deep vascular plexus, perifoveal capillary density, macular vessel density in MCI & AD - Larger mid-peripheral CFZs in cognitively unimpaired older adults at high risk for AD - Microvascular alterations in MCI, a putative warning sign for AD progression - Whole & parafoveal superficial vascular plexus vessel density inversely associated with AD - FAZ enlargement in preclinical AD & AD dementia	•Shorter acquisition time •Noninvasive imaging •No dye injection required •Quantitative analysis of retinal vessels vs. the conventional angiography •Cross-sectional vessel structure, also of retinal capillaries •Imaging of all retinal vasculature layers	•Limited field of view •Media opacities can lead to signal attenuation & shadowing artifacts •Projection artifact reflected by deeper layers •Segmentation errors •Motion artifact & motion sensitivity •Insensitive to leakage •Lower axial resolution for longer λ (~1050 nm)	(Arthur et al., 2023; Biscetti et al., 2021; Bulut et al., 2018; Chaitanuwong et al., 2023; Chiara et al., 2022; Cipolla et al., 2023; Di Pippo et al., 2023; Hu et al., 2023b; Hui et al., 2021; Jiang et al., 2018; Katsimpris et al., 2022; Lahme et al., 2018; Li et al., 2021; Ma et al., 2023; Mei et al., 2021; Moon et al., 2023; O'Bryhim et al., 2018; O'Bryhim et al., 2021; Parisi et al., 2001; Polo et al., 2017; Robbins et al., 2021; Shin et al., 2021; Sun et al., 2024; Wang et al., 2023a; Wang et al., 2022c; Wu et al., 2020; Xie et al., 2023; Zabel et al., 2019b; Zhang et al., 2019; Zhao et al., 2023)

(*continued on next page*)

Table 1 (*continued*)

Imaging modalities	Applications	Findings	Advantages	Limitations	References
		- Vascular changes correlated with MMSE - Reduced macular flow density in the superficial retina in AD, correlated with Fazekas scale - Retinal vessel density correlated with hippocampal gray matter volumes in cognitively impaired patients			
Doppler OCT	•Retinal blood flow with vascular & structural changes	•Reduced global RNFL thickness & arterial blood flow in MCI & AD •Reduced mean arterial diameter in MCI & AD •Reduced arteriovenous differences in oxygen saturation in MCI & AD •Reduced venous blood flow rate & narrowing blood column in AD	•Rapid •Consistent & economic •High spatial resolution & velocity sensitive •Real-time imaging of tissue microcirculation	•Susceptible to ocular opacity •Background noise interference •Difficult to visualize vascular leakage •Hyperreflective layers' artifact	(Berisha et al., 2007; Leitgeb et al., 2014; Szegedi et al., 2020)
PS-OCT	•Enhanced image contrast to quantitatively measure polarization properties •Used on translucent tissues •Used to detect drusen segmentation in RPE	•PS-OCT enables characterization of RNFL thickness & structural changes in the cornea & RPE in various pathological conditions: AMD, glaucoma, & during aging •Enables detection of ocular fibrosis & drusen in AMD patients	•Label-free & multi-contrast imaging •May enhance contrast for discerning, segmenting, & quantifying ocular structures •Micrometer scale resolution	•Limited to superficial locations •Speckle noise reduces the precision for birefringence measurements •Increased acquisition time •Sensitive to motion artifacts	[a] Reviewed in (Pircher et al., 2011)
PS-OCM	•Mature neuritic Aβ plaques imaging in brain tissues based on birefringent properties	•Increased intrinsic birefringent properties of Aβ plaques in postmortem brains of advanced-stage AD patients vs. control subjects •Increased birefringence in smaller vessels walls of CAA patients vs. non-CAA ones	•Label-free •No staining is required	•Not in vivo; applied only on postmortem tissue	[b] (Baumann et al., 2017; Wang et al., 2016)
cSLO/SLO	•Retinal amyloid imaging: curcumin-enhanced fluorescence of Aβ deposit •Retinal AF of Aβ deposits •Retinal fundoscopy & SLO of optic nerve fibers & cup-to-disc ratio •Vascular imaging	•<u>Amyloid Deposits:</u> - Detected retinal curcumin-bound Aβ deposits in living patients -Increased retinal amyloid deposits in MCI & AD patients -Correlated with brain amyloid, whole gray matter atrophy, & hippocampal volume loss -Increased retinal amyloid plaque count in patients with MOCA score <26 & CDR >2 -Retinal venular tortuosity, jointly with retinal deposits count in ST-mid-periphery were higher in cognitively impaired vs. cognitively normal subjects, & correlated with verbal memory loss -Detected retinal AF of Aβ deposits in MCI due to AD patients -Reduced AF after IVIG treatment -Detected retinal amyloid deposits in Down Syndrome patients •<u>Optic Nerve Fibers:</u> -Reduced number of ON fibers	•Specific to AD pathology •High spatial resolution (μm) imaging of amyloid deposits •Wider 60-degree field of view •Automated image processing & quantification •Noninvasive •Patient friendly •Cost-effective •Label-free AF imaging option •Inner retina arterial & venular imaging •Integration of adaptive optics with cSLO could enable cone photoreceptors visualization	•Oral administration of bioavailable curcumin •Pre- & post-curcumin imaging sessions •Susceptible to imaging artifacts (i.e., cataracts, eye movements) •Limited penetration to deeper retinal layers •Requires patient cooperation •AF spots may reduce Aβ specificity	(Danesh-Meyer et al., 2006; den Haan et al., 2022; Dumitrascu et al., 2020; Dumitrascu et al., 2021; Itai et al., 2003; Kile et al., 2020; Koronyo et al., 2017; Miglior et al., 1998; Ngolab et al., 2021; Patel et al., 2010; Rafii et al., 2015; Tadokoro et al., 2021b)

(*continued on next page*)

Table 1 (*continued*)

Imaging modalities	Applications	Findings	Advantages	Limitations	References
		-3-fold greater odds ratio for larger optic cup-to-disc ratio in AD			
rHSI	•Detect the optical signature of aggregates & amyloid deposits by measuring their specific spectral signature •Provides HS severity scores for potential screening of AD risk •Detects Aβ & p-tau optical signatures in retinal tissues	•Differences in the retinal reflectance spectra between individuals with high brain Aβ burden (PET^{+}), MCI patients, & brain Aβ-negative (PET^{-}) controls •Increased rHS scores in Aβ PET^{+} vs. Aβ PET^{-} cases; AUC = 0.82–0.87 •Retinal amyloid scores correlated with brain Aβ loads in MCI with MMSE scores ≥22 •Texture measure differences seen in AD, at the 450–550 nm spectral range, the spectral region known to be affected by scattering from amyloid aggregates in the retina •In retinal tissues of AD patients, spectral signatures of retinal $Aβ_{42}$ & pS396-Tau identified; enabling accurate DL prediction of retinal $Aβ_{42}$ & pS396-Tau distribution	•Specific to AD pathology •Rapid •Well tolerated •Repeated at short intervals •Near real-time semi-automated analysis of the HS data cube is possible at the time of image acquisition •Can be administered at the point-of-care •No need for contrast agents	•Spectral effects may be due to other factors such as iron accumulation, inflammation •Inter-subject spectral variability •Motion artifacts •Limited field of view & spatial resolution •Prolonged image acquisition time •Requires pupil dilation	(Du et al., 2022; Hadoux et al., 2019; Lemmens et al., 2020; More et al., 2016, 2019; Sharafi et al., 2019)
FLIO	•Measures fundus AF decays in various spectral channels & determines the mean fluorescence lifetimes of endogenous retinal fluorophores (i.e., lipofuscin, macular pigment, retinal carotenoids)	•FLIO parameters of the second fluorescent component α2 amplitude & Q2 (560–700 nm) correlated with MMSE score & CSF pTau181 in AD •FLIO-derived parameter $\tau_{m,}$ correlated with CSF Aβ & tau levels, & GCL-IPL thickness (OCT) in preclinical AD	•Not impacted by emission intensity, dye concentration, focus drift, imaging depth, light scattering, & photobleaching •Structural, metabolic, & disease-related alterations	•Susceptible to internal factors (fluorophore structure) & external factors (temperature, polarity & fluorescence quenchers) •Limited field of view •Limited disease specificity	(Jentsch et al., 2015; Sadda et al., 2019)
Ophthalmo-scopy/ Fundoscopy	•Morphology: -Retinal surface -RNFL -Optic disc (OD) -Macula •Blood vessels	•Altered microvascular network (larger venular-asymmetry factor) in cognitively impaired (CI) subjects •Lower vascular fractal dimension in CI •Lower fractal dimension & higher tortuosity of retinal vessels in AD •Vascular parameters correlated with neocortical brain amyloid plaque burden in AD	•Rapid •Widely used •Simple & painless •Economic •Accurate & consistent •Arteriole & venules features, OD geometrical pattern, & retinal detachment	•Low resolution & depth of field •Smaller magnification range •No imaging of cell layers •Requires patient's cooperation	(Cabrera DeBuc et al., 2018; Cheung et al., 2014; Frost et al., 2013; Ong et al., 2014; Williams et al., 2015)
UWF SLO	•Detect blood vessels & abnormal structures (*e.g.*, drusen) in the mid-& far-periphery of the retina	•<u>Peripheral drusen:</u> -Peripheral hard drusen formation is linked to AD pathology -Increased prevalence of peripheral hard drusen phenotype in AD -Increased drusen number in AD patients during 2-year follow up - Individuals with tAD & PCA exhibit retinal hard drusen -Less soft drusen in tAD & PCA -~3-fold increased reticular pseudodrusen formation in tAD •<u>Venular & Arteriole structure:</u> -Increased venular width gradient & decreased arterial fractal dimension in AD patients -Increased vessel branching in the midperipheral retina	•Large field of view (110°–220°), imaging from anterior edge of vortex vein ampulla & beyond to pars plana, with greater detail & in a single shot •Large view of vasculature & drusen in peripheral regions •Shorter acquisition time & minimal pupil dilation	•Lash artifacts •Peripheral distortion (far temporal & nasal periphery) where peripheral lesions can appear bigger •Sensitive to cataract severity •Limited depth perception •Expensive & limited accessibility	(Csincsik et al., 2018, 2021; Pead et al., 2023)

(*continued on next page*)

Table 1 (*continued*)

Imaging modalities	Applications	Findings	Advantages	Limitations	References
		& increased arteriolar thinning in AD dementia -MCI patients displayed increased rates of arteriolar & venular thinning, with a trend toward decreased vessel branching			
DARC by cSLO	•Visualization of ANX776-labelled apoptotic retinal neurons, mostly RGCs •Imaging of laser-induced lesions & early AMD angiogenesis	•Increased DARC counts in glaucoma •Increased apoptotic RGCs in 3xTg AD mice following intravitreal injection of fluorescent-labelled annexin-V •Detecting new wet-AMD lesions •Identification of earliest stages of angiogenesis in vivo in AMD	•Monitoring cell stress & apoptosis •Quantifiable •Single-cell resolution •Real-time response to therapy	•Invasive & painful intravitreal injections •Multiple sessions of imaging are required	[c] (Corazza et al., 2021; Cordeiro et al., 2010; Cordeiro et al., 2004; Cordeiro et al., 2022; Guo et al., 2007; Normando et al., 2015, 2020; Schmitz-Valckenberg et al., 2008; Yap et al., 2018)
FA & ICG angiography fundoscopy	•Vascular anatomy, physiology, & pathology of retina/choroidal circulation, using a sodium fluorescent dye •Visualization of central & peripheral changes in the retina, choroid, & vitreoretinal interface (ICG)	•Vascular abnormalities, such as blood flow velocity, vein occlusion, BRB leakage, & macular neovascularization in ocular diseases, mainly glaucoma & AMD •FA: Classic or occult choroidal neovascularization scars in AMD •FA: Inflammatory-related vascular lesions are detected in the retina of uveitis patients •FA: Small drusen in AMD •ICG: Increased vascular leakage in type-1 neo-vascularization disease •CG: Increased retinal lipid drusen between RPE & choroid in AMD	•Detection of abnormal circulation, vessel structure, leakage, & inflammatory angiographic signs •ICG: longer imaging window •Multimodal option of UWF fundus with FA & ICG angiography, & OCT	•Fluorescein or ICG dyes' potential side effects •Non-quantitative •Relatively expensive & lengthy •Not suitable for small pupils or diseases with unclear media •Low fluorescence signal (FA)	[c] (Bravo et al., 2023; Chen et al., 2022b; Funatsu et al., 2006; Holomcik et al., 2023; Laatikainen, 2004; Masaoka et al., 2001; Mokwa et al., 2013; Shoughy and Kozak, 2016; Witmer et al., 2013; Yamaji et al., 2004; Zola et al., 2023)
DVA	•Dynamic behavior of retinal vessels (vessel oscillations) •Changes to diameter of retinal arteries & veins over time	•Altered arterial oscillations in MCI & AD - Correlated with disease severity •Decreased arterial dilation in AD •Decreased reaction amplitude in MCI & AD •Arterial dilation & reaction amplitude correlated with CSF-Aβ •Increased retinal neuronal activity or damaged feed-back loop of neurovascular coupling with differentiating alterations across AD spectrum	•Noninvasive •Non-contact examination of the function & the regulatory mechanism of smallest retinal vessels •Examine vessel caliber •Offers quantitative assessment	•Varying responses to flickering light based on the stimulation protocol & on the vessel size •Does not provide accurate indication of blood flow	(Kotliar et al., 2017, 2022; Querques et al., 2019)
Retinal Oximetry	•Oxygen saturation in retinal blood vessels •Markers of hypoxic stress in retinal tissue	•Elevated retinal arteriolar & venular oxygen saturation in MCI & moderate AD •Decreased arteriovenous differences in MCI	•Direct, noninvasive assessment of retinal blood vessel oxygen saturation •Quick, safe, & patient-friendly •Low variability, & high reproducibility	•Pupil dilation •Sensitive to ocular opacity •Not applicable for capillary oxygenation •Influenced by retina/choroidal pigmentation, vessel size & thickness, linear blood flow velocity, & RNFL thickness	(Einarsdottir et al., 2016; Olafsdottir et al., 2018)
Retinal microperimetry	•Psychophysical method of examining fundus topographic details & light sensitivity for macular function	•Correlation between retinal sensitivity & MRI & ^{18}FDG-PET parameters related to brain neurodegeneration •Retinal sensitivity linked to cognitive status in normal cognition, MCI & AD	•Noninvasive •Simple, rapid, high sensitivity •Cost-effective •Enables exact correlation between macular pathology & functional abnormality	•Patient cooperation is necessary, especially since it relies on patient's answers on sensibility to light	Ciudin et al. (2017)
ERG or PERG	•Electrical response of neurons to light	•Altered PERG parameters:	•Objective & quantitative measurement of central	•Requires electrode placement on cornea	(Asanad et al., 2021; Byun et al., 2021; Cabrera DeBuc et al.,

(*continued on next page*)

Table 1 (*continued*)

Imaging modalities	Applications	Findings	Advantages	Limitations	References
	•Recorded response in the outer retina (photoreceptors) & inner retina (*e.g.*, RGCs)	-Reduced amplitude & prolonged implicit time in both N95 & P50 waves imply retinal dysfunction in AD Patients -Increased implicit time of P50 wave & reduced amplitudes in P50 & N95 waves in early-stage AD patients -Prolonged implicit time in cognitively normal subjects with positive brain Aβ burden •Marked RGC dysfunction in preclinical AD	retinal function via electrical activity •Vital clinical applications in unexplained vision loss •ERG changes often occur early & precede structural change	•Eye numbing •Long testing time (60–90 min) •Mild ocular discomfort •Interfering factors such as eye blinking & movement	2018; Katz et al., 1989; Krasodomska et al., 2010; Ngoo et al., 2019; Parisi et al., 2001; Sartucci et al., 2010; Sen et al., 2020; Trick et al., 1989; Zhao et al., 2020).

Abbreviations: Aβ: amyloid-beta protein; AD: Alzheimer's disease; AF: autofluorescence; aMCI: amnestic MCI; AMD: age-related macular degeneration; AUC: area under the curve; BRB: blood retinal barrier; CAA: cerebral amyloid angiopathy; CDR: clinical dementia rating; CFZ: capillary-free zone; CSF: cerebrospinal fluid; cSLO: confocal laser ophthalmoscope; DARC: detection of apoptotic retinal cells; DL: deep-learning; DVA: dynamic vessel analyzer; ERG: electroretinogram; FA: fluorescein angiography; FAD: familial AD; FAZ: foveal avascular zone; FDG-PET: fluorodeoxyglucose-PET; FLIO: fluorescence lifetime imaging ophthalmoscopy; GCL: ganglion cell layer; ICG: Indocyanine Green; INL: inner nuclear layer; IPL: inner plexiform layer; IVIG: intravenous immunoglobulin; LBD: Lewy body dementia; MCI: mild cognitive impairment; MMSE: mini–mental state examination; MOCA: Montreal cognitive assessment; MRI: magnetic resonance imaging; OCM: optical coherence microscopy; OCT: optical coherence tomography; OCTA: OCT angiography; ONL: outer nuclear layer; PCA: posterior cortical atrophy; PD: Parkinson's disease; PERG: pattern ERG; PET: positron emission tomography; PS-OCT: polarization sensitive OCT; pTau: hyperphosphorylated tau; RGC: retinal ganglion cell; rHSI: retinal hyperspectral imaging; RNFL: retinal nerve fiber layer; RPE: retinal pigment epithelium SD-OCT: spectral domain-OCT; ST: superior-temporal; tAD: typical AD; UWF-SLO: ultra-widefield SLO.

[a] No study on retina of AD patients, but in AMD and glaucomatous retina.

[b] Study on postmortem AD brain tissue.

[c] No study in AD patients, but in other ocular disease patients and animal models of AD; λ – wavelength.

retinal amyloid index in AD patients compared to age-matched healthy controls (Koronyo et al., 2017). The feasibility of noninvasively detecting and quantifying curcumin-bound retinal amyloid deposits in living patients and increased retinal amyloid deposits in preclinical, prodromal (MCI), and AD dementia patients was also reported in other studies (Dumitrascu et al., 2020, 2021; Ngolab et al., 2021; Tadokoro et al., 2021b). Additionally, increased curcumin-labelled retinal amyloid deposits, especially those in the proximal mid-periphery of the superior-temporal retina, were correlated with hippocampal volume loss and whole gray matter atrophy (Dumitrascu et al., 2020; Tadokoro et al., 2021b). Together with venular tortuosity, these observations predicted verbal memory deficit (Dumitrascu et al., 2021) (Fig. 15).

Despite at least five other studies reporting increased curcumin-labelled amyloid deposits in the AD retina (Dumitrascu et al., 2020, 2021; Koronyo et al., 2017; Ngolab et al., 2021; Tadokoro et al., 2021b), one study that used a variety of curcumin formulations (*e.g.*, Longvida®, Theracurmin® and Novasol®) was unable to show an increased retinal amyloid burden in AD patients (den Haan et al., 2022). Nevertheless, the results of this study by den Haan and colleagues (den Haan et al., 2022) also demonstrated the feasibility of detecting curcumin-positive amyloid deposits in the retina of living patients. The lack of differences between AD patients and controls can be explained by low intensity fluorescent signal from amyloid-bound curcumin, suboptimal image processing methodologies with limited scanning, threshold definition, manual counting, and/or a very low patient number used for the quantitative retinal curcumin analysis. Notably, however, an unpublished study reported initial results from 40 patients, which found increased retinal curcumin-bound deposits in brain amyloid-PET positive MCI and AD patients compared with brain amyloid-PET negative cognitively normal individuals and demonstrated a significant correlation between the amyloid burden in the retina and brain [AAIC abstract (Frost et al., 2014)]. Overall, these pilot studies, including the unpublished report, have indicated the feasibility of noninvasively detecting curcumin-enhanced fluorescence of amyloid deposits in the human retina with high spatial resolution, and most of them demonstrated increased amyloid deposits in the retina of AD patients. In addition, curcumin was utilized for retinal amyloid plaque imaging in vivo in patients with Down syndrome, further suggesting the feasibility of curcumin-amyloid imaging in the retina (Rafii et al., 2015).

Other methods have also been applied to detect increased retinal amyloidosis in AD patients, including HSI (Hadoux et al., 2019; Lemmens et al., 2020; More et al., 2019). Using cerebral PET imaging as validation for brain amyloid positivity, retinal amyloid HSI scores were greatly correlated with brain amyloid burden (Hadoux et al., 2019). Intriguingly, an additional study unveiled a significant correlation between retinal blue-light AF imaging of inclusion bodies, presumed to contain Aβ, and diminished IPL volume on SD-OCT. Moreover, these retinal inclusion bodies exhibited a notable association with neocortical amyloid burden, as quantified by florbetapir-PET imaging (Snyder et al., 2016). In agreement with human studies, several studies in transgenic murine models of AD demonstrated the feasibility of detecting and quantifying in vivo retinal curcumin-labelled Aβ deposits, alongside showing increased levels of retinal deposits in ADtg mice compared to WT littermates (Chibhabha et al., 2020; Koronyo et al., 2012; Koronyo-Hamaoui et al., 2011; Mei et al., 2020; Sidiqi et al., 2020; Vit et al., 2021a). These retinal optical imaging techniques allowed for high-resolution fluorescent detection of retinal Aβ deposits and longitudinal monitoring of the occurrence and clearance of these deposits during disease progression (Barton et al., 2021; Cao et al., 2021; Chibhabha et al., 2020; Koronyo et al., 2012, 2017; Sidiqi et al., 2020; Vit et al., 2021a).

Currently, there are no retinal imaging tools to detect tau aggregates in living patients; however, the development of a few fluorescent probes to detect abnormal tau forms holds promise for future applications. For instance, Lim and colleagues demonstrated the specific affinity of the BODIPY-fluorescence sensor (BDtau) for PHF-Tau binding in hippocampal neurons in vitro and in brain sections from transgenic murine $MAPT^{*P301L}$ models of tauopathy (Lim et al., 2017). In a recent study, Li et al. designed and synthesized a series of near infrared (NIR) probes of hydroxyethyl cycloheptatriene-BODIPY derivatives that demonstrated

strong binding specificity to NFTs and pTau aggregates in postmortem brains of advanced stage AD patients (Li et al., 2023). Among them, TNIR7–9 and TNIR7–11 showed high binding affinities toward tau aggregates but not to Aβ plaques, allowing for their specific visualization in brain tissues. TNIR7–13, modified with a fluorine atom, was further able to detect different conformational forms of tau. In mice, intravenous (i.v.) injection of TNIR7–9 or TNIR7–11 resulted in increased in vivo fluorescence signals in the brain, suggesting the potential of these probes for in vivo tau imaging (Li et al., 2023). Nuñez-Diaz et al., further reported that a fluorescent ligand, bTVBT2, exhibits high affinity and specificity to PHF-1 and AT8-positive tau forms but not to Aβ, pTDP-43, or IAPP (Nunez-Diaz et al., 2024). The bTVBT2 ligand was used to detect pathological tau forms within microglia in retinal flatmounts and brain tissues from AD patients, as well as in brains from the *App*$^{NL-F/NL-F}$ knock-in mouse model. There were increased levels of retinal bTVBT2 in microglia in patients with high Aβ compared with low Aβ levels, and retinal bTVBT2 in microglia significantly correlated with the Braak NFT staging (Nunez-Diaz et al., 2024). The identification of the spectral signature of pS396-Tau in the AD retina (Du et al., 2022) may also aid in the future development of in vivo retinal pTau imaging.

Overall, robust methodologies for assessing amyloid and tau deposition in the retina should provide clinicians with an early window into AD pathology and disease progression. Such noninvasive, high-resolution imaging technologies could aid in stratifying at-risk patients who may benefit from further Aβ- and/or pTau-clearing therapeutics. Furthermore, tracking abnormal amyloid and tau burden in the retina over time could dynamically assess the efficacy of these therapies.

3.3. Retinal vascular imaging in AD patients

Clinical studies utilizing a range of imaging techniques, such as color fundus photography, Doppler or confocal scanning laser ophthalmoscopy, OCTA, and dynamic vessel analysis, have demonstrated multiple vascular abnormalities in live AD patients compared to healthy controls. These retinal vascular changes include increases in venular caliber and density, macular avascularization, decreases in retinal and choroidal blood flow and vascular branching complexity, vein narrowing, as well as increases in fractal dimension and tortuosity (Berisha et al., 2007; Cheung et al., 2017; Chua et al., 2020; Dumitrascu et al., 2021; Feke et al., 2015; Frost et al., 2013; Golzan et al., 2017; Liew et al., 2008; Snyder et al., 2021; Williams et al., 2015; Wisely et al., 2022, 2024; Yoon et al., 2019; Zhao et al., 2023). However, some of these retinal vascular changes (*e.g.*, vein narrowing, vascular leakage) are not specific to AD and were reported in other ocular and neurodegenerative disorders, including glaucoma and AMD (Lee et al., 2006; Sperduto et al., 1998; Toulouie et al., 2022; Zola et al., 2023). Nevertheless, a growing number of studies suggest that vascular abnormalities in the retina can predict cognitive decline in AD patients (Baker et al., 2007; Cabrera DeBuc et al., 2018; Cheung et al., 2014; Deal et al., 2018; Ding et al., 2008; Wong et al., 2002).

While there is significant data demonstrating a correlation between retinal arterial and venous caliber and cognitive deficits in subjects with dementia (Cheung et al., 2022; Chua et al., 2020; Golzan et al., 2017; Jiang et al., 2018; Liew et al., 2009; Luengnaruemitchai et al., 2023; McGrory et al., 2017; Moussa et al., 2023; Wang et al., 2020b; Zhang et al., 2019), a recent meta-analysis suggests inconsistency in the results, perhaps due to variability in the underlying definition of AD (McGrory et al., 2017). Nonetheless, a significant association between vascular caliber, branching complexity, and amyloid plaque burden in the brain has been demonstrated (McGrory et al., 2017), and a significant increase in vessel density has been reported among asymptomatic monozygotic twins with amyloid-positive status compared to those with non-amyloid positive status (van de Kreeke et al., 2020). Another study successfully distinguished cerebral Aβ-positive subjects from Aβ-negative subjects with 85% accuracy based on retinal vascular measures, including vessel tortuosity and diameter assessed by hyperspectral fundus photography (Sharafi et al., 2019). Using multimodal imaging, Cabrera DeBuc and colleagues also found an association between retinal geometric vascular and functional parameters and physiological changes in the retina of cognitively impaired individuals (Cabrera DeBuc et al., 2018). Laser Doppler and other retinal imaging modalities demonstrate a decrease in blood column diameter, blood velocity, capillary vessel density, and blood flow, as well as altered vessel pulsatility and reactivity that is more significant in subjects with a clinical diagnosis of AD (Berisha et al., 2007; Feke et al., 2015; Golzan et al., 2017; Querques et al., 2019). The reported changes in retinal vascular caliber and geometry suggest that there may be concomitant changes in blood flow in AD patients.

The development of OCTA technology has enabled multi-dimensional visualization of vascular abnormalities in various retinal layers, including microaneurysms, retinal vascular non-perfusion, neovascularization, and reduced capillary density (Kashani et al., 2017). The significant potential of this technology's utility has recently led to a surge of investigations exploring retinal biomarkers in AD [reviewed in (Ibrahim et al., 2023; Lopez-Cuenca et al., 2021; Snyder et al., 2021)]. An early case-control study revealed a substantial decrease in retinal vascular density, attenuated retinal and choroidal thickness, and enlarged FAZ area in AD patients compared to healthy controls (Bulut et al., 2018). Additionally, Jiang et al., identified lower densities in the retinal vascular network, superficial vascular plexus, and deep vascular plexus in patients with MCI and AD dementia (Jiang et al., 2018). Importantly, in a well-characterized cohort of cerebral amyloid-positive AD patients, perifoveal capillary density on OCTA was significantly lower in the AD cohort, correlating with worsened Fazekas score and increased cerebrovascular lesions in AD patients (Lahme et al., 2018). Similarly, another study reported an enlarged FAZ area and decreased foveal thickness in PET amyloid and/or CSF-confirmed AD patients at the early preclinical stages (O'Bryhim et al., 2018). O'Bryhim and colleagues also found that biomarker-positive preclinical AD subjects continued to exhibit an enlarged FAZ area in a 3-year longitudinal follow-up study (O'Bryhim et al., 2021). A recent report also revealed enlarged retinal mid-peripheral capillary free zones as assessed by OCTA in cognitively unimpaired older adults who are at high risk for AD (Arthur et al., 2023). To date, case-control OCTA studies appear consistent in demonstrating retinal vascular loss and increased FAZ area in AD patients, but differ in identifying the exact vascular areas affected, namely, the superficial versus deep vessels, or parafoveal versus perifoveal vessels (Czako et al., 2020; Lahme et al., 2018; Lee et al., 2020a; Rifai et al., 2021; Wu et al., 2020; Yoon et al., 2019; Zabel et al., 2019b; Zhang et al., 2019).

In a meta-analysis of OCTA measurements across 14 studies, Rifai et al., found a significant larger FAZ area and reductions in perifoveal and whole retinal vascular densities in AD patients compared to controls (Rifai et al., 2021). Another OCTA imaging meta-analysis study by Hui et al., involving 8 reports with 195 MCI patients and 226 healthy controls, also observed significant increase in FAZ area and substantial decrease in vessel density among MCI patients compared to the healthy controls (Hui et al., 2021). Similarly, Ashraf et al., conducted a meta-analysis study in biomarker-confirmed AD patients across various disease stages, using brain PET or CSF Aβ levels for confirmation. They revealed a significant increase in FAZ area on OCTA (207 subjects) and significant reductions in arteriole and venule fractal dimensions on fundus photography (297 subjects) in AD patients (Ashraf et al., 2023). However, these meta-analysis studies also mentioned significant heterogeneity in OCTA scanning parameters and image analysis methods across the studies (Ashraf et al., 2023; Hui et al., 2021; Rifai et al., 2021). Hence, while these significant findings suggest that retinal vascular alterations are associated with AD pathology and that retinal vascular imaging has the potential to serve as a biomarker for AD, this technique requires further standardization and validation for clinical utility. Of note, OCT-adaptive optics, a promising advancement in this field, offers ultra-high-resolution imaging, including of blood vessel walls, potentially enhancing data accuracy and granularity in AD retinal studies

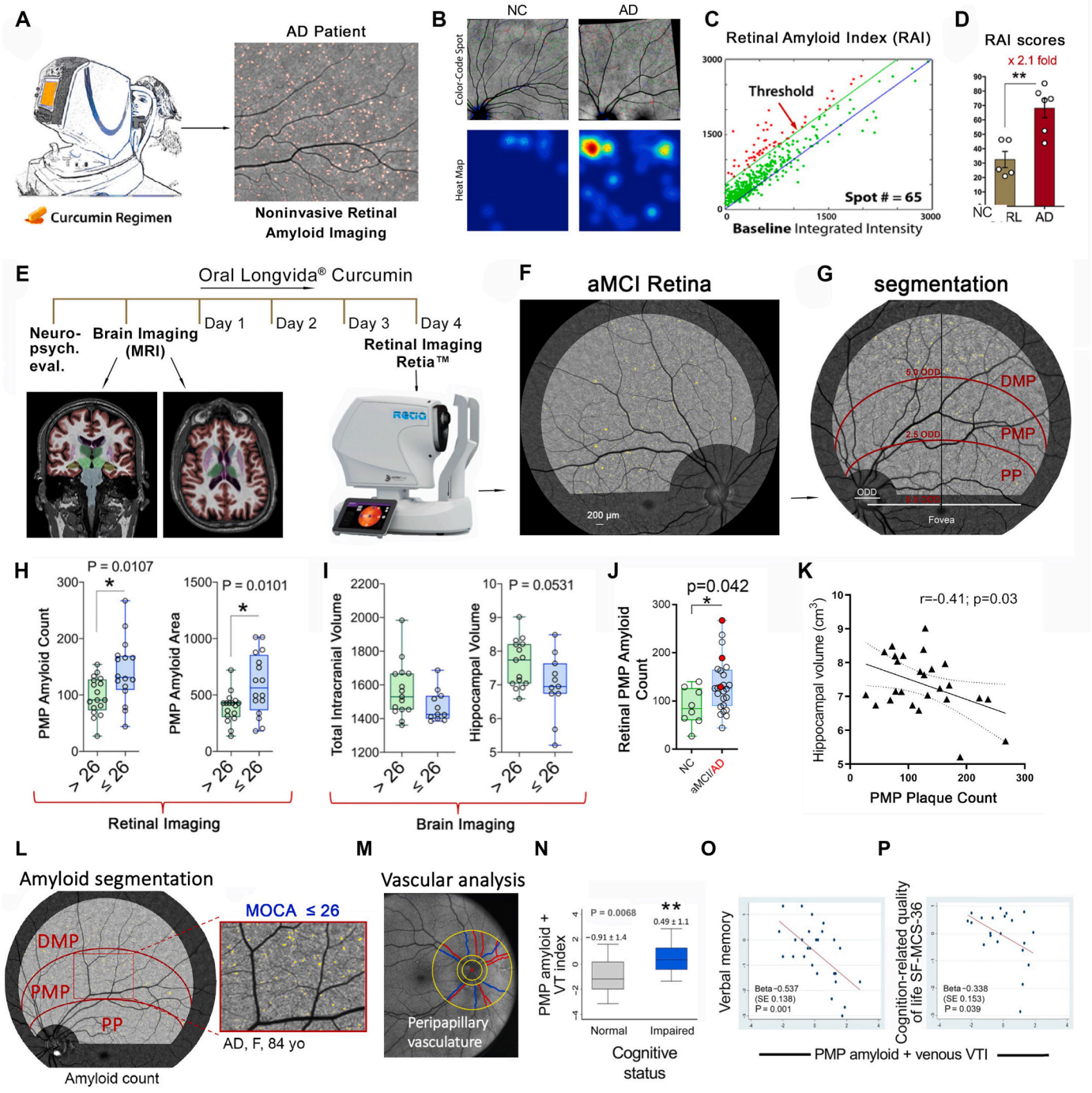

(caption on next page)

(Snyder et al., 2021). Further testing is warranted to validate its utility.

Vascular amyloidosis in the AD retina (Koronyo et al., 2017; Shi et al., 2020b, 2023) raises the question of whether retinal vascular Aβ deposition is a cause or effect of BRB abnormalities. Nevertheless, clinical studies have often indicated that retinal vascular changes can predict cognitive decline in living AD patients (Baker et al., 2007; Cabrera DeBuc et al., 2018; Deal et al., 2018). Future longitudinal studies, integrating multi-modal imaging techniques like SLO, OCT/OCTA, OCT-leakage, and fundus fluorescein angiography to assess retinal vascular parameters (*e.g.*, capillary density, branching, non-perfusion, vein narrowing, aneurysms, vascular occlusion and leakage) together with retinal amyloid and vascular amyloid imaging, will aid in discerning whether retinal vascular Aβ deposition precedes or follows observed BRB abnormalities, which is crucial for understanding disease pathogenesis. This integrated approach should allow a deeper understanding of the interplay between retinal vascular abnormalities and amyloid accumulation and may shed light onto the specific impact of retinal vascular amyloidosis on cognitive and visual functions. Indeed, further research, incorporating multi-model ophthalmic devices to comprehensively visualize diverse parameters of vascular anatomy, physiology, and pathology in the retina, optic disc, choroid, and RPE, is needed to fully understand the sequence of events and the relationships

Fig. 15. Retinal amyloid imaging in living MCI and AD patients and correlations to hippocampal atrophy and cognitive impairment. (**A**) An ophthalmic imaging illustration and a representative retinal curcumin-fluorescence amyloid image in a living AD patient, following an oral Longvida® curcumin administration. Subjects' retinas were imaged with a modified scanning-laser ophthalmoscope (SLO) prior to (day 0, baseline image) and after curcumin intake, as previously reported (Koronyo et al., 2017). Curcumin-bound amyloid deposits in AD retina are presented as yellow dots. (**B**, top) Color-coded spot overlay images in NC and AD retinas. Red spots are above the threshold and considered curcumin-positive amyloid deposits, green spots exceed 1:1 reference but not the threshold, and blue spots fall below the reference. (**B**, bottom) Heatmap images with red spot centroids. (**C**) Threshold defining increased curcumin fluorescent signal in the retina and the calculation of retinal amyloid index (RAI) scores in an AD patient. The blue line is a 1:1 reference, and the green line represents the threshold level, determined at 500 counts and above; the red spots are above the threshold. (**D**) RAI scores in AD patients (N = 6) versus age-matched NC individuals (N = 5). (**E**) Schematic of clinical study timeline, including neuropsychiatric evaluation, brain magnetic resonance imaging (MRI), and Retia™ SLO retinal amyloid imaging. (**F**) Representative post-processed image of the retinal superior-temporal (ST) quadrant from a subject with amnestic MCI (aMCI). Yellow spots indicate curcumin-bound amyloid deposits. (**G**) Predefined division of retinal ST quadrant used for quantification of retinal amyloid deposit count and area. The topographical segmentation into distal mid-periphery (DMP), proximal mid-periphery (PMP), and posterior pole (PP), is demonstrated. ODD – optic disc diameter. (**H**) Retinal PMP amyloid count and area, and (**I**) total intracranial volume and hippocampal volume, when patients are stratified by Montreal cognitive assessment (MOCA) score threshold of 26 (N = 18 for MOCA >26 and 16 for MOCA ≤26). (**J**) Retinal PMP amyloid count in MCI and AD patients (N = 25) compared to NC controls (N = 8). (**K**) Pearson's (r) correlation analysis between retinal PMP amyloid count and hippocampal volume, revealed the relationship between increased retinal amyloid burden and hippocampal volume loss (N = 26). (**L**) A representative curcumin fluorescent fundus image in an AD patient with a MOCA score ≤26, showing multiple retinal amyloid deposits (yellow dots) within the three topographical ST subregions. Magnified image is shown. (**M**) Retinal vascular analysis is shown for the region of interest, with the red circle indicating the center of the optic nerve-head, and the smallest yellow circle shows the optic nerve-head area. The two larger circles indicate the region of interest for the peripapillary vascular analysis, which were 1.5 and 4 times the diameter of the optic disc. The branching angle and tortuosity of retinal arteries (red) and veins (blue) within the region of interest were calculated. (**N**) A combined retinal PMP amyloid and venous vessel tortuosity index (VTI) in patients stratified by cognitive status [normal (N = 11) versus impaired (N = 18)]. (**O–P**) Pearson's (r) correlation analyses between combined PMP amyloid-venous VTI index and (**O**) verbal memory (N = 27) or (**P**) cognitive-related quality-of-life SF-MCS-36 Z-scores (N = 21). Statistics: Data from individual subjects (circles) as well as group means ± SEMs (D) and means ± SD (H-J, N) are shown. Fold change is shown in red. $^{*}P < 0.05$, $^{**}P < 0.01$, by two-tailed unpaired Student t-test. Panels A–D were modified from (Koronyo et al., 2017), Panels E–L were modified from (Dumitrascu et al., 2020), and Panels M–P were modified from (Dumitrascu et al., 2021) with permission.

between the development and progression of ocular vascular abnormalities and vascular amyloidosis. Additionally, the potential imaging of retinal pericytes using adaptive optics (Schallek et al., 2013) holds promise for evaluating the integrity of early neurovascular unit alterations in AD. Overall, the retinal vascular imaging methodologies, coupled with validated cognitive testing and advanced cerebral imaging techniques, may revolutionize AD diagnosis and provide a novel means of tracking disease progression in clinical practice.

3.4. Retinal imaging biomarkers in AD: challenges and future directions

A prerequisite for developing a retinal imaging biomarker is the ability to identify the molecular processes related to AD and track these pathological changes during disease progression. While noninvasive ophthalmic imaging is expected to be safe and useful for future AD detection and monitoring in clinical settings, especially in low- and middle-income countries (LMICs), this research area is still in its early developmental stage (Alber et al., 2023; Snyder et al., 2021). There are some limitations and discrepancies of results from different retinal imaging modalities that necessitate additional replication, rigorous testing, and validation against the gold-standard neuropathological examination. Hence, studies involving larger cohorts of confirmed AD patients will potentially allow the transition from the biomarker discovery phase to the biomarker validation phase (Snyder et al., 2021), with the prospect of achieving higher sensitivity and accuracy. To enhance consistency and coordination across ophthalmic devices and users for screening at-risk populations and early AD detection, standardizing retinal amyloid imaging and developing retinal tau imaging are essential. This aligns with the NIA-AA Research Framework, which defines elevated brain amyloid-PET burden as a marker of initial-stage AD, along with elevated amyloid and tau-PET accumulation in the medial temporal brain as the subsequent early-stage AD markers (Jack, 2023). Furthermore, leveraging validated retinal imaging biomarkers in AD should aid in selective participant recruitment, enhance trial designs, improve monitoring of disease progression and therapeutic target engagement, and bolster outcomes by sub-stratification of individuals to facilitate precision medicine approaches for treating AD.

Another challenge faced by several retinal imaging modalities for AD is their lack of disease specificity. While many studies have shown retinal cell layer atrophy, particularly RNFL thinning and narrowing of retinal veins in AD patients, these changes are not exclusive to AD and can also occur in other ocular or neurodegenerative conditions (Al-Mujaini et al., 2021; Balestrini et al., 2016; Celebi and Mirza, 2013; Datta et al., 2020; Garcia-Martin et al., 2016b; Lee et al., 2019; Miki et al., 2014; Shi et al., 2019; Wang et al., 2014; Woo et al., 2022; Zhang et al., 2020). However, these retinal structural changes may play a crucial role in assessing tissue degeneration processes that are pertinent to the functional deficits observed in AD. As mentioned, imaging AD core hallmarks in the retina would likely be required for specific and more reliable early AD diagnosis. In addition, longitudinal studies in large cohorts are obligatory to determine the capability of translating retinal imaging modalities from bench-to-bedside, demonstrating the feasibility of facilitating early screening and real-time tracking of AD progression and response to therapy. As previously described in MCI or AD patients (Dumitrascu et al., 2020, 2021; Hadoux et al., 2019; Kile et al., 2020; Koronyo et al., 2017; Lemmens et al., 2020; More et al., 2019; Ngolab et al., 2021; Tadokoro et al., 2021b) and animal models (Butovsky et al., 2006; Dionisio-Santos et al., 2021; Doustar et al., 2020; Frenkel et al., 2005; Koronyo et al., 2012; Koronyo-Hamaoui et al., 2009, 2011; Liu et al., 2009; Parthasarathy et al., 2015; Vit et al., 2021a), proof-of-concept longitudinal or cross-sectional noninvasive retinal amyloid imaging has allowed for assessing specific changes (*e.g.*, Aβ deposition) in various disease stages or in response to intervention. In agreement with Alber and colleagues, applying harmonized analytical methods and interpretation algorithms to the clinic for image processing and data analysis will be vital to achieve standardized information on AD-related retinal changes to make it useful to providers (Alber et al., 2023). Furthermore, the potential COU for different retinal imaging modalities would likely be beyond facilitating early and accurate diagnosis. Although currently speculative, we believe that noninvasive, affordable, and sensitive retinal biomarkers will further aid in evaluating the efficacy of therapeutic interventions as well as in predicting conversions from preclinical AD to MCI and to AD dementia.

As it relates to retinal vascular parameters, the potential of retinal vascular imaging to predict CAA status has been highlighted by several recent reports. These studies found that retinal vascular amyloidosis and other vascular abnormalities strongly correlated with CAA severity and cognitive deficits in MCI and AD patients (Alber et al., 2021; Dumitrascu et al., 2021; Shi et al., 2020b, 2021, 2023). Currently, definitive CAA diagnosis can only be made by postmortem examination of brain tissues and CAA assessment in living patients is severely limited. Nevertheless, retinal imaging offers the opportunity to not only detect the Aβ deposits but also visualize retinal venules, arterioles, and capillaries, as well as vascular amyloidosis and leakage with ultra-high spatial resolution. In a

pilot study, Alber et al., found a trend level correlation between retinal and cerebral microbleeds in CAA patients, suggesting that retinal microbleeds may reflect degree of cerebral microbleed burden (Alber et al., 2021). In another study, retinal venular tortuosity was shown to discriminate between patients with normal and impaired cognition, and the differentiation was stronger when an index combining retinal amyloid deposits in the superior-temporal mid-periphery and retinal peripapillary venular tortuosity was utilized (Dumitrascu et al., 2021). Furthermore, histopathological analyses identified a significant accumulation of vascular and perivascular Aβ deposits in postmortem retinas of MCI and AD patients (Koronyo et al., 2017; La Morgia et al., 2016; Shi et al., 2020b, 2023). In particular, retinal arteriolar $A\beta_{40}$ burden was linked to retinal pericyte and tight junction losses, and these retinal vascular changes strongly correlated with CAA severity scores (Shi et al., 2020b, 2023). Since CAA is considered a risk for developing amyloid-related imaging abnormalities (ARIA) following the anti-Aβ monoclonal antibody therapies, future studies in larger cohorts are warranted to determine the potential of noninvasive retinal vascular imaging to assess ARIA risk. Overall, while retinal imaging alone is not likely to provide a complete answer for AD detection and monitoring, we anticipate that a comprehensive clinical, behavioral, fluid and brain-imaging biomarkers, in combination with multi-modal retinal imaging will allow a more specific and sensitive assessment of AD risk, development, and progression.

To provide a balanced view of the current state of imaging technologies for examining the retina, we have compiled the advantages, limitations, and potential COU of various retinal imaging modalities used to visualize AD-related changes in Table 1.

4. Visual impairments in AD

Diverse neurocognitive dysfunctions, such as memory loss, disorientation, impaired judgment, personality changes, and emotional disturbances, are common symptoms observed in AD patients. In addition to these manifestations, visual impairment is another common sequela of AD, affecting all parts of the visual systems in AD patients (Armstrong, 1996; Bambo et al., 2015; Begde et al., 2024; Blanks et al., 1996a; Chang et al., 2014; Cormack et al., 2000; Engedal et al., 1989; Gaynor et al., 2019; Goldstein et al., 2003; Hart et al., 2016; Hutton et al., 1993; Javitt et al., 2023; Kergoat et al., 2002; Lopez-Cuenca et al., 2023; McKee et al., 2006; Mendez et al., 1990; Namazi et al., 1989; Nissen et al., 1985; Polo et al., 2017; Risacher et al., 2013, 2020; Sadun, 1988; Sadun et al., 1987; Salobrar-Garcia et al., 2019; Schlotterer et al., 1984; Takemori and Ida, 1988). The diverse neuropathological manifestations in the visual system of AD patients include the deposition of Aβ plaques in the lens (Goldstein et al., 2003) and retina (Koronyo et al., 2017), degeneration of RGCs, optic nerve atrophy, and RNFL thinning (Blanks et al., 1989, 1996a, 1996b; Carelli et al., 2017; Hinton et al., 1986; Janez-Escalada et al., 2019; Kirbas et al., 2013; Kromer et al., 2014; Liu et al., 2015; Marziani et al., 2013; Moreno-Ramos et al., 2013; Oktem et al., 2015; Shi et al., 2014), optic disc pallor atrophy and cupping (Kiyosawa et al., 1989; Sadun et al., 1987; Syed et al., 2005), accumulation of lipofuscin in the LGN (Katz and Rimmer, 1989), loss of pyramidal cells in the visual cortex (Armstrong, 1996; Hof and Morrison, 1990), and the presence of cored senile plaques and NFTs in the visual cortex (Hof and Morrison, 1990; McKee et al., 2006). These events are believed to contribute to the complex visual abnormalities observed in AD (Bature et al., 2017; Katz and Rimmer, 1989; Sadun, 1988; Sadun et al., 1987).

The common visual symptoms reported in AD patients may be linked to dysfunctions of the lens, retina, and optic nerve, including reduced color and contrast sensitivity (Cormack et al., 2000; Crow et al., 2003; Gilmore and Whitehouse, 1995; Nissen et al., 1985; Risacher et al., 2013, 2020; Sadun et al., 1987; Schlotterer et al., 1984), defective visual field and acuity, and abnormal pupillary responses (Bassi and Sadun, 1990; Gross et al., 1989; Trick et al., 1995). In addition, approximately 20% of individuals diagnosed with AD can experience visual hallucinations, particularly in those with compromised vision and severe cognitive impairment (Chiu et al., 2017). Abnormalities in eye movement and fixation, such as delayed saccadic eye movements, slowed smooth pursuit (Fletcher and Sharpe, 1988), compromised pupillary reactions, defects in motion perception, altered ocular motor function, and impaired stereopsis (Chang et al., 2014), are also reported in AD patients. These findings may be due to a combination of optic nerve dysfunction and degeneration of higher cortical areas, such as the frontal eye fields, along with fixation and saccadic centers in the parietal lobe (Fletcher and Sharpe, 1988; Sadun and Bassi, 1990).

Complex visual functions, such as reading and object/face recognition, are also impacted in AD. This plausibly results from both impaired transmission of visual information via injured RGCs to higher cortical centers, combined with dysfunction of higher cortical processing centers (Armstrong, 2009). In addition, AD patients often experience reading impairment, possibly resulting from neuropathological changes in the occipital lobes and the left temporal region, which are specialized in the high-level visual processing of written words (Glosser et al., 2002). An attenuation in reading speed has been reported in AD patients, particularly at lower contrast levels (Gilmore et al., 2005). Of note, reading latency is increased among AD patients and is more evident when irregular words are present in text (Passafiume et al., 2000). A recent longitudinal study with a large human cohort ($N = 8623$) found that decreased complex visual processing speed is associated with dementia risk, predicting dementia onset 9 years prior to the appearance of clinical symptoms (Begde et al., 2024), suggesting a link between visual processing and AD pathology.

A deficit in contrast sensitivity in AD patients greatly affects day-to-day functioning and leads to an overall reduced quality of life (Crow et al., 2003; Gilmore et al., 1994; Gilmore and Whitehouse, 1995; Hutton et al., 1993; Sadun et al., 1987). A recent study demonstrated significant associations between visual contrast sensitivity and brain-regional amyloid and tau deposition among patients with MCI and subjective cognitive decline (Risacher et al., 2020). As mentioned earlier, abnormalities, particularly in mRGCs, can result in circadian rhythm disturbances (Oh et al., 2019). This can have a spill-over effect, where abnormal sleep-wake patterns lead to a “sundowning” effect that exacerbates behavioral disturbances in these patients (Volicer et al., 2001). Sleep disturbances in turn may also impair the amyloid and tau clearance mechanisms (Holth et al., 2019; Ju et al., 2019; Wang and Holtzman, 2020; Yulug et al., 2017). Indeed, AD patients exhibit substantial circadian disturbances, including reduced interdaily stability and daytime activity, as well as rest-activity rhythm disturbances, sleep abnormalities, sundowning, and increased intradaily variability (Carrero et al., 2024; Guarnieri et al., 2020; Hoogendijk et al., 1996; Kang et al., 2021; Li et al., 2020a; Musiek et al., 2015, 2018; Niu et al., 2022; Rigat et al., 2023; Satlin et al., 1992; Sekiguchi et al., 2017; Van Someren, 1997; van Someren et al., 1996; Van Someren et al., 1997). Disruptions of normal circadian rhythms and sleep cycles have been associated with neurodegeneration and cognitive dysfunctions in AD, including in preclinical and early symptomatic AD patients (Ju et al., 2013; Lucey and Holtzman, 2015; Lucey et al., 2021; Musiek and Holtzman, 2016). In the retina of AD patients, evidence of Aβ accumulation around and inside degenerating mRGCs, a subset of ganglion cells that engage in photoentrainment and are believed to regulate circadian rhythms and sleep-wake cycles (La Morgia et al., 2016), may contribute to the sleep disturbances seen in these patients.

Furthermore, AD patients are reported to have lower thresholds for motion detection (Gilmore et al., 1994) and difficulty maintaining fixation on objects (Molitor et al., 2015). They also experience impaired semantic memory (Gaynor et al., 2019; Laatu et al., 2003), slower reaction times (Crawford et al., 2015), and reduced stereopsis (Dai et al., 2015; Lee et al., 2015). These visual deficits could stem from Aβ accumulation and associated pathological changes in the retina and higher-order visual centers, such as the LGN and visual cortex, in these patients (Grienberger et al., 2012; Javaid et al., 2016; Yan et al., 2017).

Growing evidence suggests that MCI and AD patients exhibit retinal functional impairments as assessed by pattern ERG (PERG). Numerous studies have continuously demonstrated a significant amplitude reduction in these patients compared to age-matched controls. These reductions are linked to retinal RGC dysfunction, evident even in preclinical AD cases (Asanad et al., 2021; Katz et al., 1989; Mavilio et al., 2020; Trick et al., 1989). Interestingly, preclinical AD patients with normal retinal morphology by OCT showed significant retinal dysfunction on ERG analysis compared to controls (Asanad et al., 2021). Krasodomska et al., found increased implicit time of the P50-wave in early-stage AD patients compared to the controls in PERG examination, whereas the amplitudes of P50- and N95-waves were significantly reduced in AD patients. This could be attributed to RGC and optic nerve dysfunction in early-stage AD patients (Krasodomska et al., 2010). Ngoo et al., further confirmed these PERG findings of reduced P50- and N95-waves amplitudes in AD patients (Ngoo et al., 2019). Similarly, Parisi et al., found a significant delay in N35, P50, and N95 implicit times, as well as a reduction in N35–P50 and P50–N95 amplitudes by PERG analysis of AD patients (Parisi et al., 2001). Another study further reported that the mean amplitude in the re-test PERG was significantly lower in the AD group than in the control group, while the intrinsic variability of the second harmonic phase was significantly higher in the AD group than in the control group (Mavilio et al., 2020). These findings indicate early-stage alteration of PERG in AD. Additionally, a few independent studies also revealed significant reduction of multifocal ERG wave amplitudes with delayed implicit times in AD patients, which were significantly correlated with the inner retinal layer thinning and poorer disease severity scores (Byun et al., 2021; Moschos et al., 2012; Sen et al., 2020; Strenn et al., 1991; Trick et al., 1989; Zhao et al., 2020).

Besides ERG changes, visual evoked potential (VEP) is also a critical electrophysiological process impacted in AD patients (Crow et al., 2003; Katz et al., 1989; Krasodomska et al., 2010; Ngoo et al., 2019; Sadun et al., 1987; Sartucci et al., 2010; Sen et al., 2020; Stothart et al., 2015; Zhao et al., 2020). Mounting evidence suggests a range of functional retinal impairments in pattern VEP latency and amplitude waves in MCI and AD patients. One study found a significant increase in the latency for yellow-black N-wave, whereas its amplitude was reduced in AD patients compared to the controls (Sartucci et al., 2010). Interestingly, there were no differences in the latencies and amplitudes for red-green and blue-yellow N-waves in AD and control groups. The abnormalities in yellow-black N-waves VEP in AD patients suggest an impairment of the magnocellular stream in AD patients (Sartucci et al., 2010). Similarly, Stothart et al., found a significant reduction of P1 and N1 VEP amplitudes in AD patients, whereas amnestic MCI patients showed a reduction in N1 amplitude compared to healthy older adults. The reduction in P1 amplitude in AD patients was associated with the degree of cognitive impairment (MMSE) (Stothart et al., 2015). Despite no difference in amplitude, Krasodomska et al., found a significant increase in the latency of the P100 wave in early-stage AD patients compared to controls (Krasodomska et al., 2010). Taken together, the altered latencies and amplitudes of diverse waves in pattern VEP might contribute to the visual disturbances experienced by AD patients.

AD patients may also suffer from posterior cortical atrophy (PCA), a rare visual variant causing significant visual field loss and greater visual impairment (Meyer and Hudock, 2018). PCA is characterized by a range of visual symptoms, including difficulties with reading, driving, oculomotor apraxia, object ataxia, simultanagnosia, topographical disorientation, left hemineglect, acalculia, agraphia, visual agnosia, and prosopagnosia, ultimately leading to severe visual disability (Kaeser et al., 2015). AD pathology may be also associated with cataracts, which can further impair visual acuity (Jefferis et al., 2011). These clinical studies have highlighted the impact of AD pathology on the visual system, suggesting that visual abnormalities in elderly individuals could serve as potential indicators of AD development. Likewise, in animal models of AD, the pathological processes has been linked to visual impairments and ERG disturbances (Chouhan et al., 2016; Georgevsky et al., 2019; Lim et al., 2020; O'Leary and Brown, 2009, 2022; Parnell et al., 2012; Raudino, 2018; Vit et al., 2021a, b). Our group has demonstrated color and contrast vision deficits in young and old transgenic murine models of AD (Fig. 16) (Vit et al., 2021a, 2021b). Further research is essential to deepen our understanding of the precise nature of visual impairments in AD and to elucidate their relationship with retinal pathology.

5. Parallels in retina and brain pathophysiology of AD and response to therapy

As discussed above, a growing number of studies have demonstrated the critical characteristic features of AD, such as amyloidosis, tauopathy, inflammation, vasculopathy, and neurodegeneration, manifesting in the AD retina and comparable to those detected in the AD brain (Asanad et al., 2019; Grimaldi et al., 2019; Hart de Ruyter et al., 2023; Koronyo et al., 2017, 2023; Lee et al., 2020b; Shi et al., 2020b, 2023; Walkiewicz et al., 2024; Xu et al., 2022). Table 2 summarizes the key clinical findings and histopathological evidence in the retina of MCI and AD patients. In fact, common pathophysiological processes were reported in both the retina and brain of AD patients. As it relates to Aβ plaques, Koronyo and colleagues described morphological similarities between retinal and brain deposits in AD patients (Koronyo et al., 2017), albeit typically smaller in size than plaques found in the brain (den Haan et al., 2018; Koronyo et al., 2017). Notably, these structural similarities were apparent when examining retinal flatmounts and $A\beta_{42}$-containing aggregates by TEM imaging (Cao et al., 2021; Koronyo et al., 2017, 2023; Qiu et al., 2020).

Higher levels of βAPP and $A\beta_{42}$ in postmortem retinal and brain tissues of AD patients compared with age-matched healthy controls, as measured by a sensitive biochemical assay, were also reported (Alexandrov et al., 2011). Note that the extent of βAPP and $A\beta_{42}$ increases in the AD brain was higher than that observed in the AD retina. Another study detected increased levels of high molecular weight $A\beta_{42}$, $A\beta_{40}$, and IAPP in the AD retina and levels were comparable to those detected in the hippocampi of patients (Schultz et al., 2020). Two additional reports quantified retinal $A\beta_{1\text{-}42}$ and $A\beta_{1\text{-}40}$ levels by ELISA and found significant 6- and 1.8-fold increases, respectively, in AD patients compared with age- and sex-matched cognitively normal controls (Koronyo et al., 2023; Shi et al., 2020b). Furthermore, quantification of retinal $A\beta_{42}$ immunoreactive area revealed 5- and 9-fold increases in MCI and AD patients, respectively (Koronyo et al., 2023). A rigorous study using several biochemical methods found an average 3.8-fold increase in the total Aβ levels in brains of AD patients as compared to a group of age-matched cognitively normal controls (Roberts et al., 2017). In this study, cortical $A\beta_{1\text{-}42}$ levels, as determined by ELISA, were ~4.5-fold (Tris--buffered saline fraction) and ~3-fold (Formic acid fraction) increased in AD patients compared to normal controls (Roberts et al., 2017). These results are in agreement with other groups (Adlard et al., 2014; Xia et al., 2009), and our own report detecting a 3.2-fold increase in brain Aβ plaque scores in AD patients versus NC controls (Koronyo et al., 2023). Overall, these studies suggest a similar magnitude of Aβ accumulation in the brain and retina of AD patients compared to controls.

With regards to tau pathology, several studies have identified the presence, elevation, and spreading of tau isoforms in retinal tissues from AD patients (den Haan et al., 2018; Du et al., 2022; Grimaldi et al., 2019; Hart de Ruyter et al., 2023; Nunez-Diaz et al., 2024; Schon et al., 2012; Shi et al., 2024; Walkiewicz et al., 2024), similar to observations in the AD brains. Comparable to the AD brain, reactive astrocytes and activated microglia were identified in the MCI and AD retinas, and they were closely associated and surrounded Aβ deposits, engaging in Aβ uptake (Koronyo et al., 2023; Xu et al., 2022). In addition, the degree of retinal atrophy in MCI and AD patients was similar to that of the respective brain atrophy in these patients (Koronyo et al., 2023), suggesting comparable retinal and brain neuronal vulnerability to degeneration during AD progression. Importantly, parallels in proteome

signatures, including multiple molecular and biological pathways [*e.g.*, immune responses, apoptosis, necrosis, mitochondrial dysfunction, oxidative phosphorylation, metabolic and chromatin dysregulation, and proteostasis], were similarly dysregulated in the retina and cortex of AD patients (Fig. 17) (Koronyo et al., 2023).

Multiple studies also reported strong associations between retinal and brain AD pathologies. For instances, the levels of retinal $A\beta_{42}$ and $A\beta_{40}$ correlated with corresponding hippocampal levels as well as with brain Aβ scores (Schultz et al., 2020). We reported significant correlations between retinal $A\beta_{42}$-immunoreactivity and plaque load with brain Aβ plaques in MCI and AD patients (Koronyo et al., 2017, 2023). In addition, the burden of retinal pTau isoforms (Ser202/Thr205 and

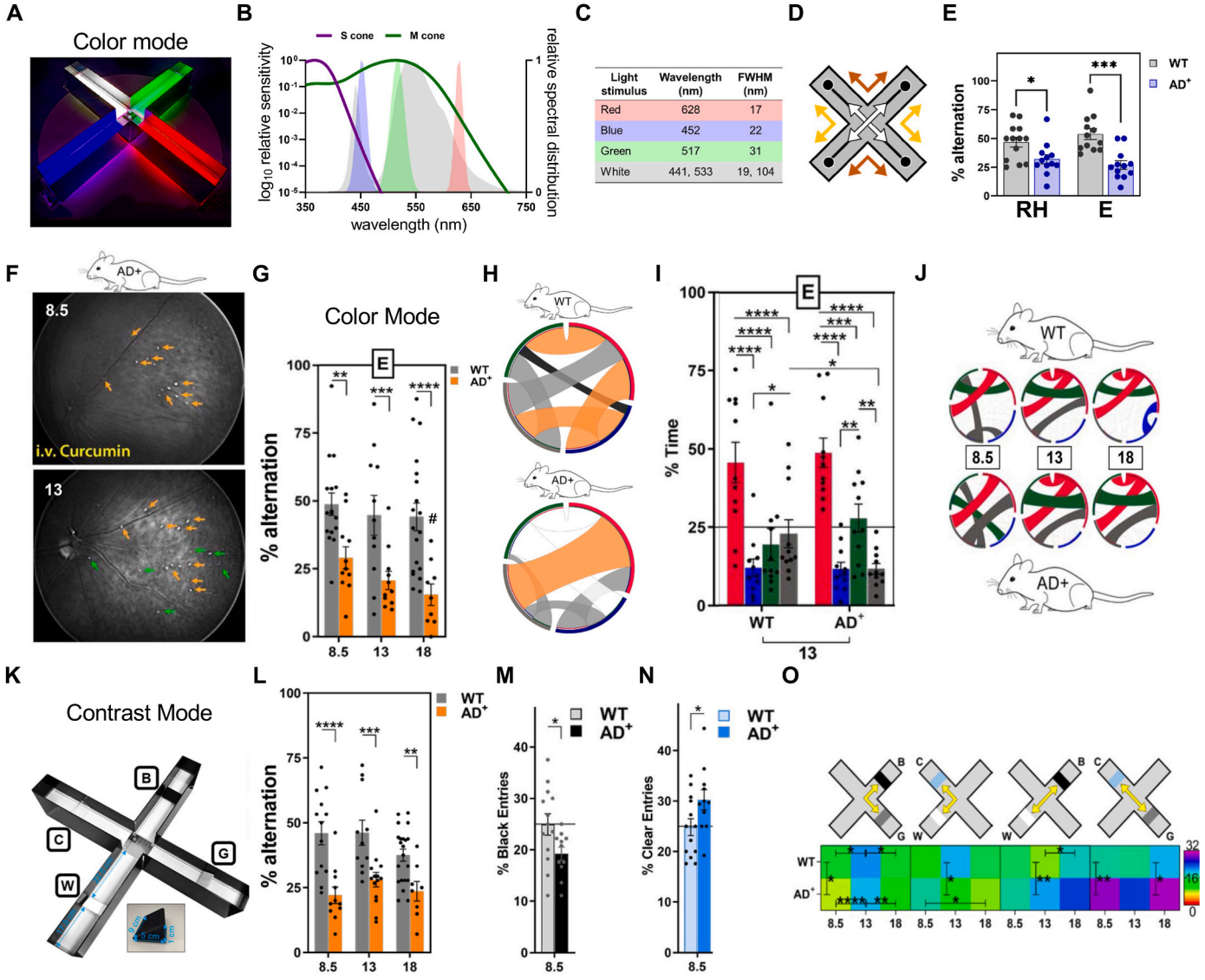

Fig. 16. Color and contrast vision impairments in young and old ADtg mice observed in the visual-stimuli X-maze test. The visual-stimuli (4-arm) X-maze (ViS4M) behavioral apparatus was used to quantitatively evaluate color and contrast vision and cognitive function in transgenic $APP_{SWE}/PS1_{\Delta E9}$ (AD^+) mice versus WT littermates. (**A**) Color mode for ViS4M text is shown. (**B**) The spectral distribution of the LED sources for each X-maze arm, corresponds to the wavelength-sensitive mouse M- and S-type opsins. (**C**) Characteristics of the light stimuli, wavelength, and full width at half maximum (FWHM), for each maze arm in the color mode. (**D**) Illustration of the spontaneous mouse alternation pathways in the ViS4M test. (**E**) Percent alternations in the red high (RH)- and the equal (E)-light intensity conditions in old AD^+ and WT mice. (**F**) Noninvasive in vivo retinal imaging of curcumin-positive amyloid deposits in the same AD^+ mouse at the age of 8.5- and 13-month-old. Orange arrows show pre-existing plaques at the 8.5-month-old mice that persisted at 13 months of age, and green arrows identify newly formed plaques at 13 months of age. (**G**) Percent alternations in E-light condition of the color mode in 8.5-, 13-, and 18-month-old AD^+ versus WT mice. (**H**) Heatmap-coded chord diagrams from the most frequent (orange) to the least frequent (black) bidirectional transitions, showing marked differences in arm transition patterns between AD^+ and WT mice. (**I**) Percent time spent in each colored arm under the E-light condition in 13-month-old AD^+ and WT mice. (**J**) Chord diagrams depicting the most frequent transitions under the E-light condition in WT (up) and AD^+ (down) mice at 3 different age groups. (**K**) Visual X maze in the contrast mode: the arms include either black (B), gray (G), white (W), or clear (C) objects, against the white floor and black walls. The dimension of the object (*e.g.*, black) in the arm is shown. (**L**) Percent alternations under the contrast mode in 8.5-, 13-, and 18-month-old WT versus AD^+ mice. (**M-N**) Percent entries in the arm containing (**M**) the black object and (**N**) the clear object in 8.5-month-old WT vs AD^+ mice. (**O**) Rainbow heatmap illustrating the percentage of bidirectional transitions between arms with gray and black objects, white and clear objects, white and black objects, and gray and clear objects (shown in top panel). The color gradient bar shows the range of percent transitions (from lowest in red to highest in purple). Mouse cohorts: 8.5-month-old WT (N = 13–16) and AD^+ (N = 11–12); 13-month-old WT (N = 11–15) and AD^+ (N = 11–15); and 18-month-old WT (N = 19) and AD^+ (N = 9). Statistics: Data from individual mouse (circles) as well as group means ± SEMs are shown. $^*P < 0.05$, $^{**}P < 0.01$, $^{***}P < 0.001$, $^{****}P < 0.0001$, by two-way ANOVA followed by post-hoc Fisher's least significant difference test. Panels were modified from (Vit et al., 2021a; Vit et al., 2021b) with permission.

Table 2
Clinical and histopathological evidence of AD pathology in the retina of MCI and AD patients.

Retinal Pathology	Findings	References
Amyloid β-protein (Aβ)	• Extra/intracellular Aβ deposits, including classical, diffused, and neuritic-like Aβ plaques in postmortem retinas of MCI and AD patients	(Du et al., 2022; Grimaldi et al., 2019; Hadoux et al., 2019; Koronyo et al., 2017, 2023; Koronyo-Hamaoui et al., 2011; La Morgia et al., 2016; Lee et al., 2020b; More et al., 2019; Tsai et al., 2014; Walkiewicz et al., 2024)
	•Ultrastructure of retinal $A\beta_{42}$ protofibrils and fibrils	
	•Spectral signature of Aβ and $A\beta_{42}$ in retinas from AD patients	
	•Increased Aβ, $A\beta_{40}$, and $A\beta_{42}$ levels in retinas from AD patients	(Alexandrov et al., 2011; Koronyo et al., 2017, 2023; Lee et al., 2020b; Schultz et al., 2020; Shi et al., 2020b, 2023)
	•Increased vascular Aβ, especially arterial $A\beta_{40}$, in retinal tissues from MCI and AD patients	
	•Increased intraneuronal Aβ oligomers, mostly in RGCs, in retinas from MCI and AD patients	Koronyo et al. (2023)
	•Aβ deposits inside and around degenerating mRGCs in the retinal tissue from AD patients	La Morgia et al. (2016)
	•Increased retinal amyloid deposits detected by curcumin-enhanced fluorescence or AF using SLO imaging in live pre-clinical, MCI, and AD patients	(Dumitrascu et al., 2020, 2021; Kile et al., 2020; Koronyo et al., 2017; Ngolab et al., 2021; Tadokoro et al., 2021b)
Abnormal tau isoforms	•pTau immunoreactivity in GCL, IPL, INL, ONL, and OPL in AD patients	(den Haan et al., 2018; Du et al., 2022; Grimaldi et al., 2019; Hart de Ruyter et al., 2023; Nilson et al., 2017; Schon et al., 2012; Walkiewicz et al., 2024)
	•pTau epitopes (3R, 4R, AT8, Ser396, AT100, pTau231, MC-1, Ser396/Ser404) in the postmortem retinas from AD patients	
	•NFT-like structures in the retina of AD patients	Koronyo et al. (2017)
	•Spectral signature of pS396-Tau in retinas from AD patients	Du et al. (2022)
Neurodegeneration	•RGC/mRGC cell loss, thinning of RNFL, GCL, IPL, INL, ONL; RGC swelling, dendritic arborization, macular degeneration, and retinal atrophy in AD patients[a]	(Almeida et al., 2019; Armstrong et al., 2021; Asanad et al., 2020; Asanad et al., 2021; Asanad et al., 2019; Ascaso et al., 2014; Bambo et al., 2015; Bayhan et al., 2015; Berisha et al., 2007; Bevan et al., 2020; Blanks et al., 1989; Cabrera DeBuc et al., 2018; Carazo-Barrios et al., 2021; Chaitanuwong et al., 2023; Chan et al., 2019; Chen et al., 2023; Cheung et al., 2015; Choi et al., 2016; Cipollini et al., 2020; Coppola et al., 2015; Cunha et al., 2017a; den Haan et al., 2019; den Haan et al., 2017; Farzinvash et al., 2022; Ferrari et al., 2017; Galvin et al., 2021; Garcia-Martin et al., 2016a; Garcia-Martin et al., 2023; Garcia-Martin et al., 2014; Girbardt et al., 2021; Hedges et al., 1996; Iseri et al., 2006; Janez-Escalada et al., 2019; Jindahra et al., 2020; Jindal, 2015; Kao et al., 2023; Kesler et al., 2011; Kim et al., 2021a; Kim et al., 2022; Kim and Kang, 2019; Kirbas et al., 2013; Koronyo et al., 2017; Koronyo et al., 2023; Kromer et al., 2014; Kwon et al., 2017; La Morgia et al., 2023; La Morgia et al., 2016; Larrosa et al., 2014; Liu et al., 2015; Lopez-de-Eguileta et al., 2019; Lu et al., 2010; Marquie et al., 2020; Marziani et al., 2013; Mathew et al., 2023; Mei et al., 2021; Mejia-Vergara et al., 2020; Moreno-Ramos et al., 2013; Moschos et al., 2012; Mutlu et al., 2018; Oktem et al., 2015; Paquet et al., 2007; Parisi et al., 2001; Polo et al., 2017; Rotenstreich et al., 2022; Sadun and Bassi, 1990; Salobrar-Garcia et al., 2019; Salobrar-Garcia et al., 2015; Sanchez et al., 2020; Santos et al., 2018; Sen et al., 2020; Shao et al., 2018; Shi et al., 2014; Shi et al., 2019; Tao et al., 2019; Trebbastoni et al., 2016; Tsai et al., 1991; Un et al., 2022; van de Kreeke et al., 2019; van der Heide et al., 2023b; Yoon et al., 2019; Zabel et al., 2019a; Zhao et al., 2023)
	•Thinning of the neuro-retinal tissue, especially in the temporal mid-periphery, of MCI and AD patients	Koronyo et al. (2023)
	•Decreased Nissl-positive neuronal counts in postmortem retinas of AD patients	Koronyo et al. (2017)
	•Increased cleaved-caspase-3 immunoreactivity in retinal tissues from AD patients	(Grimaldi et al., 2019; Koronyo et al., 2023)
Vascular abnormalities	•Decreased fractal dimensions, including column diameter, vein narrowing, branching complexity, arteriolar and venular tortuosity, and geometric optimality in AD patients, including early-stage cases	(Arthur et al., 2023; Berisha et al., 2007; Bulut et al., 2018; Cabrera DeBuc et al., 2018; Cheung et al., 2014; Cheung et al., 2022; Chiara et al., 2022; Chua et al., 2020; de Jong et al., 2011; de la Torre, 2002; Di Pippo et al., 2023; Feke et al., 2015; Frost et al., 2013; Golzan et al., 2017; Hui et al., 2021; Jiang et al., 2018; Kotliar et al., 2022; Launer, 2002; Lesage et al., 2009; Liew et al., 2009; Mei et al., 2021; Moon et al., 2023; O'Bryhim et al., 2018; Pead et al., 2023; Querques et al., 2019; Shin et al., 2021; van de Kreeke et al., 2020; Wang et al., 2023a; Wang et al., 2020b; Williams et al., 2015; Wu et al., 2020; Yeh et al., 2022; Yoon et al., 2019; Zhang et al., 2019)
	•Reduced flow speed, venous blood flow volume, parafoveal vessel loss, reduced peripapillary vessel density, and FAZ enlargement in live early- and late-stage AD patients	
	•Increased vascular and perivascular $A\beta_{40}$ and $A\beta_{42}$ deposits in postmortem retinas of MCI and AD patients	(Koronyo et al., 2017; La Morgia et al., 2016; Shi et al., 2020b, 2023)
	•Reduced pericyte/PDGFRβ levels in MCI and AD patients	
	•Reduced expression of endothelial TJ proteins (ZO-1 and Claudin-5) in retinas from MCI and AD patients	
	•Retinal arterial $A\beta_{40}$ and Claudin-5 correlated with CAA	
	•Higher $A\beta_{40}$ deposition in arteries vs. veins and capillaries in retinas from MCI and AD patients	Shi et al. (2023)
	•Increased combined retinal PMP-amyloid count and circumpapillary VT index in live patients with impaired cognition vs. normal cognition	Dumitrascu et al. (2021)
	•Inverse correlation between retinal venous brunching angle and WAIS-IV	
	•Inverse correlation between retinal venular tortuosity index and the verbal memory WMS LM-II (and other cognitive parameters) in live MCI and AD patients	

(*continued on next page*)

Table 2 (*continued*)

Retinal Pathology	Findings	References
Inflammation	•Increased macro- and microgliosis in postmortem retinas of MCI and AD patients •Increased astrocyte-to-neuron ratio in retinas from AD patients •Increased expression of microglial complement C3 and IL-1β cytokine in retinas from AD patients	(Blanks et al., 1989, 1996a; Grimaldi et al., 2019; Koronyo et al., 2023; Xu et al., 2022)
	•Microglia directly involved in Aβ uptake in retinas from MCI and AD patients •Reduced Aβ phagocytosis by microglia in retinal tissues of MCI and AD patients	(Koronyo et al., 2023; Xu et al., 2022)
	•Increased pTau uptake by microglia in retinal tissues of AD patients	Nunez-Diaz et al. (2024).

Abbreviations: Aβ: amyloid-beta protein; AD: Alzheimer's disease; AF: autofluorescence; CAA; cerebral amyloid angiopathy; FAZ: foveal avascular zone; GCL: ganglion cell layer; IL: Interleukin; INL: inner nuclear layer; IPL: inner plexiform layer; MCI: mild cognitive impairment; NFT: neurofibrillary tangle; ONL: outer nuclear layer; OPL: outer plexiform layer; PMP: proximal mid-periphery; pTau: hyperphosphorylated tau; RGC: retinal ganglion cell; mRGC: melanopsin RGC; RNFL: retinal nerve fiber layer; SLO: scanning laser ophthalmoscope; TJ: tight junctions; VT: venous tortuosity; WAIS-IV: Wechsler Adult Intelligence Scale IV; WMS LM-II: Wechsler Memory Scale Logical Memory II.

[a] Findings from both histological and live imaging studies.

Thr217) in AD patients versus controls correlated with hippocampal and cortical pTau (Ser202/Thr205) burden and Braak staging (Hart de Ruyter et al., 2023). A wide range of vascular pathologies were also commonly detected in the retina and brain of AD patients. For instance, retinal arterial $A\beta_{40}$ accumulation, and vascular pericyte-PDGFRβ and endothelial claudin-5 tight junction deficiencies, strongly correlated with CAA severity in MCI and AD patients (Shi et al., 2020b, 2023). Finally, a few imaging modalities also supported the link between retinal and brain AD pathology. Retinal amyloid reflectance spectra on HSI in AD patients correlated with brain amyloid-PET burden (Hadoux et al., 2019), and retinal curcumin-amyloid counts significantly correlated with cerebral amyloid–PET load (Ngolab et al., 2021). Taken together, these human findings, along with numerous animal model studies (Alexandrov et al., 2011; Chang et al., 2020; Chiasseu et al., 2017; Doustar et al., 2020; Grimaldi et al., 2018; Habiba et al., 2020; Koronyo-Hamaoui et al., 2011; Liu et al., 2009; Perez et al., 2009; Tsai et al., 2014; Zhang et al., 2021c), demonstrate the connection between retinal and brain pathology in AD.

In the realm of therapeutic approaches, several preclinical investigations and a pilot clinical trial have demonstrated beneficial outcomes in the retina, often mirroring the effects observed in the corresponding brain (Doustar et al., 2020; Gao et al., 2015a; He et al., 2014; Kile et al., 2020; Koronyo et al., 2012; Koronyo-Hamaoui et al., 2011; Liu et al., 2009; Parthasarathy et al., 2015; Yang et al., 2013). For instance, Kile et al. demonstrated that i.v. administration of immunoglobulin to several patients with MCI due to AD over a 2-month period resulted in similar reductions of retinal AF-amyloid deposits and brain amyloid-PET burden in most patients (Kile et al., 2020). Similar reductions in retinal and brain pathology following therapy have been described in murine models of AD. In one study, an immunomodulation therapy with myelin-derived peptide (MOG45D)-loaded dendritic cells led to significant and comparable reductions in Aβ plaques in the retina and brain of ADtg mice (Koronyo et al., 2012; Koronyo-Hamaoui et al., 2011). Additionally, Liu and colleagues reported that amyloid-peptide vaccination decreased Aβ plaques in the retina (Liu et al., 2009), a response paralleled by a reduction in brain Aβ plaques (Zhou et al., 2005). Moreover, two separate studies illustrated the feasibility of non-invasively and longitudinally tracking the dynamics of curcumin labelled Aβ plaques within the retinas of living ADtg mice, which involved observing plaque formation with disease progression and subsequent clearance following GA immunotherapy (Koronyo et al., 2012; Vit et al., 2021a). Indeed, multiple studies have shown that GA immunization leads to reduction in brain Aβ plaques, along with alleviating other pathological processes and cognitive deficits in various transgenic AD-model mouse [(Butovsky et al., 2006, 2007; Dionisio-Santos et al., 2021; Frenkel et al., 2005; Koronyo et al., 2015), reviewed in (Kasindi et al., 2022)].

Notably, in aged, late-stage ADtg mice, GA immunomodulation led to similar reductions in levels of retinal and brain $A\beta_{42}$ and $A\beta_{42}/A\beta_{40}$ ratios, as well as a strong correlation between retina and brain $A\beta_{42}$ levels and AD-related proteome markers, as depicted in Fig. 8F and G (Doustar et al., 2020). Parthasarathy and colleague further reported that Neprilysin administration reduced Aβ levels in retinal tissues of 5xFAD transgenic mice (Parthasarathy et al., 2015). Neprilysin is a well-established Aβ-degrading enzyme known to promote Aβ clearance from the brain [reviewed in (Hersh and Rodgers, 2008)]. These findings underscore the similar responses to AD therapies in both the brain and retina and highlight the potential use of noninvasive retinal imaging for monitoring therapeutic efficacy in patients.

Taken together, the identification of various pathological processes in the AD brain that are similarly found in the AD retina (Fig. 18) suggests common effects of AD on both the retina and brain during disease progression and in response to therapy.

6. Is the retina an early site of Alzheimer's pathology?

Can the retina serve as an efficient early screening target for presymptomatic AD? If so, could this early detection allow clinicians to initiate amyloid-clearing or other early therapies, potentially enhancing their therapeutic efficacy? This approach could be an exciting avenue to identify patients who may benefit from amyloid clearance before irreversible neural damage occurs.

The importance of the retina as a plausible early site for AD pathology stems from its prospective application in noninvasive detection and intervention before clinical symptoms manifest. Given that Aβ is one of the earliest core biomarkers of AD (Counts et al., 2017; Zou et al., 2020), a prerequisite for AD diagnosis (Jack, 2023), and the primary target of AD-specific therapies (McDade et al., 2022; Sims et al., 2023; van Dyck et al., 2023), the possibility of early retinal amyloid detection and longitudinal monitoring holds substantial clinical promise. Clinical trials employing Aβ plaque-clearing monoclonal antibodies that bind with high affinity to Aβ aggregates have demonstrated efficacy in slowing AD progression, particularly when initiated in early AD patients defined as those with a clinical diagnosis of MCI or mild AD dementia and positive for brain AD hallmarks (Gandy and Ehrlich, 2023; Reardon, 2023; Sims et al., 2023; Sperling et al., 2023; van Dyck et al., 2023). These trials, using Aducanumab and Lecanemab (Eisai, Biogen), which received accelerated approvals from the US regulatory agency (FDA), alongside a positive Phase 3 trial of donanemab (Eli Lilly), underscore the amyloid hypothesis in AD and highlight the therapeutic benefits of clearing brain Aβ aggregates during the early stages of the disease (Cummings et al., 2024; Markovic et al., 2023; Pang et al., 2024; Sims

et al., 2023). Notably, Lecanemab, targeting soluble Aβ protofibrils and plaques, effectively cleared brain Aβ and slowed global clinical decline by 27% as compared to placebo in the clinical dementia rating scale sum of boxes [CDR-SB] after 18 months of i.v. infusions every other week in early AD patients, with global CDR scores of 0.5–1 (Boxer and Sperling, 2023; Cummings et al., 2024; van Dyck et al., 2023). Aducanumab, targeting oligomeric Aβ and fibrillar aggregates, modestly slowed clinical decline of CDR-SB scores by 18% in MCI or mild-AD dementia patients after 76 weeks of monthly i.v. infusions of escalating dosages (Budd Haeberlein et al., 2022; Dhillon, 2021). A larger reduction in cerebral Aβ burden was associated with greater clinical benefits (Budd Haeberlein et al., 2022). Donanemab, targeting insoluble Aβ plaques and pyroglutamated Aβ, significantly slowed clinical progression by 29% (combined population CDR-SB) and by 40% in early AD patients with low/medium tau levels after i.v. administration every 4 weeks for up to 72 weeks (Boxer and Sperling, 2023; Sims et al., 2023). Hence, timely detection of AD is critical, and the potential for facilitating early screening via high-resolution retinal Aβ imaging holds promise for enhancing anti-Aβ drug efficacy and proactive preclinical disease management.

The possibility that the retina is an early site for AD pathology is supported by several studies in animal models of AD. In the double-transgenic $APP_{SWE}/PS1_{\Delta E9}$ mouse model of AD, we found that Aβ plaques in the retina preceded those detected in the respective brain of these mice (Koronyo-Hamaoui et al., 2011). Aβ plaques in the retina were detected as early as 2.5 months of age, whereas the first detectable Aβ plaques in the brain were observed at the 4–5 months of age (Garcia-Alloza et al., 2006; Koronyo-Hamaoui et al., 2011). Another

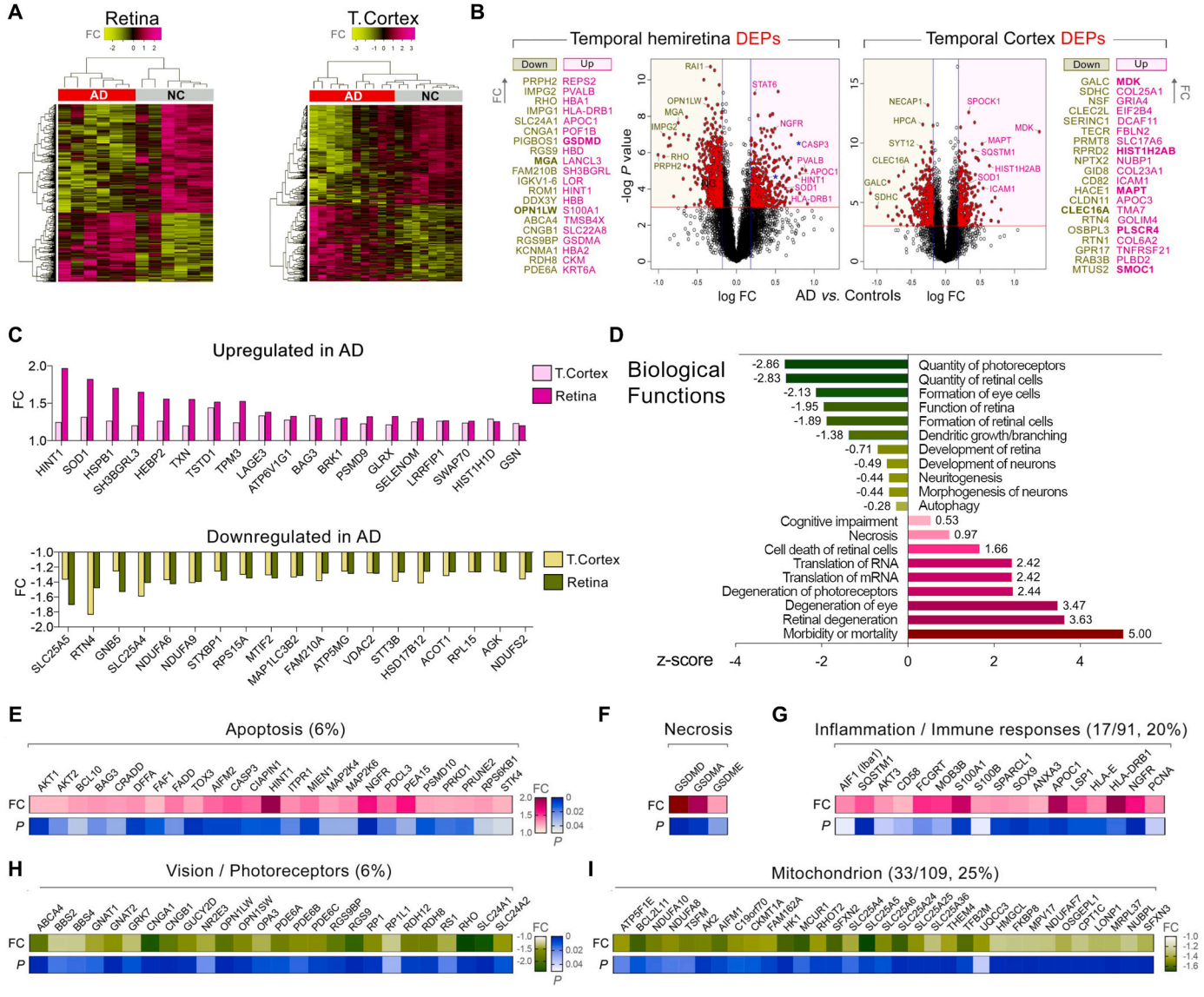

Fig. 17. Proteome landscape of the AD retina and brain. (**A**) Heatmaps display the proteomics profiling with detectable protein hierarchies as identified by mass spectrometry analysis on protein homogenates from temporal hemiretinas (N = 6 AD, N = 6 NC) and temporal (T.) cortices (N = 10 AD, N = 8 NC) of AD patients versus NC controls. The differentially expressed proteins (DEPs) and fold changes (FC) are presented for upregulated (pink) and downregulated (green) DEPs. (**B**) Volcano plots of top 20 up- or downregulated DEPs organized by FC (lowest P values highlighted in bold) in retinas and T. cortices from AD versus NC subjects (DEPs marked by red circles). (**C**) Common retinal and cortical upregulated and downregulated DEPs in AD patients versus NC controls. (**D**) Ingenuity pathway analysis of top upregulated and downregulated biological functions in AD versus NC retinas based on Z-scores. (**E-I**) DAVID biological classification analysis displays major upregulated and downregulated pathways, presenting the top upregulated DEPs (pink) related to apoptosis, necrosis, and inflammation/immune responses, as well as the top downregulated DEPs (green) associated with photoreceptor degeneration and mitochondrial dysfunction in AD versus NC retinas. Lower blue bars represent the magnitude of P values. Percentages indicate the fraction of each category of total upregulated or downregulated DEPs. All panels were adapted from (Koronyo et al., 2023) with permission.

independent study found Aβ plaques in the retina of 3-month-old $APP_{SWE}/PS1_{\Delta E9}$ mice, whereas brain Aβ plaques were not detected at this age (Habiba et al., 2021), reaffirming our previous study on early Aβ deposits in the retina in this mouse model of AD. Additionally, APP23 ADtg mice showed Aβ plaque deposition around photoreceptors in the retina earlier (at 9 months) than in the brain (12 months), which was accompanied by early onset photoreceptor degeneration (Zhang et al., 2021b). Another study using HSI revealed the presence of retinal Aβ in APP/PS1 mice at the age of 4 months in the retina but only after 8 months in the brain, further suggesting early pathologic changes in the retina (More and Vince, 2015). Furthermore, early neurodegeneration-inducing tau accumulation in the retina was observed as early as three months of age in triple ADtg mice, prior to the onset of any behavioral deficits, and preceded tau accumulation in the brain (Chiasseu et al., 2017). Color and contrast vision impairments on the Visual-Stimuli X-maze were detected in $APP_{SWE}/PS1_{\Delta E9}$ ADtg mice versus WT littermate mice as early as 8.5 months of age, prior to the detection of cognitive impairment as assessed by the Barnes maze test (Vit et al., 2021a, 2021b). Consistently, another in-vivo longitudinal study utilizing ERG analysis and OCT imaging in APP/PS1 mice at different times (3- to 12-months of age) revealed progressive functional and structural impairment in the inner retina (Georgevsky et al., 2019). Importantly, the functional ERG deficits started at 3 months, earlier than the OCT structural thinning that started at 9 months, both preceding cognitive impairment, suggesting an early onset of retinal degeneration in AD models. Findings from these animal studies affirm that the retina is a promising target to detect early pathological changes in AD, including amyloid deposition and tauopathy.

These findings support some of the early retinal changes described in human studies. The specific hallmarks, Aβ and tau pathologies, were detected in postmortem retinas of patients with early-stage AD, including MCI due to AD and mild AD dementia (Koronyo et al., 2023; Koronyo-Hamaoui et al., 2011; Shi et al., 2020b, 2023, 2024). In addition, several clinical studies have demonstrated significant increases in retinal amyloid deposits in live pre-clinical AD and MCI patients (Dumitrascu et al., 2020, 2021; Hadoux et al., 2019; More et al., 2019; Ngolab et al., 2021). The highest sensitivity for differential retinal amyloid-hyperspectral signature was found for MCI patients with $\geq$22 MMSE scores as compared to age-matched controls (More et al., 2019). A trend of increased retinal amyloid was further reported by Tadokoro and colleagues in a study with 7 MCI versus 10 NC subjects (Tadokoro et al., 2021b), whereas the increase reached significance for AD patients. In addition, other non-AD specific pathological findings were reported in early symptomatic stages of AD, in MCI patients. Utilizing OCT imaging, including meta-analysis studies, indicated significant changes such as thinning of the peripapillary and nasal RNFL and the GCL in MCI patients (Chan et al., 2019; Chen et al., 2023; den Haan et al., 2017; Lu et al., 2010; Paquet et al., 2007). Similarly, various vascular abnormalities, including reduced venous blood column diameter and enlarged FAZ, were found in early AD patients (Berisha et al., 2007; Chua et al., 2020; Hui et al., 2021; O'Bryhim et al., 2018; Shin et al., 2021; Snyder et al., 2016; Wu et al., 2020; Yeh et al., 2022). OCTA imaging also demonstrated a significant decline in parafoveal flow and vessel density in individuals with amnesic MCI and early AD patients (Zhang et al., 2019). These significant changes in retinal vascular function and structure appear to be early pathological signs that may occur during the asymptomatic or early symptomatic stages of AD (Frost et al., 2013).

Clinically, visual dysfunctions can also provide an early clue for patients who may develop AD. Testing of object recognition and discrimination showed significant differences between pre-MCI, amnestic-MCI, and dementia groups versus NC controls, suggesting that these tests can detect early visual impairments related to AD (Gaynor et al., 2019). Object recognition impairments in early AD are linked to semantic memory impairment, causing visual deficits and difficulty recognizing items, people, and places (Laatu et al., 2003). Significant visual impairments, including deficits in visual acuity, contrast sensitivity, and color perception, were further observed in MCI and mild AD dementia patients (Gaynor et al., 2019; Javitt et al., 2023; Krasodomska et al., 2010; Laatu et al., 2003; Lopez-Cuenca et al., 2023; Risacher et al., 2013, 2020; Salobrar-Garcia et al., 2019; Stothart et al., 2015; Ye et al., 2018; Zhao et al., 2020), suggesting early and substantial visual abnormalities during AD progression. In a recent clinical study, an eye-tracking test facilitated the early detection of cognitive impairment in patients with MCI and AD (Tadokoro et al., 2021a). Another longitudinal study revealed that complex visual processing speed in individuals can predict dementia risk 9 years prior to the onset of clinical symptoms (Begde et al., 2024), suggesting early visual abnormalities in AD pathology.

Overall, the presence of pathological hallmarks and structural abnormalities in the retina, alongside visual impairments in early AD patients, demonstrate the value of further studying the retina for potential early noninvasive AD detection. It is still unclear how early and common these retinal changes are in the broader population of AD patients and whether they can accurately predict disease status in the brain and cognitive decline. Additionally, future studies are required to determine whether retinal biomarkers can be used as a screening tool in asymptomatic patients who may have risk factors such as a strong family history. Hence, it is conceivable that a future healthcare plan for detecting AD would include periodic multimodal retinal scans. Asymptomatic individuals with evidence of retinal AD pathology could be referred for further assessments of AD biomarkers, including brain amyloid- and tau-PET imaging and/or fluid Aβ and pTau biomarkers, to confirm an AD diagnosis.

7. Conclusions

In our quest to enhance AD diagnostics, significant strides have been made in identifying the pathological hallmarks of AD within the accessible retina. These include the detection of abnormal forms of Aβ and tau isoforms, along with a spectrum of vascular and inflammatory abnormalities, and neurodegeneration. Notably, these changes can precede the dementia diagnosis, occurring during preclinical stages or at the onset of functional impairment (*e.g.,* MCI), and may correlate with the severity of cerebral AD pathology and cognitive deficits. This underscores the retina's potential as a predictive site for early AD detection and monitoring. A summary of retinal histopathological evidence in MCI and AD patients, alongside predicted changes during the AD continuum, is illustrated in Fig. 19. Retinal imaging stands out for its noninvasive, cost-effective, and high-resolution imaging capabilities, encompassing structural, vascular, cellular, and molecular dimensions of CNS tissue. Ophthalmic imaging technologies have advanced in capturing a range of pathological processes, some of which are widely used in clinical practice. Advances in retinal amyloid deposit and vascular functional-structural imaging may serve as future early indicators for individuals at risk and provide real-time assessment of treatments targeting amyloid. While live imaging of retinal gliosis or tauopathy remains elusive, this area harbors great promise for breakthrough innovation. The comprehensive body of literature reviewed here, along with ongoing research, emphasizes the necessity to deepen our understanding of AD pathophysiology in the retina. Future studies are critically needed to replicate previous findings in larger and more diverse cohorts with confirmed AD biomarkers. These studies must utilize standardized retinal pathology and imaging techniques to validate retinal biomarkers for AD and determine their context of use. Collectively, these efforts signal an emerging era where standardized retinal imaging has the potential to revolutionize the diagnosis and management of AD and other neurodegenerative diseases.

Funding

This work was supported by the National Institutes of Health (NIH)/ National Institute on Aging (NIA) grant numbers: R01AG056478,

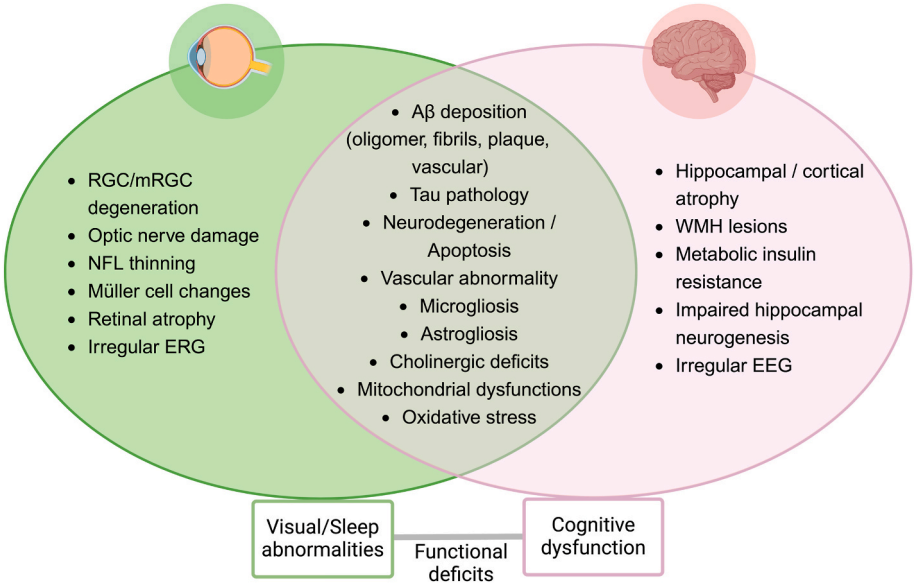

Fig. 18. Parallel AD pathological processes in the brain and retina. Various pathological hallmarks of AD observed in the brain of AD patients have also been identified in the retina. The key characteristic features of AD that the retina shares with the brain include, Aβ deposition (*e.g.*, oligomers, protofibrils and fibrils, neuritic plaques, and perivascular and vascular $A\beta_{40}$ and $A\beta_{42}$ accumulations), abnormal tau isoforms (*e.g.*, pTau, 3R and 4R tau isoforms), neurodegeneration and apoptotic cell death, vascular abnormalities, inflammatory processes (microgliosis and astrogliosis), cholinergic dysfunction, mitochondrial dysfunctions, and oxidative stress. The mRGC/RGC degeneration, optic nerve damage, RNFL thinning, Müller glia changes, retinal atrophy, and irregular ERG were reported in AD retina, whereas hippocampal and cortical atrophy, white matter hyperintensities (WMH) lesions, metabolic insulin resistance, impaired hippocampal neurogenesis, and irregular EEG were reported in the AD brain. These pathophysiological processes in the retina can contribute to visual and sleep abnormalities, and those in the brain lead to cognitive and behavioral deficits that were described in AD patients. Sharing the diverse and key pathological hallmarks of AD with the brain, the easily accessible retina may serve as a prime site for visualizing and monitoring AD.

R01AG055865, and R01AG075998 (MKH). Additionally, the work was supported by The Saban, The Wilstein, The Marciano, and The Gordon Foundations, as well as The Jona Goldrich Center Alzheimer's Disease Award and The Hertz Innovation Fund (MKH). We also acknowledge the support from The Ray Charles Foundation (MRD, OJ).

CRediT authorship contribution statement

Bhakta Prasad Gaire: Investigation, Methodology, Software, Validation, Visualization, Writing – original draft, Writing – review & editing. **Yosef Koronyo:** Data curation, Formal analysis, Investigation, Methodology, Software, Validation, Visualization, Writing – original draft, Writing – review & editing. **Dieu-Trang Fuchs:** Visualization, Writing – review & editing. **Haoshen Shi:** Data curation, Writing – review & editing. **Altan Rentsendorj:** Data curation, Writing – review & editing. **Ron Danziger:** Writing – original draft, Writing – review & editing. **Jean-Philippe Vit:** Data curation, Writing – review & editing. **Nazanin Mirzaei:** Data curation, Writing – review & editing. **Jonah Doustar:** Data curation, Writing – review & editing. **Julia Sheyn:** Data curation, Writing – review & editing. **Harald Hampel:** Writing – review & editing. **Andrea Vergallo:** Writing – review & editing. **Miyah R. Davis:** Writing – review & editing. **Ousman Jallow:** Writing – review & editing. **Filippo Baldacci:** Writing – review & editing. **Steven R. Verdooner:** Data curation, Writing – review & editing. **Ernesto Barron:** Writing – review & editing. **Mehdi Mirzaei:** Data curation, Writing – review & editing. **Vivek K. Gupta:** Writing – review & editing. **Stuart L. Graham:** Writing – review & editing. **Mourad Tayebi:** Writing – review & editing. **Roxana O. Carare:** Writing – review & editing. **Alfredo A. Sadun:** Data curation, Writing – review & editing. **Carol A. Miller:** Writing – review & editing. **Oana M. Dumitrascu:** Data curation, Writing – review & editing. **Shouri Lahiri:** Writing – review & editing. **Liang Gao:** Data curation, Writing – review & editing. **Keith L. Black:** Supervision, Writing – review & editing. **Maya Koronyo-Hamaoui:** Conceptualization, Data curation, Formal analysis, Funding acquisition, Investigation, Methodology, Resources, Software, Supervision, Validation, Visualization, Writing – original draft, Writing – review & editing.

Declaration of competing interest

HH declares no competing financial interests related to the present article. He is an employee of Eisai Inc. The present article has been initiated and prepared as part of his academic position at Sorbonne University, Paris, France, and reflects entirely and exclusively his own opinion. He serves as Senior Associate Editor for the Journal Alzheimer's & Dementia and does not receive any fees or honoraria since May 2019.

He is inventor of 11 patents and has received no royalties:

- In Vitro Multiparameter Determination Method for The Diagnosis and Early Diagnosis of Neurodegenerative Disorders Patent Number: 8916388
- In Vitro Procedure for Diagnosis and Early Diagnosis of Neurodegenerative Diseases Patent Number: 8298784
- Neurodegenerative Markers for Psychiatric Conditions Publication Number: 20120196300
- In Vitro Multiparameter Determination Method for The Diagnosis and Early Diagnosis of Neurodegenerative Disorders Publication Number: 20100062463
- In Vitro Method for The Diagnosis and Early Diagnosis of Neurodegenerative Disorders Publication Number: 20100035286
- In Vitro Procedure for Diagnosis and Early Diagnosis of Neurodegenerative Diseases Publication Number: 20090263822
- In Vitro Method for The Diagnosis of Neurodegenerative Diseases Patent Number: 7547553
- CSF Diagnostic in Vitro Method for Diagnosis of Dementias and Neuroinflammatory Diseases Publication Number: 20080206797
- In Vitro Method for The Diagnosis of Neurodegenerative Diseases Publication Number: 20080199966

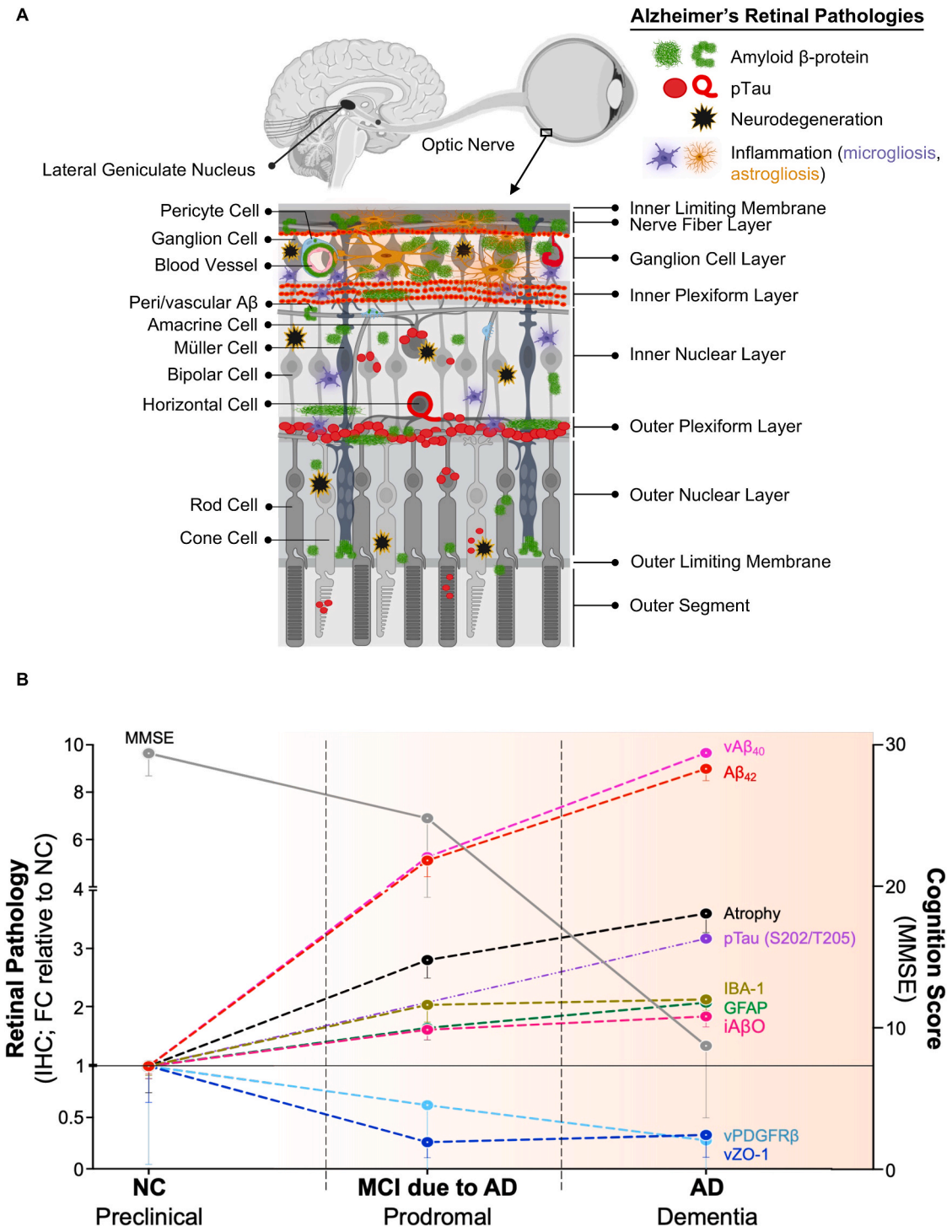

Fig. 19. Retinal pathological processes and predicted changes during AD continuum. (**A**) Schematic depiction of the pathological changes identified in different cell layers of the retina from MCI and AD patients. Aβ deposition occurs throughout the retinal layers, as well as in the retinal blood vessels, pericytes, and Müller glia endfeet. Aβ deposits are identified predominantly in the inner retina as compared to the outer retina. pTau accumulation is often observed in the OPL, along with the IPL, INL, GCL, and RNFL. Retinal neurodegeneration is detected across all retinal layers with marked ganglion cell loss, and inflammatory processes, including reactive astrocytes and activated microglia, being abundant in the inner retina (RNFL, GCL, IPL, and INL). As disease progresses, activated microglia are also found in the OPL. (**B**) Graphical illustration of the predicted changes (continues dotted lines) in retinal histopathological markers during AD progression. Experimental histopathological data of the mean fold change (FC) values quantified in retinal tissues from MCI and AD patients versus NC controls. Retinal pathologies included the $A\beta_{42}$ deposition, IBA-1 microgliosis, GFAP gliosis, intraneuronal Aβ oligomers (iAβO), and atrophy (Koronyo et al., 2023), vascular (v)$A\beta_{40}$, vPDGFRβ, (Shi et al., 2020b) and vZO-1 (Shi et al., 2023), as well as pTau (S202/T205) (Hart de Ruyter et al., 2023), plotted against the reported MMSE scores (Koronyo et al., 2023). The FC values of pTau (S202/T205) was calculated by dividing the mean surface percentage of pTau (S202/205) in the AD retina by the average mean surface percentage of pTau (S202/205) in controls with Braak scores of 0 or I-III. pTau (S202/205) IR area was analyzed in the mid- and far-peripheral retinal regions and does not include MCI patients. All other biomarkers represent retinal changes from central, mid-, and far-peripheral ST and IT subregions, in the three diagnostic groups. The black line represents the threshold FC value of 1 relative to NC controls.

- Neurodegenerative Markers for Psychiatric Conditions Publication Number: 20080131921
- Method for diagnosis of dementias and neuroinflammatory diseases based on an increased level of procalcitonin in cerebrospinal fluid: Publication number: United States Patent 10921330.

AV declares no competing financial interests related to the present article. AV contribution to this work relates to his previous academic position at Sorbonne University, Paris, France. AV was an employee of Eisai Inc. (Nov 2019–June 2021). AV does not receive any fees or honoraria since November 2019. Before November 2019 he had he received lecture honoraria from Roche, MagQu LLC, and Servier.

YK and MKH are co-founding members and consultants of NeuroVision Imaging, Inc., 1395 Garden Highway, Suite 250, Sacramento, CA 95833, USA. KLB is chair and SV is CEO, co-founders and shareholders of NeuroVision Imaging, Inc., 1395 Garden Highway, Suite 250, Sacramento, CA 95833, USA.

All other authors declare no competing interests related to this article.

Data availability

Data will be made available on request.

Acknowledgement and dedication

We thank Elijiah Maxfield for English editing. Figs. 3A, 13A, 18, and 19A were prepared using Biorender.com. This article is dedicated in Memoriam to our friend and colleague Prof. David R. Hinton, MD, FARVO, of the Department of Pathology and the Keck School of Medicine, USC. The article is also dedicated to the memory of Dr. Salomon Moni Hamaoui and Lillian Jones Black, both of whom passed away from Alzheimer's disease.

References

Abbasi, J., 2017. A retinal scan for Alzheimer disease. JAMA 318, 1314.
Adlard, P.A., Li, Q.X., McLean, C., Masters, C.L., Bush, A.I., Fodero-Tavoletti, M., Villemagne, V., Barnham, K.J., 2014. beta-amyloid in biological samples: not all Abeta detection methods are created equal. Front. Aging Neurosci. 6, 203.
Akiyama, H., Barger, S., Barnum, S., Bradt, B., Bauer, J., Cole, G.M., Cooper, N.R., Eikelenboom, P., Emmerling, M., Fiebich, B.L., Finch, C.E., Frautschy, S., Griffin, W. S., Hampel, H., Hull, M., Landreth, G., Lue, L., Mrak, R., Mackenzie, I.R., McGeer, P. L., O'Banion, M.K., Pachter, J., Pasinetti, G., Plata-Salaman, C., Rogers, J., Rydel, R., Shen, Y., Streit, W., Strohmeyer, R., Tooyoma, I., Van Muiswinkel, F.L., Veerhuis, R., Walker, D., Webster, S., Wegrzyniak, B., Wenk, G., Wyss-Coray, T., 2000. Inflammation and Alzheimer's disease. Neurobiol. Aging 21, 383–421.
Al-Mujaini, A.S., Al-Mujaini, M.S., Sabt, B.I., 2021. Retinal nerve fiber layer thickness in multiple sclerosis with and without optic neuritis: a four-year follow-up study from Oman. BMC Ophthalmol. 21, 391.
Alber, J., Arthur, E., Goldfarb, D., Drake, J., Boxerman, J.L., Silver, B., Ott, B.R., Johnson, L.N., Snyder, P.J., 2021. The relationship between cerebral and retinal microbleeds in cerebral amyloid angiopathy (CAA): a pilot study. J. Neurol. Sci. 423, 117383.
Alber, J., Bouwman, F., den Haan, J., Rissman, R.A., De Groef, L., Koronyo-Hamaoui, M., Lengyel, I., Thal, D.R., Alzheimer's Association ISTAART "The Eye as a Biomarker for AD" Professional Interest Area, 2023. Retina pathology as a target for biomarkers for Alzheimer's disease: current status, ophthalmopathological background, challenges, and future directions. Alzheimers Dement.
Alber, J., Goldfarb, D., Thompson, L.I., Arthur, E., Hernandez, K., Cheng, D., DeBuc, D.C., Cordeiro, F., Provetti-Cunha, L., den Haan, J., Van Stavern, G.P., Salloway, S.P., Sinoff, S., Snyder, P.J., 2020. Developing retinal biomarkers for the earliest stages of Alzheimer's disease: what we know, what we don't, and how to move forward. Alzheimers Dement 16, 229–243.
Alexandrov, P.N., Pogue, A., Bhattacharjee, S., Lukiw, W.J., 2011. Retinal amyloid peptides and complement factor H in transgenic models of Alzheimer's disease. Neuroreport 22, 623–627.
Almeida, A.L.M., Pires, L.A., Figueiredo, E.A., Costa-Cunha, L.V.F., Zacharias, L.C., Preti, R.C., Monteiro, M.L.R., Cunha, L.P., 2019. Correlation between cognitive impairment and retinal neural loss assessed by swept-source optical coherence tomography in patients with mild cognitive impairment. Alzheimers Dement. (Amst) 11, 659–669.
Alzheimer, A., 1906. Über einen eigenartigen schweren Erkrankungsprozeβ der Hirnrincle. Neurol Central 25, 1134.
Alzheimer, A., Stelzmann, R.A., Schnitzlein, H.N., Murtagh, F.R., 1995. An English translation of Alzheimer's 1907 paper, "Uber eine eigenartige Erkankung der Hirnrinde". Clin. Anat. 8, 429–431.
Alzheimer's, A., 2023. 2023 Alzheimer's disease facts and figures. Alzheimers Dement 19, 1598–1695.
Amthor, F.R., Tootle, J.S., Gawne, T.J., 2005. Retinal ganglion cell coding in simulated active vision. Vis. Neurosci. 22, 789–806.
Antes, R., Salomon-Zimri, S., Beck, S.C., Garcia Garrido, M., Livnat, T., Maharshak, I., Kadar, T., Seeliger, M., Weinberger, D., Michaelson, D.M., 2015. VEGF mediates ApoE4-induced neovascularization and synaptic pathology in the choroid and retina. Curr. Alzheimer Res. 12, 323–334.
Armstrong, G.W., Kim, L.A., Vingopoulos, F., Park, J.Y., Garg, I., Kasetty, M., Silverman, R.F., Zeng, R., Douglas, V.P., Lopera, F., Baena, A., Giraldo, M., Norton, D., Cronin-Golomb, A., Arboleda-Velasquez, J.F., Quiroz, Y.T., Miller, J.B., 2021. Retinal imaging findings in carriers with PSEN1-associated early-onset familial Alzheimer disease before onset of cognitive symptoms. JAMA Ophthalmol 139, 49–56.
Armstrong, R.A., 1996. Visual field defects in Alzheimer's disease patients may reflect differential pathology in the primary visual cortex. Optom. Vis. Sci. 73, 677–682.
Armstrong, R.A., 2009. Alzheimer's disease and the eye. J. Opt. 2, 103–111.
Armulik, A., Genove, G., Betsholtz, C., 2011. Pericytes: developmental, physiological, and pathological perspectives, problems, and promises. Dev. Cell 21, 193–215.
Arthur, E., Ravichandran, S., Snyder, P.J., Alber, J., Strenger, J., Bittner, A.K., Khankan, R., Adams, S.L., Putnam, N.M., Lypka, K.R., Piantino, J.A., Sinoff, S., 2023. Retinal mid-peripheral capillary free zones are enlarged in cognitively unimpaired older adults at high risk for Alzheimer's disease. Alzheimer's Res. Ther. 15, 172.
Arvanitakis, Z., Leurgans, S.E., Wang, Z., Wilson, R.S., Bennett, D.A., Schneider, J.A., 2011. Cerebral amyloid angiopathy pathology and cognitive domains in older persons. Ann. Neurol. 69, 320–327.
Asanad, S., Fantini, M., Sultan, W., Nassisi, M., Felix, C.M., Wu, J., Karanjia, R., Ross-Cisneros, F.N., Sagare, A.P., Zlokovic, B.V., Chui, H.C., Pogoda, J.M., Arakaki, X., Fonteh, A.N., Sadun, A.A., Harrington, M.G., 2020. Retinal nerve fiber layer thickness predicts CSF amyloid/tau before cognitive decline. PLoS One 15, e0232785.
Asanad, S., Felix, C.M., Fantini, M., Harrington, M.G., Sadun, A.A., Karanjia, R., 2021. Retinal ganglion cell dysfunction in preclinical Alzheimer's disease: an electrophysiologic biomarker signature. Sci. Rep. 11, 6344.
Asanad, S., Ross-Cisneros, F.N., Nassisi, M., Barron, E., Karanjia, R., Sadun, A.A., 2019. The retina in Alzheimer's disease: histomorphometric analysis of an Ophthalmologic biomarker. Invest. Ophthalmol. Vis. Sci. 60, 1491–1500.
Ascaso, F.J., Cruz, N., Modrego, P.J., Lopez-Anton, R., Santabarbara, J., Pascual, L.F., Lobo, A., Cristobal, J.A., 2014. Retinal alterations in mild cognitive impairment and Alzheimer's disease: an optical coherence tomography study. J. Neurol. 261, 1522–1530.
Ashraf, G., McGuinness, M., Khan, M.A., Obtinalla, C., Hadoux, X., van Wijngaarden, P., 2023. Retinal imaging biomarkers of Alzheimer's disease: a systematic review and meta-analysis of studies using brain amyloid beta status for case definition. Alzheimers Dement. (Amst) 15, e12421.
Baker, M.L., Marino Larsen, E.K., Kuller, L.H., Klein, R., Klein, B.E., Siscovick, D.S., Bernick, C., Manolio, T.A., Wong, T.Y., 2007. Retinal microvascular signs, cognitive function, and dementia in older persons: the Cardiovascular Health Study. Stroke 38, 2041–2047.
Bakker, E.N., Bacskai, B.J., Arbel-Ornath, M., Aldea, R., Bedussi, B., Morris, A.W., Weller, R.O., Carare, R.O., 2016. Lymphatic clearance of the brain: perivascular, Paravascular and significance for neurodegenerative diseases. Cell. Mol. Neurobiol. 36, 181–194.
Balestrini, S., Clayton, L.M., Bartmann, A.P., Chinthapalli, K., Novy, J., Coppola, A., Wandschneider, B., Stern, W.M., Acheson, J., Bell, G.S., Sander, J.W., Sisodiya, S.M., 2016. Retinal nerve fibre layer thinning is associated with drug resistance in epilepsy. J. Neurol. Neurosurg. Psychiatry 87, 396–401.
Ballatore, C., Lee, V.M., Trojanowski, J.Q., 2007. Tau-mediated neurodegeneration in Alzheimer's disease and related disorders. Nat. Rev. Neurosci. 8, 663–672.
Bambo, M.P., Garcia-Martin, E., Otin, S., Pinilla, J., Larrosa, J.M., Polo, V., Pablo, L.E., 2015. Visual function and retinal nerve fibre layer degeneration in patients with Alzheimer disease: correlations with severity of dementia. Acta Ophthalmol. 93, e507–e508.
Banks, W.A., Robinson, S.M., Verma, S., Morley, J.E., 2003. Efflux of human and mouse amyloid beta proteins 1-40 and 1-42 from brain: impairment in a mouse model of Alzheimer's disease. Neuroscience 121, 487–492.
Bao, W., Jia, H., Finnema, S., Cai, Z., Carson, R.E., Huang, Y.H., 2017. PET imaging for early detection of Alzheimer's disease: from pathologic to physiologic biomarkers. Pet. Clin. 12, 329–350.
Bartley, S.C., Proctor, M.T., Xia, H., Ho, E., Kang, D.S., Schuster, K., Bicca, M.A., Seckler, H.S., Viola, K.L., Patrie, S.M., Kelleher, N.L., De Mello, F.G., Klein, W.L., 2022. An essential role for Alzheimer's-linked amyloid beta oligomers in Neurodevelopment: transient expression of multiple Proteoforms during retina Histogenesis. Int. J. Mol. Sci. 23.
Barton, S.M., To, E., Rogers, B.P., Whitmore, C., Uppal, M., Matsubara, J.A., Pham, W., 2021. Inhalable thioflavin S for the detection of amyloid beta deposits in the retina. Molecules 26.
Barucker, C., Bittner, H.J., Chang, P.K., Cameron, S., Hancock, M.A., Liebsch, F., Hossain, S., Harmeier, A., Shaw, H., Charron, F.M., Gensler, M., Dembny, P., Zhuang, W., Schmitz, D., Rabe, J.P., Rao, Y., Lurz, R., Hildebrand, P.W., McKinney, R.A., Multhaup, G., 2015. Abeta42-oligomer Interacting Peptide (AIP) neutralizes toxic amyloid-beta42 species and protects synaptic structure and function. Sci. Rep. 5, 15410.

Bassi, C.J., Sadun, A.A., 1990. Alzheimer's disease and vision: correlation versus causation, revisited. Ophthalmology 97, 395–397.
Bateman, R.J., Xiong, C., Benzinger, T.L., Fagan, A.M., Goate, A., Fox, N.C., Marcus, D.S., Cairns, N.J., Xie, X., Blazey, T.M., Holtzman, D.M., Santacruz, A., Buckles, V., Oliver, A., Moulder, K., Aisen, P.S., Ghetti, B., Klunk, W.E., McDade, E., Martins, R. N., Masters, C.L., Mayeux, R., Ringman, J.M., Rossor, M.N., Schofield, P.R., Sperling, R.A., Salloway, S., Morris, J.C., Dominantly Inherited Alzheimer, N., 2012. Clinical and biomarker changes in dominantly inherited Alzheimer's disease. N. Engl. J. Med. 367, 795–804.
Bature, F., Guinn, B.A., Pang, D., Pappas, Y., 2017. Signs and symptoms preceding the diagnosis of Alzheimer's disease: a systematic scoping review of literature from 1937 to 2016. BMJ Open 7, e015746.
Baumann, B., Woehrer, A., Ricken, G., Augustin, M., Mitter, C., Pircher, M., Kovacs, G.G., Hitzenberger, C.K., 2017. Visualization of neuritic plaques in Alzheimer's disease by polarization-sensitive optical coherence microscopy. Sci. Rep. 7, 43477.
Bayhan, H.A., Aslan Bayhan, S., Celikbilek, A., Tanik, N., Gurdal, C., 2015. Evaluation of the chorioretinal thickness changes in Alzheimer's disease using spectral-domain optical coherence tomography. Clin. Exp. Ophthalmol. 43, 145–151.
Begde, A., Wilcockson, T., Brayne, C., Hogervorst, E., 2024. Visual processing speed and its association with future dementia development in a population-based prospective cohort: EPIC-Norfolk. Sci. Rep. 14, 5016.
Bell, R.D., Zlokovic, B.V., 2009. Neurovascular mechanisms and blood-brain barrier disorder in Alzheimer's disease. Acta Neuropathol. 118, 103–113.
Ben-Nejma, I.R.H., Keliris, A.J., Vanreusel, V., Ponsaerts, P., Van der Linden, A., Keliris, G.A., 2023. Altered dynamics of glymphatic flow in a mature-onset Tet-off APP mouse model of amyloidosis. Alzheimer's Res. Ther. 15, 23.
Bennett, D., 2001. Public health importance of vascular dementia and Alzheimer's disease with cerebrovascular disease. Int. J. Clin. Pract. Suppl. 41–48.
Bergers, G., Song, S., 2005. The role of pericytes in blood-vessel formation and maintenance. Neuro Oncol. 7, 452–464.
Berisha, F., Feke, G.T., Trempe, C.L., McMeel, J.W., Schepens, C.L., 2007. Retinal abnormalities in early Alzheimer's disease. Invest. Ophthalmol. Vis. Sci. 48, 2285–2289.
Bevan, R.J., Hughes, T.R., Williams, P.A., Good, M.A., Morgan, B.P., Morgan, J.E., 2020. Retinal ganglion cell degeneration correlates with hippocampal spine loss in experimental Alzheimer's disease. Acta Neuropathol. Commun. 8, 216.
Biffi, A., Greenberg, S.M., 2011. Cerebral amyloid angiopathy: a systematic review. J. Clin. Neurol. 7, 1–9.
Binnewijzend, M.A., Benedictus, M.R., Kuijer, J.P., van der Flier, W.M., Teunissen, C.E., Prins, N.D., Wattjes, M.P., van Berckel, B.N., Scheltens, P., Barkhof, F., 2016. Cerebral perfusion in the predementia stages of Alzheimer's disease. Eur. Radiol. 26, 506–514.
Biron, K.E., Dickstein, D.L., Gopaul, R., Jefferies, W.A., 2011. Amyloid triggers extensive cerebral angiogenesis causing blood brain barrier permeability and hypervascularity in Alzheimer's disease. PLoS One 6, e23789.
Biscetti, L., Lupidi, M., Luchetti, E., Eusebi, P., Gujar, R., Vergaro, A., Cagini, C., Parnetti, L., 2021. Novel noninvasive biomarkers of prodromal Alzheimer disease: the role of optical coherence tomography and optical coherence tomography-angiography. Eur. J. Neurol. 28, 2185–2191.
Bitel, C.L., Kasinathan, C., Kaswala, R.H., Klein, W.L., Frederikse, P.H., 2012. Amyloid-beta and tau pathology of Alzheimer's disease induced by diabetes in a rabbit animal model. J. Alzheimers Dis. 32, 291–305.
Blanks, J.C., Hinton, D.R., Sadun, A.A., Miller, C.A., 1989. Retinal ganglion cell degeneration in Alzheimer's disease. Brain Res. 501, 364–372.
Blanks, J.C., Schmidt, S.Y., Torigoe, Y., Porrello, K.V., Hinton, D.R., Blanks, R.H., 1996a. Retinal pathology in Alzheimer's disease. II. Regional neuron loss and glial changes in GCL. Neurobiol. Aging 17, 385–395.
Blanks, J.C., Torigoe, Y., Hinton, D.R., Blanks, R.H., 1996b. Retinal pathology in Alzheimer's disease. I. Ganglion cell loss in foveal/parafoveal retina. Neurobiol. Aging 17, 377–384.
Bonte, F.J., Ross, E.D., Chehabi, H.H., Devous, M.D., 1986. SPECT study of regional cerebral blood flow in Alzheimer disease. J. Comput. Assist. Tomogr. 10, 579–583.
Boxer, A.L., Sperling, R., 2023. Accelerating Alzheimer's therapeutic development: the past and future of clinical trials. Cell 186, 4757–4772.
Bravo, F.J.V., Ayliffe, W., Stanga, S.F.E., Reinstein, U.I., Moxham, R., Tariq, Z., Downes, S.M., Stanga, P.E., 2023. New imaging technology for Simultaneous Multiwavelength-UWF fundus fluorescein angiography and indocyanine green angiography with Navigated central and peripheral SS-OCT. Ophthalmic Surg Lasers Imaging Retina 54, 401–410.
Buccarello, L., Sclip, A., Sacchi, M., Castaldo, A.M., Bertani, I., ReCecconi, A., Maestroni, S., Zerbini, G., Nucci, P., Borsello, T., 2017. The c-jun N-terminal kinase plays a key role in ocular degenerative changes in a mouse model of Alzheimer disease suggesting a correlation between ocular and brain pathologies. Oncotarget 8, 83038–83051.
Buchhave, P., Minthon, L., Zetterberg, H., Wallin, A.K., Blennow, K., Hansson, O., 2012. Cerebrospinal fluid levels of beta-amyloid 1-42, but not of tau, are fully changed already 5 to 10 years before the onset of Alzheimer dementia. Arch. Gen. Psychiatr. 69, 98–106.
Budd Haeberlein, S., Aisen, P.S., Barkhof, F., Chalkias, S., Chen, T., Cohen, S., Dent, G., Hansson, O., Harrison, K., von Hehn, C., Iwatsubo, T., Mallinckrodt, C., Mummery, C.J., Muralidharan, K.K., Nestorov, I., Nisenbaum, L., Rajagovindan, R., Skordos, L., Tian, Y., van Dyck, C.H., Vellas, B., Wu, S., Zhu, Y., Sandrock, A., 2022. Two randomized phase 3 studies of Aducanumab in early Alzheimer's disease. J. Prev. Alzheimers Dis. 9, 197–210.
Bulut, M., Kurtulus, F., Gozkaya, O., Erol, M.K., Cengiz, A., Akidan, M., Yaman, A., 2018. Evaluation of optical coherence tomography angiographic findings in Alzheimer's type dementia. Br. J. Ophthalmol. 102, 233–237.
Burgaletto, C., Platania, C.B.M., Di Benedetto, G., Munafo, A., Giurdanella, G., Federico, C., Caltabiano, R., Saccone, S., Conti, F., Bernardini, R., Bucolo, C., Cantarella, G., 2021. Targeting the miRNA-155/TNFSF10 network restrains inflammatory response in the retina in a mouse model of Alzheimer's disease. Cell Death Dis. 12, 905.
Buscho, S., Palacios, E., Xia, F., Shi, S., Li, S., Luisi, J., Kayed, R., Motamedi, M., Zhang, W., Liu, H., 2022. Longitudinal characterization of retinal vasculature alterations with optical coherence tomography angiography in a mouse model of tauopathy. Exp. Eye Res. 224, 109240.
Butovsky, O., Koronyo-Hamaoui, M., Kunis, G., Ophir, E., Landa, G., Cohen, H., Schwartz, M., 2006. Glatiramer acetate fights against Alzheimer's disease by inducing dendritic-like microglia expressing insulin-like growth factor 1. Proc. Natl. Acad. Sci. U. S. A. 103, 11784–11789.
Butovsky, O., Kunis, G., Koronyo-Hamaoui, M., Schwartz, M., 2007. Selective ablation of bone marrow-derived dendritic cells increases amyloid plaques in a mouse Alzheimer's disease model. Eur. J. Neurosci. 26, 413–416.
Byerly, M.S., Blackshaw, S., 2009. Vertebrate retina and hypothalamus development. Wiley interdisciplinary reviews. Systems biology and medicine 1, 380–389.
Byun, M.S., Park, S.W., Lee, J.H., Yi, D., Jeon, S.Y., Choi, H.J., Joung, H., Ghim, U.H., Park, U.C., Kim, Y.K., Shin, S.A., Yu, H.G., Lee, D.Y., Group, K.R., 2021. Association of retinal changes with Alzheimer disease Neuroimaging biomarkers in cognitively normal individuals. JAMA Ophthalmol 139, 548–556.
Cabrera DeBuc, D., Somfai, G.M., Arthur, E., Kostic, M., Oropesa, S., Mendoza Santiesteban, C., 2018. Investigating multimodal diagnostic eye biomarkers of cognitive impairment by measuring vascular and neurogenic changes in the retina. Front. Physiol. 9, 1721.
Cai, Z., Qiao, P.F., Wan, C.Q., Cai, M., Zhou, N.K., Li, Q., 2018. Role of blood-brain barrier in Alzheimer's disease. J. Alzheimers Dis. 63, 1223–1234.
Calsolaro, V., Edison, P., 2016. Neuroinflammation in Alzheimer's disease: current evidence and future directions. Alzheimers Dement 12, 719–732.
Campbell, M., Humphries, P., 2012. The blood-retina barrier: tight junctions and barrier modulation. Adv. Exp. Med. Biol. 763, 70–84.
Cao, K.J., Kim, J.H., Kroeger, H., Gaffney, P.M., Lin, J.H., Sigurdson, C.J., Yang, J., 2021. ARCAM-1 facilitates fluorescence detection of amyloid-containing deposits in the retina. Transl Vis Sci Technol 10, 5.
Carazo-Barrios, L., Archidona-Arranz, A., Claros-Ruiz, A., Garcia-Basterra, I., Garzon-Maldonado, F.J., Serrano-Castro, V., Gutierrez-Bedmar, M., Barbancho, M.A., De la Cruz Cosme, C., Garcia-Campos, J.M., Garcia-Casares, N., 2021. Correlation between retinal nerve fibre layer thickness and white matter lesions in Alzheimer's disease. Int. J. Geriatr. Psychiatr. 36, 935–942.
Carelli, V., La Morgia, C., Ross-Cisneros, F.N., Sadun, A.A., 2017. Optic neuropathies: the tip of the neurodegeneration iceberg. Hum. Mol. Genet. 26, R139–R150.
Carrero, L., Antequera, D., Municio, C., Carro, E., 2024. Circadian rhythm disruption and retinal dysfunction: a bidirectional link in Alzheimer's disease? Neural Regen Res 19, 1967–1972.
Castellani, G., Schwartz, M., 2020. Immunological features of non-neuronal brain cells: implications for Alzheimer's disease immunotherapy. Trends Immunol. 41, 794–804.
Castillo-Carranza, D.L., Nilson, A.N., Van Skike, C.E., Jahrling, J.B., Patel, K., Garach, P., Gerson, J.E., Sengupta, U., Abisambra, J., Nelson, P., Troncoso, J., Ungvari, Z., Galvan, V., Kayed, R., 2017. Cerebral microvascular accumulation of tau oligomers in Alzheimer's disease and related tauopathies. Aging Dis 8, 257–266.
Celebi, A.R., Mirza, G.E., 2013. Age-related change in retinal nerve fiber layer thickness measured with spectral domain optical coherence tomography. Invest. Ophthalmol. Vis. Sci. 54, 8095–8103.
Chaitanuwong, P., Jariyakosol, S., Apinyawasisuk, S., Hirunwiwatkul, P., Lawanlattanagul, H., Hemrungrojn, S., Chongpison, Y., 2023. Changes in ocular biomarkers from normal cognitive aging to Alzheimer's disease: a pilot study. Eye Brain 15, 15–23.
Chan, V.T.T., Sun, Z., Tang, S., Chen, L.J., Wong, A., Tham, C.C., Wong, T.Y., Chen, C., Ikram, M.K., Whitson, H.E., Lad, E.M., Mok, V.C.T., Cheung, C.Y., 2019. Spectral-domain OCT measurements in Alzheimer's disease: a systematic review and meta-analysis. Ophthalmology 126, 497–510.
Chang, L.Y., Ardiles, A.O., Tapia-Rojas, C., Araya, J., Inestrosa, N.C., Palacios, A.G., Acosta, M.L., 2020. Evidence of synaptic and Neurochemical remodeling in the retina of aging degus. Front. Neurosci. 14, 161.
Chang, L.Y., Lowe, J., Ardiles, A., Lim, J., Grey, A.C., Robertson, K., Danesh-Meyer, H., Palacios, A.G., Acosta, M.L., 2014. Alzheimer's disease in the human eye. Clinical tests that identify ocular and visual information processing deficit as biomarkers. Alzheimers Dement 10, 251–261.
Chang, L.Y., Palanca-Castan, N., Neira, D., Palacios, A.G., Acosta, M.L., 2021. Ocular health of Octodon degus as a clinical marker for age-related and age-independent neurodegeneration. Front. Integr. Neurosci. 15, 665467.
Charidimou, A., Boulouis, G., Gurol, M.E., Ayata, C., Bacskai, B.J., Frosch, M.P., Viswanathan, A., Greenberg, S.M., 2017. Emerging concepts in sporadic cerebral amyloid angiopathy. Brain 140, 1829–1850.
Chaudhury, A.R., Gerecke, K.M., Wyss, J.M., Morgan, D.G., Gordon, M.N., Carroll, S.L., 2003. Neuregulin-1 and erbB4 immunoreactivity is associated with neuritic plaques in Alzheimer disease brain and in a transgenic model of Alzheimer disease. J. Neuropathol. Exp. Neurol. 62, 42–54.
Chen, C.W., Lin, W.Y., Chen, K.B., Wu, Y.S., Kuo, Y.C., Liu, H.P., Li, C.Y., 2013. Inhalational anesthetic sevoflurane rescues retina function in Alzheimer's disease transgenic Drosophila. Curr. Alzheimer Res. 10, 1005–1014.

Chen, F., Chen, Y., Wang, Y., Ke, Q., Cui, L., 2022a. The COVID-19 pandemic and Alzheimer's disease: mutual risks and mechanisms. Transl. Neurodegener. 11, 40.
Chen, L., Yang, P., Curcio, C.A., 2022b. Visualizing lipid behind the retina in aging and age-related macular degeneration, via indocyanine green angiography (ASHS-LIA). Eye (Lond) 36, 1735–1746.
Chen, S., Zhang, D., Zheng, H., Cao, T., Xia, K., Su, M., Meng, Q., 2023. The association between retina thinning and hippocampal atrophy in Alzheimer's disease and mild cognitive impairment: a meta-analysis and systematic review. Front. Aging Neurosci. 15, 1232941.
Cheung, C.Y., Ikram, M.K., Chen, C., Wong, T.Y., 2017. Imaging retina to study dementia and stroke. Prog. Retin. Eye Res. 57, 89–107.
Cheung, C.Y., Mok, V., Foster, P.J., Trucco, E., Chen, C., Wong, T.Y., 2021. Retinal imaging in Alzheimer's disease. J. Neurol. Neurosurg. Psychiatry 92, 983–994.
Cheung, C.Y., Ong, Y.T., Hilal, S., Ikram, M.K., Low, S., Ong, Y.L., Venketasubramanian, N., Yap, P., Seow, D., Chen, C.L., Wong, T.Y., 2015. Retinal ganglion cell analysis using high-definition optical coherence tomography in patients with mild cognitive impairment and Alzheimer's disease. J. Alzheimers Dis. 45, 45–56.
Cheung, C.Y., Ong, Y.T., Ikram, M.K., Ong, S.Y., Li, X., Hilal, S., Catindig, J.A., Venketasubramanian, N., Yap, P., Seow, D., Chen, C.P., Wong, T.Y., 2014. Microvascular network alterations in the retina of patients with Alzheimer's disease. Alzheimers Dement 10, 135–142.
Cheung, C.Y., Wong, W.L.E., Hilal, S., Kan, C.N., Gyanwali, B., Tham, Y.C., Schmetterer, L., Xu, D., Lee, M.L., Hsu, W., Venketasubramanian, N., Tan, B.Y., Wong, T.Y., Chen, C., 2022. Deep-learning retinal vessel calibre measurements and risk of cognitive decline and dementia. Brain Commun 4, fcac212.
Chiara, C., Gilda, C., Daniela, M., Antonio, C., Miriana, M., Marcello, M., Elena, S., Roberta, L., Ciro, C., Vincenzo, B.M., 2022. A two-year longitudinal study of retinal vascular impairment in patients with amnestic mild cognitive impairment. Front. Aging Neurosci. 14, 993621.
Chiasseu, M., Alarcon-Martinez, L., Belforte, N., Quintero, H., Dotigny, F., Destroismaisons, L., Vande Velde, C., Panayi, F., Louis, C., Di Polo, A., 2017. Tau accumulation in the retina promotes early neuronal dysfunction and precedes brain pathology in a mouse model of Alzheimer's disease. Mol. Neurodegener. 12, 58.
Chibhabha, F., Yang, Y., Ying, K., Jia, F., Zhang, Q., Ullah, S., Liang, Z., Xie, M., Li, F., 2020. Non-invasive optical imaging of retinal Abeta plaques using curcumin loaded polymeric micelles in APP(swe)/PS1(DeltaE9) transgenic mice for the diagnosis of Alzheimer's disease. J. Mater. Chem. B 8, 7438–7452.
Chiquita, S., Campos, E.J., Castelhano, J., Ribeiro, M., Sereno, J., Moreira, P.I., Castelo-Branco, M., Ambrosio, A.F., 2019. Retinal thinning of inner sub-layers is associated with cortical atrophy in a mouse model of Alzheimer's disease: a longitudinal multimodal in vivo study. Alzheimer's Res. Ther. 11, 90.
Chiu, K., Chan, T.F., Wu, A., Leung, I.Y., So, K.F., Chang, R.C., 2012. Neurodegeneration of the retina in mouse models of Alzheimer's disease: what can we learn from the retina? Age (Dordr) 34, 633–649.
Chiu, P.Y., Hsu, M.H., Wang, C.W., Tsai, C.T., Pai, M.C., 2017. Visual hallucinations in Alzheimer's disease is significantly associated with clinical diagnostic features of dementia with Lewy bodies. PLoS One 12, e0186886.
Choi, S.H., Park, S.J., Kim, N.R., 2016. Macular ganglion cell -inner plexiform layer thickness is associated with clinical progression in mild cognitive impairment and Alzheimers disease. PLoS One 11, e0162202.
Chouhan, A.K., Guo, C., Hsieh, Y.C., Ye, H., Senturk, M., Zuo, Z., Li, Y., Chatterjee, S., Botas, J., Jackson, G.R., Bellen, H.J., Shulman, J.M., 2016. Uncoupling neuronal death and dysfunction in Drosophila models of neurodegenerative disease. Acta Neuropathol. Commun. 4, 62.
Chua, J., Hu, Q., Ke, M., Tan, B., Hong, J., Yao, X., Hilal, S., Venketasubramanian, N., Garhofer, G., Cheung, C.Y., Wong, T.Y., Chen, C.L., Schmetterer, L., 2020. Retinal microvasculature dysfunction is associated with Alzheimer's disease and mild cognitive impairment. Alzheimer's Res. Ther. 12, 161.
Chua, J., Li, C., Ho, L.K.H., Wong, D., Tan, B., Yao, X., Gan, A., Schwarzhans, F., Garhofer, G., Sng, C.C.A., Hilal, S., Venketasubramanian, N., Cheung, C.Y., Fischer, G., Vass, C., Wong, T.Y., Chen, C.L., Schmetterer, L., 2022. A multi-regression framework to improve diagnostic ability of optical coherence tomography retinal biomarkers to discriminate mild cognitive impairment and Alzheimer's disease. Alzheimer's Res. Ther. 14, 41.
Cipolla, J.A., Jiang, H., Simms, A.Y., Baumel, B., Rundek, T., Wang, J., 2023. Impaired retinal capillary function in patients with Alzheimer disease. J. Neuro Ophthalmol.
Cipollini, V., Abdolrahimzadeh, S., Troili, F., De Carolis, A., Calafiore, S., Scuderi, L., Giubilei, F., Scuderi, G., 2020. Neurocognitive assessment and retinal thickness alterations in Alzheimer disease: is there a correlation? J. Neuro Ophthalmol. 40, 370–377.
Ciudin, A., Simo-Servat, O., Hernandez, C., Arcos, G., Diego, S., Sanabria, A., Sotolongo, O., Hernandez, I., Boada, M., Simo, R., 2017. Retinal Microperimetry: a new tool for identifying patients with type 2 diabetes at risk for developing Alzheimer disease. Diabetes 66, 3098–3104.
Claudio, L., 1996. Ultrastructural features of the blood-brain barrier in biopsy tissue from Alzheimer's disease patients. Acta Neuropathol. 91, 6–14.
Cohen, S.I., Linse, S., Luheshi, L.M., Hellstrand, E., White, D.A., Rajah, L., Otzen, D.E., Vendruscolo, M., Dobson, C.M., Knowles, T.P., 2013. Proliferation of amyloid-beta42 aggregates occurs through a secondary nucleation mechanism. Proc. Natl. Acad. Sci. U. S. A. 110, 9758–9763.
Coppola, G., Di Renzo, A., Ziccardi, L., Martelli, F., Fadda, A., Manni, G., Barboni, P., Pierelli, F., Sadun, A.A., Parisi, V., 2015. Optical coherence tomography in Alzheimer's disease: a meta-analysis. PLoS One 10, e0134750.
Corazza, P., Maddison, J., Bonetti, P., Guo, L., Luong, V., Garfinkel, A., Younis, S., Cordeiro, M.F., 2021. Predicting wet age-related macular degeneration (AMD) using DARC (detecting apoptosing retinal cells) AI (artificial intelligence) technology. Expert Rev. Mol. Diagn 21, 109–118.
Cordeiro, M.F., Guo, L., Coxon, K.M., Duggan, J., Nizari, S., Normando, E.M., Sensi, S.L., Sillito, A.M., Fitzke, F.W., Salt, T.E., Moss, S.E., 2010. Imaging multiple phases of neurodegeneration: a novel approach to assessing cell death in vivo. Cell Death Dis. 1, e3.
Cordeiro, M.F., Guo, L., Luong, V., Harding, G., Wang, W., Jones, H.E., Moss, S.E., Sillito, A.M., Fitzke, F.W., 2004. Real-time imaging of single nerve cell apoptosis in retinal neurodegeneration. Proc. Natl. Acad. Sci. U. S. A. 101, 13352–13356.
Cordeiro, M.F., Hill, D., Patel, R., Corazza, P., Maddison, J., Younis, S., 2022. Detecting retinal cell stress and apoptosis with DARC: progression from lab to clinic. Prog. Retin. Eye Res. 86, 100976.
Cormack, F.K., Tovee, M., Ballard, C., 2000. Contrast sensitivity and visual acuity in patients with Alzheimer's disease. Int. J. Geriatr. Psychiatr. 15, 614–620.
Counts, S.E., Ikonomovic, M.D., Mercado, N., Vega, I.E., Mufson, E.J., 2017. Biomarkers for the early detection and progression of Alzheimer's disease. Neurotherapeutics 14, 35–53.
Crawford, T.J., Devereaux, A., Higham, S., Kelly, C., 2015. The disengagement of visual attention in Alzheimer's disease: a longitudinal eye-tracking study. Front. Aging Neurosci. 7, 118.
Crews, L., Masliah, E., 2010. Molecular mechanisms of neurodegeneration in Alzheimer's disease. Hum. Mol. Genet. 19, R12–R20.
Crow, R.W., Levin, L.B., LaBree, L., Rubin, R., Feldon, S.E., 2003. Sweep visual evoked potential evaluation of contrast sensitivity in Alzheimer's dementia. Invest. Ophthalmol. Vis. Sci. 44, 875–878.
Csincsik, L., MacGillivray, T.J., Flynn, E., Pellegrini, E., Papanastasiou, G., Barzegar-Befroei, N., Csutak, A., Bird, A.C., Ritchie, C.W., Peto, T., Lengyel, I., 2018. Peripheral retinal imaging biomarkers for Alzheimer's disease: a pilot study. Ophthalmic Res. 59, 182–192.
Csincsik, L., Quinn, N., Yong, K.X.X., Crutch, S.J., Peto, T., Lengyel, I., 2021. Retinal phenotyping of variants of Alzheimer's disease using ultra-widefield retinal images. Alzheimers Dement. (Amst) 13, e12232.
Cummings, J., Osse, A.M.L., Cammann, D., Powell, J., Chen, J., 2024. Anti-amyloid monoclonal antibodies for the treatment of Alzheimer's disease. BioDrugs 38, 5–22.
Cunha, J.P., Proenca, R., Dias-Santos, A., Almeida, R., Aguas, H., Alves, M., Papoila, A.L., Louro, C., Castanheira-Dinis, A., 2017a. In Alzheimer's disease: thinning of the RNFL and superior hemiretina. Graefes Arch. Clin. Exp. Ophthalmol. 255, 1827–1835.
Cunha, J.P., Proenca, R., Dias-Santos, A., Melancia, D., Almeida, R., Aguas, H., Santos, B. O., Alves, M., Ferreira, J., Papoila, A.L., Louro, C., Castanheira-Dinis, A., 2017b. Choroidal thinning: Alzheimer's disease and aging. Alzheimers Dement. (Amst) 8, 11–17.
Cunha, L.P., Almeida, A.L., Costa-Cunha, L.V., Costa, C.F., Monteiro, M.L., 2016a. The role of optical coherence tomography in Alzheimer's disease. Int J Retina Vitreous 2, 24.
Cunha, L.P., Lopes, L.C., Costa-Cunha, L.V., Costa, C.F., Pires, L.A., Almeida, A.L., Monteiro, M.L., 2016b. Macular thickness measurements with frequency domain-OCT for quantification of retinal neural loss and its correlation with cognitive impairment in Alzheimer's disease. PLoS One 11, e0153830.
Cutler, T., Sarkar, A., Moran, M., Steffensmeier, A., Puli, O.R., Mancini, G., Tare, M., Gogia, N., Singh, A., 2015. Drosophila eye model to study neuroprotective role of CREB binding protein (CBP) in Alzheimer's disease. PLoS One 10, e0137691.
Czako, C., Kovacs, T., Ungvari, Z., Csiszar, A., Yabluchanskiy, A., Conley, S., Csipo, T., Lipecz, A., Horvath, H., Sandor, G.L., Istvan, L., Logan, T., Nagy, Z.Z., Kovacs, I., 2020. Retinal biomarkers for Alzheimer's disease and vascular cognitive impairment and dementia (VCID): implication for early diagnosis and prognosis. Geroscience 42, 1499–1525.
Dai, B., Mao, Z., Wu, B., Mei, Y.J., Levkoff, S., Wang, H., 2015. Family Caregiver's Perception of Alzheimer's disease and caregiving in Chinese culture. Soc. Work. Publ. Health 30, 185–196.
Danesh-Meyer, H.V., Birch, H., Ku, J.Y., Carroll, S., Gamble, G., 2006. Reduction of optic nerve fibers in patients with Alzheimer disease identified by laser imaging. Neurology 67, 1852–1854.
Datta, S., Baidya, K., Banerjee, M., Mahapatra, S., Mukherjee, S., 2020. Retinal nerve fibre layer thinning in patients with Thalassaemia, Iron deficiency anaemia, and anaemia of chronic diseases. J. Ophthalmol., 9268364
de Jong, F.J., Schrijvers, E.M., Ikram, M.K., Koudstaal, P.J., de Jong, P.T., Hofman, A., Vingerling, J.R., Breteler, M.M., 2011. Retinal vascular caliber and risk of dementia: the Rotterdam study. Neurology 76, 816–821.
de la Torre, J.C., 2002. Alzheimer disease as a vascular disorder: nosological evidence. Stroke 33, 1152–1162.
de Ruyter, F.J., 2020. Early tau phosphorylation as a poterntial retinal biomarker for AD and other tauopathies. Alzheimers Dement 16, e040924.
De-Paula, V.J., Radanovic, M., Diniz, B.S., Forlenza, O.V., 2012. Alzheimer's disease. Subcell. Biochem. 65, 329–352.
Deal, J.A., Sharrett, A.R., Rawlings, A.M., Gottesman, R.F., Bandeen-Roche, K., Albert, M., Knopman, D., Selvin, E., Wasserman, B.A., Klein, B., Klein, R., 2018. Retinal signs and 20-year cognitive decline in the atherosclerosis risk in Communities study. Neurology 90, e1158–e1166.
DeMattos, R.B., Bales, K.R., Cummins, D.J., Paul, S.M., Holtzman, D.M., 2002. Brain to plasma amyloid-beta efflux: a measure of brain amyloid burden in a mouse model of Alzheimer's disease. Science 295, 2264–2267.
den Haan, J., Hart de Ruyter, F.J., Lochocki, B., Kroon, M., Kemper, E.M., Teunissen, C. E., van Berckel, B., Scheltens, P., Hoozemans, J.J., van de Kreeke, A., Verbraak, F.D., de Boer, J.F., Bouwman, F.H., 2022. No difference in retinal fluorescence after oral curcumin intake in amyloid-proven AD cases compared to controls. Alzheimers Dement. (Amst) 14, e12347.

den Haan, J., Morrema, T.H.J., Verbraak, F.D., de Boer, J.F., Scheltens, P., Rozemuller, A. J., Bergen, A.A.B., Bouwman, F.H., Hoozemans, J.J., 2018. Amyloid-beta and phosphorylated tau in post-mortem Alzheimer's disease retinas. Acta Neuropathol. Commun. 6, 147.

den Haan, J., van de Kreeke, J.A., Konijnenberg, E., ten Kate, M., den Braber, A., Barkhof, F., van Berckel, B.N., Teunissen, C.E., Scheltens, P., Visser, P.J., Verbraak, F.D., Bouwman, F.H., 2019. Retinal thickness as a potential biomarker in patients with amyloid-proven early- and late-onset Alzheimer's disease. Alzheimers Dement. (Amst) 11, 463–471.

den Haan, J., Verbraak, F.D., Visser, P.J., Bouwman, F.H., 2017. Retinal thickness in Alzheimer's disease: a systematic review and meta-analysis. Alzheimers Dement. (Amst) 6, 162–170.

Desai, B.S., Schneider, J.A., Li, J.L., Carvey, P.M., Hendey, B., 2009. Evidence of angiogenic vessels in Alzheimer's disease. J. Neural. Transm. 116, 587–597.

Dhillon, S., 2021. Aducanumab: first approval. Drugs 81, 1437–1443.

Di Pippo, M., Cipollini, V., Giubilei, F., Scuderi, G., Abdolrahimzadeh, S., 2023. Retinal and Choriocapillaris vascular changes in early Alzheimer disease patients using optical coherence tomography angiography. J. Neuro Ophthalmol.

Ding, J., Patton, N., Deary, I.J., Strachan, M.W., Fowkes, F.G., Mitchell, R.J., Price, J.F., 2008. Retinal microvascular abnormalities and cognitive dysfunction: a systematic review. Br. J. Ophthalmol. 92, 1017–1025.

Dionisio-Santos, D.A., Karaahmet, B., Belcher, E.K., Owlett, L.D., Trojanczyk, L.A., Olschowka, J.A., O'Banion, M.K., 2021. Evaluating effects of glatiramer acetate treatment on amyloid deposition and tau phosphorylation in the 3xTg mouse model of Alzheimer's disease. Front. Neurosci. 15, 758677.

Do, T.M., Dodacki, A., Alata, W., Calon, F., Nicolic, S., Scherrmann, J.M., Farinotti, R., Bourasset, F., 2016. Age-dependent regulation of the blood-brain barrier influx/efflux Equilibrium of amyloid-beta peptide in a mouse model of Alzheimer's disease (3xTg-AD). J. Alzheimers Dis. 49, 287–300.

Dolan, D., Troncoso, J., Resnick, S.M., Crain, B.J., Zonderman, A.B., O'Brien, R.J., 2010a. Age, Alzheimer's disease and dementia in the Baltimore longitudinal study of ageing. Brain 133, 2225–2231.

Dolan, H., Crain, B., Troncoso, J., Resnick, S.M., Zonderman, A.B., Obrien, R.J., 2010b. Atherosclerosis, dementia, and Alzheimer disease in the Baltimore longitudinal study of aging cohort. Ann. Neurol. 68, 231–240.

Douaud, G., Lee, S., Alfaro-Almagro, F., Arthofer, C., Wang, C., McCarthy, P., Lange, F., Andersson, J.L.R., Griffanti, L., Duff, E., Jbabdi, S., Taschler, B., Keating, P., Winkler, A.M., Collins, R., Matthews, P.M., Allen, N., Miller, K.L., Nichols, T.E., Smith, S.M., 2022. SARS-CoV-2 is associated with changes in brain structure in UK Biobank. Nature 604, 697–707.

Doustar, J., Rentsendorj, A., Torbati, T., Regis, G.C., Fuchs, D.T., Sheyn, J., Mirzaei, N., Graham, S.L., Shah, P.K., Mastali, M., Van Eyk, J.E., Black, K.L., Gupta, V.K., Mirzaei, M., Koronyo, Y., Koronyo-Hamaoui, M., 2020. Parallels between retinal and brain pathology and response to immunotherapy in old, late-stage Alzheimer's disease mouse models. Aging Cell, e13246.

Doustar, J., Torbati, T., Black, K.L., Koronyo, Y., Koronyo-Hamaoui, M., 2017. Optical coherence tomography in Alzheimer's disease and other neurodegenerative diseases. Front. Neurol. 8, 701.

Du, L.Y., Chang, L.Y., Ardiles, A.O., Tapia-Rojas, C., Araya, J., Inestrosa, N.C., Palacios, A.G., Acosta, M.L., 2015. Alzheimer's disease-related protein expression in the retina of Octodon degus. PLoS One 10, e0135499.

Du, X., Koronyo, Y., Mirzaei, N., Yang, C., Fuchs, D.T., Black, K.L., Koronyo-Hamaoui, M., Gao, L., 2022. Label-free hyperspectral imaging and deep-learning prediction of retinal amyloid beta-protein and phosphorylated tau. PNAS Nexus 1, pgac164.

Dubois, B., Hampel, H., Feldman, H.H., Scheltens, P., Aisen, P., Andrieu, S., Bakardjian, H., Benali, H., Bertram, L., Blennow, K., Broich, K., Cavedo, E., Crutch, S., Dartigues, J.F., Duyckaerts, C., Epelbaum, S., Frisoni, G.B., Gauthier, S., Genthon, R., Gouw, A.A., Habert, M.O., Holtzman, D.M., Kivipelto, M., Lista, S., Molinuevo, J.L., O'Bryant, S.E., Rabinovici, G.D., Rowe, C., Salloway, S., Schneider, L.S., Sperling, R., Teichmann, M., Carrillo, M.C., Cummings, J., Jack Jr., C.R., 2016. Proceedings of the Meeting of the International Working, G., the American Alzheimer's Association on "The Preclinical State of, A.D., July, Washington Dc, U.S.A., 2016. Preclinical Alzheimer's disease: Definition, natural history, and diagnostic criteria. Alzheimers Dement 12, 292–323.

Dumitrascu, O.M., Doustar, J., Fuchs, D.T., Koronyo, Y., Sherman, D.S., Miller, M.S., Johnson, K.O., Carare, R.O., Verdooner, S.R., Lyden, P.D., Schneider, J.A., Black, K. L., Koronyo-Hamaoui, M., 2024. Distinctive retinal peri-arteriolar versus peri-venular amyloid plaque distribution correlates with the cognitive performance. bioRxiv. https://doi.org/10.1101/2024.02.27.580733 [Preprint].

Dumitrascu, O.M., Lyden, P.D., Torbati, T., Sheyn, J., Sherzai, A., Sherzai, D., Sherman, D.S., Rosenberry, R., Cheng, S., Johnson, K.O., Czeszynski, A.D., Verdooner, S., Frautschy, S., Black, K.L., Koronyo, Y., Koronyo-Hamaoui, M., 2020. Sectoral segmentation of retinal amyloid imaging in subjects with cognitive decline. Alzheimers Dement. (Amst) 12, e12109.

Dumitrascu, O.M., Rosenberry, R., Sherman, D.S., Khansari, M.M., Sheyn, J., Torbati, T., Sherzai, A., Sherzai, D., Johnson, K.O., Czeszynski, A.D., Verdooner, S., Black, K.L., Frautschy, S., Lyden, P.D., Shi, Y., Cheng, S., Koronyo, Y., Koronyo-Hamaoui, M., 2021. Retinal Venular Tortuosity Jointly with Retinal Amyloid Burden Correlates with Verbal Memory Loss: A Pilot Study. Cells 10.

Dutescu, R.M., Li, Q.X., Crowston, J., Masters, C.L., Baird, P.N., Culvenor, J.G., 2009. Amyloid precursor protein processing and retinal pathology in mouse models of Alzheimer's disease. Graefes Arch. Clin. Exp. Ophthalmol. 247, 1213–1221.

Edwards, M.M., Rodriguez, J.J., Gutierrez-Lanza, R., Yates, J., Verkhratsky, A., Lutty, G. A., 2014. Retinal macroglia changes in a triple transgenic mouse model of Alzheimer's disease. Exp. Eye Res. 127, 252–260.

Einarsdottir, A.B., Hardarson, S.H., Kristjansdottir, J.V., Bragason, D.T., Snaedal, J., Stefansson, E., 2016. Retinal oximetry imaging in Alzheimer's disease. J. Alzheimers Dis. 49, 79–83.

El-Darzi, N., Mast, N., Buchner, D.A., Saadane, A., Dailey, B., Trichonas, G., Pikuleva, I. A., 2022. Low-Dose Anti-HIV Drug Efavirenz Mitigates Retinal Vascular Lesions in a Mouse Model of Alzheimer's Disease. Front. Pharmacol. 13, 902254.

Ellis, R.J., Olichney, J.M., Thal, L.J., Mirra, S.S., Morris, J.C., Beekly, D., Heyman, A., 1996. Cerebral amyloid angiopathy in the brains of patients with Alzheimer's disease: the CERAD experience, Part XV. Neurology 46, 1592–1596.

Engedal, K., Oftedal, S.I., Lilleaas, F., Laake, P., 1989. Electroencephalography, visual evoked potentials, and cerebral CAT-scan as diagnostic tools in senile dementia of Alzheimer type. Aging (Milano) 1, 139–145.

Erskine, D., Taylor, J.P., Firbank, M.J., Patterson, L., Onofrj, M., O'Brien, J.T., McKeith, I. G., Attems, J., Thomas, A.J., Morris, C.M., Khundakar, A.A., 2016. Changes to the lateral geniculate nucleus in Alzheimer's disease but not dementia with Lewy bodies. Neuropathol. Appl. Neurobiol. 42, 366–376.

Fagan, A.M., Xiong, C., Jasielec, M.S., Bateman, R.J., Goate, A.M., Benzinger, T.L., Ghetti, B., Martins, R.N., Masters, C.L., Mayeux, R., Ringman, J.M., Rossor, M.N., Salloway, S., Schofield, P.R., Sperling, R.A., Marcus, D., Cairns, N.J., Buckles, V.D., Ladenson, J.H., Morris, J.C., Holtzman, D.M., Dominantly Inherited Alzheimer, N., 2014. Longitudinal change in CSF biomarkers in autosomal-dominant Alzheimer's disease. Sci. Transl. Med. 6, 226ra230.

Farzinvash, Z., Abutorabi-Zarchi, M., Manaviat, M., Zare Mehrjerdi, H., 2022. Retinal Ganglion Cell Complex in Alzheimer Disease: Comparing Ganglion Cell Complex and Central Macular Thickness in Alzheimer Disease and Healthy Subjects Using Spectral Domain-Optical Coherence Tomography. Basic Clin. Neurosci. 13, 675–684.

Feke, G.T., Hyman, B.T., Stern, R.A., Pasquale, L.R., 2015. Retinal blood flow in mild cognitive impairment and Alzheimer's disease. Alzheimers Dement. (Amst) 1, 144–151.

Ferrari, L., Huang, S.C., Magnani, G., Ambrosi, A., Comi, G., Leocani, L., 2017. Optical Coherence Tomography Reveals Retinal Neuroaxonal Thinning in Frontotemporal Dementia as in Alzheimer's Disease. J. Alzheimers Dis. 56, 1101–1107.

Ferri, C.P., Prince, M., Brayne, C., Brodaty, H., Fratiglioni, L., Ganguli, M., Hall, K., Hasegawa, K., Hendrie, H., Huang, Y., Jorm, A., Mathers, C., Menezes, P.R., Rimmer, E., Scazufca, M., Alzheimer's Disease, I., 2005. Global prevalence of dementia: a Delphi consensus study. Lancet 366, 2112–2117.

Fischer, V.W., Siddiqi, A., Yusufaly, Y., 1990. Altered angioarchitecture in selected areas of brains with Alzheimer's disease. Acta Neuropathol. 79, 672–679.

Fisher, R.A., Miners, J.S., Love, S., 2022. Pathological changes within the cerebral vasculature in Alzheimer's disease: New perspectives. Brain Pathol. 32, e13061.

Fletcher, W.A., Sharpe, J.A., 1988. Smooth pursuit dysfunction in Alzheimer's disease. Neurology 38, 272–277.

Frenkel, D., Maron, R., Burt, D.S., Weiner, H.L., 2005. Nasal vaccination with a proteosome-based adjuvant and glatiramer acetate clears beta-amyloid in a mouse model of Alzheimer disease. J. Clin. Invest. 115, 2423–2433.

Frost, S., Kanagasingam, Y., Sohrabi, H., Vignarajan, J., Bourgeat, P., Salvado, O., Villemagne, V., Rowe, C.C., Macaulay, S.L., Szoeke, C., Ellis, K.A., Ames, D., Masters, C.L., Rainey-Smith, S., Martins, R.N., Group, A.R., 2013. Retinal vascular biomarkers for early detection and monitoring of Alzheimer's disease. Transl. Psychiatry 3, e233.

Frost, S., Kanagasingam, Y., Macaulay, L., Koronyo-Hamaoui, M., Koronyo, Y., Biggs, D., Verdooner, S., Black, K., Taddei, K., Shah, T., Rainey-Smith, S., Bourgeat, P., Salvado, O., Doecke, J., Wilson, B., Villemagne, V., Rowe, C.C., Martins, R., AIBL Research Group, 2014. O3-13-01: retinal amyloid fluorescence imaging predicts cerebral amyloid burden and Alzheimer's disease. Alzheimer's Dementia 10, P234–P235. https://doi.org/10.1016/j.jalz.2014.04.341 [AAIC conference abstract]. Available at: https://alz-journals.onlinelibrary.wiley.com/doi/full/10.1016/j.jalz.2014.04.341.

Frost, S., Martins, R.N., Kanagasingam, Y., 2010. Ocular biomarkers for early detection of Alzheimer's disease. J. Alzheimers Dis. 22, 1–16.

Frozza, R.L., Lourenco, M.V., De Felice, F.G., 2018. Challenges for Alzheimer's Disease Therapy: Insights from Novel Mechanisms Beyond Memory Defects. Front. Neurosci. 12, 37.

Funatsu, H., Sakata, K., Harino, S., Okuzawa, Y., Noma, H., Hori, S., 2006. Tracing method in the assessment of retinal capillary blood flow velocity by fluorescein angiography with scanning laser ophthalmoscope. Jpn. J. Ophthalmol. 50, 25–32.

Gabin, J.M., Tambs, K., Saltvedt, I., Sund, E., Holmen, J., 2017. Association between blood pressure and Alzheimer disease measured up to 27 years prior to diagnosis: the HUNT Study. Alzheimer's Res. Ther. 9, 37.

Gallardo, G., Holtzman, D.M., 2017. Antibody Therapeutics Targeting Abeta and Tau. Cold Spring Harb Perspect Med 7.

Galvin, J.E., Kleiman, M.J., Walker, M., 2021. Using Optical Coherence Tomography to Screen for Cognitive Impairment and Dementia. J. Alzheimers Dis. 84, 723–736.

Gandy, S., Ehrlich, M.E., 2023. Moving the Needle on Alzheimer's Disease with an Anti-Oligomer Antibody. N. Engl. J. Med. 388, 80–81.

Gao, L., Chen, X., Tang, Y., Zhao, J., Li, Q., Fan, X., Xu, H., Yin, Z.Q., 2015a. Neuroprotective effect of memantine on the retinal ganglion cells of APPswe/PS1DeltaE9 mice and its immunomodulatory mechanisms. Exp. Eye Res. 135, 47–58.

Gao, L., Liu, Y., Li, X., Bai, Q., Liu, P., 2015b. Abnormal retinal nerve fiber layer thickness and macula lutea in patients with mild cognitive impairment and Alzheimer's disease. Arch. Gerontol. Geriatr. 60, 162–167.

Garcia-Alloza, M., Robbins, E.M., Zhang-Nunes, S.X., Purcell, S.M., Betensky, R.A., Raju, S., Prada, C., Greenberg, S.M., Bacskai, B.J., Frosch, M.P., 2006. Characterization of amyloid deposition in the APPswe/PS1dE9 mouse model of Alzheimer disease. Neurobiol. Dis. 24, 516–524.

Garcia-Martin, E., Bambo, M.P., Marques, M.L., Satue, M., Otin, S., Larrosa, J.M., Polo, V., Pablo, L.E., 2016a. Ganglion cell layer measurements correlate with disease severity in patients with Alzheimer's disease. Acta Ophthalmol. 94, e454–e459.
Garcia-Martin, E., Garcia-Campayo, J., Puebla-Guedea, M., Ascaso, F.J., Roca, M., Gutierrez-Ruiz, F., Vilades, E., Polo, V., Larrosa, J.M., Pablo, L.E., Satue, M., 2016b. Fibromyalgia Is Correlated with Retinal Nerve Fiber Layer Thinning. PLoS One 11, e0161574.
Garcia-Martin, E., Jimeno-Huete, D., Dongil-Moreno, F.J., Boquete, L., Sanchez-Morla, E. M., Miguel-Jimenez, J.M., Lopez-Dorado, A., Vilades, E., Fuertes, M.I., Pueyo, A., Ortiz Del Castillo, M., 2023. Differential Study of Retinal Thicknesses in the Eyes of Alzheimer's Patients, Multiple Sclerosis Patients and Healthy Subjects. Biomedicines 11.
Garcia-Martin, E.S., Rojas, B., Ramirez, A.I., de Hoz, R., Salazar, J.J., Yubero, R., Gil, P., Trivino, A., Ramirez, J.M., 2014. Macular thickness as a potential biomarker of mild Alzheimer's disease. Ophthalmology 121, 1149–1151 e1143.
Gaynor, L.S., Curiel Cid, R.E., Penate, A., Rosselli, M., Burke, S.N., Wicklund, M., Loewenstein, D.A., Bauer, R.M., 2019. Visual Object Discrimination Impairment as an Early Predictor of Mild Cognitive Impairment and Alzheimer's Disease. J. Int. Neuropsychol. Soc. 25, 688–698.
Georgevsky, D., Retsas, S., Raoufi, N., Shimoni, O., Golzan, S.M., 2019. A longitudinal assessment of retinal function and structure in the APP/PS1 transgenic mouse model of Alzheimer's disease. Transl. Neurodegener. 8, 30.
Gharbiya, M., Trebbastoni, A., Parisi, F., Manganiello, S., Cruciani, F., D'Antonio, F., De Vico, U., Imbriano, L., Campanelli, A., De Lena, C., 2014. Choroidal thinning as a new finding in Alzheimer's disease: evidence from enhanced depth imaging spectral domain optical coherence tomography. J. Alzheimers Dis. 40, 907–917.
Gilmore, G.C., Groth, K.E., Thomas, C.W., 2005. Stimulus contrast and word reading speed in Alzheimer's disease. Exp. Aging Res. 31, 15–33.
Gilmore, G.C., Wenk, H.E., Naylor, L.A., Koss, E., 1994. Motion perception and Alzheimer's disease. J. Gerontol. 49, P52–P57.
Gilmore, G.C., Whitehouse, P.J., 1995. Contrast sensitivity in Alzheimer's disease: a 1-year longitudinal analysis. Optom. Vis. Sci. 72, 83–91.
Girbardt, J., Luck, T., Kynast, J., Rodriguez, F.S., Wicklein, B., Wirkner, K., Engel, C., Girbardt, C., Wang, M., Polyakova, M., Witte, A.V., Loeffler, M., Villringer, A., Riedel-Heller, S.G., Schroeter, M.L., Elze, T., Rauscher, F.G., 2021. Reading cognition from the eyes: association of retinal nerve fibre layer thickness with cognitive performance in a population-based study. Brain Commun 3, fcab258.
Glosser, G., Baker, K.M., de Vries, J.J., Alavi, A., Grossman, M., Clark, C.M., 2002. Disturbed visual processing contributes to impaired reading in Alzheimer's disease. Neuropsychologia 40, 902–909.
Goldstein, L.E., Muffat, J.A., Cherny, R.A., Moir, R.D., Ericsson, M.H., Huang, X., Mavros, C., Coccia, J.A., Faget, K.Y., Fitch, K.A., Masters, C.L., Tanzi, R.E., Chylack Jr., L.T., Bush, A.I., 2003. Cytosolic beta-amyloid deposition and supranuclear cataracts in lenses from people with Alzheimer's disease. Lancet 361, 1258–1265.
Golzan, S.M., Goozee, K., Georgevsky, D., Avolio, A., Chatterjee, P., Shen, K., Gupta, V., Chung, R., Savage, G., Orr, C.F., Martins, R.N., Graham, S.L., 2017. Retinal vascular and structural changes are associated with amyloid burden in the elderly: ophthalmic biomarkers of preclinical Alzheimer's disease. Alzheimer's Res. Ther. 9, 13.
Gonzalez-Ortiz, F., Turton, M., Kac, P.R., Smirnov, D., Premi, E., Ghidoni, R., Benussi, L., Cantoni, V., Saraceno, C., Rivolta, J., Ashton, N.J., Borroni, B., Galasko, D., Harrison, P., Zetterberg, H., Blennow, K., Karikari, T.K., 2022. Brain-derived tau: a novel blood-based biomarker for Alzheimer's disease-type neurodegeneration. Brain.
Grammas, P., Ovase, R., 2001. Inflammatory factors are elevated in brain microvessels in Alzheimer's disease. Neurobiol. Aging 22, 837–842.
Greenberg, S.M., Bacskai, B.J., Hernandez-Guillamon, M., Pruzin, J., Sperling, R., van Veluw, S.J., 2020. Cerebral amyloid angiopathy and Alzheimer disease - one peptide, two pathways. Nat. Rev. Neurol. 16, 30–42.
Grienberger, C., Rochefort, N.L., Adelsberger, H., Henning, H.A., Hill, D.N., Reichwald, J., Staufenbiel, M., Konnerth, A., 2012. Staged decline of neuronal function in vivo in an animal model of Alzheimer's disease. Nat. Commun. 3, 774.
Grimaldi, A., Brighi, C., Peruzzi, G., Ragozzino, D., Bonanni, V., Limatola, C., Ruocco, G., Di Angelantonio, S., 2018. Inflammation, neurodegeneration and protein aggregation in the retina as ocular biomarkers for Alzheimer's disease in the 3xTg-AD mouse model. Cell Death Dis. 9, 685.
Grimaldi, A., Pediconi, N., Oieni, F., Pizzarelli, R., Rosito, M., Giubettini, M., Santini, T., Limatola, C., Ruocco, G., Ragozzino, D., Di Angelantonio, S., 2019. Neuroinflammatory Processes, A1 Astrocyte Activation and Protein Aggregation in the Retina of Alzheimer's Disease Patients, Possible Biomarkers for Early Diagnosis. Front. Neurosci. 13, 925.
Gross, J.G., Sadun, A.A., Wiley, C.A., Freeman, W.R., 1989. Severe visual loss related to isolated peripapillary retinal and optic nerve head cytomegalovirus infection. Am. J. Ophthalmol. 108, 691–698.
Grundke-Iqbal, I., Iqbal, K., Tung, Y.C., Quinlan, M., Wisniewski, H.M., Binder, L.I., 1986. Abnormal phosphorylation of the microtubule-associated protein tau (tau) in Alzheimer cytoskeletal pathology. Proc. Natl. Acad. Sci. U. S. A. 83, 4913–4917.
Guarnieri, B., Maestri, M., Cucchiara, F., Lo Gerfo, A., Schirru, A., Arnaldi, D., Mattioli, P., Nobili, F., Lombardi, G., Cerroni, G., Bartoli, A., Manni, R., Sinforiani, E., Terzaghi, M., Arena, M.G., Silvestri, R., La Morgia, C., Di Perri, M.C., Franzoni, F., Tognoni, G., Mancuso, M., Sorbi, S., Bonuccelli, U., Siciliano, G., Faraguna, U., Bonanni, E., 2020. Multicenter Study on Sleep and Circadian Alterations as Objective Markers of Mild Cognitive Impairment and Alzheimer's Disease Reveals Sex Differences. J. Alzheimers Dis. 78, 1707–1719.
Guo, J., Xu, C., Ni, S., Zhang, S., Li, Q., Zeng, P., Pi, G., Liu, E., Sun, D.S., Liu, Y., Wang, Z., Chen, H., Yang, Y., Wang, J.Z., 2019. Elevation of pS262-Tau and Demethylated PP2A in Retina Occurs Earlier than in Hippocampus During Hyperhomocysteinemia. J. Alzheimers Dis. 68, 367–381.
Guo, L., Ravindran, N., Shamsher, E., Hill, D., Cordeiro, M.F., 2021. Retinal Changes in Transgenic Mouse Models of Alzheimer's Disease. Curr. Alzheimer Res. 18, 89–102.
Guo, L., Salt, T.E., Luong, V., Wood, N., Cheung, W., Maass, A., Ferrari, G., Russo-Marie, F., Sillito, A.M., Cheetham, M.E., Moss, S.E., Fitzke, F.W., Cordeiro, M.F., 2007. Targeting amyloid-beta in glaucoma treatment. Proc. Natl. Acad. Sci. U. S. A. 104, 13444–13449.
Gupta, V.B., Chitranshi, N., den Haan, J., Mirzaei, M., You, Y., Lim, J.K., Basavarajappa, D., Godinez, A., Di Angelantonio, S., Sachdev, P., Salekdeh, G.H., Bouwman, F., Graham, S., Gupta, V., 2021. Retinal changes in Alzheimer's disease-integrated prospects of imaging, functional and molecular advances. Prog. Retin. Eye Res. 82, 100899.
Gupta, V.K., Chitranshi, N., Gupta, V.B., Golzan, M., Dheer, Y., Wall, R.V., Georgevsky, D., King, A.E., Vickers, J.C., Chung, R., Graham, S., 2016. Amyloid beta accumulation and inner retinal degenerative changes in Alzheimer's disease transgenic mouse. Neurosci. Lett. 623, 52–56.
Haass, C., Selkoe, D., 2022. If amyloid drives Alzheimer disease, why have anti-amyloid therapies not yet slowed cognitive decline? PLoS Biol. 20, e3001694.
Habiba, U., Descallar, J., Kreilaus, F., Adhikari, U.K., Kumar, S., Morley, J.W., Bui, B.V., Koronyo-Hamaoui, M., Tayebi, M., 2021. Detection of retinal and blood Abeta oligomers with nanobodies. Alzheimers Dement. (Amst) 13, e12193.
Habiba, U., Merlin, S., Lim, J.K.H., Wong, V.H.Y., Nguyen, C.T.O., Morley, J.W., Bui, B. V., Tayebi, M., 2020. Age-Specific Retinal and Cerebral Immunodetection of Amyloid-beta Plaques and Oligomers in a Rodent Model of Alzheimer's Disease. J. Alzheimers Dis. 76, 1135–1150.
Haddad, H.W., Malone, G.W., Comardelle, N.J., Degueure, A.E., Poliwoda, S., Kaye, R.J., Murnane, K.S., Kaye, A.M., Kaye, A.D., 2022. Aduhelm, a novel anti-amyloid monoclonal antibody, for the treatment of Alzheimer's Disease: A comprehensive review. Health Psychol Res 10, 37023.
Hadoux, X., Hui, F., Lim, J.K.H., Masters, C.L., Pebay, A., Chevalier, S., Ha, J., Loi, S., Fowler, C.J., Rowe, C., Villemagne, V.L., Taylor, E.N., Fluke, C., Soucy, J.P., Lesage, F., Sylvestre, J.P., Rosa-Neto, P., Mathotaarachchi, S., Gauthier, S., Nasreddine, Z.S., Arbour, J.D., Rheaume, M.A., Beaulieu, S., Dirani, M., Nguyen, C.T. O., Bui, B.V., Williamson, R., Crowston, J.G., van Wijngaarden, P., 2019. Non-invasive in vivo hyperspectral imaging of the retina for potential biomarker use in Alzheimer's disease. Nat. Commun. 10, 4227.
Hameed, S., Fuh, J.L., Senanarong, V., Ebenezer, E.G.M., Looi, I., Dominguez, J.C., Park, K.W., Karanam, A.K., Simon, O., 2020. Role of Fluid Biomarkers and PET Imaging in Early Diagnosis and its Clinical Implication in the Management of Alzheimer's Disease. J Alzheimers Dis Rep 4, 21–37.
Hamilton, N.B., Attwell, D., Hall, C.N., 2010. Pericyte-mediated regulation of capillary diameter: a component of neurovascular coupling in health and disease. Front. Neuroenergetics 2.
Hampel, H., Caraci, F., Cuello, A.C., Caruso, G., Nistico, R., Corbo, M., Baldacci, F., Toschi, N., Garaci, F., Chiesa, P.A., Verdooner, S.R., Akman-Anderson, L., Hernandez, F., Avila, J., Emanuele, E., Valenzuela, P.L., Lucia, A., Watling, M., Imbimbo, B.P., Vergallo, A., Lista, S., 2020. A Path Toward Precision Medicine for Neuroinflammatory Mechanisms in Alzheimer's Disease. Front. Immunol. 11, 456.
Hampel, H., Cummings, J., Blennow, K., Gao, P., Jack Jr., C.R., Vergallo, A., 2021a. Developing the ATX(N) classification for use across the Alzheimer disease continuum. Nat. Rev. Neurol. 17, 580–589.
Hampel, H., Hardy, J., Blennow, K., Chen, C., Perry, G., Kim, S.H., Villemagne, V.L., Aisen, P., Vendruscolo, M., Iwatsubo, T., Masters, C.L., Cho, M., Lannfelt, L., Cummings, J.L., Vergallo, A., 2021b. The Amyloid-beta Pathway in Alzheimer's Disease. Mol. Psychiatr. 26, 5481–5503.
Hampel, H., Lista, S., Neri, C., Vergallo, A., 2019. Time for the systems-level integration of aging: Resilience enhancing strategies to prevent Alzheimer's disease. Prog. Neurobiol. 181, 101662.
Hampel, H., O'Bryant, S.E., Molinuevo, J.L., Zetterberg, H., Masters, C.L., Lista, S., Kiddle, S.J., Batrla, R., Blennow, K., 2018. Blood-based biomarkers for Alzheimer disease: mapping the road to the clinic. Nat. Rev. Neurol. 14, 639–652.
Hanseeuw, B.J., Betensky, R.A., Jacobs, H.I.L., Schultz, A.P., Sepulcre, J., Becker, J.A., Cosio, D.M.O., Farrell, M., Quiroz, Y.T., Mormino, E.C., Buckley, R.F., Papp, K.V., Amariglio, R.A., Dewachter, I., Ivanoiu, A., Huijbers, W., Hedden, T., Marshall, G.A., Chhatwal, J.P., Rentz, D.M., Sperling, R.A., Johnson, K., 2019. Association of Amyloid and Tau With Cognition in Preclinical Alzheimer Disease: A Longitudinal Study. JAMA Neurol. 76, 915–924.
Hansen, D.V., Hanson, J.E., Sheng, M., 2018. Microglia in Alzheimer's disease. J. Cell Biol. 217, 459–472.
Harrison, I.F., Ismail, O., Machhada, A., Colgan, N., Ohene, Y., Nahavandi, P., Ahmed, Z., Fisher, A., Meftah, S., Murray, T.K., Ottersen, O.P., Nagelhus, E.A., O'Neill, M.J., Wells, J.A., Lythgoe, M.F., 2020. Impaired glymphatic function and clearance of tau in an Alzheimer's disease model. Brain 143, 2576–2593.
Hart de Ruyter, F.J., Morrema, T.H.J., den Haan, J., Netherlands Brain, B., Twisk, J.W.R., de Boer, J.F., Scheltens, P., Boon, B.D.C., Thal, D.R., Rozemuller, A.J., Verbraak, F. D., Bouwman, F.H., Hoozemans, J.J.M., 2023. Phosphorylated tau in the retina correlates with tau pathology in the brain in Alzheimer's disease and primary tauopathies. Acta Neuropathol. 145, 197–218.
Hart, N.J., Koronyo, Y., Black, K.L., Koronyo-Hamaoui, M., 2016. Ocular indicators of Alzheimer's: exploring disease in the retina. Acta Neuropathol. 132, 767–787.
Harwerth, R.S., Wheat, J.L., Rangaswamy, N.V., 2008. Age-related losses of retinal ganglion cells and axons. Invest. Ophthalmol. Vis. Sci. 49, 4437–4443.
Hassler, O., 1965. Vascular changes in senile brains. A micro-angiographic study. Acta Neuropathol. 5, 40–53.

He, Y., Zhao, H., Su, G., 2014. Ginsenoside Rg1 decreases neurofibrillary tangles accumulation in retina by regulating activities of neprilysin and PKA in retinal cells of AD mice model. J. Mol. Neurosci. 52, 101–106.
Hedges, T.R., Perez Galves, R., Speigelman, D., Barbas, N.R., Peli, E., Yardley, C.J., 1996. Retinal nerve fiber layer abnormalities in Alzheimer's disease. Acta Ophthalmol. Scand. 74, 271–275.
Heneka, M.T., Carson, M.J., El Khoury, J., Landreth, G.E., Brosseron, F., Feinstein, D.L., Jacobs, A.H., Wyss-Coray, T., Vitorica, J., Ransohoff, R.M., Herrup, K., Frautschy, S. A., Finsen, B., Brown, G.C., Verkhratsky, A., Yamanaka, K., Koistinaho, J., Latz, E., Halle, A., Petzold, G.C., Town, T., Morgan, D., Shinohara, M.L., Perry, V.H., Holmes, C., Bazan, N.G., Brooks, D.J., Hunot, S., Joseph, B., Deigendesch, N., Garaschuk, O., Boddeke, E., Dinarello, C.A., Breitner, J.C., Cole, G.M., Golenbock, D. T., Kummer, M.P., 2015. Neuroinflammation in Alzheimer's disease. Lancet Neurol. 14, 388–405.
Hersh, L.B., Rodgers, D.W., 2008. Neprilysin and amyloid beta peptide degradation. Curr. Alzheimer Res. 5, 225–231.
Hickman, S.E., Allison, E.K., El Khoury, J., 2008. Microglial dysfunction and defective beta-amyloid clearance pathways in aging Alzheimer's disease mice. J. Neurosci. 28, 8354–8360.
Hinton, D.R., Sadun, A.A., Blanks, J.C., Miller, C.A., 1986. Optic-nerve degeneration in Alzheimer's disease. N. Engl. J. Med. 315, 485–487.
Hirsch, C., Bartenstein, P., Minoshima, S., Mosch, D., Willoch, F., Buch, K., Schad, D., Schwaiger, M., Kurz, A., 1997. Reduction of regional cerebral blood flow and cognitive impairment in patients with Alzheimer's disease: evaluation of an observer-independent analytic approach. Dement. Geriatr. Cogn. Disord 8, 98–104.
Ho, C.Y., Troncoso, J.C., Knox, D., Stark, W., Eberhart, C.G., 2014. Beta-amyloid, phospho-tau and alpha-synuclein deposits similar to those in the brain are not identified in the eyes of Alzheimer's and Parkinson's disease patients. Brain Pathol. 24, 25–32.
Hof, P.R., Morrison, J.H., 1990. Quantitative analysis of a vulnerable subset of pyramidal neurons in Alzheimer's disease: II. Primary and secondary visual cortex. J. Comp. Neurol. 301, 55–64.
Holmes, C., Boche, D., Wilkinson, D., Yadegarfar, G., Hopkins, V., Bayer, A., Jones, R.W., Bullock, R., Love, S., Neal, J.W., Zotova, E., Nicoll, J.A., 2008. Long-term effects of Abeta42 immunisation in Alzheimer's disease: follow-up of a randomised, placebo-controlled phase I trial. Lancet 372, 216–223.
Holomcik, D., Seebock, P., Gerendas, B.S., Mylonas, G., Najeeb, B.H., Schmidt-Erfurth, U., Deak, G., 2023. Segmentation of macular neovascularization and leakage in fluorescein angiography images in neovascular age-related macular degeneration using deep learning. Eye (Lond) 37, 1439–1444.
Holth, J.K., Fritschi, S.K., Wang, C., Pedersen, N.P., Cirrito, J.R., Mahan, T.E., Finn, M.B., Manis, M., Geerling, J.C., Fuller, P.M., Lucey, B.P., Holtzman, D.M., 2019. The sleep-wake cycle regulates brain interstitial fluid tau in mice and CSF tau in humans. Science 363, 880–884.
Holtzman, D.M., Morris, J.C., Goate, A.M., 2011. Alzheimer's disease: the challenge of the second century. Sci. Transl. Med. 3, 77sr71.
Hong, S., Beja-Glasser, V.F., Nfonoyim, B.M., Frouin, A., Li, S., Ramakrishnan, S., Merry, K.M., Shi, Q., Rosenthal, A., Barres, B.A., Lemere, C.A., Selkoe, D.J., Stevens, B., 2016. Complement and microglia mediate early synapse loss in Alzheimer mouse models. Science 352, 712–716.
Honig, L.S., Kukull, W., Mayeux, R., 2005. Atherosclerosis and AD: analysis of data from the US National Alzheimer's Coordinating Center. Neurology 64, 494–500.
Hoogendijk, W.J., van Someren, E.J., Mirmiran, M., Hofman, M.A., Lucassen, P.J., Zhou, J.N., Swaab, D.F., 1996. Circadian rhythm-related behavioral disturbances and structural hypothalamic changes in Alzheimer's disease. Int. Psychogeriatr. 8 (Suppl. 3), 245–252. ; discussion 269-272.
Hu, X., Meier, M., Pruessner, J., 2023a. Challenges and opportunities of diagnostic markers of Alzheimer's disease based on structural magnetic resonance imaging. Brain Behav 13, e2925.
Hu, Z., Wang, L., Zhu, D., Qin, R., Sheng, X., Ke, Z., Shao, P., Zhao, H., Xu, Y., Bai, F., 2023b. Retinal Alterations as Potential Biomarkers of Structural Brain Changes in Alzheimer's Disease Spectrum Patients. Brain Sci. 13.
Hughes, T.M., Kuller, L.H., Barinas-Mitchell, E.J., Mackey, R.H., McDade, E.M., Klunk, W.E., Aizenstein, H.J., Cohen, A.D., Snitz, B.E., Mathis, C.A., Dekosky, S.T., Lopez, O.L., 2013. Pulse wave velocity is associated with beta-amyloid deposition in the brains of very elderly adults. Neurology 81, 1711–1718.
Hui, J., Zhao, Y., Yu, S., Liu, J., Chiu, K., Wang, Y., 2021. Detection of retinal changes with optical coherence tomography angiography in mild cognitive impairment and Alzheimer's disease patients: A meta-analysis. PLoS One 16, e0255362.
Hutton, J.T., Morris, J.L., Elias, J.W., Poston, J.N., 1993. Contrast sensitivity dysfunction in Alzheimer's disease. Neurology 43, 2328–2330.
Iadanza, M.G., Jackson, M.P., Radford, S.E., Ranson, N.A., 2016. MpUL-multi: Software for Calculation of Amyloid Fibril Mass per Unit Length from TB-TEM Images. Sci. Rep. 6, 21078.
Ibrahim, Y., Xie, J., Macerollo, A., Sardone, R., Shen, Y., Romano, V., Zheng, Y., 2023. A Systematic Review on Retinal Biomarkers to Diagnose Dementia from OCT/OCTA Images. J Alzheimers Dis Rep 7, 1201–1235.
Iseri, P.K., Altinas, O., Tokay, T., Yuksel, N., 2006. Relationship between cognitive impairment and retinal morphological and visual functional abnormalities in Alzheimer disease. J. Neuro Ophthalmol. 26, 18–24.
Ishida, K., Yamada, K., Nishiyama, R., Hashimoto, T., Nishida, I., Abe, Y., Yasui, M., Iwatsubo, T., 2022. Glymphatic system clears extracellular tau and protects from tau aggregation and neurodegeneration. J. Exp. Med. 219.
Itai, N., Tanito, M., Chihara, E., 2003. Comparison of optic disc topography measured by Retinal Thickness Analyzer with measurement by Heidelberg Retina Tomograph II. Jpn. J. Ophthalmol. 47, 214–220.
Jack Jr., C.R., 2023. Revised Criteria for Diagnosis and Staging of Alzheimer's Disease: Alzheimer's Association Workgroup. Alzheimer's Associations International Conference.
Jadhav, S., Cubinkova, V., Zimova, I., Brezovakova, V., Madari, A., Cigankova, V., Zilka, N., 2015. Tau-mediated synaptic damage in Alzheimer's disease. Transl. Neurosci. 6, 214–226.
Jaeger, L.B., Dohgu, S., Hwang, M.C., Farr, S.A., Murphy, M.P., Fleegal-DeMotta, M.A., Lynch, J.L., Robinson, S.M., Niehoff, M.L., Johnson, S.N., Kumar, V.B., Banks, W.A., 2009. Testing the neurovascular hypothesis of Alzheimer's disease: LRP-1 antisense reduces blood-brain barrier clearance, increases brain levels of amyloid-beta protein, and impairs cognition. J. Alzheimers Dis. 17, 553–570.
Janez-Escalada, L., Janez-Garcia, L., Salobrar-Garcia, E., Santos-Mayo, A., de Hoz, R., Yubero, R., Gil, P., Ramirez, J.M., 2019. Spatial analysis of thickness changes in ten retinal layers of Alzheimer's disease patients based on optical coherence tomography. Sci. Rep. 9, 13000.
Jansen, I.E., Savage, J.E., Watanabe, K., Bryois, J., Williams, D.M., Steinberg, S., Sealock, J., Karlsson, I.K., Hagg, S., Athanasiu, L., Voyle, N., Proitsi, P., Witoelar, A., Stringer, S., Aarsland, D., Almdahl, I.S., Andersen, F., Bergh, S., Bettella, F., Bjornsson, S., Braekhus, A., Brathen, G., de Leeuw, C., Desikan, R.S., Djurovic, S., Dumitrescu, L., Fladby, T., Hohman, T.J., Jonsson, P.V., Kiddle, S.J., Rongve, A., Saltvedt, I., Sando, S.B., Selbaek, G., Shoai, M., Skene, N.G., Snaedal, J., Stordal, E., Ulstein, I.D., Wang, Y., White, L.R., Hardy, J., Hjerling-Leffler, J., Sullivan, P.F., van der Flier, W.M., Dobson, R., Davis, L.K., Stefansson, H., Stefansson, K., Pedersen, N. L., Ripke, S., Andreassen, O.A., Posthuma, D., 2019. Genome-wide meta-analysis identifies new loci and functional pathways influencing Alzheimer's disease risk. Nat. Genet. 51, 404–413.
Javaid, F.Z., Brenton, J., Guo, L., Cordeiro, M.F., 2016. Visual and Ocular Manifestations of Alzheimer's Disease and Their Use as Biomarkers for Diagnosis and Progression. Front. Neurol. 7, 55.
Javitt, D.C., Martinez, A., Sehatpour, P., Beloborodova, A., Habeck, C., Gazes, Y., Bermudez, D., Razlighi, Q.R., Devanand, D.P., Stern, Y., 2023. Disruption of early visual processing in amyloid-positive healthy individuals and mild cognitive impairment. Alzheimer's Res. Ther. 15, 42.
Jefferis, J.M., Mosimann, U.P., Clarke, M.P., 2011. Cataract and cognitive impairment: a review of the literature. Br. J. Ophthalmol. 95, 17–23.
Jellinger, K.A., 2010. Prevalence and impact of cerebrovascular lesions in Alzheimer and lewy body diseases. Neurodegener. Dis. 7, 112–115.
Jentsch, S., Schweitzer, D., Schmidtke, K.U., Peters, S., Dawczynski, J., Bar, K.J., Hammer, M., 2015. Retinal fluorescence lifetime imaging ophthalmoscopy measures depend on the severity of Alzheimer's disease. Acta Ophthalmol. 93, e241–e247.
Jiang, H., Wei, Y., Shi, Y., Wright, C.B., Sun, X., Gregori, G., Zheng, F., Vanner, E.A., Lam, B.L., Rundek, T., Wang, J., 2018. Altered Macular Microvasculature in Mild Cognitive Impairment and Alzheimer Disease. J. Neuro Ophthalmol. 38, 292–298.
Jindahra, P., Hengsiri, N., Witoonpanich, P., Poonyathalang, A., Pulkes, T., Tunlayadechanont, S., Thadanipon, K., Vanikieti, K., 2020. Evaluation of Retinal Nerve Fiber Layer and Ganglion Cell Layer Thickness in Alzheimer's Disease Using Optical Coherence Tomography. Clin. Ophthalmol. 14, 2995–3000.
Jindal, V., 2015. Interconnection between brain and retinal neurodegenerations. Mol. Neurobiol. 51, 885–892.
Jorge, L., Canario, N., Quental, H., Bernardes, R., Castelo-Branco, M., 2019. Is the Retina a Mirror of the Aging Brain? Aging of Neural Retina Layers and Primary Visual Cortex Across the Lifespan. Front. Aging Neurosci. 11, 360.
Ju, Y.E., McLeland, J.S., Toedebusch, C.D., Xiong, C., Fagan, A.M., Duntley, S.P., Morris, J.C., Holtzman, D.M., 2013. Sleep quality and preclinical Alzheimer disease. JAMA Neurol. 70, 587–593.
Ju, Y.S., Zangrilli, M.A., Finn, M.B., Fagan, A.M., Holtzman, D.M., 2019. Obstructive sleep apnea treatment, slow wave activity, and amyloid-beta. Ann. Neurol. 85, 291–295.
Kaeser, P.F., Ghika, J., Borruat, F.X., 2015. Visual signs and symptoms in patients with the visual variant of Alzheimer disease. BMC Ophthalmol. 15, 65.
Kalaria, R.N., 2016. Neuropathological diagnosis of vascular cognitive impairment and vascular dementia with implications for Alzheimer's disease. Acta Neuropathol. 131, 659–685.
Kang, J., Choi, H.J., Isaacs, G.D., Sung, W., Kim, H.J., 2021. Amyloid Burden in Alzheimer's Disease Patients Is Associated with Alterations in Circadian Rhythm. Dement Neurocogn Disord 20, 99–107.
Kao, C.C., Hsieh, H.M., Chang, Y.C., Chu, H.C., Yang, Y.H., Sheu, S.J., 2023. Optical Coherence Tomography Assessment of Macular Thickness in Alzheimer's Dementia with Different Neuropsychological Severities. J. Personalized Med. 13.
Karch, C.M., Goate, A.M., 2015. Alzheimer's disease risk genes and mechanisms of disease pathogenesis. Biol. Psychiatr. 77, 43–51.
Kashani, A.H., Chen, C.L., Gahm, J.K., Zheng, F., Richter, G.M., Rosenfeld, P.J., Shi, Y., Wang, R.K., 2017. Optical coherence tomography angiography: A comprehensive review of current methods and clinical applications. Prog. Retin. Eye Res. 60, 66–100.
Kasindi, A., Fuchs, D.T., Koronyo, Y., Rentsendorj, A., Black, K.L., Koronyo-Hamaoui, M., 2022. Glatiramer Acetate Immunomodulation: Evidence of Neuroprotection and Cognitive Preservation. Cells 11.
Katsimpris, A., Karamaounas, A., Sideri, A.M., Katsimpris, J., Georgalas, I., Petrou, P., 2022. Optical coherence tomography angiography in Alzheimer's disease: a systematic review and meta-analysis. Eye (Lond) 36, 1419–1426.
Katz, B., Rimmer, S., 1989. Ophthalmologic manifestations of Alzheimer's disease. Surv. Ophthalmol. 34, 31–43.
Katz, B., Rimmer, S., Iragui, V., Katzman, R., 1989. Abnormal pattern electroretinogram in Alzheimer's disease: evidence for retinal ganglion cell degeneration? Ann. Neurol. 26, 221–225.

Kelly, L., Brown, C., Michalik, D., Hawkes, C.A., Aldea, R., Agarwal, N., Salib, R., Alzetani, A., Ethell, D.W., Counts, S.E., de Leon, M., Fossati, S., Koronyo-Hamaoui, M., Piazza, F., Rich, S.A., Wolters, F.J., Snyder, H., Ismail, O., Elahi, F., Proulx, S.T., Verma, A., Wunderlich, H., Haack, M., Dodart, J.C., Mazer, N., Carare, R.O., 2024. Clearance of interstitial fluid (ISF) and CSF (CLIC) group-part of Vascular Professional Interest Area (PIA), updates in 2022-2023. Cerebrovascular disease and the failure of elimination of Amyloid-beta from the brain and retina with age and Alzheimer's disease: Opportunities for therapy. Alzheimers Dement 20, 1421–1435.

Keren-Shaul, H., Spinrad, A., Weiner, A., Matcovitch-Natan, O., Dvir-Szternfeld, R., Ulland, T.K., David, E., Baruch, K., Lara-Astaiso, D., Toth, B., Itzkovitz, S., Colonna, M., Schwartz, M., Amit, I., 2017. A Unique Microglia Type Associated with Restricting Development of Alzheimer's Disease. Cell 169, 1276–1290 e1217.

Kergoat, H., Kergoat, M.J., Justino, L., Chertkow, H., Robillard, A., Bergman, H., 2002. Visual retinocortical function in dementia of the Alzheimer type. Gerontology 48, 197–203.

Kesler, A., Vakhapova, V., Korczyn, A.D., Naftaliev, E., Neudorfer, M., 2011. Retinal thickness in patients with mild cognitive impairment and Alzheimer's disease. Clin. Neurol. Neurosurg. 113, 523–526.

Kile, S., Au, W., Parise, C., Sohi, J., Yarbrough, T., Czeszynski, A., Johnson, K., Redline, D., Donnel, T., Hankins, A., Rose, K., 2020. Reduction of Amyloid in the Brain and Retina After Treatment With IVIG for Mild Cognitive Impairment. Am J Alzheimers Dis Other Demen 35, 1533317519899800.

Kim, B.J., Lee, V., Lee, E.B., Saludades, A., Trojanowski, J.Q., Dunaief, J.L., Grossman, M., Irwin, D.J., 2021a. Retina tissue validation of optical coherence tomography determined outer nuclear layer loss in FTLD-tau. Acta Neuropathol. Commun. 9, 184.

Kim, D.G., Krenz, A., Toussaint, L.E., Maurer, K.J., Robinson, S.A., Yan, A., Torres, L., Bynoe, M.S., 2016. Non-alcoholic fatty liver disease induces signs of Alzheimer's disease (AD) in wild-type mice and accelerates pathological signs of AD in an AD model. J. Neuroinflammation 13, 1.

Kim, H.M., Han, J.W., Park, Y.J., Bae, J.B., Woo, S.J., Kim, K.W., 2022. Association Between Retinal Layer Thickness and Cognitive Decline in Older Adults. JAMA Ophthalmol 140, 683–690.

Kim, J.I., Kang, B.H., 2019. Decreased retinal thickness in patients with Alzheimer's disease is correlated with disease severity. PLoS One 14, e0224180.

Kim, J.W., Rizzo, J.F., Lessell, S., 2005. Delayed visual decline in patients with "stable" optic neuropathy. Arch. Ophthalmol. 123, 785–788.

Kim, S.H., Ahn, J.H., Yang, H., Lee, P., Koh, G.Y., Jeong, Y., 2020. Cerebral amyloid angiopathy aggravates perivascular clearance impairment in an Alzheimer's disease mouse model. Acta Neuropathol. Commun. 8, 181.

Kim, T.H., Son, T., Klatt, D., Yao, X., 2021b. Concurrent OCT and OCT angiography of retinal neurovascular degeneration in the 5XFAD Alzheimer's disease mice. Neurophotonics 8, 035002.

Kimbrough, I.F., Robel, S., Roberson, E.D., Sontheimer, H., 2015. Vascular amyloidosis impairs the gliovascular unit in a mouse model of Alzheimer's disease. Brain 138, 3716–3733.

Kirbas, S., Turkyilmaz, K., Anlar, O., Tufekci, A., Durmus, M., 2013. Retinal nerve fiber layer thickness in patients with Alzheimer disease. J. Neuro Ophthalmol. 33, 58–61.

Kiyosawa, M., Bosley, T.M., Chawluk, J., Jamieson, D., Schatz, N.J., Savino, P.J., Sergott, R.C., Reivich, M., Alavi, A., 1989. Alzheimer's disease with prominent visual symptoms. Clinical and metabolic evaluation. Ophthalmology 96, 1077–1085. ; discussion 1085-1076.

Koronyo, Y., Biggs, D., Barron, E., Boyer, D.S., Pearlman, J.A., Au, W.J., Kile, S.J., Blanco, A., Fuchs, D.T., Ashfaq, A., Frautschy, S., Cole, G.M., Miller, C.A., Hinton, D. R., Verdooner, S.R., Black, K.L., Koronyo-Hamaoui, M., 2017. Retinal amyloid pathology and proof-of-concept imaging trial in Alzheimer's disease. JCI Insight 2.

Koronyo, Y., Rentsendorj, A., Mirzaei, N., Regis, G.C., Sheyn, J., Shi, H., Barron, E., Cook-Wiens, G., Rodriguez, A.R., Medeiros, R., Paulo, J.A., Gupta, V.B., Kramerov, A.A., Ljubimov, A.V., Van Eyk, J.E., Graham, S.L., Gupta, V.K., Ringman, J.M., Hinton, D. R., Miller, C.A., Black, K.L., Cattaneo, A., Meli, G., Mirzaei, M., Fuchs, D.T., Koronyo-Hamaoui, M., 2023. Retinal pathological features and proteome signatures of Alzheimer's disease. Acta Neuropathol. 145, 409–438.

Koronyo, Y., Salumbides, B.C., Black, K.L., Koronyo-Hamaoui, M., 2012. Alzheimer's disease in the retina: imaging retinal abeta plaques for early diagnosis and therapy assessment. Neurodegener. Dis. 10, 285–293.

Koronyo, Y., Salumbides, B.C., Sheyn, J., Pelissier, L., Li, S., Ljubimov, V., Moyseyev, M., Daley, D., Fuchs, D.T., Pham, M., Black, K.L., Rentsendorj, A., Koronyo-Hamaoui, M., 2015. Therapeutic effects of glatiramer acetate and grafted CD115(+) monocytes in a mouse model of Alzheimer's disease. Brain 138, 2399–2422.

Koronyo-Hamaoui, M., Ko, M.K., Koronyo, Y., Azoulay, D., Seksenyan, A., Kunis, G., Pham, M., Bakhsheshian, J., Rogeri, P., Black, K.L., Farkas, D.L., Schwartz, M., 2009. Attenuation of AD-like neuropathology by harnessing peripheral immune cells: local elevation of IL-10 and MMP-9. J. Neurochem. 111, 1409–1424.

Koronyo-Hamaoui, M., Koronyo, Y., Ljubimov, A.V., Miller, C.A., Ko, M.K., Black, K.L., Schwartz, M., Farkas, D.L., 2011. Identification of amyloid plaques in retinas from Alzheimer's patients and noninvasive in vivo optical imaging of retinal plaques in a mouse model. Neuroimage 54 (Suppl. 1), S204–S217.

Koronyo-Hamaoui, M., Sheyn, J., Hayden, E.Y., Li, S., Fuchs, D.T., Regis, G.C., Lopes, D. H.J., Black, K.L., Bernstein, K.E., Teplow, D.B., Fuchs, S., Koronyo, Y., Rentsendorj, A., 2020. Peripherally derived angiotensin converting enzyme-enhanced macrophages alleviate Alzheimer-related disease. Brain 143, 336–358.

Kosik, K.S., Joachim, C.L., Selkoe, D.J., 1986. Microtubule-associated protein tau (tau) is a major antigenic component of paired helical filaments in Alzheimer disease. Proc. Natl. Acad. Sci. U. S. A. 83, 4044–4048.

Kotliar, K., Hauser, C., Ortner, M., Muggenthaler, C., Diehl-Schmid, J., Angermann, S., Hapfelmeier, A., Schmaderer, C., Grimmer, T., 2017. Altered neurovascular coupling as measured by optical imaging: a biomarker for Alzheimer's disease. Sci. Rep. 7, 12906.

Kotliar, K., Ortner, M., Conradi, A., Hacker, P., Hauser, C., Gunthner, R., Moser, M., Muggenthaler, C., Diehl-Schmid, J., Priller, J., Schmaderer, C., Grimmer, T., 2022. Altered retinal cerebral vessel oscillation frequencies in Alzheimer's disease compatible with impaired amyloid clearance. Neurobiol. Aging 120, 117–127.

Krabbe, G., Halle, A., Matyash, V., Rinnenthal, J.L., Eom, G.D., Bernhardt, U., Miller, K. R., Prokop, S., Kettenmann, H., Heppner, F.L., 2013. Functional impairment of microglia coincides with Beta-amyloid deposition in mice with Alzheimer-like pathology. PLoS One 8, e60921.

Krasemann, S., Madore, C., Cialic, R., Baufeld, C., Calcagno, N., El Fatimy, R., Beckers, L., O'Loughlin, E., Xu, Y., Fanek, Z., Greco, D.J., Smith, S.T., Tweet, G., Humulock, Z., Zrzavy, T., Conde-Sanroman, P., Gacias, M., Weng, Z., Chen, H., Tjon, E., Mazaheri, F., Hartmann, K., Madi, A., Ulrich, J.D., Glatzel, M., Worthmann, A., Heeren, J., Budnik, B., Lemere, C., Ikezu, T., Heppner, F.L., Litvak, V., Holtzman, D. M., Lassmann, H., Weiner, H.L., Ochando, J., Haass, C., Butovsky, O., 2017. The TREM2-APOE Pathway Drives the Transcriptional Phenotype of Dysfunctional Microglia in Neurodegenerative Diseases. Immunity 47, 566–581 e569.

Krasodomska, K., Lubinski, W., Potemkowski, A., Honczarenko, K., 2010. Pattern electroretinogram (PERG) and pattern visual evoked potential (PVEP) in the early stages of Alzheimer's disease. Doc. Ophthalmol. 121, 111–121.

Kromer, R., Serbecic, N., Hausner, L., Froelich, L., Aboul-Enein, F., Beutelspacher, S.C., 2014. Detection of Retinal Nerve Fiber Layer Defects in Alzheimer's Disease Using SD-OCT. Front. Psychiatr. 5, 22.

Kumaraswamy, P., Sethuraman, S., Krishnan, U.M., 2013. Mechanistic insights of curcumin interactions with the core-recognition motif of beta-amyloid peptide. J. Agric. Food Chem. 61, 3278–3285.

Kwon, J.Y., Yang, J.H., Han, J.S., Kim, D.G., 2017. Analysis of the Retinal Nerve Fiber Layer Thickness in Alzheimer Disease and Mild Cognitive Impairment. Kor. J. Ophthalmol. 31, 548–556.

La Morgia, C., Mitolo, M., Romagnoli, M., Stanzani Maserati, M., Evangelisti, S., De Matteis, M., Capellari, S., Bianchini, C., Testa, C., Vandewalle, G., Santoro, A., Carbonelli, M., D'Agati, P., Filardi, M., Avanzini, P., Barboni, P., Zenesini, C., Baccari, F., Liguori, R., Tonon, C., Lodi, R., Carelli, V., 2023. Multimodal investigation of melanopsin retinal ganglion cells in Alzheimer's disease. Ann Clin Transl Neurol 10, 918–932.

La Morgia, C., Ross-Cisneros, F.N., Koronyo, Y., Hannibal, J., Gallassi, R., Cantalupo, G., Sambati, L., Pan, B.X., Tozer, K.R., Barboni, P., Provini, F., Avanzini, P., Carbonelli, M., Pelosi, A., Chui, H., Liguori, R., Baruzzi, A., Koronyo-Hamaoui, M., Sadun, A.A., Carelli, V., 2016. Melanopsin retinal ganglion cell loss in Alzheimer disease. Ann. Neurol. 79, 90–109.

La Morgia, C., Ross-Cisneros, F.N., Sadun, A.A., Carelli, V., 2017. Retinal Ganglion Cells and Circadian Rhythms in Alzheimer's Disease, Parkinson's Disease, and Beyond. Front. Neurol. 8, 162.

Laatikainen, L., 2004. The fluorescein angiography revolution: a breakthrough with sustained impact. Acta Ophthalmol. Scand. 82, 381–392.

Laatu, S., Revonsuo, A., Jaykka, H., Portin, R., Rinne, J.O., 2003. Visual object recognition in early Alzheimer's disease: deficits in semantic processing. Acta Neurol. Scand. 108, 82–89.

Lahiri, S., Regis, G.C., Koronyo, Y., Fuchs, D.T., Sheyn, J., Kim, E.H., Mastali, M., Van Eyk, J.E., Rajput, P.S., Lyden, P.D., Black, K.L., Ely, E.W., H, D.J., Koronyo-Hamaoui, M., 2019. Acute neuropathological consequences of short-term mechanical ventilation in wild-type and Alzheimer's disease mice. Crit. Care 23, 63.

Lahme, L., Esser, E.L., Mihailovic, N., Schubert, F., Lauermann, J., Johnen, A., Eter, N., Duning, T., Alnawaiseh, M., 2018. Evaluation of Ocular Perfusion in Alzheimer's Disease Using Optical Coherence Tomography Angiography. J. Alzheimers Dis. 66, 1745–1752.

Lambert, J.C., Ibrahim-Verbaas, C.A., Harold, D., Naj, A.C., Sims, R., Bellenguez, C., DeStafano, A.L., Bis, J.C., Beecham, G.W., Grenier-Boley, B., Russo, G., Thorton-Wells, T.A., Jones, N., Smith, A.V., Chouraki, V., Thomas, C., Ikram, M.A., Zelenika, D., Vardarajan, B.N., Kamatani, Y., Lin, C.F., Gerrish, A., Schmidt, H., Kunkle, B., Dunstan, M.L., Ruiz, A., Bihoreau, M.T., Choi, S.H., Reitz, C., Pasquier, F., Cruchaga, C., Craig, D., Amin, N., Berr, C., Lopez, O.L., De Jager, P.L., Deramecourt, V., Johnston, J.A., Evans, D., Lovestone, S., Letenneur, L., Moron, F.J., Rubinsztein, D.C., Eiriksdottir, G., Sleegers, K., Goate, A.M., Fievet, N., Huentelman, M.W., Gill, M., Brown, K., Kamboh, M.I., Keller, L., Barberger-Gateau, P., McGuiness, B., Larson, E.B., Green, R., Myers, A.J., Dufouil, C., Todd, S., Wallon, D., Love, S., Rogaeva, E., Gallacher, J., St George-Hyslop, P., Clarimon, J., Lleo, A., Bayer, A., Tsuang, D.W., Yu, L., Tsolaki, M., Bossu, P., Spalletta, G., Proitsi, P., Collinge, J., Sorbi, S., Sanchez-Garcia, F., Fox, N.C., Hardy, J., Deniz Naranjo, M.C., Bosco, P., Clarke, R., Brayne, C., Galimberti, D., Mancuso, M., Matthews, F., European Alzheimer's Disease, I., Genetic, Environmental Risk in Alzheimer's, D., Alzheimer's Disease Genetic, C., Cohorts for, H., Aging Research in Genomic, E., Moebus, S., Mecocci, P., Del Zompo, M., Maier, W., Hampel, H., Pilotto, A., Bullido, M., Panza, F., Caffarra, P., Nacmias, B., Gilbert, J.R., Mayhaus, M., Lannefelt, L., Hakonarson, H., Pichler, S., Carrasquillo, M.M., Ingelsson, M., Beekly, D., Alvarez, V., Zou, F., Valladares, O., Younkin, S.G., Coto, E., Hamilton-Nelson, K.L., Gu, W., Razquin, C., Pastor, P., Mateo, I., Owen, M.J., Faber, K.M., Jonsson, P.V., Combarros, O., O'Donovan, M.C., Cantwell, L.B., Soininen, H., Blacker, D., Mead, S., Mosley Jr., T.H., Bennett, D.A., Harris, T.B., Fratiglioni, L., Holmes, C., de Bruijn, R.F., Passmore, P., Montine, T.J., Bettens, K., Rotter, J.I., Brice, A., Morgan, K., Foroud, T.M., Kukull, W.A., Hannequin, D., Powell, J.F., Nalls, M.A., Ritchie, K., Lunetta, K.L., Kauwe, J.S., Boerwinkle, E., Riemenschneider, M., Boada, M., Hiltuenen, M., Martin, E.R., Schmidt, R.,

Rujescu, D., Wang, L.S., Dartigues, J.F., Mayeux, R., Tzourio, C., Hofman, A., Nothen, M.M., Graff, C., Psaty, B.M., Jones, L., Haines, J.L., Holmans, P.A., Lathrop, M., Pericak-Vance, M.A., Launer, L.J., Farrer, L.A., van Duijn, C.M., Van Broeckhoven, C., Moskvina, V., Seshadri, S., Williams, J., Schellenberg, G.D., Amouyel, P., 2013. Meta-analysis of 74,046 individuals identifies 11 new susceptibility loci for Alzheimer's disease. Nat. Genet. 45, 1452–1458.

Lan, G., Cai, Y., Li, A., Liu, Z., Ma, S., Guo, T., Alzheimer's Disease Neuroimaging, I, 2022. Association of Presynaptic Loss with Alzheimer's Disease and Cognitive Decline. Ann. Neurol. 92, 1001–1015.

Landhuis, E., 2024. Researchers call for a major rethink of how Alzheimer's treatments are evaluated. Nature 627, S18–S20.

Larrosa, J.M., Garcia-Martin, E., Bambo, M.P., Pinilla, J., Polo, V., Otin, S., Satue, M., Herrero, R., Pablo, L.E., 2014. Potential new diagnostic tool for Alzheimer's disease using a linear discriminant function for Fourier domain optical coherence tomography. Invest. Ophthalmol. Vis. Sci. 55, 3043–3051.

Latina, V., Giacovazzo, G., Cordella, F., Balzamino, B.O., Micera, A., Varano, M., Marchetti, C., Malerba, F., Florio, R., Ercole, B.B., La Regina, F., Atlante, A., Coccurello, R., Di Angelantonio, S., Calissano, P., Amadoro, G., 2021. Systemic delivery of a specific antibody targeting the pathological N-terminal truncated tau peptide reduces retinal degeneration in a mouse model of Alzheimer's Disease. Acta Neuropathol. Commun. 9, 38.

Launer, L.J., 2002. Demonstrating the case that AD is a vascular disease: epidemiologic evidence. Ageing Res. Rev. 1, 61–77.

Launer, L.J., Ross, G.W., Petrovitch, H., Masaki, K., Foley, D., White, L.R., Havlik, R.J., 2000. Midlife blood pressure and dementia: the Honolulu-Asia aging study. Neurobiol. Aging 21, 49–55.

Lee, A., Kondapalli, C., Virga, D.M., Lewis Jr., T.L., Koo, S.Y., Ashok, A., Mairet-Coello, G., Herzig, S., Foretz, M., Viollet, B., Shaw, R., Sproul, A., Polleux, F., 2022. Abeta42 oligomers trigger synaptic loss through CAMKK2-AMPK-dependent effectors coordinating mitochondrial fission and mitophagy. Nat. Commun. 13, 4444.

Lee, C.N., Ko, D., Suh, Y.W., Park, K.W., 2015. Cognitive functions and stereopsis in patients with Parkinson's disease and Alzheimer's disease using 3-dimensional television: a case controlled trial. PLoS One 10, e0123229.

Lee, C.Y., Landreth, G.E., 2010. The role of microglia in amyloid clearance from the AD brain. J. Neural. Transm. 117, 949–960.

Lee, J.S., Seong, G.J., Kim, C.Y., Lee, S.Y., Bae, H.W., 2019. Risk factors associated with progressive nerve fiber layer thinning in open-angle glaucoma with mean intraocular pressure below 15 mmHg. Sci. Rep. 9, 19811.

Lee, J.Y., Kim, J.P., Jang, H., Kim, J., Kang, S.H., Kim, J.S., Lee, J., Jung, Y.H., Na, D.L., Seo, S.W., Oh, S.Y., Kim, H.J., 2020a. Optical coherence tomography angiography as a potential screening tool for cerebral small vessel diseases. Alzheimer's Res. Ther. 12, 73.

Lee, S., Jiang, K., McIlmoyle, B., To, E., Xu, Q.A., Hirsch-Reinshagen, V., Mackenzie, I.R., Hsiung, G.R., Eadie, B.D., Sarunic, M.V., Beg, M.F., Cui, J.Z., Matsubara, J.A., 2020b. Amyloid Beta Immunoreactivity in the Retinal Ganglion Cell Layer of the Alzheimer's Eye. Front. Neurosci. 14, 758.

Lee, S., Varvel, N.H., Konerth, M.E., Xu, G., Cardona, A.E., Ransohoff, R.M., Lamb, B.T., 2010. CX3CR1 deficiency alters microglial activation and reduces beta-amyloid deposition in two Alzheimer's disease mouse models. Am. J. Pathol. 177, 2549–2562.

Lee, S., Wang, J.W., Yu, W., Lu, B., 2012. Phospho-dependent ubiquitination and degradation of PAR-1 regulates synaptic morphology and tau-mediated Abeta toxicity in Drosophila. Nat. Commun. 3, 1312.

Lee, S.J., Lee, J.J., Kim, S.D., 2006. Multiple retinal hemorrhage following anterior chamber paracentesis in uveitic glaucoma. Kor. J. Ophthalmol. 20, 128–130.

Leitgeb, R.A., Werkmeister, R.M., Blatter, C., Schmetterer, L., 2014. Doppler optical coherence tomography. Prog. Retin. Eye Res. 41, 26–43.

Lemmens, S., Van Craenendonck, T., Van Eijgen, J., De Groef, L., Bruffaerts, R., de Jesus, D.A., Charle, W., Jayapala, M., Sunaric-Megevand, G., Standaert, A., Theunis, J., Van Keer, K., Vandenbulcke, M., Moons, L., Vandenberghe, R., De Boever, P., Stalmans, I., 2020. Combination of snapshot hyperspectral retinal imaging and optical coherence tomography to identify Alzheimer's disease patients. Alzheimer's Res. Ther. 12, 144.

Lesage, S.R., Mosley, T.H., Wong, T.Y., Szklo, M., Knopman, D., Catellier, D.J., Cole, S.R., Klein, R., Coresh, J., Coker, L.H., Sharrett, A.R., 2009. Retinal microvascular abnormalities and cognitive decline: the ARIC 14-year follow-up study. Neurology 73, 862–868.

Li, H., Guo, Q., Inoue, T., Polito, V.A., Tabuchi, K., Hammer, R.E., Pautler, R.G., Taffet, G. E., Zheng, H., 2014. Vascular and parenchymal amyloid pathology in an Alzheimer disease knock-in mouse model: interplay with cerebral blood flow. Mol. Neurodegener. 9, 28.

Li, P., Gao, L., Gaba, A., Yu, L., Cui, L., Fan, W., Lim, A.S.P., Bennett, D.A., Buchman, A. S., Hu, K., 2020a. Circadian disturbances in Alzheimer's disease progression: a prospective observational cohort study of community-based older adults. Lancet Healthy Longev 1, e96–e105.

Li, S., Hayden, E.Y., Garcia, V.J., Fuchs, D.T., Sheyn, J., Daley, D.A., Rentsendorj, A., Torbati, T., Black, K.L., Rutishauser, U., Teplow, D.B., Koronyo, Y., Koronyo-Hamaoui, M., 2020b. Activated Bone Marrow-Derived Macrophages Eradicate Alzheimer's-Related Abeta(42) Oligomers and Protect Synapses. Front. Immunol. 11, 49.

Li, Y., Tian, C., Xie, T., Zhang, Q.L., Liu, J., Yan, X.X., Dai, J., Liang, Y., Cui, M., 2023. Hydroxyethyl-Modified Cycloheptatriene-BODIPY Derivatives as Specific Tau Imaging Probes. ACS Med. Chem. Lett. 14, 1108–1112.

Li, Z.B., Lin, Z.J., Li, N., Yu, H., Wu, Y.L., Shen, X., 2021. Evaluation of retinal and choroidal changes in patients with Alzheimer's type dementia using optical coherence tomography angiography. Int. J. Ophthalmol. 14, 860–868.

Lian, T.H., Jin, Z., Qu, Y.Z., Guo, P., Guan, H.Y., Zhang, W.J., Ding, D.Y., Li, D.N., Li, L. X., Wang, X.M., Zhang, W., 2020. The Relationship Between Retinal Nerve Fiber Layer Thickness and Clinical Symptoms of Alzheimer's Disease. Front. Aging Neurosci. 12, 584244.

Liew, G., Mitchell, P., Wong, T.Y., Lindley, R.I., Cheung, N., Kaushik, S., Wang, J.J., 2009. Retinal microvascular signs and cognitive impairment. J. Am. Geriatr. Soc. 57, 1892–1896.

Liew, G., Wang, J.J., Mitchell, P., Wong, T.Y., 2008. Retinal vascular imaging: a new tool in microvascular disease research. Circ Cardiovasc Imaging 1, 156–161.

Lim, J.K.H., Li, Q.X., He, Z., Vingrys, A.J., Chinnery, H.R., Mullen, J., Bui, B.V., Nguyen, C.T.O., 2020. Retinal Functional and Structural Changes in the 5xFAD Mouse Model of Alzheimer's Disease. Front. Neurosci. 14, 862.

Lim, S., Haque, M.M., Su, D., Kim, D., Lee, J.S., Chang, Y.T., Kim, Y.K., 2017. Development of a BODIPY-based fluorescent probe for imaging pathological tau aggregates in live cells. Chem. Commun. 53, 1607–1610.

Lim, Y.Y., Ellis, K.A., Harrington, K., Kamer, A., Pietrzak, R.H., Bush, A.I., Darby, D., Martins, R.N., Masters, C.L., Rowe, C.C., Savage, G., Szoeke, C., Villemagne, V.L., Ames, D., Maruff, P., Group, A.R., 2013. Cognitive consequences of high Abeta amyloid in mild cognitive impairment and healthy older adults: implications for early detection of Alzheimer's disease. Neuropsychology 27, 322–332.

Lista, S., Vergallo, A., Teipel, S.J., Lemercier, P., Giorgi, F.S., Gabelle, A., Garaci, F., Mercuri, N.B., Babiloni, C., Gaire, B.P., Koronyo, Y., Koronyo-Hamaoui, M., Hampel, H., Nistico, R., Neurodegeneration Precision Medicine, I., 2022. Determinants of approved acetylcholinesterase inhibitor response outcomes in Alzheimer's disease: relevance for precision medicine in neurodegenerative diseases. Ageing Res. Rev., 101819

Liu, B., Rasool, S., Yang, Z., Glabe, C.G., Schreiber, S.S., Ge, J., Tan, Z., 2009. Amyloid-peptide vaccinations reduce {beta}-amyloid plaques but exacerbate vascular deposition and inflammation in the retina of Alzheimer's transgenic mice. Am. J. Pathol. 175, 2099–2110.

Liu, D., Zhang, L., Li, Z., Zhang, X., Wu, Y., Yang, H., Min, B., Zhang, X., Ma, D., Lu, Y., 2015. Thinner changes of the retinal nerve fiber layer in patients with mild cognitive impairment and Alzheimer's disease. BMC Neurol. 15, 14.

Liu, J., Sanes, J.R., 2017. Cellular and Molecular Analysis of Dendritic Morphogenesis in a Retinal Cell Type That Senses Color Contrast and Ventral Motion. J. Neurosci. 37, 12247–12262.

Liu, Y., Feng, D., Wang, H., 2019. Distinct forms of motion sensitivity impairments in Alzheimer's disease. Sci. Rep. 9, 12931.

London, A., Benhar, I., Schwartz, M., 2013. The retina as a window to the brain-from eye research to CNS disorders. Nat. Rev. Neurol. 9, 44–53.

Lopez-Cuenca, I., Nebreda, A., Garcia-Colomo, A., Salobrar-Garcia, E., de Frutos-Lucas, J., Bruna, R., Ramirez, A.I., Ramirez-Torano, F., Salazar, J.J., Barabash, A., Gil, P., Maestu, F., Ramirez, J.M., de Hoz, R., 2023. Early visual alterations in individuals at-risk of Alzheimer's disease: a multidisciplinary approach. Alzheimer's Res. Ther. 15, 19.

Lopez-Cuenca, I., Salobrar-Garcia, E., Elvira-Hurtado, L., Fernandez-Albarral, J.A., Sanchez-Puebla, L., Salazar, J.J., Ramirez, J.M., Ramirez, A.I., de Hoz, R., 2021. The Value of OCT and OCTA as Potential Biomarkers for Preclinical Alzheimer's Disease: A Review Study. Life 11.

Lopez-de-Eguileta, A., Lage, C., Lopez-Garcia, S., Pozueta, A., Garcia-Martinez, M., Kazimierczak, M., Bravo, M., de Arcocha-Torres, M., Banzo, I., Jimenez-Bonilla, J., Cervero, A., Goikoetxea, A., Rodriguez-Rodriguez, E., Sanchez-Juan, P., Casado, A., 2020. Evaluation of choroidal thickness in prodromal Alzheimer's disease defined by amyloid PET. PLoS One 15, e0239484.

Lopez-de-Eguileta, A., Lage, C., Lopez-Garcia, S., Pozueta, A., Garcia-Martinez, M., Kazimierczak, M., Bravo, M., de Arcocha-Torres, M., Banzo, I., Jimenez-Bonilla, J., Cervero, A., Rodriguez-Rodriguez, E., Sanchez-Juan, P., Casado, A., 2019. Ganglion cell layer thinning in prodromal Alzheimer's disease defined by amyloid PET. Alzheimers Dement (N Y) 5, 570–578.

Lu, Y., Li, Z., Zhang, X., Ming, B., Jia, J., Wang, R., Ma, D., 2010. Retinal nerve fiber layer structure abnormalities in early Alzheimer's disease: evidence in optical coherence tomography. Neurosci. Lett. 480, 69–72.

Lucey, B.P., Holtzman, D.M., 2015. How amyloid, sleep and memory connect. Nat. Neurosci. 18, 933–934.

Lucey, B.P., Wisch, J., Boerwinkle, A.H., Landsness, E.C., Toedebusch, C.D., McLeland, J. S., Butt, O.H., Hassenstab, J., Morris, J.C., Ances, B.M., Holtzman, D.M., 2021. Sleep and longitudinal cognitive performance in preclinical and early symptomatic Alzheimer's disease. Brain 144, 2852–2862.

Luengnaruemitchai, G., Kaewmahanin, W., Munthuli, A., Phienphanich, P., Puangarom, S., Sangchocanonta, S., Jariyakosol, S., Hirunwiwatkul, P., Tantibundhit, C., 2023. Alzheimer's Together with Mild Cognitive Impairment Screening Using Polar Transformation of Middle Zone of Fundus Images Based Deep Learning. Annu Int Conf IEEE Eng Med Biol Soc 2023, 1–4.

Ma, X., Xie, Z., Wang, H., Tian, Z., Bi, Y., Li, Y., Zhang, L., 2023. A cross-sectional study of retinal vessel changes based on optical coherence tomography angiography in Alzheimer's disease and mild cognitive impairment. Front. Aging Neurosci. 15, 1101950.

Markovic, M., Milosevic, J., Wang, W., Cao, Y., 2023. Passive Immunotherapies Targeting Amyloid-beta in Alzheimer's Disease: A Quantitative Systems Pharmacology Perspective. Mol. Pharmacol. 105, 1–13.

Marquie, M., Valero, S., Castilla-Marti, M., Martinez, J., Rodriguez-Gomez, O., Sanabria, A., Tartari, J.P., Monte-Rubio, G.C., Sotolongo-Grau, O., Alegret, M., Perez-Cordon, A., Roberto, N., de Rojas, I., Moreno-Grau, S., Montrreal, L.,

Hernandez, I., Rosende-Roca, M., Mauleon, A., Vargas, L., Abdelnour, C., Gil, S., Esteban-De Antonio, E., Espinosa, A., Ortega, G., Lomena, F., Pavia, J., Vivas, A., Tejero, M.A., Gomez-Chiari, M., Simo, R., Ciudin, A., Hernandez, C., Orellana, A., Benaque, A., Ruiz, A., Tarraga, L., Boada, M., group, F.s., 2020. Association between retinal thickness and beta-amyloid brain accumulation in individuals with subjective cognitive decline: Fundacio ACE Healthy Brain Initiative. Alzheimer's Res. Ther. 12, 37.

Marziani, E., Pomati, S., Ramolfo, P., Cigada, M., Giani, A., Mariani, C., Staurenghi, G., 2013. Evaluation of retinal nerve fiber layer and ganglion cell layer thickness in Alzheimer's disease using spectral-domain optical coherence tomography. Invest. Ophthalmol. Vis. Sci. 54, 5953–5958.

Masaoka, N., Nakaya, K., Koura, Y., Ohsaki, M., 2001. Hemodynamic changes in two patients with retinal circulatory disturbances shown by fluorescein angiography using a scanning laser ophthalmoscope. Retina 21, 155–160.

Masters, C.L., Simms, G., Weinman, N.A., Multhaup, G., McDonald, B.L., Beyreuther, K., 1985. Amyloid plaque core protein in Alzheimer disease and Down syndrome. Proc. Natl. Acad. Sci. U. S. A. 82, 4245–4249.

Masuda, Y., Fukuchi, M., Yatagawa, T., Tada, M., Takeda, K., Irie, K., Akagi, K., Monobe, Y., Imazawa, T., Takegoshi, K., 2011. Solid-state NMR analysis of interaction sites of curcumin and 42-residue amyloid beta-protein fibrils. Bioorg. Med. Chem. 19, 5967–5974.

Matei, N., Leahy, S., Blair, N.P., Burford, J., Rahimi, M., Shahidi, M., 2022. Retinal Vascular Physiology Biomarkers in a 5XFAD Mouse Model of Alzheimer's Disease. Cells 11.

Mathew, S., WuDunn, D., Mackay, D.D., Vosmeier, A., Tallman, E.F., Deardorff, R., Harris, A., Farlow, M.R., Brosch, J.R., Gao, S., Apostolova, L.G., Saykin, A.J., Risacher, S.L., 2023. Association of Brain Volume and Retinal Thickness in the Early Stages of Alzheimer's Disease. J. Alzheimers Dis. 91, 743–752.

Mavilio, A., Sisto, D., Prete, F., Guadalupi, V., Dammacco, R., Alessio, G., 2020. RE-PERG in early-onset Alzheimer's disease: A double-blind, electrophysiological pilot study. PLoS One 15, e0236568.

Mawuenyega, K.G., Sigurdson, W., Ovod, V., Munsell, L., Kasten, T., Morris, J.C., Yarasheski, K.E., Bateman, R.J., 2010. Decreased clearance of CNS beta-amyloid in Alzheimer's disease. Science 330, 1774.

McAlpine, F.E., Tansey, M.G., 2008. Neuroinflammation and tumor necrosis factor signaling in the pathophysiology of Alzheimer's disease. J. Inflamm. Res. 1, 29–39.

McDade, E., Cummings, J.L., Dhadda, S., Swanson, C.J., Reyderman, L., Kanekiyo, M., Koyama, A., Irizarry, M., Kramer, L.D., Bateman, R.J., 2022. Lecanemab in patients with early Alzheimer's disease: detailed results on biomarker, cognitive, and clinical effects from the randomized and open-label extension of the phase 2 proof-of-concept study. Alzheimer's Res. Ther. 14, 191.

McGeer, P.L., McGeer, E.G., 2004. Inflammation and the degenerative diseases of aging. Ann. N. Y. Acad. Sci. 1035, 104–116.

McGrory, S., Cameron, J.R., Pellegrini, E., Warren, C., Doubal, F.N., Deary, I.J., Dhillon, B., Wardlaw, J.M., Trucco, E., MacGillivray, T.J., 2017. The application of retinal fundus camera imaging in dementia: A systematic review. Alzheimers Dement. (Amst) 6, 91–107.

McKee, A.C., Au, R., Cabral, H.J., Kowall, N.W., Seshadri, S., Kubilus, C.A., Drake, J., Wolf, P.A., 2006. Visual association pathology in preclinical Alzheimer disease. J. Neuropathol. Exp. Neurol. 65, 621–630.

Mei, X., Qiu, C., Zhou, Q., Chen, Z., Chen, Y., Xu, Z., Zou, C., 2021. Changes in retinal multilayer thickness and vascular network of patients with Alzheimer's disease. Biomed. Eng. Online 20, 97.

Mei, X., Yang, M., Zhu, L., Zhou, Q., Li, X., Chen, Z., Zou, C., 2020. Retinal Levels of Amyloid Beta Correlate with Cerebral Levels of Amyloid Beta in Young APPswe/PS1dE9 Transgenic Mice before Onset of Alzheimer's Disease. Behav. Neurol., 1574816

Mejia-Vergara, A.J., Restrepo-Jimenez, P., Pelak, V.S., 2020. Optical Coherence Tomography in Mild Cognitive Impairment: A Systematic Review and Meta-Analysis. Front. Neurol. 11, 578698.

Mendez, M.F., Mendez, M.A., Martin, R., Smyth, K.A., Whitehouse, P.J., 1990. Complex visual disturbances in Alzheimer's disease. Neurology 40, 439–443.

Meyer, M.A., Hudock, S.A., 2018. Posterior cortical atrophy: A rare variant of Alzheimer's disease. Neurol. Int. 10, 7665.

Miglior, S., Rossetti, L., Lonati, C., Orzalesi, N., 1998. Scanning laser ophthalmoscopy of the optic disc at the level of the lamina cribrosa. Curr. Eye Res. 17, 453–461.

Miki, A., Medeiros, F.A., Weinreb, R.N., Jain, S., He, F., Sharpsten, L., Khachatryan, N., Hammel, N., Liebmann, J.M., Girkin, C.A., Sample, P.A., Zangwill, L.M., 2014. Rates of retinal nerve fiber layer thinning in glaucoma suspect eyes. Ophthalmology 121, 1350–1358.

Mirzaei, N., Shi, H., Oviatt, M., Doustar, J., Rentsendorj, A., Fuchs, D.T., Sheyn, J., Black, K.L., Koronyo, Y., Koronyo-Hamaoui, M., 2020. Alzheimer's Retinopathy: Seeing Disease in the Eyes. Front. Neurosci. 14, 921.

Mokwa, N.F., Ristau, T., Keane, P.A., Kirchhof, B., Sadda, S.R., Liakopoulos, S., 2013. Grading of Age-Related Macular Degeneration: Comparison between Color Fundus Photography, Fluorescein Angiography, and Spectral Domain Optical Coherence Tomography. J. Ophthalmol. 2013, 385915.

Molitor, R.J., Ko, P.C., Ally, B.A., 2015. Eye movements in Alzheimer's disease. J. Alzheimers Dis. 44, 1–12.

Montagne, A., Zhao, Z., Zlokovic, B.V., 2017. Alzheimer's disease: A matter of blood-brain barrier dysfunction? J. Exp. Med. 214, 3151–3169.

Moon, S., Jeon, S., Seo, S.K., Kim, D.E., Jung, N.Y., Kim, S.J., Lee, M.J., Lee, J., Kim, E.J., 2023. Comparison of Retinal Structural and Neurovascular Changes between Patients with and without Amyloid Pathology. J. Clin. Med. 12.

More, S.S., Beach, J.M., McClelland, C., Mokhtarzadeh, A., Vince, R., 2019. In Vivo Assessment of Retinal Biomarkers by Hyperspectral Imaging: Early Detection of Alzheimer's Disease. ACS Chem. Neurosci. 10, 4492–4501.

More, S.S., Beach, J.M., Vince, R., 2016. Early Detection of Amyloidopathy in Alzheimer's Mice by Hyperspectral Endoscopy. Invest. Ophthalmol. Vis. Sci. 57, 3231–3238.

More, S.S., Vince, R., 2015. Hyperspectral imaging signatures detect amyloidopathy in Alzheimer's mouse retina well before onset of cognitive decline. ACS Chem. Neurosci. 6, 306–315.

Moreno-Ramos, T., Benito-Leon, J., Villarejo, A., Bermejo-Pareja, F., 2013. Retinal nerve fiber layer thinning in dementia associated with Parkinson's disease, dementia with Lewy bodies, and Alzheimer's disease. J. Alzheimers Dis. 34, 659–664.

Moschos, M.M., Markopoulos, I., Chatziralli, I., Rouvas, A., Papageorgiou, S.G., Ladas, I., Vassilopoulos, D., 2012. Structural and functional impairment of the retina and optic nerve in Alzheimer's disease. Curr. Alzheimer Res. 9, 782–788.

Moussa, M., Falfoul, Y., Nasri, A., El Matri, K., Kacem, I., Mrabet, S., Chebil, A., Gharbi, A., Gouider, R., El Matri, L., 2023. Optical coherence tomography and angiography in Alzheimer's disease and other cognitive disorders. Eur. J. Ophthalmol. 33, 1706–1717.

Moya-Alvarado, G., Gershoni-Emek, N., Perlson, E., Bronfman, F.C., 2016. Neurodegeneration and Alzheimer's disease (AD). What Can Proteomics Tell Us About the Alzheimer's Brain? Mol. Cell. Proteomics 15, 409–425.

Musiek, E.S., Bhimasani, M., Zangrilli, M.A., Morris, J.C., Holtzman, D.M., Ju, Y.S., 2018. Circadian Rest-Activity Pattern Changes in Aging and Preclinical Alzheimer Disease. JAMA Neurol. 75, 582–590.

Musiek, E.S., Holtzman, D.M., 2016. Mechanisms linking circadian clocks, sleep, and neurodegeneration. Science 354, 1004–1008.

Musiek, E.S., Xiong, D.D., Holtzman, D.M., 2015. Sleep, circadian rhythms, and the pathogenesis of Alzheimer disease. Exp. Mol. Med. 47, e148.

Mutlu, U., Colijn, J.M., Ikram, M.A., Bonnemaijer, P.W.M., Licher, S., Wolters, F.J., Tiemeier, H., Koudstaal, P.J., Klaver, C.C.W., Ikram, M.K., 2018. Association of Retinal Neurodegeneration on Optical Coherence Tomography With Dementia: A Population-Based Study. JAMA Neurol. 75, 1256–1263.

Mutsuga, M., Chambers, J.K., Uchida, K., Tei, M., Makibuchi, T., Mizorogi, T., Takashima, A., Nakayama, H., 2012. Binding of curcumin to senile plaques and cerebral amyloid angiopathy in the aged brain of various animals and to neurofibrillary tangles in Alzheimer's brain. J. Vet. Med. Sci. 74, 51–57.

Namazi, K.H., Rosner, T.T., Calkins, M.P., 1989. Visual barriers to prevent ambulatory Alzheimer's patients from exiting through an emergency door. Gerontol. 29, 699–702.

Nazari, H.K., Karimaghaei, C., van der Merwe, R., Montalbano, M., Taglialatela, G., Vargas, G., Zhang, W., Motamedi, M., 2022. Age dependence of retinal vascular plexus attenuation in the triple transgenic mouse model of Alzheimer's disease. Exp. Eye Res. 214, 108879.

Nedergaard, M., 2013. Neuroscience. Garbage truck of the brain. Science 340, 1529–1530.

Ngolab, J., Donohue, M., Belsha, A., Salazar, J., Cohen, P., Jaiswal, S., Tan, V., Gessert, D., Korouri, S., Aggarwal, N.T., Alber, J., Johnson, K., Jicha, G., van Dyck, C., Lah, J., Salloway, S., Sperling, R.A., Aisen, P.S., Rafii, M.S., Rissman, R.A., 2021. Feasibility study for detection of retinal amyloid in clinical trials: The Anti-Amyloid Treatment in Asymptomatic Alzheimer's Disease (A4) trial. Alzheimers Dement. (Amst) 13, e12199.

Ngoo, Q.Z., Wan Hitam, W.H., Ab Razak, A., 2019. Evaluation of Retinal Nerve Fiber Layer Thickness, Electroretinogram and Visual Evoked Potential in Patients with Alzheimer's Disease. J. Ophthalmol. 2019, 6248185.

Ni Chasaide, C., Lynch, M.A., 2020. The role of the immune system in driving neuroinflammation. Brain Neurosci Adv 4, 2398212819901082.

Nilson, A.N., English, K.C., Gerson, J.E., Barton Whittle, T., Nicolas Crain, C., Xue, J., Sengupta, U., Castillo-Carranza, D.L., Zhang, W., Gupta, P., Kayed, R., 2017. Tau Oligomers Associate with Inflammation in the Brain and Retina of Tauopathy Mice and in Neurodegenerative Diseases. J. Alzheimers Dis. 55, 1083–1099.

Ning, A., Cui, J., To, E., Ashe, K.H., Matsubara, J., 2008. Amyloid-beta deposits lead to retinal degeneration in a mouse model of Alzheimer disease. Invest. Ophthalmol. Vis. Sci. 49, 5136–5143.

Nissen, M.J., Corkin, S., Buonanno, F.S., Growdon, J.H., Wray, S.H., Bauer, J., 1985. Spatial vision in Alzheimer's disease. General findings and a case report. Arch. Neurol. 42, 667–671.

Niu, L., Zhang, F., Xu, X., Yang, Y., Li, S., Liu, H., Le, W., 2022. Chronic sleep deprivation altered the expression of circadian clock genes and aggravated Alzheimer's disease neuropathology. Brain Pathol. 32, e13028.

Noah, A.M., Almghairbi, D., Moppett, I.K., 2020. Optical coherence tomography in mild cognitive impairment - Systematic review and meta-analysis. Clin. Neurol. Neurosurg. 196, 106036.

Normando, E.M., Dehabadi, M.H., Guo, L., Turner, L.A., Pollorsi, G., Cordeiro, M.F., 2015. Real-time imaging of retinal cell apoptosis by confocal scanning laser ophthalmoscopy. Methods Mol. Biol. 1254, 227–237.

Normando, E.M., Yap, T.E., Maddison, J., Miodragovic, S., Bonetti, P., Almonte, M., Mohammad, N.G., Ameen, S., Crawley, L., Ahmed, F., Bloom, P.A., Cordeiro, M.F., 2020. A CNN-aided method to predict glaucoma progression using DARC (Detection of Apoptosing Retinal Cells). Expert Rev. Mol. Diagn 20, 737–748.

Nunez-Diaz, C., Andersson, E., Schultz, N., Poceviciute, D., Hansson, O., Netherlands Brain, B., Nilsson, K.P.R., Wennstrom, M., 2024. The fluorescent ligand bTVBT2 reveals increased p-tau uptake by retinal microglia in Alzheimer's disease patients and App(NL-F/NL-F) mice. Alzheimer's Res. Ther. 16, 4.

O'Bryhim, B.E., Apte, R.S., Kung, N., Coble, D., Van Stavern, G.P., 2018. Association of Preclinical Alzheimer Disease With Optical Coherence Tomographic Angiography Findings. JAMA Ophthalmol 136, 1242–1248.
O'Bryhim, B.E., Lin, J.B., Van Stavern, G.P., Apte, R.S., 2021. Angiography Findings in Preclinical Alzheimer's Disease: 3-Year Follow-Up. Ophthalmology 128, 1489–1491.
O'Leary, T.P., Brown, R.E., 2009. Visuo-spatial learning and memory deficits on the Barnes maze in the 16-month-old APPswe/PS1dE9 mouse model of Alzheimer's disease. Behav. Brain Res. 201, 120–127.
O'Leary, T.P., Brown, R.E., 2022. Visuo-spatial learning and memory impairments in the 5xFAD mouse model of Alzheimer's disease: Effects of age, sex, albinism, and motor impairments. Gene Brain Behav. 21, e12794.
Oh, A.J., Amore, G., Sultan, W., Asanad, S., Park, J.C., Romagnoli, M., La Morgia, C., Karanjia, R., Harrington, M.G., Sadun, A.A., 2019. Pupillometry evaluation of melanopsin retinal ganglion cell function and sleep-wake activity in pre-symptomatic Alzheimer's disease. PLoS One 14, e0226197.
Oktem, E.O., Derle, E., Kibaroglu, S., Oktem, C., Akkoyun, I., Can, U., 2015. The relationship between the degree of cognitive impairment and retinal nerve fiber layer thickness. Neurol. Sci. 36, 1141–1146.
Olabarria, M., Noristani, H.N., Verkhratsky, A., Rodriguez, J.J., 2010. Concomitant astroglial atrophy and astrogliosis in a triple transgenic animal model of Alzheimer's disease. Glia 58, 831–838.
Olafsdottir, O.B., Saevarsdottir, H.S., Hardarson, S.H., Hannesdottir, K.H., Traustadottir, V.D., Karlsson, R.A., Einarsdottir, A.B., Jonsdottir, K.D., Stefansson, E., Snaedal, J., 2018. Retinal oxygen metabolism in patients with mild cognitive impairment. Alzheimers Dement. (Amst) 10, 340–345.
Oliveira-Souza, F.G., DeRamus, M.L., van Groen, T., Lambert, A.E., Bolding, M.S., Strang, C.E., 2017. Retinal changes in the Tg-SwDI mouse model of Alzheimer's disease. Neuroscience 354, 43–53.
Ong, Y.T., Hilal, S., Cheung, C.Y., Xu, X., Chen, C., Venketasubramanian, N., Wong, T.Y., Ikram, M.K., 2014. Retinal vascular fractals and cognitive impairment. Dement. Geriatr. Cogn. Dis. Extra 4, 305–313.
Osborne, O.M., Naranjo, O., Heckmann, B.L., Dykxhoorn, D., Toborek, M., 2023. Anti-amyloid: An antibody to cure Alzheimer's or an attitude. iScience 26, 107461.
Pang, M., Gabelle, A., Saha-Chaudhuri, P., Huijbers, W., Gafson, A., Matthews, P.M., Tian, L., Rubino, I., Hughes, R., de Moor, C., Belachew, S., Shen, C., 2024. Precision medicine analysis of heterogeneity in individual-level treatment response to amyloid beta removal in early Alzheimer's disease. Alzheimers Dement 20, 1102–1111.
Paquet, C., Boissonnot, M., Roger, F., Dighiero, P., Gil, R., Hugon, J., 2007. Abnormal retinal thickness in patients with mild cognitive impairment and Alzheimer's disease. Neurosci. Lett. 420, 97–99.
Paresce, D.M., Ghosh, R.N., Maxfield, F.R., 1996. Microglial cells internalize aggregates of the Alzheimer's disease amyloid beta-protein via a scavenger receptor. Neuron 17, 553–565.
Parisi, V., 2003. Correlation between morphological and functional retinal impairment in patients affected by ocular hypertension, glaucoma, demyelinating optic neuritis and Alzheimer's disease. Semin. Ophthalmol. 18, 50–57.
Parisi, V., Restuccia, R., Fattapposta, F., Mina, C., Bucci, M.G., Pierelli, F., 2001. Morphological and functional retinal impairment in Alzheimer's disease patients. Clin. Neurophysiol. 112, 1860–1867.
Park, S.W., Kim, J.H., Mook-Jung, I., Kim, K.W., Park, W.J., Park, K.H., Kim, J.H., 2014. Intracellular amyloid beta alters the tight junction of retinal pigment epithelium in 5XFAD mice. Neurobiol. Aging 35, 2013–2020.
Parnell, M., Guo, L., Abdi, M., Cordeiro, M.F., 2012. Ocular manifestations of Alzheimer's disease in animal models. Int. J. Alzheimer's Dis. 2012, 786494.
Parthasarathy, R., Chow, K.M., Derafshi, Z., Fautsch, M.P., Hetling, J.R., Rodgers, D.W., Hersh, L.B., Pepperberg, D.R., 2015. Reduction of amyloid-beta levels in mouse eye tissues by intra-vitreally delivered neprilysin. Exp. Eye Res. 138, 134–144.
Pascoal, T.A., Benedet, A.L., Ashton, N.J., Kang, M.S., Therriault, J., Chamoun, M., Savard, M., Lussier, F.Z., Tissot, C., Karikari, T.K., Ottoy, J., Mathotaarachchi, S., Stevenson, J., Massarweh, G., Scholl, M., de Leon, M.J., Soucy, J.P., Edison, P., Blennow, K., Zetterberg, H., Gauthier, S., Rosa-Neto, P., 2021. Microglial activation and tau propagate jointly across Braak stages. Nat. Med. 27, 1592–1599.
Passafiume, D., Di Giacomo, D., Giubilei, F., 2000. Reading latency of words and nonwords in Alzheimer's patients. Cortex 36, 293–298.
Patel, N.N., Shulman, J.P., Chin, K.J., Finger, P.T., 2010. Optical coherence tomography/scanning laser ophthalmoscopy imaging of optic nerve head drusen. Ophthalmic Surg. Laser. Imag. 41, 614–621.
Pauwels, K., Williams, T.L., Morris, K.L., Jonckheere, W., Vandersteen, A., Kelly, G., Schymkowitz, J., Rousseau, F., Pastore, A., Serpell, L.C., Broersen, K., 2012. Structural basis for increased toxicity of pathological abeta42:abeta40 ratios in Alzheimer disease. J. Biol. Chem. 287, 5650–5660.
Pead, E., Thompson, A.C., Grewal, D.S., McGrory, S., Robbins, C.B., Ma, J.P., Johnson, K. G., Liu, A.J., Hamid, C., Trucco, E., Ritchie, C.W., Muniz, G., Lengyel, I., Dhillon, B., Fekrat, S., MacGillivray, T., 2023. Retinal Vascular Changes in Alzheimer's Dementia and Mild Cognitive Impairment: A Pilot Study Using Ultra-Widefield Imaging. Transl Vis Sci Technol 12, 13.
Pelkmans, W., Shekari, M., Brugulat-Serrat, A., Sanchez-Benavides, G., Minguillon, C., Fauria, K., Molinuevo, J.L., Grau-Rivera, O., Gonzalez Escalante, A., Kollmorgen, G., Carboni, M., Ashton, N.J., Zetterberg, H., Blennow, K., Suarez-Calvet, M., Gispert, J. D., study, A., 2024. Astrocyte biomarkers GFAP and YKL-40 mediate early Alzheimer's disease progression. Alzheimers Dement 20, 483–493.
Peng, F., Zhao, Y., Huang, X., Chen, C., Sun, L., Zhuang, L., Xue, L., 2015. Loss of Polo ameliorates APP-induced Alzheimer's disease-like symptoms in Drosophila. Sci. Rep. 5, 16816.
Perez, S.E., Lumayag, S., Kovacs, B., Mufson, E.J., Xu, S., 2009. Beta-amyloid deposition and functional impairment in the retina of the APPswe/PS1DeltaE9 transgenic mouse model of Alzheimer's disease. Invest. Ophthalmol. Vis. Sci. 50, 793–800.
Perrin, R.J., Fagan, A.M., Holtzman, D.M., 2009. Multimodal techniques for diagnosis and prognosis of Alzheimer's disease. Nature 461, 916–922.
Petersen, R.C., Smith, G.E., Waring, S.C., Ivnik, R.J., Tangalos, E.G., Kokmen, E., 1999. Mild cognitive impairment: clinical characterization and outcome. Arch. Neurol. 56, 303–308.
Petzold, A., 2016. Retinal glymphatic system: an explanation for transient retinal layer volume changes? Brain 139, 2816–2819.
Pircher, M., Hitzenberger, C.K., Schmidt-Erfurth, U., 2011. Polarization sensitive optical coherence tomography in the human eye. Prog. Retin. Eye Res. 30, 431–451.
Pogue, A.I., Dua, P., Hill, J.M., Lukiw, W.J., 2015. Progressive inflammatory pathology in the retina of aluminum-fed 5xFAD transgenic mice. J. Inorg. Biochem. 152, 206–209.
Polans, J., Keller, B., Carrasco-Zevallos, O.M., LaRocca, F., Cole, E., Whitson, H.E., Lad, E.M., Farsiu, S., Izatt, J.A., 2017. Wide-field retinal optical coherence tomography with wavefront sensorless adaptive optics for enhanced imaging of targeted regions. Biomed. Opt Express 8, 16–37.
Polo, V., Rodrigo, M.J., Garcia-Martin, E., Otin, S., Larrosa, J.M., Fuertes, M.I., Bambo, M.P., Pablo, L.E., Satue, M., 2017. Visual dysfunction and its correlation with retinal changes in patients with Alzheimer's disease. Eye (Lond) 31, 1034–1041.
Porsteinsson, A.P., Isaacson, R.S., Knox, S., Sabbagh, M.N., Rubino, I., 2021. Diagnosis of Early Alzheimer's Disease: Clinical Practice in 2021. J. Prev. Alzheimers Dis. 8, 371–386.
Purves, D., Fitzpatrick, D., 2001. The Retina, second ed. Sinauer Associates Sunderland, MA.
Qiu, Y., Jin, T., Mason, E., Campbell, M.C.W., 2020. Predicting Thioflavin Fluorescence of Retinal Amyloid Deposits Associated With Alzheimer's Disease from Their Polarimetric Properties. Transl Vis Sci Technol 9, 47.
Querques, G., Borrelli, E., Sacconi, R., De Vitis, L., Leocani, L., Santangelo, R., Magnani, G., Comi, G., Bandello, F., 2019. Functional and morphological changes of the retinal vessels in Alzheimer's disease and mild cognitive impairment. Sci. Rep. 9, 63.
Rafii, M.S., Wishnek, H., Brewer, J.B., Donohue, M.C., Ness, S., Mobley, W.C., Aisen, P.S., Rissman, R.A., 2015. The down syndrome biomarker initiative (DSBI) pilot: proof of concept for deep phenotyping of Alzheimer's disease biomarkers in down syndrome. Front. Behav. Neurosci. 9, 239.
Rajendran, L., Paolicelli, R.C., 2018. Microglia-Mediated Synapse Loss in Alzheimer's Disease. J. Neurosci. 38, 2911–2919.
Raudino, F., 2018. Ocular and Visual Manifestation of the Alzheimer's Disease: A Literature Review, Part I: Animal Models and Human Pathology. Arch Neurosci 5, e74225.
Reardon, S., 2023. Alzheimer's drug donanemab helps most when taken at earliest disease stage, study finds. Nature 619, 682–683.
Reitz, C., Tang, M.X., Manly, J., Mayeux, R., Luchsinger, J.A., 2007. Hypertension and the risk of mild cognitive impairment. Arch. Neurol. 64, 1734–1740.
Rifai, O.M., McGrory, S., Robbins, C.B., Grewal, D.S., Liu, A., Fekrat, S., MacGillivray, T. J., 2021. The application of optical coherence tomography angiography in Alzheimer's disease: A systematic review. Alzheimers Dement. (Amst) 13, e12149.
Rigat, L., Ouk, K., Kramer, A., Priller, J., 2023. Dysfunction of circadian and sleep rhythms in the early stages of Alzheimer's disease. Acta Physiol. 238, e13970.
Risacher, S.L., Wudunn, D., Pepin, S.M., MaGee, T.R., McDonald, B.C., Flashman, L.A., Wishart, H.A., Pixley, H.S., Rabin, L.A., Pare, N., Englert, J.J., Schwartz, E., Curtain, J.R., West, J.D., O'Neill, D.P., Santulli, R.B., Newman, R.W., Saykin, A.J., 2013. Visual contrast sensitivity in Alzheimer's disease, mild cognitive impairment, and older adults with cognitive complaints. Neurobiol. Aging 34, 1133–1144.
Risacher, S.L., WuDunn, D., Tallman, E.F., West, J.D., Gao, S., Farlow, M.R., Brosch, J.R., Apostolova, L.G., Saykin, A.J., 2020. Visual contrast sensitivity is associated with the presence of cerebral amyloid and tau deposition. Brain Commun 2, fcaa019.
Robbins, C.B., Grewal, D.S., Stinnett, S.S., Soundararajan, S., Yoon, S.P., Polascik, B.W., Liu, A.J., Burke, J.R., Fekrat, S., 2021. Assessing the Retinal Microvasculature in Individuals With Early and Late-Onset Alzheimer's Disease. Ophthalmic Surg Lasers Imaging Retina 52, 336–344.
Roberts, B.R., Lind, M., Wagen, A.Z., Rembach, A., Frugier, T., Li, Q.X., Ryan, T.M., McLean, C.A., Doecke, J.D., Rowe, C.C., Villemagne, V.L., Masters, C.L., 2017. Biochemically-defined pools of amyloid-beta in sporadic Alzheimer's disease: correlation with amyloid PET. Brain 140, 1486–1498.
Rotenstreich, Y., Sharvit-Ginon, I., Sher, I., Zloto, O., Fabian, I.D., Abd-Elkader, A., Weller, A., Heymann, A., Beeri, M.S., Ravona-Springer, R., 2022. Thicker macula in asymptomatic APOE E4 middle-aged adults at high AD risk. Alzheimers Dement. (Amst) 14, e12275.
Ryu, E.K., Choe, Y.S., Lee, K.H., Choi, Y., Kim, B.T., 2006. Curcumin and dehydrozingerone derivatives: synthesis, radiolabeling, and evaluation for beta-amyloid plaque imaging. J. Med. Chem. 49, 6111–6119.
Ryu, J.K., McLarnon, J.G., 2009. A leaky blood-brain barrier, fibrinogen infiltration and microglial reactivity in inflamed Alzheimer's disease brain. J. Cell Mol. Med. 13, 2911–2925.
Sadda, S.R., Borrelli, E., Fan, W., Ebraheem, A., Marion, K.M., Harrington, M., Kwon, S., 2019. A pilot study of fluorescence lifetime imaging ophthalmoscopy in preclinical Alzheimer's disease. Eye (Lond) 33, 1271–1279.
Sadda, S.V.A.S., Wilkinson, C., Hinton, D., Wiedemann, P., Freund, K.B., Saraf, D., 2022. Ryan's Retina, seventh ed. Elsevier (eBook ISBN: 9780323722148; Hardcover ISBN: 9780323722131.

Sadun, A.A., 1988. Assessing vision in patients with Alzheimer's disease. West. J. Med. 148, 693.
Sadun, A.A., Bassi, C.J., 1990. Optic nerve damage in Alzheimer's disease. Ophthalmology 97, 9–17.
Sadun, A.A., Borchert, M., DeVita, E., Hinton, D.R., Bassi, C.J., 1987. Assessment of visual impairment in patients with Alzheimer's disease. Am. J. Ophthalmol. 104, 113–120.
Sagare, A.P., Bell, R.D., Zhao, Z., Ma, Q., Winkler, E.A., Ramanathan, A., Zlokovic, B.V., 2023. Author Correction: Pericyte loss influences Alzheimer-like neurodegeneration in mice. Nat. Commun. 14, 6151.
Salobrar-Garcia, E., de Hoz, R., Ramirez, A.I., Lopez-Cuenca, I., Rojas, P., Vazirani, R., Amarante, C., Yubero, R., Gil, P., Pinazo-Duran, M.D., Salazar, J.J., Ramirez, J.M., 2019. Changes in visual function and retinal structure in the progression of Alzheimer's disease. PLoS One 14, e0220535.
Salobrar-Garcia, E., Hoyas, I., Leal, M., de Hoz, R., Rojas, B., Ramirez, A.I., Salazar, J.J., Yubero, R., Gil, P., Trivino, A., Ramirez, J.M., 2015. Analysis of Retinal Peripapillary Segmentation in Early Alzheimer's Disease Patients. BioMed Res. Int. 2015, 636548.
Salobrar-Garcia, E., Lopez-Cuenca, I., Sanchez-Puebla, L., de Hoz, R., Fernandez-Albarral, J.A., Ramirez, A.I., Bravo-Ferrer, I., Medina, V., Moro, M.A., Saido, T.C., Saito, T., Salazar, J.J., Ramirez, J.M., 2020a. Retinal Thickness Changes Over Time in a Murine AD Model APP (NL-F/NL-F). Front. Aging Neurosci. 12, 625642.
Salobrar-Garcia, E., Rodrigues-Neves, A.C., Ramirez, A.I., de Hoz, R., Fernandez-Albarral, J.A., Lopez-Cuenca, I., Ramirez, J.M., Ambrosio, A.F., Salazar, J.J., 2020b. Microglial Activation in the Retina of a Triple-Transgenic Alzheimer's Disease Mouse Model (3xTg-AD). Int. J. Mol. Sci. 21.
Salter, M.W., Stevens, B., 2017. Microglia emerge as central players in brain disease. Nat. Med. 23, 1018–1027.
Sanchez, D., Castilla-Marti, M., Marquie, M., Valero, S., Moreno-Grau, S., Rodriguez-Gomez, O., Piferrer, A., Martinez, G., Martinez, J., Rojas, I., Hernandez, I., Abdelnour, C., Rosende-Roca, M., Vargas, L., Mauleon, A., Gil, S., Alegret, M., Ortega, G., Espinosa, A., Perez-Cordon, A., Sanabria, A., Roberto, N., Ciudin, A., Simo, R., Hernandez, C., Tarraga, L., Boada, M., Ruiz, A., 2020. Evaluation of macular thickness and volume tested by optical coherence tomography as biomarkers for Alzheimer's disease in a memory clinic. Sci. Rep. 10, 1580.
Sanchez, D., Castilla-Marti, M., Rodriguez-Gomez, O., Valero, S., Piferrer, A., Martinez, G., Martinez, J., Serra, J., Moreno-Grau, S., Hernandez-Olasagarre, B., De Rojas, I., Hernandez, I., Abdelnour, C., Rosende-Roca, M., Vargas, L., Mauleon, A., Santos-Santos, M.A., Alegret, M., Ortega, G., Espinosa, A., Perez-Cordon, A., Sanabria, A., Ciudin, A., Simo, R., Hernandez, C., Villoslada, P., Ruiz, A., Tarraga, L., Boada, M., 2018. Usefulness of peripapillary nerve fiber layer thickness assessed by optical coherence tomography as a biomarker for Alzheimer's disease. Sci. Rep. 8, 16345.
Sanchez-Puebla, L., Lopez-Cuenca, I., Salobrar-Garcia, E., Ramirez, A.I., Fernandez-Albarral, J.A., Matamoros, J.A., Elvira-Hurtado, L., Salazar, J.J., Ramirez, J.M., de Hoz, R., 2024. Imaging in Murine Models of Alzheimer's Disease in a Systematic Review: Findings, Methodology and Future Perspectives. Biomedicines 12.
Santangelo, R., Huang, S.C., Bernasconi, M.P., Falautano, M., Comi, G., Magnani, G., Leocani, L., 2020. Neuro-Retina Might Reflect Alzheimer's Disease Stage. J. Alzheimers Dis. 77, 1455–1468.
Santos, C.Y., Johnson, L.N., Sinoff, S.E., Festa, E.K., Heindel, W.C., Snyder, P.J., 2018. Change in retinal structural anatomy during the preclinical stage of Alzheimer's disease. Alzheimers Dement. (Amst) 10, 196–209.
Sarkar, A., Gogia, N., Glenn, N., Singh, A., Jones, G., Powers, N., Srivastava, A., Kango-Singh, M., Singh, A., 2018. A soy protein Lunasin can ameliorate amyloid-beta 42 mediated neurodegeneration in Drosophila eye. Sci. Rep. 8, 13545.
Sartucci, F., Borghetti, D., Bocci, T., Murri, L., Orsini, P., Porciatti, V., Origlia, N., Domenici, L., 2010. Dysfunction of the magnocellular stream in Alzheimer's disease evaluated by pattern electroretinograms and visual evoked potentials. Brain Res. Bull. 82, 169–176.
Satlin, A., Volicer, L., Ross, V., Herz, L., Campbell, S., 1992. Bright light treatment of behavioral and sleep disturbances in patients with Alzheimer's disease. Am. J. Psychiatr. 149, 1028–1032.
Schallek, J., Geng, Y., Nguyen, H., Williams, D.R., 2013. Morphology and topography of retinal pericytes in the living mouse retina using in vivo adaptive optics imaging and ex vivo characterization. Invest. Ophthalmol. Vis. Sci. 54, 8237–8250.
Scheltens, P., Blennow, K., Breteler, M.M., de Strooper, B., Frisoni, G.B., Salloway, S., Van der Flier, W.M., 2016. Alzheimer's disease. Lancet 388, 505–517.
Schlotterer, G., Moscovitch, M., Crapper-McLachlan, D., 1984. Visual processing deficits as assessed by spatial frequency contrast sensitivity and backward masking in normal ageing and Alzheimer's disease. Brain 107 (Pt 1), 309–325.
Schmitz-Valckenberg, S., Guo, L., Maass, A., Cheung, W., Vugler, A., Moss, S.E., Munro, P.M., Fitzke, F.W., Cordeiro, M.F., 2008. Real-time in vivo imaging of retinal cell apoptosis after laser exposure. Invest. Ophthalmol. Vis. Sci. 49, 2773–2780.
Schon, C., Hoffmann, N.A., Ochs, S.M., Burgold, S., Filser, S., Steinbach, S., Seeliger, M. W., Arzberger, T., Goedert, M., Kretzschmar, H.A., Schmidt, B., Herms, J., 2012. Long-term in vivo imaging of fibrillar tau in the retina of P301S transgenic mice. PLoS One 7, e53547.
Schultz, N., Byman, E., Netherlands Brain, B., Wennstrom, M., 2020. Levels of Retinal Amyloid-beta Correlate with Levels of Retinal IAPP and Hippocampal Amyloid-beta in Neuropathologically Evaluated Individuals. J. Alzheimers Dis. 73, 1201–1209.
Sekiguchi, H., Iritani, S., Fujita, K., 2017. Bright light therapy for sleep disturbance in dementia is most effective for mild to moderate Alzheimer's type dementia: a case series. Psychogeriatrics 17, 275–281.
Selkoe, D.J., 2008. Soluble oligomers of the amyloid beta-protein impair synaptic plasticity and behavior. Behav. Brain Res. 192, 106–113.
Sen, S., Saxena, R., Vibha, D., Tripathi, M., Sharma, P., Phuljhele, S., Tandon, R., Kumar, P., 2020. Detection of structural and electrical disturbances in macula and optic nerve in Alzheimer's patients and their correlation with disease severity. Semin. Ophthalmol. 35, 116–125.
Sengillo, J.D., Winkler, E.A., Walker, C.T., Sullivan, J.S., Johnson, M., Zlokovic, B.V., 2013. Deficiency in mural vascular cells coincides with blood-brain barrier disruption in Alzheimer's disease. Brain Pathol. 23, 303–310.
Shajahan, S.R., Kumar, S., Ramli, M.D.C., 2023. Unravelling the connection between COVID-19 and Alzheimer's disease: a comprehensive review. Front. Aging Neurosci. 15, 1274452.
Shankar, G.M., Li, S., Mehta, T.H., Garcia-Munoz, A., Shepardson, N.E., Smith, I., Brett, F. M., Farrell, M.A., Rowan, M.J., Lemere, C.A., Regan, C.M., Walsh, D.M., Sabatini, B. L., Selkoe, D.J., 2008. Amyloid-beta protein dimers isolated directly from Alzheimer's brains impair synaptic plasticity and memory. Nat. Med. 14, 837–842.
Shao, Y., Jiang, H., Wei, Y., Shi, Y., Shi, C., Wright, C.B., Sun, X., Vanner, E.A., Rodriguez, A.D., Lam, B.L., Rundek, T., Baumel, B.S., Gameiro, G.R., Dong, C., Wang, J., 2018. Visualization of Focal Thinning of the Ganglion Cell-Inner Plexiform Layer in Patients with Mild Cognitive Impairment and Alzheimer's Disease. J. Alzheimers Dis. 64, 1261–1273.
Sharafi, S.M., Sylvestre, J.P., Chevrefils, C., Soucy, J.P., Beaulieu, S., Pascoal, T.A., Arbour, J.D., Rheaume, M.A., Robillard, A., Chayer, C., Rosa-Neto, P., Mathotaarachchi, S.S., Nasreddine, Z.S., Gauthier, S., Lesage, F., 2019. Vascular retinal biomarkers improves the detection of the likely cerebral amyloid status from hyperspectral retinal images. Alzheimers Dement (N Y) 5, 610–617.
Shi, H., Koronyo, Y., Fuchs, D.T., Sheyn, J., Jallow, O., Mandalia, K., Graham, S.L., Gupta, V.K., Mirzaei, M., Kramerov, A.A., Ljubimov, A.V., Hawes, D., Miller, C.A., Black, K.L., Carare, R.O., Koronyo-Hamaoui, M., 2023. Retinal arterial Abeta(40) deposition is linked with tight junction loss and cerebral amyloid angiopathy in MCI and AD patients. Alzheimers Dement.
Shi, H., Koronyo, Y., Fuchs, D.T., Sheyn, J., Wawrowsky, K., Lahiri, S., Black, K.L., Koronyo-Hamaoui, M., 2020a. Retinal capillary degeneration and blood-retinal barrier disruption in murine models of Alzheimer's disease. Acta Neuropathol. Commun. 8, 202.
Shi, H., Koronyo, Y., Rentsendorj, A., Fuchs, D.T., Sheyn, J., Black, K.L., Mirzaei, N., Koronyo-Hamaoui, M., 2021. Retinal Vasculopathy in Alzheimer's Disease. Front. Neurosci. 15, 731614.
Shi, H., Koronyo, Y., Rentsendorj, A., Regis, G.C., Sheyn, J., Fuchs, D.T., Kramerov, A.A., Ljubimov, A.V., Dumitrascu, O.M., Rodriguez, A.R., Barron, E., Hinton, D.R., Black, K.L., Miller, C.A., Mirzaei, N., Koronyo-Hamaoui, M., 2020b. Identification of early pericyte loss and vascular amyloidosis in Alzheimer's disease retina. Acta Neuropathol. 139, 813–836.
Shi, H., Mirzaei, N., Koronyo, Y., Davis, M.R., Robinson, E., Braun, G.M., Jallow, O., Rentsendorj, A., Ramanujan, V.K., Fert-Bober, J., Kramerov, A.A., Ljubimov, A.V., Schneider, L.S., Tourtellotte, W.G., Hawes, D., Schneider, J.A., Black, K.L., Kayed, R., Selenica, M.B., Lee, D.C., Fuchs, D.T., Koronyo-Hamaoui, M., 2024. Identification of retinal tau oligomers, citrullinated tau, and other tau isoforms in early and advanced AD and relations to disease status. bioRxiv. https://doi.org/10.1101/2024.02.13.579999 [Preprint].
Shi, H., Yin, Z., Koronyo, Y., Fuchs, D.T., Sheyn, J., Davis, M.R., Wilson, J.W., Margeta, M.A., Pitts, K.M., Herron, S., Ikezu, S., Ikezu, T., Graham, S.L., Gupta, V.K., Black, K.L., Mirzaei, M., Butovsky, O., Koronyo-Hamaoui, M., 2022. Regulating microglial miR-155 transcriptional phenotype alleviates Alzheimer's-induced retinal vasculopathy by limiting Clec7a/Galectin-3(+) neurodegenerative microglia. Acta Neuropathol. Commun. 10, 136.
Shi, Z., Wu, Y., Wang, M., Cao, J., Feng, W., Cheng, Y., Li, C., Shen, Y., 2014. Greater attenuation of retinal nerve fiber layer thickness in Alzheimer's disease patients. J. Alzheimers Dis. 40, 277–283.
Shi, Z., Zheng, H., Hu, J., Jiang, L., Cao, X., Chen, Y., Mei, X., Li, C., Shen, Y., 2019. Retinal Nerve Fiber Layer Thinning Is Associated With Brain Atrophy: A Longitudinal Study in Nondemented Older Adults. Front. Aging Neurosci. 11, 69.
Shin, J.Y., Choi, E.Y., Kim, M., Lee, H.K., Byeon, S.H., 2021. Changes in retinal microvasculature and retinal layer thickness in association with apolipoprotein E genotype in Alzheimer's disease. Sci. Rep. 11, 1847.
Shoughy, S.S., Kozak, I., 2016. Selective and complementary use of Optical Coherence Tomography and Fluorescein Angiography in retinal practice. Eye Vis (Lond) 3, 26.
Sidiqi, A., Wahl, D., Lee, S., Ma, D., To, E., Cui, J., To, E., Beg, M.F., Sarunic, M., Matsubara, J.A., 2020. In vivo Retinal Fluorescence Imaging With Curcumin in an Alzheimer Mouse Model. Front. Neurosci. 14, 713.
Silva, I., Silva, J., Ferreira, R., Trigo, D., 2021. Glymphatic system, AQP4, and their implications in Alzheimer's disease. Neurol Res Pract 3, 5.
Sims, J.R., Zimmer, J.A., Evans, C.D., Lu, M., Ardayfio, P., Sparks, J., Wessels, A.M., Shcherbinin, S., Wang, H., Monkul Nery, E.S., Collins, E.C., Solomon, P., Salloway, S., Apostolova, L.G., Hansson, O., Ritchie, C., Brooks, D.A., Mintun, M., Skovronsky, D.M., Investigators, T.-A., 2023. Donanemab in Early Symptomatic Alzheimer Disease: The TRAILBLAZER-ALZ 2 Randomized Clinical Trial. JAMA 330, 512–527.
Sloane, P.D., Zimmerman, S., Suchindran, C., Reed, P., Wang, L., Boustani, M., Sudha, S., 2002. The public health impact of Alzheimer's disease, 2000-2050: potential implication of treatment advances. Annu. Rev. Publ. Health 23, 213–231.
Smith, A.J., Duan, T., Verkman, A.S., 2019. Aquaporin-4 reduces neuropathology in a mouse model of Alzheimer's disease by remodeling peri-plaque astrocyte structure. Acta Neuropathol. Commun. 7, 74.
Snyder, P.J., Alber, J., Alt, C., Bain, L.J., Bouma, B.E., Bouwman, F.H., DeBuc, D.C., Campbell, M.C.W., Carrillo, M.C., Chew, E.Y., Cordeiro, M.F., Duenas, M.R., Fernandez, B.M., Koronyo-Hamaoui, M., La Morgia, C., Carare, R.O., Sadda, S.R.,

van Wijngaarden, P., Snyder, H.M., 2021. Retinal imaging in Alzheimer's and neurodegenerative diseases. Alzheimers Dement 17, 103–111.
Snyder, P.J., Johnson, L.N., Lim, Y.Y., Santos, C.Y., Alber, J., Maruff, P., Fernandez, B., 2016. Nonvascular retinal imaging markers of preclinical Alzheimer's disease. Alzheimers Dement. (Amst) 4, 169–178.
Song, G., Steelman, Z.A., Finkelstein, S., Yang, Z., Martin, L., Chu, K.K., Farsiu, S., Arshavsky, V.Y., Wax, A., 2020. Multimodal Coherent Imaging of Retinal Biomarkers of Alzheimer's Disease in a Mouse Model. Sci. Rep. 10, 7912.
Sperduto, R.D., Hiller, R., Chew, E., Seigel, D., Blair, N., Burton, T.C., Farber, M.D., Gragoudas, E.S., Haller, J., Seddon, J.M., Yannuzzi, L.A., 1998. Risk factors for hemiretinal vein occlusion: comparison with risk factors for central and branch retinal vein occlusion: the eye disease case-control study. Ophthalmology 105, 765–771.
Sperling, R.A., Aisen, P.S., Beckett, L.A., Bennett, D.A., Craft, S., Fagan, A.M., Iwatsubo, T., Jack Jr., C.R., Kaye, J., Montine, T.J., Park, D.C., Reiman, E.M., Rowe, C.C., Siemers, E., Stern, Y., Yaffe, K., Carrillo, M.C., Thies, B., Morrison-Bogorad, M., Wagster, M.V., Phelps, C.H., 2011. Toward defining the preclinical stages of Alzheimer's disease: recommendations from the National Institute on Aging-Alzheimer's Association workgroups on diagnostic guidelines for Alzheimer's disease. Alzheimers Dement 7, 280–292.
Sperling, R.A., Donohue, M.C., Raman, R., Rafii, M.S., Johnson, K., Masters, C.L., van Dyck, C.H., Iwatsubo, T., Marshall, G.A., Yaari, R., Mancini, M., Holdridge, K.C., Case, M., Sims, J.R., Aisen, P.S., Team, A.S., 2023. Trial of Solanezumab in Preclinical Alzheimer's Disease. N. Engl. J. Med. 389, 1096–1107.
Sperling, R.A., Karlawish, J., Johnson, K.A., 2013. Preclinical Alzheimer disease-the challenges ahead. Nat. Rev. Neurol. 9, 54–58.
Stothart, G., Kazanina, N., Naatanen, R., Haworth, J., Tales, A., 2015. Early visual evoked potentials and mismatch negativity in Alzheimer's disease and mild cognitive impairment. J. Alzheimers Dis. 44, 397–408.
Strenn, K., Dal-Bianco, P., Weghaupt, H., Koch, G., Vass, C., Gottlob, I., 1991. Pattern electroretinogram and luminance electroretinogram in Alzheimer's disease. J. Neural. Transm. Suppl. 33, 73–80.
Sun, Y., Zhang, L., Ye, H., Leng, L., Chen, Y., Su, Y., Ren, P., Lu, H., Peng, G., 2024. Potential ocular indicators to distinguish posterior cortical atrophy and typical Alzheimer's disease: a cross-section study using optical coherence tomography angiography. Alzheimer's Res. Ther. 16, 64.
Sweeney, M.D., Sagare, A.P., Zlokovic, B.V., 2018. Blood-brain barrier breakdown in Alzheimer disease and other neurodegenerative disorders. Nat. Rev. Neurol. 14, 133–150.
Syed, A.B., Armstrong, R.A., Smith, C.U., 2005. A quantitative analysis of optic nerve axons in elderly control subjects and patients with Alzheimer's disease. Folia Neuropathol. 43, 1–6.
Szegedi, S., Dal-Bianco, P., Stogmann, E., Traub-Weidinger, T., Rainer, M., Masching, A., Schmidl, D., Werkmeister, R.M., Chua, J., Schmetterer, L., Garhofer, G., 2020. Anatomical and functional changes in the retina in patients with Alzheimer's disease and mild cognitive impairment. Acta Ophthalmol. 98, e914–e921.
Tadokoro, K., Yamashita, T., Fukui, Y., Nomura, E., Ohta, Y., Ueno, S., Nishina, S., Tsunoda, K., Wakutani, Y., Takao, Y., Miyoshi, T., Higashi, Y., Osakada, Y., Sasaki, R., Matsumoto, N., Kawahara, Y., Omote, Y., Takemoto, M., Hishikawa, N., Morihara, R., Abe, K., 2021a. Early detection of cognitive decline in mild cognitive impairment and Alzheimer's disease with a novel eye tracking test. J. Neurol. Sci. 427, 117529.
Tadokoro, K., Yamashita, T., Kimura, S., Nomura, E., Ohta, Y., Omote, Y., Takemoto, M., Hishikawa, N., Morihara, R., Morizane, Y., Abe, K., 2021b. Retinal Amyloid Imaging for Screening Alzheimer's Disease. J. Alzheimers Dis. 83, 927–934.
Takemori, S., Ida, M., 1988. Dementia and eye movements. Adv. Oto-Rhino-Laryngol. 42, 213–216.
Tao, Q., Ang, T.F.A., DeCarli, C., Auerbach, S.H., Devine, S., Stein, T.D., Zhang, X., Massaro, J., Au, R., Qiu, W.Q., 2018. Association of Chronic Low-grade Inflammation With Risk of Alzheimer Disease in ApoE4 Carriers. JAMA Netw. Open 1, e183597.
Tao, R., Lu, Z., Ding, D., Fu, S., Hong, Z., Liang, X., Zheng, L., Xiao, Y., Zhao, Q., 2019. Perifovea retinal thickness as an ophthalmic biomarker for mild cognitive impairment and early Alzheimer's disease. Alzheimers Dement. (Amst) 11, 405–414.
Tarasoff-Conway, J.M., Carare, R.O., Osorio, R.S., Glodzik, L., Butler, T., Fieremans, E., Axel, L., Rusinek, H., Nicholson, C., Zlokovic, B.V., Frangione, B., Blennow, K., Menard, J., Zetterberg, H., Wisniewski, T., de Leon, M.J., 2015. Clearance systems in the brain-implications for Alzheimer disease. Nat. Rev. Neurol. 11, 457–470.
Teunissen, C.E., Verberk, I.M.W., Thijssen, E.H., Vermunt, L., Hansson, O., Zetterberg, H., van der Flier, W.M., Mielke, M.M., Del Campo, M., 2022. Blood-based biomarkers for Alzheimer's disease: towards clinical implementation. Lancet Neurol. 21, 66–77.
Thomson, K.L., Yeo, J.M., Waddell, B., Cameron, J.R., Pal, S., 2015. A systematic review and meta-analysis of retinal nerve fiber layer change in dementia, using optical coherence tomography. Alzheimers Dement. (Amst) 1, 136–143.
Tolar, M., Abushakra, S., Hey, J.A., Porsteinsson, A., Sabbagh, M., 2020. Aducanumab, gantenerumab, BAN2401, and ALZ-801-the first wave of amyloid-targeting drugs for Alzheimer's disease with potential for near term approval. Alzheimer's Res. Ther. 12, 95.
Toulouie, S., Chang, S., Pan, J., Snyder, K., Yiu, G., 2022. Relationship of Retinal Vessel Caliber with Age-Related Macular Degeneration. J. Ophthalmol. 2022, 8210599.
Trebbastoni, A., D'Antonio, F., Bruscolini, A., Marcelli, M., Cecere, M., Campanelli, A., Imbriano, L., de Lena, C., Gharbiya, M., 2016. Retinal nerve fibre layer thickness changes in Alzheimer's disease: Results from a 12-month prospective case series. Neurosci. Lett. 629, 165–170.
Trick, G.L., Barris, M.C., Bickler-Bluth, M., 1989. Abnormal pattern electroretinograms in patients with senile dementia of the Alzheimer type. Ann. Neurol. 26, 226–231.
Trick, G.L., Trick, L.R., Morris, P., Wolf, M., 1995. Visual field loss in senile dementia of the Alzheimer's type. Neurology 45, 68–74.
Tripathy, D., Thirumangalakudi, L., Grammas, P., 2007. Expression of macrophage inflammatory protein 1-alpha is elevated in Alzheimer's vessels and is regulated by oxidative stress. J. Alzheimers Dis. 11, 447–455.
Trost, A., Lange, S., Schroedl, F., Bruckner, D., Motloch, K.A., Bogner, B., Kaser-Eichberger, A., Strohmaier, C., Runge, C., Aigner, L., Rivera, F.J., Reitsamer, H.A., 2016. Brain and Retinal Pericytes: Origin, Function and Role. Front. Cell. Neurosci. 10, 20.
Tsai, C.S., Ritch, R., Schwartz, B., Lee, S.S., Miller, N.R., Chi, T., Hsieh, F.Y., 1991. Optic nerve head and nerve fiber layer in Alzheimer's disease. Arch. Ophthalmol. 109, 199–204.
Tsai, Y., Lu, B., Ljubimov, A.V., Girman, S., Ross-Cisneros, F.N., Sadun, A.A., Svendsen, C.N., Cohen, R.M., Wang, S., 2014. Ocular changes in TgF344-AD rat model of Alzheimer's disease. Invest. Ophthalmol. Vis. Sci. 55, 523–534.
Uddin, N., Rutar, M., 2022. Ocular Lymphatic and Glymphatic Systems: Implications for Retinal Health and Disease. Int. J. Mol. Sci. 23.
Un, Y., Alpaslan, F., Dikmen, N.T., Sonmez, M., 2022. Posterior pole analysis and ganglion cell layer measurements in Alzheimer's disease. Hosp. Pract. 50, 282–288.
van de Haar, H.J., Burgmans, S., Jansen, J.F., van Osch, M.J., van Buchem, M.A., Muller, M., Hofman, P.A., Verhey, F.R., Backes, W.H., 2016a. Blood-Brain Barrier Leakage in Patients with Early Alzheimer Disease. Radiology 281, 527–535.
van de Haar, H.J., Jansen, J.F.A., van Osch, M.J.P., van Buchem, M.A., Muller, M., Wong, S.M., Hofman, P.A.M., Burgmans, S., Verhey, F.R.J., Backes, W.H., 2016b. Neurovascular unit impairment in early Alzheimer's disease measured with magnetic resonance imaging. Neurobiol. Aging 45, 190–196.
van de Kreeke, J.A., Nguyen, H.T., den Haan, J., Konijnenberg, E., Tomassen, J., den Braber, A., Ten Kate, M., Collij, L., Yaqub, M., van Berckel, B., Lammertsma, A.A., Boomsma, D.I., Tan, H.S., Verbraak, F.D., Visser, P.J., 2019. Retinal layer thickness in preclinical Alzheimer's disease. Acta Ophthalmol. 97, 798–804.
van de Kreeke, J.A., Nguyen, H.T., Konijnenberg, E., Tomassen, J., den Braber, A., Ten Kate, M., Yaqub, M., van Berckel, B., Lammertsma, A.A., Boomsma, D.I., Tan, S.H., Verbraak, F., Visser, P.J., 2020. Optical coherence tomography angiography in preclinical Alzheimer's disease. Br. J. Ophthalmol. 104, 157–161.
van der Heide, F.C.T., Khawaja, A., Berendschot, T., Littlejohns, T.J., Kuzma, E., Luben, R., Patel, P.J., Foster, P.J., Maastricht Study, C., Bertelsen, G., von Hanno, T., Johnsen, B., Schirmer, H., Reboucas, S.C.L., Grasset, L., Delcourt, C., Helmer, C., Eye, U.K.B., Vision, C., consortium, E., Stehouwer, C.D.A., 2023a. Associations of inner retinal layers with risk of incident dementia: An individual participant data analysis of four prospective cohort studies. Alzheimers Dement.
van der Heide, F.C.T., Steens, I.L.M., Limmen, B., Mokhtar, S., van Boxtel, M.P.J., Schram, M.T., Kohler, S., Kroon, A.A., van der Kallen, C.J.H., Dagnelie, P.C., van Dongen, M., Eussen, S., Berendschot, T., Webers, C.A.B., van Greevenbroek, M.M.J., Koster, A., van Sloten, T.T., Jansen, J.F.A., Backes, W.H., Stehouwer, C.D.A., 2023b. Thinner inner retinal layers are associated with lower cognitive performance, lower brain volume, and altered white matter network structure-The Maastricht Study. Alzheimers Dement.
van Dyck, C.H., Swanson, C.J., Aisen, P., Bateman, R.J., Chen, C., Gee, M., Kanekiyo, M., Li, D., Reyderman, L., Cohen, S., Froelich, L., Katayama, S., Sabbagh, M., Vellas, B., Watson, D., Dhadda, S., Irizarry, M., Kramer, L.D., Iwatsubo, T., 2023. Lecanemab in Early Alzheimer's Disease. N. Engl. J. Med. 388, 9–21.
Van Someren, E.J., 1997. Actigraphic monitoring of movement and rest-activity rhythms in aging, Alzheimer's disease, and Parkinson's disease. IEEE Trans. Rehabil. Eng. 5, 394–398.
van Someren, E.J., Hagebeuk, E.E., Lijzenga, C., Scheltens, P., de Rooij, S.E., Jonker, C., Pot, A.M., Mirmiran, M., Swaab, D.F., 1996. Circadian rest-activity rhythm disturbances in Alzheimer's disease. Biol. Psychiatr. 40, 259–270.
Van Someren, E.J., Kessler, A., Mirmiran, M., Swaab, D.F., 1997. Indirect bright light improves circadian rest-activity rhythm disturbances in demented patients. Biol. Psychiatr. 41, 955–963.
Vandenabeele, M., Veys, L., Lemmens, S., Hadoux, X., Gelders, G., Masin, L., Serneels, L., Theunis, J., Saito, T., Saido, T.C., Jayapala, M., De Boever, P., De Strooper, B., Stalmans, I., van Wijngaarden, P., Moons, L., De Groef, L., 2021. The App(NL-G-F) mouse retina is a site for preclinical Alzheimer's disease diagnosis and research. Acta Neuropathol. Commun. 9, 6.
Varga, E., Juhasz, G., Bozso, Z., Penke, B., Fulop, L., Szegedi, V., 2015. Amyloid-beta1-42 Disrupts Synaptic Plasticity by Altering Glutamate Recycling at the Synapse. J. Alzheimers Dis. 45, 449–456.
Vinters, H.V., 1987. Cerebral amyloid angiopathy. A critical review. Stroke 18, 311–324.
Vinters, H.V., Gilbert, J.J., 1983. Cerebral amyloid angiopathy: incidence and complications in the aging brain. II. The distribution of amyloid vascular changes. Stroke 14, 924–928.
Viswanathan, A., Greenberg, S.M., 2011. Cerebral amyloid angiopathy in the elderly. Ann. Neurol. 70, 871–880.
Vit, J.P., Fuchs, D.T., Angel, A., Levy, A., Lamensdorf, I., Black, K.L., Koronyo, Y., Koronyo-Hamaoui, M., 2021a. Color and contrast vision in mouse models of aging and Alzheimer's disease using a novel visual-stimuli four-arm maze. Sci. Rep. 11, 1255.
Vit, J.P., Fuchs, D.T., Angel, A., Levy, A., Lamensdorf, I., Black, K.L., Koronyo, Y., Koronyo-Hamaoui, M., 2021b. Visual-stimuli Four-arm Maze test to Assess Cognition and Vision in Mice. Bio Protoc 11, e4234.
Volicer, L., Harper, D.G., Manning, B.C., Goldstein, R., Satlin, A., 2001. Sundowning and circadian rhythms in Alzheimer's disease. Am. J. Psychiatr. 158, 704–711.

Walkiewicz, G., Ronisz, A., Van Ginderdeuren, R., Lemmens, S., Bouwman, F.H., Hoozemans, J.J.M., Morrema, T.H.J., Rozemuller, A.J., Hart de Ruyter, F.J., De Groef, L., Stalmans, I., Thal, D.R., 2024. Primary retinal tauopathy: A tauopathy with a distinct molecular pattern. Alzheimers Dement 20, 330–340.
Wang, C., Holtzman, D.M., 2020. Bidirectional relationship between sleep and Alzheimer's disease: role of amyloid, tau, and other factors. Neuropsychopharmacology 45, 104–120.
Wang, D., Li, Y., Wang, C., Xu, L., You, Q.S., Wang, Y.X., Zhao, L., Wei, W.B., Zhao, X., Jonas, J.B., 2014. Localized retinal nerve fiber layer defects and stroke. Stroke 45, 1651–1656.
Wang, H., Akkin, T., Magnain, C., Wang, R., Dubb, J., Kostis, W.J., Yaseen, M.A., Cramer, A., Sakadzic, S., Boas, D., 2016. Polarization sensitive optical coherence microscopy for brain imaging. Opt Lett 41, 2213–2216.
Wang, L., Davis, P.B., Volkow, N.D., Berger, N.A., Kaelber, D.C., Xu, R., 2022a. Association of COVID-19 with New-Onset Alzheimer's Disease. J. Alzheimers Dis. 89, 411–414.
Wang, L., Hu, Z., Chen, H., Sheng, X., Qin, R., Shao, P., Yang, Z., Yao, W., Zhao, H., Xu, Y., Bai, F., 2023a. Applying Retinal Vascular Structures Characteristics Coupling with Cortical Visual System in Alzheimer's Disease Spectrum Patients. Brain Sci. 13.
Wang, S., Jiang, X., Peng, W., Yang, S., Pi, R., Zhou, S., 2023b. Acrolein Induces Retinal Abnormalities of Alzheimer's Disease in Mice. Int. J. Mol. Sci. 24.
Wang, X., Jiao, B., Liu, H., Wang, Y., Hao, X., Zhu, Y., Xu, B., Xu, H., Zhang, S., Jia, X., Xu, Q., Liao, X., Zhou, Y., Jiang, H., Wang, J., Guo, J., Yan, X., Tang, B., Zhao, R., Shen, L., 2022b. Machine learning based on Optical Coherence Tomography images as a diagnostic tool for Alzheimer's disease. CNS Neurosci. Ther. 28, 2206–2217.
Wang, X., Lou, N., Eberhardt, A., Yang, Y., Kusk, P., Xu, Q., Forstera, B., Peng, S., Shi, M., Ladron-de-Guevara, A., Delle, C., Sigurdsson, B., Xavier, A.L.R., Erturk, A., Libby, R. T., Chen, L., Thrane, A.S., Nedergaard, M., 2020a. An ocular glymphatic clearance system removes beta-amyloid from the rodent eye. Sci. Transl. Med. 12.
Wang, X., Wang, Y., Liu, H., Zhu, X., Hao, X., Zhu, Y., Xu, B., Zhang, S., Jia, X., Weng, L., Liao, X., Zhou, Y., Tang, B., Zhao, R., Jiao, B., Shen, L., 2022c. Macular Microvascular Density as a Diagnostic Biomarker for Alzheimer's Disease. J. Alzheimers Dis. 90, 139–149.
Wang, X., Zhao, Q., Tao, R., Lu, H., Xiao, Z., Zheng, L., Ding, D., Ding, S., Ma, Y., Lu, Z., Xiao, Y., 2020b. Decreased Retinal Vascular Density in Alzheimer's Disease (AD) and Mild Cognitive Impairment (MCI): An Optical Coherence Tomography Angiography (OCTA) Study. Front. Aging Neurosci. 12, 572484.
Welikovitch, L.A., Do Carmo, S., Magloczky, Z., Malcolm, J.C., Loke, J., Klein, W.L., Freund, T., Cuello, A.C., 2020. Early intraneuronal amyloid triggers neuron-derived inflammatory signaling in APP transgenic rats and human brain. Proc. Natl. Acad. Sci. U. S. A. 117, 6844–6854.
WHO, 2023. World Health Organization. Dementia: Key Facts.
Wiese, L.A.K., Gibson, A., Guest, M.A., Nelson, A.R., Weaver, R., Gupta, A., Carmichael, O., Lewis, J.P., Lindauer, A., Loi, S., Peterson, R., Radford, K., Rhodus, E.K., Wong, C.G., Zuelsdorff, M., Saidi, L.G., Valdivieso-Mora, E., Franzen, S., Pope, C.N., Killian, T.S., Shrestha, H.L., Heyn, P.C., Ng, T.K.S., Prusaczyk, B., John, S., Kulshreshtha, A., Sheffler, J.L., Besser, L., Daniel, V., Tolea, M.I., Miller, J., Musyimi, C., Corkey, J., Yank, V., Williams, C.L., Rahemi, Z., Park, J., Magzamen, S., Newton Jr., R.L., Harrington, C., Flatt, J.D., Arora, S., Walter, S., Griffin, P., Babulal, G.M., 2023. Global rural health disparities in Alzheimer's disease and related dementias: State of the science. Alzheimers Dement.
Williams, E.A., McGuone, D., Frosch, M.P., Hyman, B.T., Laver, N., Stemmer-Rachamimov, A., 2017. Absence of Alzheimer Disease Neuropathologic Changes in Eyes of Subjects With Alzheimer Disease. J. Neuropathol. Exp. Neurol. 76, 376–383.
Williams, M.A., McGowan, A.J., Cardwell, C.R., Cheung, C.Y., Craig, D., Passmore, P., Silvestri, G., Maxwell, A.P., McKay, G.J., 2015. Retinal microvascular network attenuation in Alzheimer's disease. Alzheimers Dement. (Amst) 1, 229–235.
Williams, P.A., Thirgood, R.A., Oliphant, H., Frizzati, A., Littlewood, E., Votruba, M., Good, M.A., Williams, J., Morgan, J.E., 2013. Retinal ganglion cell dendritic degeneration in a mouse model of Alzheimer's disease. Neurobiol. Aging 34, 1799–1806.
Williams, S., Chalmers, K., Wilcock, G.K., Love, S., 2005. Relationship of neurofibrillary pathology to cerebral amyloid angiopathy in Alzheimer's disease. Neuropathol. Appl. Neurobiol. 31, 414–421.
Wilson, R.S., Leurgans, S.E., Boyle, P.A., Schneider, J.A., Bennett, D.A., 2010. Neurodegenerative basis of age-related cognitive decline. Neurology 75, 1070–1078.
Wisely, C.E., Richardson, A., Henao, R., Robbins, C.B., Ma, J.P., Wang, D., Johnson, K.G., Liu, A.J., Grewal, D.S., Fekrat, S., 2024. A Convolutional Neural Network Using Multimodal Retinal Imaging for Differentiation of Mild Cognitive Impairment from Normal Cognition. Ophthalmol Sci 4, 100355.
Wisely, C.E., Wang, D., Henao, R., Grewal, D.S., Thompson, A.C., Robbins, C.B., Yoon, S. P., Soundararajan, S., Polascik, B.W., Burke, J.R., Liu, A., Carin, L., Fekrat, S., 2022. Convolutional neural network to identify symptomatic Alzheimer's disease using multimodal retinal imaging. Br. J. Ophthalmol. 106, 388–395.
Witmer, M.T., Parlitsis, G., Patel, S., Kiss, S., 2013. Comparison of ultra-widefield fluorescein angiography with the Heidelberg Spectralis((R)) noncontact ultra-widefield module versus the Optos((R)) Optomap((R)). Clin. Ophthalmol. 7, 389–394.
Wong, T.Y., Klein, R., Sharrett, A.R., Nieto, F.J., Boland, L.L., Couper, D.J., Mosley, T.H., Klein, B.E., Hubbard, L.D., Szklo, M., 2002. Retinal microvascular abnormalities and cognitive impairment in middle-aged persons: the Atherosclerosis Risk in Communities Study. Stroke 33, 1487–1492.
Woo, K.A., Shin, J.Y., Kim, H., Ahn, J., Jeon, B., Lee, J.Y., 2022. Peripapillary retinal nerve fiber layer thinning in patients with progressive supranuclear palsy. J. Neurol. 269, 3216–3225.
Wostyn, P., De Groot, V., Van Dam, D., Audenaert, K., De Deyn, P.P., Killer, H.E., 2016. The Glymphatic System: A New Player in Ocular Diseases? Invest. Ophthalmol. Vis. Sci. 57, 5426–5427.
Wostyn, P., De Groot, V., Van Dam, D., Audenaert, K., Killer, H.E., De Deyn, P.P., 2017. The Glymphatic Hypothesis of Glaucoma: A Unifying Concept Incorporating Vascular, Biomechanical, and Biochemical Aspects of the Disease. BioMed Res. Int. 2017, 5123148.
Wostyn, P., Van Dam, D., Audenaert, K., Killer, H.E., De Deyn, P.P., De Groot, V., 2015. A new glaucoma hypothesis: a role of glymphatic system dysfunction. Fluids Barriers CNS 12, 16.
Wu, J., Zhang, X., Azhati, G., Li, T., Xu, G., Liu, F., 2020. Retinal microvascular attenuation in mental cognitive impairment and Alzheimer's disease by optical coherence tomography angiography. Acta Ophthalmol. 98, e781–e787.
Wyss-Coray, T., Loike, J.D., Brionne, T.C., Lu, E., Anankov, R., Yan, F., Silverstein, S.C., Husemann, J., 2003. Adult mouse astrocytes degrade amyloid-beta in vitro and in situ. Nat. Med. 9, 453–457.
Xia, W., Yang, T., Shankar, G., Smith, I.M., Shen, Y., Walsh, D.M., Selkoe, D.J., 2009. A specific enzyme-linked immunosorbent assay for measuring beta-amyloid protein oligomers in human plasma and brain tissue of patients with Alzheimer disease. Arch. Neurol. 66, 190–199.
Xie, J., Yi, Q., Wu, Y., Zheng, Y., Liu, Y., Macerollo, A., Fu, H., Xu, Y., Zhang, J., Behera, A., Fan, C., Frangi, A.F., Liu, J., Lu, Q., Qi, H., Zhao, Y., 2023. Deep segmentation of OCTA for evaluation and association of changes of retinal microvasculature with Alzheimer's disease and mild cognitive impairment. Br. J. Ophthalmol.
Xu, Q.A., Boerkoel, P., Hirsch-Reinshagen, V., Mackenzie, I.R., Hsiung, G.R., Charm, G., To, E.F., Liu, A.Q., Schwab, K., Jiang, K., Sarunic, M., Beg, M.F., Pham, W., Cui, J., To, E., Lee, S., Matsubara, J.A., 2022. Muller cell degeneration and microglial dysfunction in the Alzheimer's retina. Acta Neuropathol. Commun. 10, 145.
Xu, Z., Xiao, N., Chen, Y., Huang, H., Marshall, C., Gao, J., Cai, Z., Wu, T., Hu, G., Xiao, M., 2015. Deletion of aquaporin-4 in APP/PS1 mice exacerbates brain Abeta accumulation and memory deficits. Mol. Neurodegener. 10, 58.
Yamaji, H., Shiraga, F., Tsuchida, Y., Yamamoto, Y., Ohtsuki, H., 2004. Evaluation of arteriovenous crossing sheathotomy for branch retinal vein occlusion by fluorescein videoangiography and image analysis. Am. J. Ophthalmol. 137, 834–841.
Yan, Z., Liao, H., Chen, H., Deng, S., Jia, Y., Deng, C., Lin, J., Ge, J., Zhuo, Y., 2017. Elevated Intraocular Pressure Induces Amyloid-beta Deposition and Tauopathy in the Lateral Geniculate Nucleus in a Monkey Model of Glaucoma. Invest. Ophthalmol. Vis. Sci. 58, 5434–5443.
Yanagisawa, D., Shirai, N., Amatsubo, T., Taguchi, H., Hirao, K., Urushitani, M., Morikawa, S., Inubushi, T., Kato, M., Kato, F., Morino, K., Kimura, H., Nakano, I., Yoshida, C., Okada, T., Sano, M., Wada, Y., Wada, K.N., Yamamoto, A., Tooyama, I., 2010. Relationship between the tautomeric structures of curcumin derivatives and their Abeta-binding activities in the context of therapies for Alzheimer's disease. Biomaterials 31, 4179–4185.
Yanagisawa, D., Taguchi, H., Yamamoto, A., Shirai, N., Hirao, K., Tooyama, I., 2011. Curcuminoid binds to amyloid-beta1-42 oligomer and fibril. J. Alzheimers Dis. 24 (Suppl. 2), 33–42.
Yang, Y., Shiao, C., Hemingway, J.F., Jorstad, N.L., Shalloway, B.R., Chang, R., Keene, C. D., 2013. Suppressed retinal degeneration in aged wild type and APPswe/PS1DeltaE9 mice by bone marrow transplantation. PLoS One 8, e64246.
Yao, Q., Jiang, K., Lin, F., Zhu, T., Khan, N.H., Jiang, E., 2023. Pathophysiological Association of Alzheimer's Disease and Hypertension: A Clinical Concern for Elderly Population. Clin. Interv. Aging 18, 713–728.
Yap, T.E., Donna, P., Almonte, M.T., Cordeiro, M.F., 2018. Real-Time Imaging of Retinal Ganglion Cell Apoptosis. Cells 7.
Yarns, B.C., Holiday, K.A., Carlson, D.M., Cosgrove, C.K., Melrose, R.J., 2022. Pathophysiology of Alzheimer's Disease. Psychiatr. Clin. 45, 663–676.
Ye, F., Ye, M., An, J., Wang, D., Wang, Q., Chen, Y., Peng, X., 2018. Motion-induced position shift in early Alzheimer's disease. Sci. Rep. 8, 9833.
Yeh, T.C., Kuo, C.T., Chou, Y.B., 2022. Retinal Microvascular Changes in Mild Cognitive Impairment and Alzheimer's Disease: A Systematic Review, Meta-Analysis, and Meta-Regression. Front. Aging Neurosci. 14, 860759.
Yin, X., Zhang, S., Lee, J.H., Dong, H., Mourgkos, G., Terwilliger, G., Kraus, A., Geraldo, L.H., Poulet, M., Fischer, S., Zhou, T., Mohammed, F.S., Zhou, J., Wang, Y., Malloy, S., Rohner, N., Sharma, L., Salinas, I., Eichmann, A., Thomas, J.L., Saltzman, W.M., Huttner, A., Zeiss, C., Ring, A., Iwasaki, A., Song, E., 2024. Compartmentalized ocular lymphatic system mediates eye-brain immunity. Nature 628, 204–211.
Yoon, S.P., Grewal, D.S., Thompson, A.C., Polascik, B.W., Dunn, C., Burke, J.R., Fekrat, S., 2019. Retinal Microvascular and Neurodegenerative Changes in Alzheimer's Disease and Mild Cognitive Impairment Compared with Control Participants. Ophthalmol Retina 3, 489–499.
Yulug, B., Hanoglu, L., Kilic, E., 2017. Does sleep disturbance affect the amyloid clearance mechanisms in Alzheimer's disease? Psychiatr. Clin. Neurosci. 71, 673–677.
Zabel, P., Kaluzny, J.J., Wilkosc-Debczynska, M., Gebska-Toloczko, M., Suwala, K., Kucharski, R., Araszkiewicz, A., 2019a. Peripapillary Retinal Nerve Fiber Layer Thickness in Patients with Alzheimer's Disease: A Comparison of Eyes of Patients with Alzheimer's Disease, Primary Open-Angle Glaucoma, and Preperimetric Glaucoma and Healthy Controls. Med Sci Monit 25, 1001–1008.
Zabel, P., Kaluzny, J.J., Wilkosc-Debczynska, M., Gebska-Toloczko, M., Suwala, K., Zabel, K., Zaron, A., Kucharski, R., Araszkiewicz, A., 2019b. Comparison of Retinal Microvasculature in Patients With Alzheimer's Disease and Primary Open-Angle Glaucoma by Optical Coherence Tomography Angiography. Invest. Ophthalmol. Vis. Sci. 60, 3447–3455.

Zempel, H., Luedtke, J., Kumar, Y., Biernat, J., Dawson, H., Mandelkow, E., Mandelkow, E.M., 2013. Amyloid-beta oligomers induce synaptic damage via Tau-dependent microtubule severing by TTLL6 and spastin. EMBO J. 32, 2920–2937.
Zenaro, E., Piacentino, G., Constantin, G., 2017. The blood-brain barrier in Alzheimer's disease. Neurobiol. Dis. 107, 41–56.
Zhang, H., Cao, Y., Ma, L., Wei, Y., Li, H., 2021a. Possible Mechanisms of Tau Spread and Toxicity in Alzheimer's Disease. Front. Cell Dev. Biol. 9, 707268.
Zhang, J., Gao, F., Ma, Y., Xue, T., Shen, Y., 2021b. Identification of early-onset photoreceptor degeneration in transgenic mouse models of Alzheimer's disease. iScience 24, 103327.
Zhang, M., Zhong, L., Han, X., Xiong, G., Xu, D., Zhang, S., Cheng, H., Chiu, K., Xu, Y., 2021c. Brain and Retinal Abnormalities in the 5xFAD Mouse Model of Alzheimer's Disease at Early Stages. Front. Neurosci. 15, 681831.
Zhang, Y., Shi, C., Chen, Y., Wang, W., Huang, S., Han, Z., Lin, X., Lu, F., Shen, M., 2020. Retinal Structural and Microvascular Alterations in Different Acute Ischemic Stroke Subtypes. J. Ophthalmol. 2020, 8850309.
Zhang, Y.S., Zhou, N., Knoll, B.M., Samra, S., Ward, M.R., Weintraub, S., Fawzi, A.A., 2019. Parafoveal vessel loss and correlation between peripapillary vessel density and cognitive performance in amnestic mild cognitive impairment and early Alzheimer's Disease on optical coherence tomography angiography. PLoS One 14, e0214685.
Zhao, A., Fang, F., Li, B., Chen, Y., Qiu, Y., Wu, Y., Xu, W., Deng, Y., 2020. Visual Abnormalities Associate With Hippocampus in Mild Cognitive Impairment and Early Alzheimer's Disease. Front. Aging Neurosci. 12, 597491.
Zhao, B., Yan, Y., Wu, X., Geng, Z., Wu, Y., Xiao, G., Wang, L., Zhou, S., Wei, L., Wang, K., Liao, R., 2023. The correlation of retinal neurodegeneration and brain degeneration in patients with Alzheimer's disease using optical coherence tomography angiography and MRI. Front. Aging Neurosci. 15, 1089188.
Zhao, H., Chang, R., Che, H., Wang, J., Yang, L., Fang, W., Xia, Y., Li, N., Ma, Q., Wang, X., 2013. Hyperphosphorylation of tau protein by calpain regulation in retina of Alzheimer's disease transgenic mouse. Neurosci. Lett. 551, 12–16.
Zhao, X., Stafford, B.K., Godin, A.L., King, W.M., Wong, K.Y., 2014. Photoresponse diversity among the five types of intrinsically photosensitive retinal ganglion cells. J. Physiol. 592, 1619–1636.
Zhao, Z., Sagare, A.P., Ma, Q., Halliday, M.R., Kong, P., Kisler, K., Winkler, E.A., Ramanathan, A., Kanekiyo, T., Bu, G., Owens, N.C., Rege, S.V., Si, G., Ahuja, A., Zhu, D., Miller, C.A., Schneider, J.A., Maeda, M., Maeda, T., Sugawara, T., Ichida, J. K., Zlokovic, B.V., 2015. Central role for PICALM in amyloid-beta blood-brain barrier transcytosis and clearance. Nat. Neurosci. 18, 978–987.
Zhong, L., Wang, Z., Wang, D., Wang, Z., Martens, Y.A., Wu, L., Xu, Y., Wang, K., Li, J., Huang, R., Can, D., Xu, H., Bu, G., Chen, X.F., 2018. Amyloid-beta modulates microglial responses by binding to the triggering receptor expressed on myeloid cells 2 (TREM2). Mol. Neurodegener. 13, 15.
Zhou, J., Fonseca, M.I., Kayed, R., Hernandez, I., Webster, S.D., Yazan, O., Cribbs, D.H., Glabe, C.G., Tenner, A.J., 2005. Novel Abeta peptide immunogens modulate plaque pathology and inflammation in a murine model of Alzheimer's disease. J. Neuroinflammation 2, 28.
Zipser, B.D., Johanson, C.E., Gonzalez, L., Berzin, T.M., Tavares, R., Hulette, C.M., Vitek, M.P., Hovanesian, V., Stopa, E.G., 2007. Microvascular injury and blood-brain barrier leakage in Alzheimer's disease. Neurobiol. Aging 28, 977–986.
Zlokovic, B.V., 2011. Neurovascular pathways to neurodegeneration in Alzheimer's disease and other disorders. Nat. Rev. Neurosci. 12, 723–738.
Zlokovic, B.V., Ghiso, J., Mackic, J.B., McComb, J.G., Weiss, M.H., Frangione, B., 1993. Blood-brain barrier transport of circulating Alzheimer's amyloid beta. Biochem. Biophys. Res. Commun. 197, 1034–1040.
Zola, M., Bousquet, E., Favard, C., Gigon, A., Mantel, I., Behar-Cohen, F., 2023. Indocyanine Green Angiography of Type 1 Macular Neovascularization in Age-Related Macular Degeneration and Central Serous Chorioretinopathy Reveals Different Disease Mechanisms. Retina 43, 1255–1263.
Zou, K., Abdullah, M., Michikawa, M., 2020. Current Biomarkers for Alzheimer's Disease: From CSF to Blood. J. Personalized Med. 10.
Zuroff, L., Daley, D., Black, K.L., Koronyo-Hamaoui, M., 2017. Clearance of cerebral Abeta in Alzheimer's disease: reassessing the role of microglia and monocytes. Cell. Mol. Life Sci. 74, 2167–2201.